SEDIMENT HANDLING IN HIMALAYAN RIVERS USING HYDROCYCLONES

by

Hari Prasad Pandit

A Dissertation submitted in partial fulfillment of the requirements for the degree of Doctor of Engineering

Supervisors   : Prof. Dr. N. M. Shakya , IOE, TU
                                     Prof. Dr. Haakon Stole, NTNU, Norway
                                     Prof. Dr. N.K. Garg, IIT, Delhi

Hari Prasad Pandit
Nationality   Nepali
Previous Degrees   MSc., Hydraulic Engineering
                          International Institute for Infrastructural, Hydraulic &
                          Environmental Engineering (IHE), Delft, The Netherlands

                          MSc.(Hons), Civil Engineering
                          Rostov Civil Engineering Institute
                          Russia (Former USSR)

Civil Engineering Department
Institute of Engineering
Tribhuvan University
Kathmandu, Nepal
May 2009

TABLE OF CONTENTS
SYNOPSIS
TABLE OF CONTENTS
LIST OF FIGURES
LIST OF TABLES

iii

REFERENCES

APPENDICES
APPENDIX 1: List of Publications Made During Research Period

LIST OF FIGURES

v

LIST OF TABLES

1 INTRODUCTION

1.1 Background

The steep catchments of the Himalayan Rivers endowed with abundant water offer a huge potential of hydropower generation accounting a gross potential of 83,000 MW in Nepalese rivers alone (MWRN, 2003). This very little harnessed (< 2 %) resources so far and emerging energy markets both at home and in the neighborhood signify a glimpse of prosperity of the country and its populace.

However, harnessing this huge resources from the Himalayan Rivers is a very challenging task. Severe land erosion is the inherent natural phenomenon in Himalayan river basins. The inherent, incessant and stochastic character of rainfall in this geologically rugged and fragile region generates extreme sediment load due to catchment, bank and bed erosion (Galay et al., 2003; Stole,1993) ,which has been found one of the major obstacles in developing hydropower projects. Sediment load as high as 25,000 ppm are regularly recorded on major rivers such as the Narayani in Nepal (Carson, 1985). Sediment load up to 50,000 ppm have been frequently observed on smaller rivers like the Jhimruk in Nepal (Basnyat, 1997). Therefore, only the Run-of–Rivers (RoR) hydropower projects are viable alternatives in most of the stretches of the Himalayan rivers due to enormous sediment load and topographical limitations (Stole, 1993).

Tunnel type excluder, settling basins and lately, vortex chamber type extractors are used for excluding sediment in RoR projects (Garde and Ranga Raju, 2000; Paul et al., 1991; Ranga Raju et al., 1999). Among them the use of settling basins is most common. Such units are normally designed to trap sediment coarser than 200 micron in size and avoid passing them into the turbines and accessories of the hydropower plant and minimize wear and tear of hydro-mechanical equipment appreciably.

Nevertheless, there are ample examples that even the particles finer than 200 micron have been found to cause enormous wear and tear in hydro-mechanical equipment of medium and high head power plants. This is mainly due to the presence of hard minerals like quartz and feldspar as chief constituents in the sediment of the Himalayan rivers. For example, Jhimruk Hydropower plant of Nepal suffers each year severe wear and tear of turbines and accessories, where more than 80% sediment particles finer than 90 micron have been

observed (Basnyat, 1997). Severe erosion followed by cavitation have been observed in a high head (920 m) Pelton turbine subject to a flow containing 77 % sediment particles finer than 63 micron and 99 % particles finer than 125 micron shortly after 600 hours of operation (Brekke et al., 2002).

Recent studies have also indicated that sediment load is one of the major factors for such wear and tear (Bajracharya, 2007; Biswakarma, 2008). The continuing wear and tear of turbines reduce the efficiency of the plant considerably, thereby necessitating frequent maintenance. Annual operation and maintenance cost of the sediment affected power plants can reach as high as 5.0% of the capital cost, against about 1.5% in plants with little sediment load (Naidu, 1997). In addition to the high cost of repair or replacement of damaged turbines and accessories, the plant also loses substantial revenue due to outage of the plant (Naidu, 1996; Basnyat, 1997; Hydro Lab, 2004). These facts call for the exclusion of fine sand as well as coarse silt from the withdrawn flow in most of the hydropower plants.

On the other hand, exclusion of such fine particles from entering into the turbines and accessories using conventional method need larger settling basins. But it is difficult quite often to avail required space for larger settling basin in a rugged and fragile Himalayan terrain. Even if such space is managed, the cost involved will be huge. To cope with these constraints, alternative methods for the removal of suspended sediment particles in medium and high head hydropower plants of Himalayan region are sought.

The alternative concept of centrifugal separation has been applied to exclude fine particles in many fields such as water supply and wastewater engineering, mineral processing, chemical engineering and coal refineries (Svarovsky, 1990). In such devices, a higher velocity flow stream is introduced tangentially into a cylindrical body having an orifice at the center of its bottom (Fig.1.1). This gives rise to Rankine type vortex conditions with forced vortex forming near the orifice and free vortex forming in the outer region toward the periphery. As a result, sediment concentration gradient builds up across the vortex and a diffusive flux proportional but opposite to the centrifugal flux is induced (Julien, 1986).

The sediment particles present in the flow move along a helicoidal path towards the orifice, thereby obtaining a long settling length compared to the dimension of the separator. Materials that are denser than the carrier medium are separated from the stream during this downward flow and are removed through the 'underflow' outlet at the bottom of the cone continuously. Whereas, the relatively sediment free flow containing fine sediment and most of the flow leaves through the 'overflow' outlet located at the top of the hydrocyclone.
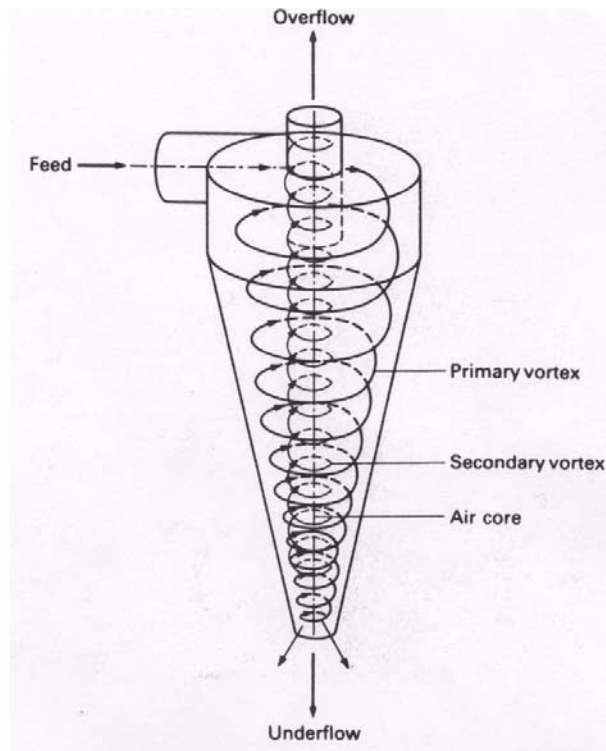
Fig. 1.1   Schematic sketch of a hydrocyclone

Paul et al., 1991; Dhillon, 1996 and Sakhuja, 1996 have observed much better efficiency of a vortex settling basin compared to classical settling basin. Athar et al.(2002) found a better geometry for such basin. Sakhuja (1996) observed satisfactory results from field applications. However, despite their higher efficiency in removing coarser particles, the degree of removal of finer particles required in most of the hydropower plants is under question. This necessitates the use of devices capable of producing strong centrifugal acceleration. Hydrocyclones are the preferred devices for such purposes in the industries (Wills, 1985 Svarovsky, 1991). Efficiency of removal of fine particles by this device is much higher than that can be expected from the theory of single particle sedimentation. This inherent property of hydrocyclone popularly known as 'fish-hook' effect (Plitt, 1971; Nageswararao 2000; Majumder et al., 2003) is the major advantage over the classical and vortex settling basins.

But the geometry of hydrocyclone is very sensitive to particle removal efficiency. Hydrocyclone with geometries due to Rietema (1961) and Bradley (1965) are two well-known devices adopted for solid liquid separation. Bradley's design with long conical section gives higher separation efficiency for finer particles. However, Rietema's geometry works efficiently for coarser particles. Krebs Engineers (2000) therefore combined both of

these advantages by using sharper upper cone to accelerate tangential velocity and then a gradual tapering lower cone to provide residence time for a finer separation resulting in a new geometry (gMax series) and better separation efficiency (Turner et al., 2001).

Despite their excellent removal efficiency, hydrocyclones are often criticized for the considerable amount of energy they require for processing the flow. Moreover, the available head for such a purpose is often a limitation in many water projects. The short circuiting of flow near the inlet resulting in bypassing of coarser particles directly to the overflow is yet another weakness of hydrocyclones (Bradley, 1965). The significant energy loss incurred in the hydrocyclone has been observed near the inlet and outlet (Boadway, 1984; Pandit et al., 2007). The migration of coarse particles due to short-circuiting is also believed due to the excessive turbulence near the inlet. Therefore, there is a need of an efficient geometry of a hydrocyclone in terms of hydraulics as well as particle separation to address these issues.

1.2   Objectives

Cyclone type separators have been used in industries for a long time. They have been used primarily in mineral processing and chemical engineering, where relatively smaller feed discharge, but higher feed concentration has to be handled. However, the studies of hydrocyclones as a sediment separator in handling large discharge in hydraulic engineering, such as Hydropower and Irrigation Engineering have not been carried out. Therefore, considering the prospects of using hydrocyclones in large water sector projects, the present study intended to identify a new geometry of a hydrocyclone and a suitable test rig capable of simulating a hydrocyclone in the context of a hydropower system. Improvement of flow near the inlet and outlet and minimizing the headloss and short-circuiting effect are the focal points. The specific objectives to achieve the main objective are as follows:
  • Review of solid liquid separation techniques in industries and water sector projects
  • Design a test rig and investigate hydrocyclones of conventional geometrical features and assess their performance for a range of design and operating variables
  • Find out the strength and weakness of the hydrocyclone in terms of requirements in hydropower plants
  • Design a suitable test rig and modified geometry of a hydrocyclone minimizing the shortcomings due to conventional design

- Investigate the cyclone for a range of design and operating variables and assess the performance of the system
- Compare the performance of hydrocyclone with that of conventional gravity settling basin designed for a hydropower project

1.3 Research Methodology

The study was carried out in different stages as outlined below.

1.3.1 Literature Review

The primary objective of the literature review was to determine the state of the art development in the area of research envisaged. The major sources of information include scientific journals, magazine, publications of academic and research institutions, web pages and research reports. Since very few studies have been carried out in the area of water resources engineering, review of literature in peripheral areas have been conducted. Sedimentation process in the Himalayas, sediment handling in Himalayan Rivers and particles separation using centrifugal techniques were the areas of major concern during literature review.

1.3.2 Finalization of Research Proposal

The literature review carried out for a period of about one year has given valuable inputs to the researcher. The problems in handling the sediment in Himalayan Rivers have been better understood. The strength and weakness of the conventional methods of sediment handling techniques have been assessed and found room for improvement. Considerable damages to hydro-electro- mechanical equipment and appreciable revenue loss have been noticed. Therefore, based on this reality and the knowledge gained from pre-requisite courses the research proposal has been updated to carry out a study on alternative methods of sediment handling, with a central focus on study of a cyclone type separator.

1.3.3 Planning and Design of Laboratory Study

The next step of the research was to decide the type of model to use. Non-distorted prototype rigs were designed and set up. However, later it was interpreted as a scale model to predict the performance of larger cyclones using the basic principles of Froude as well as Reynolds Laws. The design parameters of hydrocyclone and the test rig for carrying out the experiment were computed for various scenarios. The main decision variables were the design parameters defining the geometry of the hydrocyclone and the test rig and operating parameters characterizing the flow and sediment properties. The availability of

the space and facilities available in the laboratories were duly considered while deciding the design and operating variables.

Conceptualizing the hydrocyclone and the test rig, an inventory of pieces of equipment and materials required for model construction was prepared. Similarly, the methods and procedures for simulation of model was worked out. The record keeping methods and procedures for monitoring the flow characteristics, hydraulics and process observation were established.

1.3.4 Setting Up Test Rig and Experimental Investigation

The experimental test rigs with the designated hydrocyclones were set up based on the design parameters estimated. Experimental investigations were carried out in two stages. A test rig equipped with a smaller hydrocyclone (D = 0.22 m) having a standard geometry was installed in the beginning. The output and the feed back from this test rig served as input to the larger model, set up a later stage facilitating more advanced studies

The experiments in both the test rigs were conducted for different scenarios. Variation in design variables, mainly the geometrical parameters of the hydrocyclone, and operating variables, primarily, discharge, sediment load and characteristics and pressure drop formed the basis for different scenarios of experimentation.

1.3.5 Data Analysis

The recorded data were analyzed using appropriate tools. In most of the cases, the statistical tools available in the MS EXCEL program were sufficient for analysis. The validity of the methods of data collection, simulation and reliability of data were ascertained and calibrated whenever needed. The results obtained from different alternatives were compared to analyze the performance of the modified hydrocyclone. Finally, the sensitivity of the model with respect to various parameters, especially discharge, sediment load and characteristics as well as pressure drop were carried out.

1.3.6 Dissemination of Outcome of the Research

The interim results of the research were disseminated periodically. The outcomes were shared through conferences, workshops, seminars and journals. The list of publications made during the study period are presented in Appendix 1 of this thesis.

1.4 Outline of the Dissertation

The thesis is written in seven chapters. The first chapter includes background information and depicts the shortcomings of the conventional settling basins leading to erosion problems in hydro-mechanical equipment of hydropower plants. Further, the objectives are presented, which is followed by research methodology applied to achieve the objectives.

Both Chapter 2 and Chapter 3 present the findings of the state of the art literature review. The first part of the Chapter 2 comprises the review of the particle separation techniques primarily in industries, with major focus on centrifugal separation. Whereas the second part encompasses the techniques of sediment exclusion in comparatively large water sector projects. Shortcomings of settling basin, a commonly adopted device in water sector projects are highlighted and the erosion problems thereof experienced in hydro-mechanical units of some of the hydropower projects are presented.

Review of literature on hydrocyclone is presented in Chapter 3. The hydraulics inside the hydrocyclone is depicted in the beginning, which is followed by the theories of hydrocyclone and correlations describing its performance. The next part of the chapter includes the effect of design and operating variables.

Details on experimental investigations are given in Chapter 4. Design of hydrocyclones and experimental setups with 0.22 m and 0.38 m diameter hydrocyclones are discussed in the beginning. The next part of the chapter includes the characteristic design and operating parameters as well as testing procedures applied.

Data analysis and results and discussions are presented in Chapter 5. The first part of the chapter depicts the results obtained from a smaller rig, its merits and shortcomings are highlighted, which forms the basis of the modification of test rig and geometry of the hydrocyclone. The results obtained from the modified test rig with improved geometries is dealt with in the second part, which is followed by discussions concentrating mainly on the performance of hydrocyclones.

Chapter 6 compares the performance of hydrocyclones with that of conventional settling basins. A case study of Jhimruk Hydropower Plant is presented. Suggestions, including the

application of hydrocyclones are made to minimize the excessive wear and tear in the plant.

Finally, conclusions are drawn in Chapter 7. The recommendations for application as well as further study and proposed measures to minimize abrasive erosion in hydropower plants are also presented.

2   SEPARATION OF SOLID PARTICLES FROM FLUID

The problems of separating solid particles according to their physical properties has arisen on a large scale in the mining industries, where it is necessary to separate valuable constituents in a mineral from the adhering material, usually of lower density. Therefore, many of the methods of separation and types of equipment have been developed for using in mining and metallurgical industries (Coulson et al., 1991). This method of separating mixtures of solid particles (minerals) into two or more products on the basis of the velocity with which the grains fall through a fluid medium is commonly known as classification (Wills, 1985). And water is the commonly used fluid for such purpose.

The separation depends on the selection of a process in which the behavior of the material is highly influenced by their physical properties. Generally, large particles are separated into size fractions by means of screens, and small particles, which would clog the fine apertures of the screen are separated in a fluid (Coulson et al., 1991).

2.1   Basic Principles of Particles Separation

The separation of solid particles from a fluid is highly influenced by the physical properties of particles as well as fluid and the flow characteristics. If the particles are separated using gravitational acceleration, then the particle terminal fall velocity (or simply the fall velocity) is the most important parameter. On the other hand, if the separation takes place using centrifugal acceleration, then magnitude of centrifugal acceleration as well as density difference between the particles and fluid (ρ_s -ρ) play a dominant role.

2.1.1   Fall Velocity of a Particle

A solid body immersed in a fluid is subjected to a buoyant force. In a flowing fluid (or if the particle is falling in a quiescent fluid), there is an additional resisting force resulting due to the skin friction (or viscous drag) and the form drag (due to the pressure distribution). According to Newton, this drag force can be expressed in terms of a drag coefficient, C_D, stagnation pressure $\rho V^2/2$ and area of the solid surface, A which provides resistance. And, mathematically,

$$F_D = C_D \rho A V^2 / 2 \hspace{4cm} \text{Eq. 2-1}$$

If the particle is falling in a quiescent liquid, ($V = \omega$), force balance between buoyant weight of the particle and the drag forces results in fall velocity of particle, ω. With the submerged weight of a spherical particle of diameter, d as

$$W_s = \frac{1}{6}\pi d^3(\rho_s - \rho)g$$

<div align="right">Eq. 2-2</div>

the fall velocity is given by the relation

$$\omega = \left(\frac{4}{3}\frac{gd^3}{C_D}\frac{\rho_s - \rho}{\rho}\right)^{1/2}$$

<div align="right">Eq. 2-3</div>

While the submerged weight of the particles remains constant, the drag force varies considerably, as the drag coefficient is highly dependent on flow parameter, and primarily on particle Reynolds number, $R_e{}^{'}$ (Rouse,1937). Since the drag coefficient highly varies with the state of the flow and has a non linear character, deducing a general relation solving basic flow equations is almost an impossible task. Therefore, various investigators have made effort to establish this relation experimentally as well as empirically. Among others, Rouse (1937), Vanoni (1975), Simons and Senturk (1977), Yang (1996), Coulson et al. (1995) and Garde and Ranga Raju (2000) have reviewed the works of previous researchers. The most prominent and the earliest work in this field was due to Stokes, who was able to solve the Navier-Stokes equations, for the case of creeping flow (Re < 1) of velocity, V, relative to the particle of diameter, d, and to define the drag force, F_D, which is described as

$$F_D = 3\pi\mu dV$$

<div align="right">Eq. 2-4</div>

where μ is the fluid viscosity and skin friction constitutes two-thirds of the total drag.

If the particle is falling in a quiescent liquid, ($V = \omega$), then the fall velocity of the particle is given by the following relation

$$\omega = \frac{d^2(\rho_s - \rho)g}{18\mu}$$

<div align="right">Eq. 2-5</div>

And, when the applied force is due to centrifugal acceleration and assuming that Stokes' law is still valid the particle fall velocity, can be described by the following relation

$$\omega = \frac{d^2(\rho_s - \rho)}{18\mu}\frac{V_t^2}{r}$$

<div align="right">Eq. 2-6</div>

with V_t and r being the tangential velocity and radius of rotation. Along with the size and density of the particles, the inertial forces, the shape of the particles and the temperature of the fluid influence the fall velocity.

2.1.2 Acceleration of Particles in a Gravitational Field

The behavior of a particle undergoing acceleration or retardation has been the subject of a very large number of investigations. Among others, Torobin and Gauvin (1959) have critically reviewed these investigations. The results of different investigators are not consistent, however, it has been shown that the drag factor is dependent not only on Reynolds number, but also the distance traveled by the particle since the initiation of motion (Coulson et al.,1992).

To consider the acceleration of particle in a simplistic approach, additional mass of fluid can be considered (Mironer, 1979). For a spherical particle, this added or hydrodynamic mass is equal to one half of that of the sphere. Total mass, m' thus becomes,

$$m' = \frac{\pi}{6}d^3\rho_s + \frac{\pi}{12}d^3\rho = m(1 + \frac{\rho}{2\rho_s})$$

Eq. 2-7

Considering the motion of a particle of mass in the earth's gravitational field, with a velocity, V (Fig. 2.1), the equation of motion in x and y direction can be written as follows (Coulson et al., 1995):
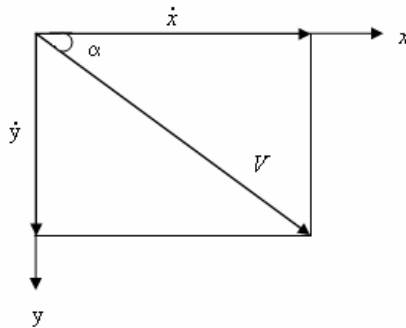
Fig. 2.1   Motion of particle in a two-dimensional field

$$m\ddot{x} = -\frac{R'}{\rho V^2}\rho A'\dot{x}\sqrt{\dot{x}^2 + \dot{y}^2}$$

Eq. 2-8

and

$$m\ddot{y} = -\frac{R'}{\rho V^2}\rho A'\dot{y}\sqrt{\dot{x}^2 + \dot{y}^2} + mg(1 - \frac{\rho}{\rho_s})$$

Eq. 2-9

where, $\dot{x}\dot{y}$ and $\ddot{x}\,\ddot{y}$ are first order and second order derivatives of the displacement in x and y directions with respect to time; $R'=F/A'$, the drag force per unit area.

If the added mass is to be considered, then m should be substituted with m'. Then

$$\ddot{x} = -\frac{R'}{\rho V^2} \frac{3}{d} \frac{\rho}{(2\rho_s + \rho)} \dot{x}\sqrt{\dot{x}^2 + \dot{y}^2}$$

Eq. 2-10

$$\ddot{y} = \pm\frac{R'}{\rho V^2} \frac{3}{d} \frac{\rho}{(2\rho_s + \rho)} \dot{y}\sqrt{\dot{x}^2 + \dot{y}^2} + \frac{2g(\rho_s - \rho)}{(2\rho_s + \rho)}$$

Eq. 2-11

where the minus and plus signs in equations 2.10 and 2.11 is applicable for downward and upward motions respectively. As these equations are coupled with $\dot{x}$ and $\dot{y}$ appearing in each of the equations, general solutions is possible only in the Stokes range. Further, since the velocity of the particles and the fluid inside the hydrocyclone is almost same, Stoke's law applies with reasonable accuracy to separations in cyclones of conventional design (Wills, 1985; Coulson et al., 1991).

2.1.3 *Motion of a Sphere in the Stokes Range*

In Stokes range,

$$\frac{R'}{\rho V^2} = \frac{12}{R'_e} = \frac{12\mu}{d\rho\sqrt{\dot{x}^2 + \dot{y}^2}}$$

Eq. 2-12

With substitution of this relationship to Eq. 2.10 and 2.11 and further simplification

$$\ddot{x} = \frac{18\mu}{d^2\rho_s}\dot{x} = -a\dot{x}$$

Eq. 2-13

And considering added mass

$$\ddot{x} = \frac{36\mu}{d^2(2\rho_s + \rho)}x = -a'\dot{x}$$

Eq. 2-14

Similarly,

$$\ddot{y} = -\frac{18\mu}{d^2\rho_s}\dot{y} + g(1 - \frac{\rho}{\rho_s}) = -a\dot{y} + b$$

Eq. 2-15

And considering added mass

$$\ddot{y} = -\frac{36\mu}{d^2(2\rho_s + \rho)}\dot{y} + \frac{2g(2\rho_s - \rho)}{2\rho_s + \rho} = -a'y' + b'$$

Eq. 2-16

Integration of these equations, ignoring added mass with suitable boundary conditions and $\dot{y} = V$, leads to

$$y = \frac{b}{a}t + \frac{V}{a} - \frac{b}{a^2} + (\frac{b}{a^2} - \frac{V}{a})e^{-at}$$

Eq. 2-17

$$x = \frac{V_{x_0}}{a}(1 - e^{-at})$$

Eq. 2-18

with V_{x0} as initial velocity component in x direction

$$a = \frac{18\mu}{d^2\rho_s} ; \quad b = (1 - \frac{\rho}{\rho_s})g ; \quad \frac{b}{a} = \omega_0$$

Eq. 2-19

Then the time required for displacement, x is

$$t = -\frac{1}{a}\ln(1 - \frac{ax}{V_{x0}})$$

Eq. 2-20

2.1.4 Acceleration of particles in a Centrifugal Field

In most practical cases, where a particle moves in a fluid under the action of a centrifugal field, gravitational effects are comparatively small and can be neglected. The equation of motion for particles in this case can be derived replacing g by $\omega^2 r$, where r is the radius of rotation and ω is the angular velocity.

If the velocity of the fluid with respect to the particles is quite small and the flow is streamlined, the equation of motion for Stokes range can be written as

$$\frac{\pi}{6}d^3(\rho_s - \rho)\omega^2 r - 3\pi\mu d\frac{dr}{dt} = \frac{\pi}{6}d^3\rho_s\frac{d^2r}{dt^2}$$

Eq. 2-21

As the particle moves outwards, the accelerating force increases and therefore, it never acquires an equilibrium velocity in the fluid. If the inertial terms on the right hand side of Eq. 2.21 is neglected

$$\frac{dr}{dt} = \frac{d^2(\rho_s - \rho)\omega^2 r}{18\mu} = \frac{gd^2(\rho_s - \rho)}{18\mu}\frac{\omega^2 r}{g} = \omega_0\frac{\omega^2 r}{g}$$

Eq. 2-22

Therefore, instantaneous velocity dr/dt is equal to the terminal fall velocity ω_0 in the gravitational field, increased by $\omega^2 r/g$.

Returning to the exact form of Eq. 2.23,

$$\frac{d^2r}{dt^2} + \frac{18\mu}{d^2\rho_s}\frac{dr}{dt} - \frac{(\rho_s - \rho)}{\rho_s}\omega^2 r = 0$$

Eq. 2-23

or

$$\frac{d^2r}{dt^2} + a\frac{dr}{dt} - nr = 0$$

Eq. 2-24

The solution of above equation leads to the form (Coulson et al. 1995)

$$r = B_1 e^{-\left[a/2 + \sqrt{a^2/4 + n}\right]t} + B_2 e^{-\left[a/2 - \sqrt{a^2/4 + n}\right]t}$$

Eq. 2-25

or, $r = e^{-at/2}\{B_1 e^{-kt} + B_2 e^{kt}\}$

Eq. 2-26

where, $a = \dfrac{18\mu}{d^2\rho_s}$, $\qquad n = (1-\dfrac{\rho}{\rho_s})\omega^2 r$, $k = \sqrt{a^2/4 + n}$ **Eq. 2-27**

The effects of added mass, which have not been taken into account in the above equations, require the replacement of a by a' and n by n'

where, $a = \dfrac{36\mu}{d^2(2\rho_s + \rho)}$ and $n' = \dfrac{2(\rho_s - \rho)}{2\rho_s + \rho}\omega^2$ **Eq. 2-28**

Applying boundary conditions the solution of Eq. 2.26 leads to

$$\frac{r}{r_1} = e^{-at/2}\left\{\cosh kt + \frac{a}{2k}\sinh kt\right\}$$ **Eq. 2-29**

Time of Settling

If the effects of particle acceleration can be neglected, the Eq. 2.24 simplifies to

$$a\frac{dr}{dt} - nr = 0$$ **Eq. 2-30**

And the direct integration of the Eq. 2-30 leads to

$$\ln\frac{r}{r_1} = \frac{n}{a}t = \frac{d^2(\rho_s - \rho)\omega^2}{18\mu}t$$ **Eq. 2-31**

Thus the time taken for a particle to move to a radius r from an initial radius r_0 is given by

$$t = \frac{18\mu}{d^2\omega^2(\rho_s - \rho)}\ln\frac{r}{r_0}$$ **Eq. 2-32**

2.2 Methods of Particles Separation in Industries

The choice of methods of particles separation in a fluid is attributed mainly to the inherent physical characteristics of the particles to be separated. Scope and purpose of the separation also often plays a decisive role. However, overall economy of the whole process has been accepted as the major criterion for selection of a particular method.

Based on principles applied for separation, Svarovsky (1977, 2000) divided the methods of particles separation into two main groups (Fig. 2.2). In the first group of separation, the liquid is constrained in a stationary or rotating vessel, where the particles move freely within the liquid. Here the separation takes place due to mass forces acting on the particles because of an external or internal field of acceleration that might be the gravity, centrifugal or magnetic field. Difference in densities between the fluid and the particles plays major role (except for floatation) in the separation of gravity and centrifugal fields. Here, continuous operation of equipment can be realized, which often results in a cheaper solution than filtration. Therefore,

the gravity sedimentation and floatation is usually looked as possible alternatives in the early stage of equipment selection (Svarovsky,2000).
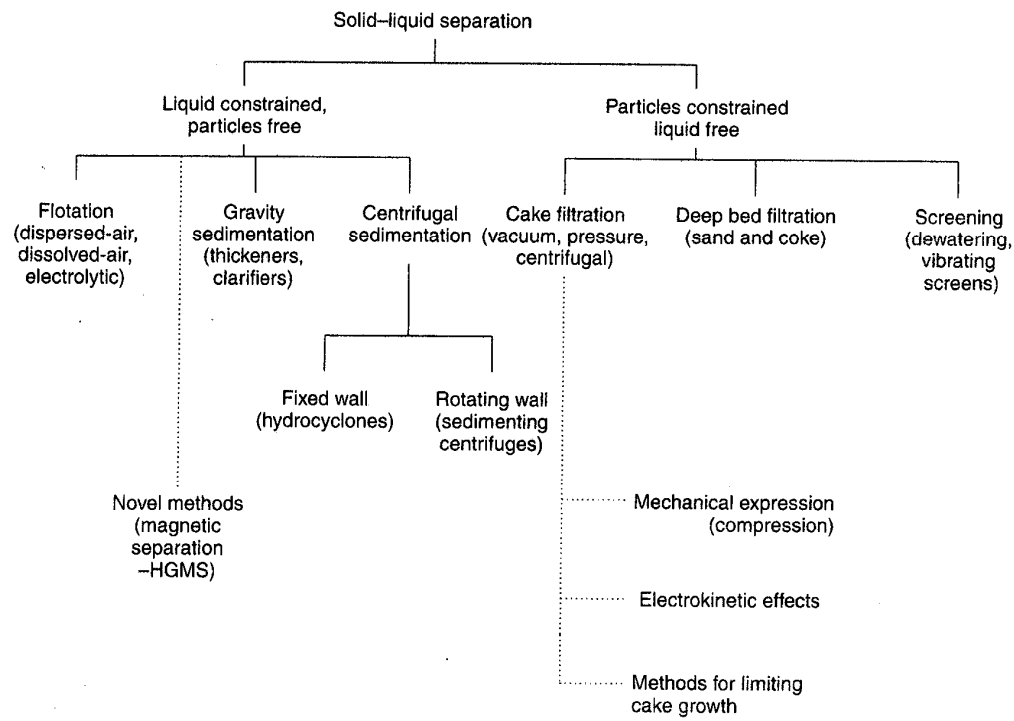
Fig. 2.2 Classification of solid-liquid separation processes (Svarovky, 2000)

In the second group, which is often called filtration, particles are constrained by a medium through which liquid is allowed to flow freely. Here, density difference between the fluid and particles is not required for particles separation. Nevertheless, a truly continuous operation is usually not possible to achieve, which results in often a much higher cost compared to sedimentation and floatation.

While the particles are usually separated being constrained or free in the fluid, conventionally, they can be classified using one of the next methods: floatation, sedimentation, filtration and screening (Fig.2.2). Pretreatment of fine suspensions, for example, coagulation and flocculation is sometimes applied to enhance the separation procedure. Coagulation brings particles into contact to form agglomerates by the addition of inorganic chemicals such as hydrolysis coagulants like alum or ferric salts or lime. Similarly, flocculation uses flocculating agents, usually in the form of natural or synthetic polyelectrolyte of high molecular weight, which interconnect and enmesh the colloidal particles into giant flocs up to 10 mm in size. Basic processes applied and the equipment used in the solid liquid separation are briefly discussed below.

2.2.1 Floatation

Floatation is a kind of gravity separation process based on the attachment of air or gas bubbles to solid particles, which are then carried to the liquid surface, where they accumulate as a float and can be skimmed off. The process consists of two stages: the production of small bubbles in the first stage and their attachment to the particles in the second stage. Depending upon the method of bubble production, floatation is classified as dispersed air, dissolved air or electrolytic type (Svarovsky, 2000).

Floatation can be applied to fine suspensions. It offers a viable alternative to gravity sedimentation as it can operate at much higher overflow rates and use smaller, more compact equipment of lower capital cost. The typical overflow rate (hydraulic loading) per unit plan area of the floatation cell is 1.5-17 meters per hour (Svarovsky, 2000). Most industrial applications of dissolved air floatation are in pulp and paper industries, refineries and waste water treatment, where the particles might often be oily by nature.

2.2.2 Magnetic Separation

Magnetic separation is used to remove ferromagnetic particles from a suspension. In mineral processing, permanent magnets have been used for removing tramp iron and for concentrating magnetic ores. Continuous magnetic separators such as the drum separators are widely used for beneficiation of ores and recycling of magnetic or ferrosilicon from the heavy madia pulps used for coal washing, or in water treatment (Svarovsky, 2000).

Much stronger magnetic fields and gradients can be produced by the high gradient magnetic separators (HGMS). They can be used for separation of very fine and weakly paramagnetic particles on a large scale. The main advantage of HGMS is their high efficiency of separation even at relatively high flow rates and minimum pressure drops across the filter. As the capital cost is very high, only the large installations are viable.

2.2.3 Gravity Sedimentation

The gravity sedimentation utilizes density difference between the solid particles and the fluid medium. The available gravity sedimentation equipment can be divided into batch operated settling tanks and continuously operated classifiers. The batch operated settling tanks are used where relatively small quantity of liquid is to be treated. The bulk of the processing by gravity sedimentation, however is carried out in continuously operated classifiers. The classifiers are

further divided into thickeners and clarifiers (Svarovsky 1977, 2000). If the primary purpose is to produce solids in a highly concentrated slurry, then the process is called thickening and the equipment is known as the gravity thickener. Whereas, if the purpose is to have relatively clean overflow, then the equipment used is known as clarifier. The feed to a thickener is usually more concentrated than that to a clarifier. Classifier types vary with the application. However, based on the principles of operation they can be divided into the following four sub groups (Fig. 2.3): settling tank, cylindrical tank classifier, Cone type classifier and mechanical classifier (Kelly and Spottiswood, 1982; Coulson et al., 1991; Wills, 1985).

(a)

(b)

$I = Inflow; O_{(-)} = Overflow; O_{(+)} = Underflow$

(c)

(d)
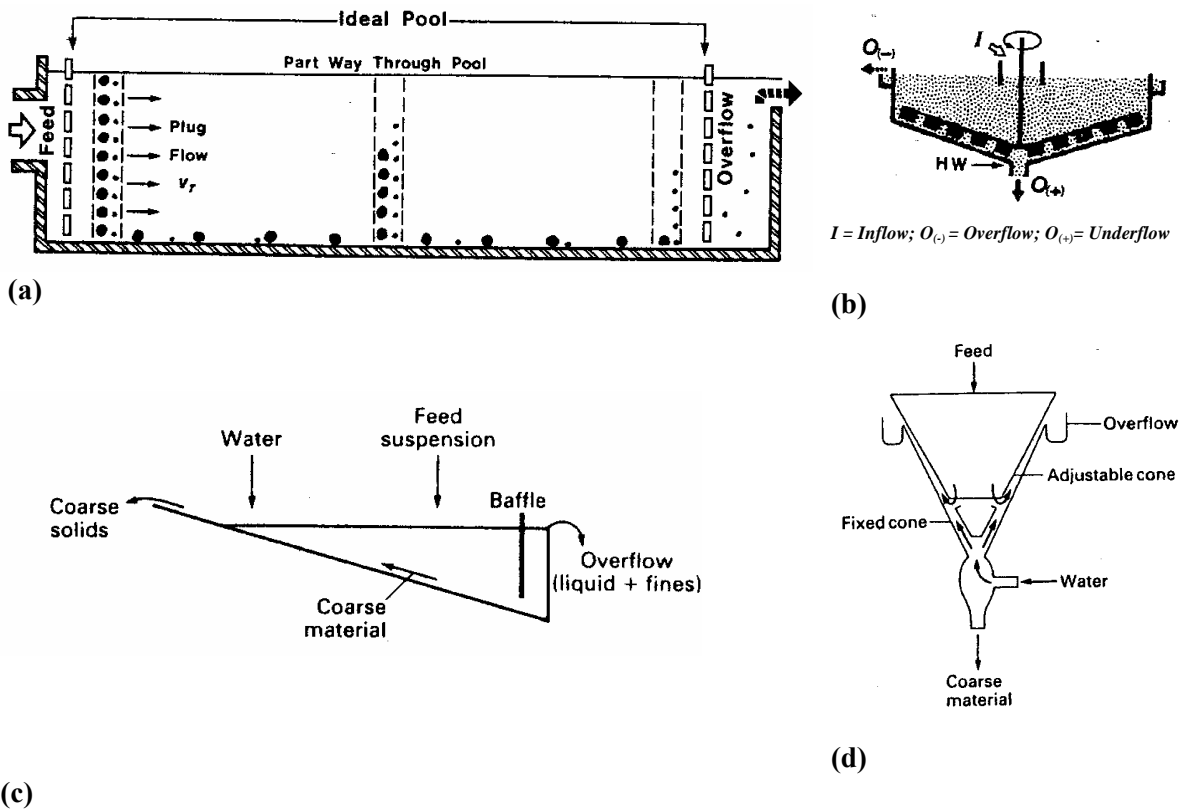
Fig. 2.3 Basic principles of operation of different gravity sedimentation classifier: (a) Settling tank by Finch(1962) (b) Cylindrical Tank classifier (c) Mechanical classifier (d) Cone classifier (Source: (a) and (b) Kelly and Spottiswood,1982; (c) and (d) Coulson et al., 1992)

2.2.4 Centrifugal Sedimentation

The devices in this category classify the feed utilizing centrifugal force to accelerate the settling rate of particles. There are two main groups of equipment in this category. The first group of equipment having fixed wall is known as hydrocyclone (Fig. 2.4.a), whereas the second one having rotating wall is called centrifuge (Fig. 2.4.b).
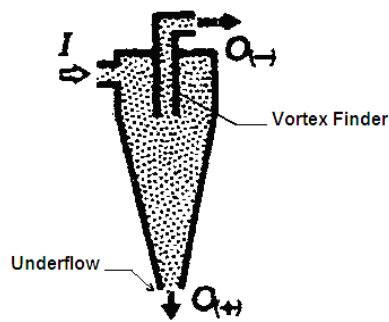
I = Inflow; $O_{(-)}$ = Overflow; $O_{(+)}$= Underflow

(a)
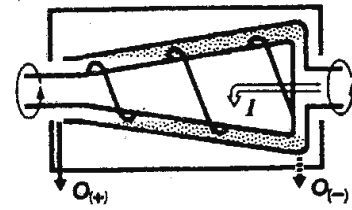
I = Inflow; $O_{(-)}$ = Overflow; $O_{(+)}$= Underflow

(b)

Fig. 2.4 Basic operating principles of operation of centrifugal sedimentation classifier: (a) Hydrocyclone (b) Bowl type centrifuge (Source: Kelly and Spottiswood,1982)

2.2.4.1   Hydrocyclone

This is a continuously operating classifying device that utilizes centrifugal force to accelerate the settling rate of particles. Its main use in mineral processing is as a classifier, which has proved extremely efficient to separate fine particles. It has been successfully used for classification, de-sliming, de-gritting, thickening and washing of fine coal (Wills, 1985).

A typical hydrocyclone consists of a conically shaped vessel, open at its apex (underflow), joined to a cylindrical section, which has a tangential feed inlet (Fig. 2.4.a). The top of the cylindrical section is closed with a plate through which passes an overflow pipe. The overflow pipe is extended into the body of the cyclone, known as vortex finder, which prevents short-circuiting of feed directly to the overflow.

The raw feed is introduced under pressure through the tangential entry, which imparts a swirling motion to the flow. This generates a vortex in the cyclone, with a low pressure zone along the vertical axis. An air core develops along the axis, normally connected to the atmosphere through the apex opening.

The classical theory of hydrocyclone actions is that particles within the flow pattern are subjected to two opposing forces- an outward centrifugal force and inwardly acting drag. The centrifugal force developed accelerates the settling rate of the particles, thereby separating particles according to size and specific gravity. Faster settling particles move to the wall of the cyclone, where the velocity is lowest, and migrate to the apex opening. Due to the action of

2-10

the drag force, the slower settling particles move towards the zone of low pressure along the axis and carried upward through the vortex-finder to the overflow (Wills,1985).

The diameter of individual cyclone ranges 10 mm to 2.5 m. Flow rate of such unit ranges from 0.1 m^3/hr to 7200 m^3/hr. The operating pressure drop varies from 3.4 m to 60 m with smaller units usually operated at higher pressure than the larger ones (Svarovsky, 2000).

Hydrocyclones can be used to classify the particles from 5µm to 300 µm with high efficiency of fine particles. These device can handle feed and underflow concentrations (V/V) up to 35% and 50% respectively (Kelly and Spottiswood, 1982). In contrast to sedimentation centrifuge, hydrocyclones do not have any rotating parts. Because of the simplicity, high efficiency with continuous operating feature, these devices are cheaper than other classifiers. Therefore, they are recognized as one of the most important devices used in mineral industries (Wills, 1985; Kelly and Spottiswood, 1982).

2.2.4.2   Centrifuges

In a centrifuge, the suspension is fed into a imperforated bowl, which rotates at high speed together with the feed (Fig. 2.4.b). The liquid is removed through a skimming tube or over a weir while the solid particles either remain in the bowl or are intermittently (or continuously) discharged from the bowl. Depending upon the design of the bowl and solid collection mechanism, they are further classified to tabular, multi-chamber, imperforate basket, scroll type and disc centrifuges (Svarovsky, 2000).

Most of the centrifuges are capable of producing cut size well into the sub-micron region. They are widely used in chemical industry, coal processing industries and other mineral processing applications. They are also often used in dewatering of coarse solids. Although they are quite efficient in separation, in solid-liquid separation, centrifuges are often compared with the Rolls-Royces in the car industry: they perform well but the capital and running costs are very high.

2.2.5   Filtration

The method of filtration can be divided into two broad groups; cake filtration and deep bed filtration. In cake filtration the solids are deposited in the form of cake by passing suspension through a permeable, relatively thin medium. As soon as the first layer of cake is formed, the subsequent filtration takes place on top of this cake and the medium provides only a

2-11

supporting function. Depending upon the pressure drop required, surface filters are classified into vacuum, pressure and centrifugal filters.

On the other hand, in deep bed filtration, the suspension passes through a deep filter medium having pore size much greater than the particles meant to remove. No cake should form on the face of the medium but particles penetrate into the medium where they separate due to gravity settling, diffusion and inertial forces. Attachment to the medium, is due to molecular and electrostatic forces (Svarovsky, 1977). Sand and gravel are the most common media. When the bed is full of solids, the flow is interrupted and backwashed from the bed. Deep bed filtration were originally developed for drinking water treatment. They are also increasingly applied in industrial waste water treatment.

Despite the perfect separation of solids in filtration, the filtration units require large floor areas. Therefore their capital cost is very high. Mechanical power is applied in surface filtration. Flow rate is relatively low. Continuous process is expensive to achieve.

2.2.6   Screening

Screening is an operation by which particles are introduced to a screen of a given aperture size and thus have an opportunity of either passing through if they are smaller than the apertures, or being retained on the screen if they are larger (Svarovsky, 2000). The bulk of the screens in industry are used for size grading but they have been also used in dewatering function, often combined with washing.

2.2.7   Selection of Equipment for Particles Separation

A wide range of equipment for particles separation is given in Perry and Chilton (1973). Llyod and Ward (1975) developed a very informative diagram, which schematically shows the range of solid liquid separation equipment based on particle size range (Fig.2.5). The spectrum of particle size together with the position of the common material as well as the broad range of application of membrane separation, filtration and screening processes due to Osmonics, Inc. (1984) is also helpful in selecting proper device. The grade efficiency curves of various types of equipment (Fig. 2.6) working under floatation and sedimentation processes also gives valuable information in selecting the type of equipment (Svarovsky, 2000).
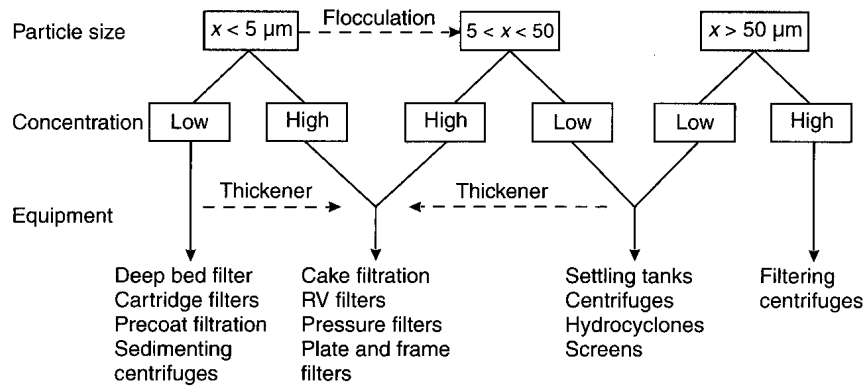
Fig. 2.5 Relation between particle size and type of equipment to be used for separation (Source: Llyod and Ward, 1975)
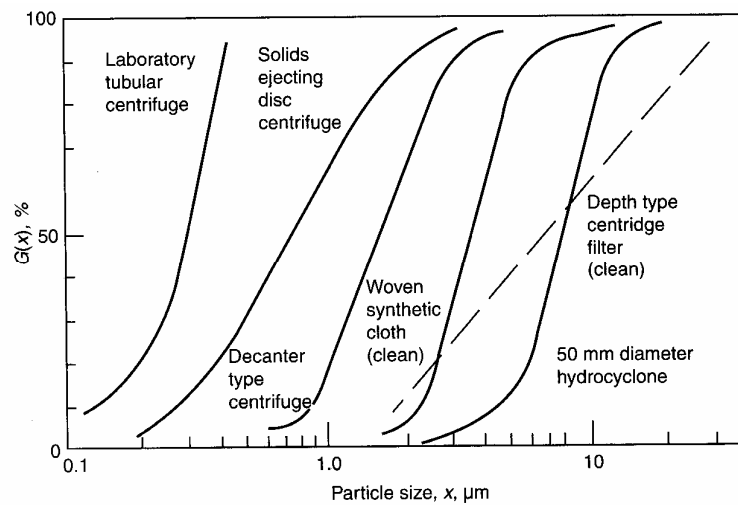
Fig. 2.6 Grade Efficiency Curves of various types of equipment (Source: Svarovsky, 2000)

Kelly and Spottiswood (1982) have reviewed the types of equipment used in this field and presented more common types of equipment with illustrations. Introducing each equipment type, the authors have presented range of data pertaining to size of the equipment, feed characteristics (size, rate, concentration), power requirement as well as the discussion on their suitability and applications.

2.3 Suspended Sediment Removal Practices in Water Sector Projects

While the separation of most of the solid particles is desirable in most of the processing industries, the removal of only the coarser particles is of greater concern in water sector projects, such as hydropower and irrigation. The coarse particles in hydropower projects cause enormous wear and tear in hydro mechanical equipment and accessories. The deposition of sediment along the conveyance causes conveyance loss. The transport of sand particles as well

2-13

as coarse silt particles to farm land drastically reduce the fertility of the land. The terminology 'sediment removal' as against 'separation of solid particles' is commonly adopted in water sector projects. Hence, the same is used in ensuing sub-chapters. The approach to sediment removal in storage projects is much different from that applied in RoR projects. The present study attempts to address the issues of RoR projects only.

One of the earliest studies carried out on sediment control measures in water projects is due to Lane (1953), who suggested one or several methods (devices) to remove sediment from flowing water: (i) slot, (ii) step, (iii) settling basin,(iv) deflecting vanes (v) skimming weir (vi) drawing off of slow-moving currents,(vii) separation of top and bottom water, (viii) curved vanes, (ix) sluices, (x) still pond, and (xi) grillage (bottom rack). However, most of the devices except for settling basins are applicable for excluding bed load at river headworks and intake.

Vanoni (1975), Garde and Ranga Raju (2000) have reviewed the methods of sediment control in canals, especially in irrigation project. The latter also reviewed most of the relations developed earlier for trapping efficiency estimation and recommended more refined relations. On the other hand, Mosonyi, 1991 has reviewed sediment control works carried out mostly on hydropower projects.

Sediment removal in water projects is carried out in two stages (Vanoni, 1975; Avery, 1989; Garde and Ranga Raju, 2000): bed load and heavily concentrated bottom layer is separated using excluders at intake (headworks), whereas the suspended sediment load is removed using mostly the ejectors in large irrigation projects but settling basins in hydropower projects.

2.3.1 *Sediment Extraction from Diverted Flow*

The structures used to remove bed load from the river water at headworks are of little value in the removal of suspended sediment particles. Because of the fragile and rugged nature of Himalayan catchment, a considerable amount of sediment load (up to 85%) in normal flood is transported in suspended mode (SMEC, 1989; Galay, 2003). Because of the velocity and resulting turbulence in the flow at headworks most of the suspended load enters into the off-taking conveyance. And, in most of the cases, this excess sediment has to be removed. Conventionally, the devices used for such purpose are called ejectors (Garde and Ranga Raju, 2000). The ejectors in common use are as follows:

2.3.1.1 Conventional Gravity Setting Basins

Setting basins are most common type of ejector used in water projects. It consists of an enlarged section of the conveyance or other arrangement in which the velocity is low enough to permit the suspended particles to settle out. They are designed to trap particles which cause undesirable consequences in water projects. As the hydro-mechanical equipment and accessories are usually subjected to very high velocity, the plants subjected to the hardest and abrasive particles such as quartz and feldspar suffer severe wear and tear. Unfortunately, quartz particles predominate the sediment of most of the Himalayan rivers (Thapa,2004).

a) Design of Settling Basins

Setting basins are designed in such a way that the criteria for trapping certain particles size are met stringently and flushing of settled particles is carried out effectively. For a setting basin to perform well, there are two important conditions: proper shaping, sizing, and the efficient flushing of trapped sediment particles.

As the quartz particles cause enormous damage to the hydro-mechanical equipment and accessories and are chiefly available in most of the rivers, the physical properties of quartz particles are therefore normally used as a reference for designing a setting basin (Stole, 1993). And, it is the fall velocity of these quartz particles to be excluded, that governs the settling basin design. The trapping of reference particle sizes with desired efficiency is the most important parameter governing the sizing of a settling basin.

b) What Particle Size to Exclude?

Stole (1993) suggests to exclude most particles larger than 150-300 micron to minimize costs related to turbine wear and generation losses. However, as the severity increases with the increase of head, the removal of particles should be done accordingly. Mosonyi,1991 suggests removal of quartz particles larger than 250 micron in medium head plants (15 m < H< 50 m) and 100-200 micron at high head plants (50 < H< 250m). *"Undue wear of mechanical equipment installed at plants operating under very high heads of several hundred meters, may sometimes be prevented only by removing particles of size as small as 10- 50 micron"* the author further mentions.

The experience with a high-head (650 m) Khimti hydropower plant in eastern Nepal emphasizes the compliance of Mosonyi's criteria in the Himalayan region. Despite trapping

2-15

97% of quartz particles larger than 200 micron and 85% of quartz particles larger than 130 micron, the plant suffers considerable loss due to wear and tear (Deshar, 2007).

Equipped with three Francis turbines, Marsyandi Hydropower plant in central Nepal generates 69 MW of power utilizing a net head of 95 m. 400 m long, 75 m wide setting basin having a transit velocity of 0.16 m/sec traps most of the particles larger than 50 micron (Mosonyi, 1991; Kayastha and Regmi, 1991; Kayastha, 1992). Nevertheless, the turbine and accessories, which are inspected every third year suffer considerable wear and tear. Abrasion as high as 40 mm was observed in turbine guide vanes, whereas the turbines and accessories were subjected to maximum concentration of 6,000 ppm of sediment load (Kayastha, 1992).

Six Francis turbines installed at Nathpa Jhankri Hydropower Plant in India utilize 425 m head to generate 1500 MW of power. Although settling basins were designed to exclude 98% quartz particles larger than 200 micron, turbines and accessories suffered from the first year of operation. Sediment load as high as 20,000 ppm was recorded. (Chopra and Arya, 1996).

Three Francis turbines and accessories installed in Jhiruk Hydropower Project in Western Nepal suffer massive damage each year despite settling basins trap most of the particles larger than 200 micron. Observation of sediment concentration and efficiency revealed that the efficiency loss of the units after operating for just 71 days (Sept 1, 2003 - Nov 11, 2003) under mild sediment load has been recorded at 4 percent at best efficiency point and 8 percent at 25 percent load (Fig. 2.7, Hydro Lab, 2003).
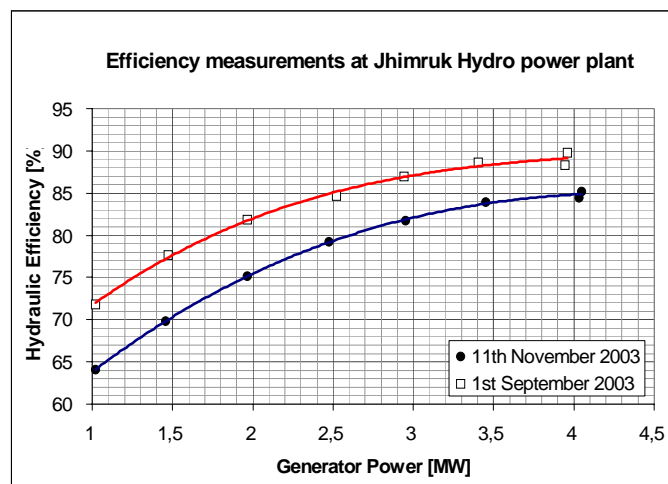
Fig. 2.7 Hydraulic efficiency of the turbine of Jhimruk Hydropower Plant before and after the operation for 71 days (Hydro Lab, 2003)

Two Turgo turbines, installed at Piluwa Hydropower Project located in Eastern Nepal generate 3 MW of power utilizing a gross head of 113 m and a flow of 3.5 m^3/s. Although the Turgo units have been considered to be much better than Francis in terms of sediment induced erosion resistance, they were out of order after working for three monsoon seasons. The settling basins have been designed to trap most of the particles larger than 200 micron.

Despite the removal of most of the sediment particles larger than 200 micron, the buckets, needles and nozzle liners of four Pelton turbines installed at Chukha Hydropower Plant in the Wangchhu River, Bhutan, working under a head of 428 m, and each generating 84 m have been severely damaged (Chandra and Sinha, 1996).

The settling basin in Maneri Stage I hydropower plant in the Bhagirathi river in India is quite small, which was designed to fully trap particles larger than 600 micron. As a result, three Francis turbines and accessories subjected to a head of 147.5 m to generate 90 MW of power suffered substantial damage from the early stage of operation. As a precaution measure, the power plant is shut down, once the sediment concentration exceeds 2000 ppm, which results in a revenue loss of 40% during monsoon months (Chandra and Sinha, 1996; Nagpal and Tyagi, 1996).

Four Kaplan turbines installed in Chilla Hydropower plant in the Ganga River subjected to a head of mere 32.5 m and generating 144 MW of power have been damaged due to sediment induced wear and tear. Silt ejector has been used to control the sediment. The PSD analysis of the samples collected from the powerhouse revealed that 98% particles larger than 530 micron were excluded, whereas 63% particles entering the machine peripherals were smaller than 149 micron (Chandra and Sinha, 1996).

Sediment related damage on intake; conveyance and power house equipment have been found to be very much alarming in other parts of the world as well. Mosonyi, 1991 refers to a case where abrasion caused by sharp-edged coarse sediment resulted annually in a wear of 6 to 7 mm of the buckets of a Pelton wheel. The author further reports some of the remarkable examples as follows. The buckets of the Pelton wheels in the Parenthen plant, III River, Austria, operating under a head of 800 m showed signs of extensive wear after a brief operating period. The efficiency of a turbine operating under a relatively low head (42 m)

suffered, owing to tear, a loss of 13 percent at full load, and effective output dropped to zero at a wheel discharge of 25 per cent. The turbines of the Florida Alta Plant in Chile operating under a head of 95 m were completely worn after the operation of 200 hours.

Severe erosion followed by cavitation have been observed in a high head (920 m) Pelton turbine subject to a flow containing 77 % sediment particles finer than 63 micron and 99 % particles finer than 125 micron shortly after 600 hours of operation (Brekke et al., 2002).

These evidences show that the velocity with which the particles strike the surface as well as the sediment characteristics (mainly the mineral content, size and load) are detrimental to hydro-mechanical equipment and accessories. The erosion rate of steel subjected to a flow containing quartz particles was found to be proportional to sediment load and velocity of the flow to a power of 3 to 4 (Lysne, et al.,2003, Bajracharya, 2007). Biswakarma (2008) also found erosion in hydro-mechanical equipment to be directly related to sediment load. Therefore, the settling basins of hydropower plants have to trap much finer particles compared to those in other projects such as irrigation.

c) Proper Sizing of Settling Basin

The settling basins as well as hydro mechanical equipment and accessories constitute major cost components in a hydropower plant. Increased trapping of finer particles usually reduces direct cost related to wear and tear as well as the revenue loss due to decreased efficiency, while adding the capital cost on civil works. Whereas, saving the cost of settling basin, allowing more sediment to pass to powerhouse highly increases the operation cost of turbines and accessories including the revenue loss due to decreased efficiency. Therefore, it is often a trade off between sediment trapping versus wear and tear of turbine and accessories. And, such an analysis should be performed in order to decide reference particles size to trap and degree of removal desired.

Settling conditions in any sedimentation basin are achieved by decreasing the transit velocity of water so that the bed shear stress and turbulence is decreased. The transit velocity in the basin should be less than the critical velocity in order to avoid the particles once settled being picked up by the flow (Camp, 1946). At an early stage of planning a transit velocity of 0.2 m/sec is normally adopted (Lysne et al., 2003).

The sizing of the basin is mainly guided by the fall velocity of the particles to be excluded and the degree of removal (trapping) of sediment required. Mosonyi (1991), Garde and Ranga Raju (2000), Lysne et al. (2003) have reviewed the previous work on the design of a setting basin.

The most commonly used methods for estimating the dimension of the settling basin are particles approach and concentration approach. The effect of turbulence in particles approach can be considered using Camp's diagram (Camp,1946). With the advent of modern computers, modeling of flow and sediment is possible using computational fluid dynamics (CFD) approach (Olsen,1991). Good agreement has been found with the results obtained by physical model (Lysne et al., 1995). However, the numerical models have not yet found widespread application, because of their relative complexity and sometimes unknown calibration coefficients for the particular case under investigation (Schrimpf, 1991; Ranga Raju et al. 1999).

2.3.1.2 Split and Settle Concept

Invented by Stole (1997), Split and Settle is a relatively new concept to exclude sediment in water projects. The principle of Split and Settle is similar to the gravity settling basin, but it utilizes the concentration difference in any conveyance. The dirtiest water (bottom layer) from the parent conveyance is diverted to the settling conveyance while the relatively clean water (upper layer) continues to travel along the main conveyance, thereby requiring settling space only for part of the flow. This concept saves the cost of the settling basins, especially when they are arranged underground. A cost comparison was made for such an arrangement in Kaligandaki-A project in Nepal, which resulted in overall economy of 35% compared to conventional underground arrangement (Bajracharya, 1996).

2.3.2   Flushing of Deposits

The removal of sediment particles from settling basins is among the most difficult tasks to address in hydropower plants operating in Himalayan region (Stole,1993). There are principally two types of arrangements for this purpose:

2.3.2.1 Intermittent Flushing

The flushing of deposits in this mode is carried out shutting down the power plant either by conventional gravity flushing arrangement or manual/mechanical excavation. Kaligandaki-A, Marsyangdi ,Trisuli, Sunkoshi, Bhotekoshi hydropower plants in Nepal are equipped with

conventional gravity flushing arrangement. The settling basin of Sunsari Morang Irrigation Project in Nepal is equipped with two mechanical dredgers for removing the deposits. Although such arrangement is considered reliable from operational point of view, considerable revenue loss is incurred due to shutdown of the plants. For example, Marsyangdi Hydropower plant loses 3.53 GWh annually due to flushing (Stole, 1993). When the removal of deposits is carried out manually or by mechanical means, it usually involves a huge cost in addition to the complexity on mechanical equipment and power requirement. Furthermore, generation needs often overrule flushing requirement leading to the reduction of trapping capacity and increased wear and tear of hydro-mechanical equipment due to excess sediment load.

2.3.2.2 Continuous Flushing

Continuous or intermittent flushing mode is usually adopted in this arrangement keeping the plant in operation. As the space for sediment deposition is not required, such an arrangement usually results in a cheaper solution. Optimum quantity of flushing discharge also increases the trapping efficiency of basin (Ranga Raju et al.,1999). This type of basin arrangement is always preferred as flushing can be carried out as often as required. A swift velocity, close to the particles should be maintained to scour the deposits and transport them along with the flushing water without mixing with the main flow of the basin. This criterion, however, is not quite often realized in a continuous flushing mode equipped with conventional settling basin, leading to reduced trapping efficiency of the basin. Therefore, the following methods have been applied in hydropower projects operated in continuous flushing mode.

2.3.2.3 Hopper Type Basin

Intermittent sediment flushing is realized in a Hopper type basin. In spite of advantage of continuous operation thereby minimizing power losses, the hydraulics of the manifold, involving many valves and small sized pipes, is quite complex. Therefore, the operation is complex. The system may clog if it is applied at sites, where gravel enters the basin (WECS, 1987).

2.3.2.4 Bieri Desander

The Bieri desander concept, developed in Switzerland is better than the hopper type in terms of design, construction and operation features. The shutter mechanism installed in series at the bottom of the basin consisting of two plates and operated by servo motor facilitates flushing. The major drawback of the system include: the moving parts in exposed environment is

2-20

subjected to sediment wear, gravels and pebbles entered into the basin causes operational problems (Stole,1993).

2.3.2.5 Serpent Sediment Sluicing System (S4)

The major drawbacks of Hopper and Bieri desanders have been addressed in S4 (Stole,1993). Invented by Prof. Haakon Stole, the S4 system consists of a float unit (serpent), which covers a long continuous flushing channel at the bottom of the settling basin while the former is filled with water. Once the float unit is de-watered, it becomes buoyant, which facilitates flushing of deposited sediment by opening the flushing channel. The unit requires nominal amount of water (10 %), which is utilized only during flushing period. The advantage of S4 is simplicity and relatively inexpensive structure compared to Bieri and hopper systems (Stole, 1993). Satisfactory performance of S4 has been reported from several hydropower projects in Nepal.

2.3.2.6 Sediment Ejectors

Continuous flushing in large irrigation canals from alluvial streams have been usually carried out mostly by sediment ejectors/extractors. An ejector consists of a horizontal slab a little above the canal bed, which separates the sediment-laden bottom layers from the top layers. Under the slab (diaphragm) are tunnels, which carry these bottom layers into an escape channel. The velocity in the tunnel is kept about 3 m/s utilizing about 20-25 per cent of the canal discharge (Garde and Ranga Raju, 2000). Vittal and Rao (1994) have given a method of determination of the height of diaphragm wall and method of estimating reliable removal efficiency.

2.3.2.7 Vortex Tube

Vortex tube type of extractor is one of the very effective extracting devices, though its use is still limited. Vortex tube is an open tube placed across the canal bottom in which the flow enters tangentially. Due to the vortex motion, a high swirl is developed, which keeps the sediment in suspension. Due to the pressure difference at exit point, the sediment in suspension moves downstream to get flushed through the outlet. Considerable number of research work has been carried out at Hydraulics laboratory of Fort Collins (US) and Wallingford (UK) to develop ejectors based on the vortex flow. White (1981) and Atkinson (1990) have developed design guidelines for dimensioning and arranging such ejectors. Such an arrangement has been successfully implemented in Dera Gazi irrigation canal in Pakistan, which carries a flow of 417 m^3/s . Such an arrangement is able to eject 80% sediment coarser than 500 micron (Garde and Ranga Raju, 2000).Nevertheless, such a device works efficiently,

when a critical flow is maintained near the vortex tube, which is not possible to maintain always.

2.3.2.8 Vortex Settling Basins

Vortex settling is a relatively recent continuous flushing method, which utilizes centrifugal acceleration to separate sediment particles from the flow. In such devices, a higher velocity flow stream is introduced tangentially into a cylindrical body having an orifice at the center of its bottom. Materials that are denser than the carrier medium are flushed out through the bottom orifice continuously.

Paul et al. (1991); Dhillon (1996) and Sakhuja (1996) have observed much better efficiency of a vortex settling basin compared to classical settling basin. Athar et al. (2002) found a better geometry for such a basin. Sakhuja (1996) observed satisfactory results from field applications. However, despite their higher efficiency in removing coarser particles, the degree of removal of finer particles required in most of the hydropower plants is under question.

2.4   Discussions and Conclusions

The time taken to trap solid particles, especially fine ones in a gravitational field is much higher than that in a centrifugal field. For particles finer than 100 μm, detention time in the centrifugal sedimentation devices is shorter by 100 times or more. Therefore, centrifugal separation, especially use of hydrocyclones have gained popular application in industries. The flow rate of such devices being high compared to other processing devices, they have been applied whenever the quantity to process is huge. And the cost effectiveness of such devices has been highly commended.

Sediment particles in water sector projects have been separated using different methods. However, most of them, one way or the other utilize gravity field as a separating force. These methods differ only from the perspective of removal technique applied. Settling basins have been commonly used, especially in hydropower projects. Exclusion of particles larger than 200 μm has been conventionally adopted as a design criterion while designing such a basin. New methods such as Serpent Sediment Sluicing System (S4) and Split and Settle concepts may improve the performance of conventional settling basins. The evidences of cost effectiveness of such concepts over conventional settling basins have been witnessed.

Nevertheless, the turbines and accessories of hydropower plants, especially medium and high head ones from Himalayan region have been severely damaged due to high sediment load of fine particles containing hard minerals such as quartz. This necessitates to exclude even finer particles using larger settling basins. However, it is very unlikely to avail such a space for large settling basins in a rugged and highly fragile Himalayan terrain. Even if such space is available, the cost involved will be quite high. Therefore, there is a need to use more efficient devices such as hydrocyclones in water sector projects to minimize sediment related wear and tear of turbine and accessories and resulting revenue loss.

3   SEPARATION OF PARTICLES BY A HYDROCYCLONE

3.1   *Flow Phenomena in a Hydrocyclone*

The most significant flow pattern in a conventional hydrocyclone is a 'spiral within a spiral' (Fig. 3.1). The feed mixture entered tangentially from the top commences downward flow in the outer regions of the cyclone body. The downward flow combined with rotational
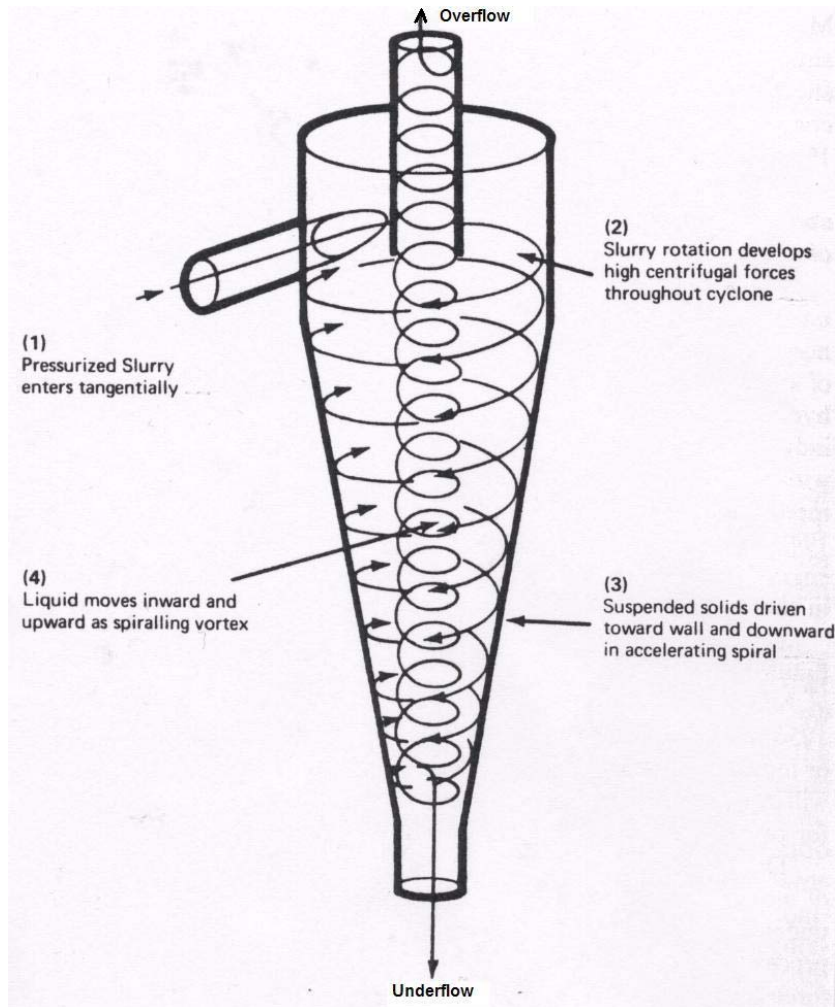
Fig. 3.1   Typical actions within a hydrocyclone by Picenco Int'l, Inc.

motion to which it is constrained creates the outer spiral. The existence of two axial outlets located centrally, but in opposite ends and inability of all the flow (under normal pressure and flow conditions) to leave through the lower apex compel inward migration of some of the fluid. The amount of inward migration increases towards the cone apex. The fluid migrating inward ultimately reverses its vertical velocity direction, and flows along a spiral path upward to the

overflow outlet via the vortex finder. The flow in a cyclone is therefore essentially a- three dimensional, highly turbulent and thus fairly complicated.

Early researchers believed that the flow pattern in a hydrocyclone has a symmetry with exception of the region in and around tangential inlet duct (Kelsall, 1952; Svarovsky,1977, 1990). However, recently it was found such an assumption to be detrimental (He et al., 1999; and Ma et al.,2000). And more recently, the application of both the computational fluid dynamics (CFD) and experimental observation, have shown that the flow throughout the hydrocyclone is asymmetric by virtue of the asymmetry of the geometry of the inlet (Cullivan et al.,2004). Other features occurring in a hydrocyclone are discussed below.

a) *Short-Circuit Flow*

Generally, a flow path across the roof of a hydrocyclone exists due to tangential velocity(Fig. 3.2). The lower pressure region in the proximity of the cyclone walls together with the lower pressure in the inner regions cause a proportion of the feed liquid to pass directly across the cyclone roof and join the overflow stream within the vortex finder (Bradley, 1965). In fact the main reason for providing the vortex finder is to minimize this flow. The quantity of short circuit flow might be quite significant in a hydrocyclone. Kelsall (1953) has measured such a flow as much as 15 per cent.
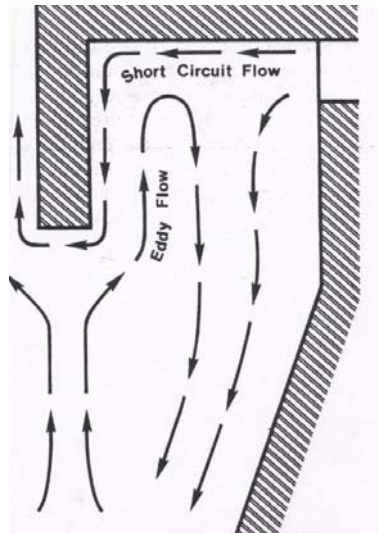
Fig. 3.2 Flow pattern in the upper region of a hydrocyclone (Bradley 1965)

b) *Eddy Flows*

The underflow outlet usually pass small part of the discharge through it, therefore most part of the flow returns towards the overflow in a form of natural vortex. As the vortex finder cannot fully accommodate this rising vortex, a vertical flow can exist in the region outside the radius of the outer wall of the vortex finder (Fig 3.2) leading to re-circulating eddy flows.

c) *The Locus of Zero Vertical Velocity (LZVV)*

The existence of an outer region of downward flow and an inner region of upward flow necessitates a space at which there is no vertical velocity. The LZVV extends from the apex to the stationary layer (Fig. 3.3) below the vortex finder, where the axial and radial velocities are zero (Fontein,1958 ;Bradley & Pulling, 1959).
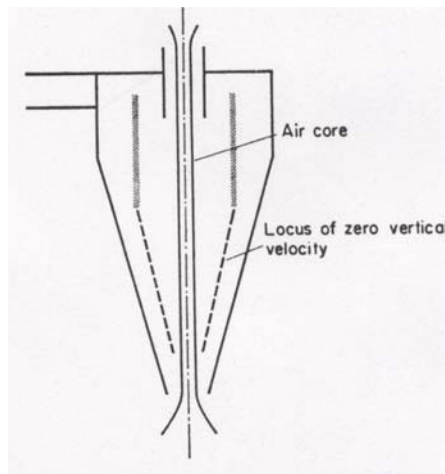
Fig. 3.3 Schematic representation of LZVV and the air core (Bradley, 1965)

c) *The Central Core*

The rotational motion of the fluid inside a hydrocyclone creates a low pressure axial core (Fig 3.3). As the outlets of the hydrocyclone are usually exposed to the atmospheric pressure, the central core is filled with air. In case there is no communication with atmospheric pressure, the core can still exist filled either with vapor and gases from the mixture or cavities depending upon the pressure gradient in the cyclone (Bradley,1965).

The formation of the air core indicates the stability of the vortex (Bradley 1965). However, Bradley didn't comment about the influence of the air core on the overall performance of the hydrocyclone. Recent studies have shown that the presence of air core is detrimental to the performance of the hydrocyclone (Luo et al.,1989; Xu et al., 1990; Chu et al., 2000, 2004).

Analyzing the results obtained in a 75 mm diameter hydrocyclone, Chu et al. (2004) were able to notice the significant increase in capacity of cyclone by the introduction of air core suppressor. The other important aspect is the significant reduction in energy consumption while handling the same of volume of fluid.

The estimation of the diameter of the air core is possible only in a highly idealized conditions (Binnie,1948). The diameter of air core increases with the increase in flow rate up to a point where further increase has no apparent effect. The decrease in the diameter or even collapse of air core can be observed with the impediment of rotational velocity adjacent to the air core for instance due to the accumulation of solids in the apex or operation of cyclone below 3.5 m of pressure head (Bradley 1965).

The diameter of the air core varies from 0.06 to 0.33 D_c (Tarjan, 1962). Bradley (1965) noticed increase in diameter with the increase in cone angle. On the other hand, Fontein et al. (1962) observed the increase in air core diameter with the increase in overflow diameter. However, they found no effect with the change in underflow diameter.

d) *The Flow Pattern in Underflow*

In most of the applications, underflow discharges free, which lead to three types of discharge based on the flow volume and solid load at the apex (Bradley,1965):

- Vortex, where the solids and liquid discharge in a violent spray in the shape of a hollow cone, through which the air core passes.
- "Sausage" like or "Rope" like, where the discharge is a rotating solid spiral.
- Overloaded, where the discharge is a straight "lazy" stream with no spiral motion.

If the performance criteria is maximum removal of solids from the overflow stream, vortex discharge should be chosen. If the criterion is the removal of solids with a minimum of liquid then "sausage" like discharge may be the correct choice. This decreases the efficiency of removal of the fine material, while the overloading produces a marked decrease in the efficiency of removal of material of all sizes.

3.2   Velocity Distributions

The velocity of liquid or solid particle at any point in a hydrocyclone may be resolved into three orthogonal components: i) tangential velocity (V_t); ii) axial velocity (V_a); and, iii) radial velocity (V_r). The most useful and significant of these components in separation of particles is the tangential velocity. Using an optical method, not interfering the flow and microscope fitted with rotating objectives, Kelsall (1952) was able to measure and derive velocity components of fine aluminum particles directly in a 75 mm diameter cyclone at selected positions, which are considered to be the most reliable indication of liquid flow pattern. Despite their limitations because of the special conditions of the observations, measurement and the cyclone dimensions, these data have been formed the basis of theoretical correlations for analyzing the cyclone performance.

3.2.1   Tangential Velocity (V_t)

The tangential velocity in a liquid cyclone in the outer region decreases with the increase in radius, r and across any horizontal levels obeys the relationship (Kelsall,1952;Fig 3.4):

$$V_t r^n = C \qquad\qquad \textbf{Eq- 3.1}$$

where, n is a coefficient and normally has values between 0.6 and 0.9 (Svarovsky 1990) and C is a constant. When compared with the outer region of a free vortex, where angular momentum is conserved, the relationship is

$$V_t r = C \qquad\qquad \textbf{Eq- 3.2}$$

that is, the hydrocyclone tends to approximate a free vortex as n tends to unity (Fig 3.5). Therefore, a cyclone is basically different to a centrifuge in which the fluid rotates as if it were a solid body that is with constant angular velocity:

$$V_t r^{-1} = C \qquad\qquad \textbf{Eq- 3.3}$$
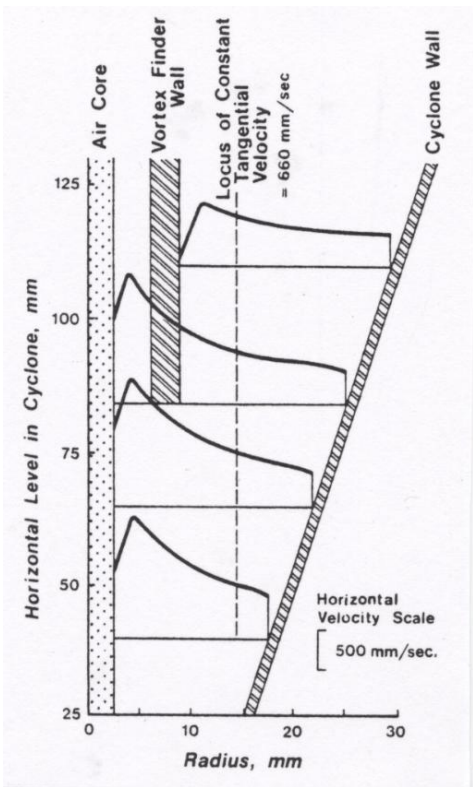
Fig. 3.4 Tangential velocity distribution of fluid measured by Kelsall,1952 (Kelly & Spottiswood, 1985)
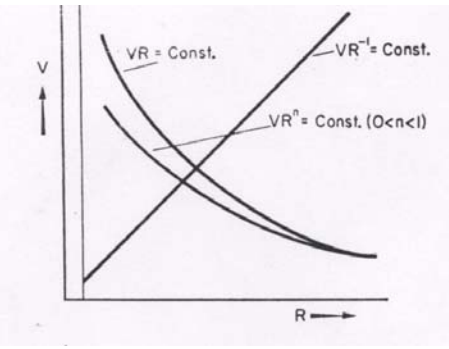
Fig. 3.5 Tangential velocity distributions corresponding to given relationships (Bradley, 1965)

In a vortex relationship, it can be seen that V_t approaches infinity as r approaches zero (Fig. 3.5). Because of the inner spiral and vortex core at the center, the relationship holds only until some small values of radii are reached, when the velocity begins to fall with further decrease in radius. The relationship in this region is governed by constant angular velocity that is a forced vortex. This relationship holds good until the core interface is reached.

Kelsall (1952) found the maximum tangential velocity at a radius of 4.5 mm, which did not change with other design variables, such as overflow and underflow openings as well as flow

rate (feed pressure). Bradley & Pulling (1959) also confirmed the results of Kelsall (1952) for a wide variety of design changes.
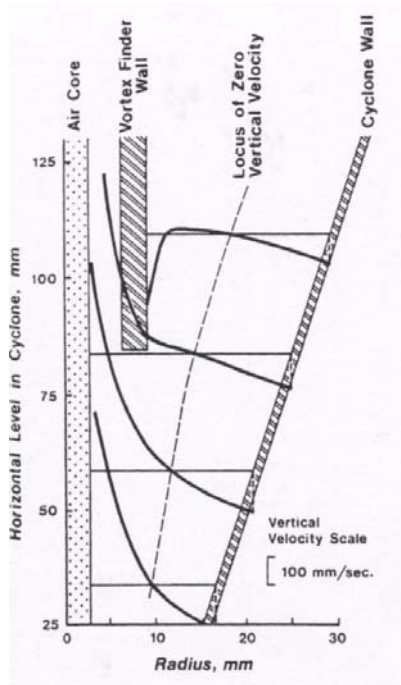
Fig. 3.6 Axial velocity distribution of fluid by Kelsall, 1952 (Kelly & Spottiswood, 1985)

3.2.2 Axial Velocity (V_a)

The axial velocity component of the flow relates to the volumetric distribution of underflow and overflow. A strong downward current usually exists along the outer wall of the cyclone (Fig. 3.6). The downward current is partially counterbalanced by an upward flow in the core region, depending on the split ratio, S. Above the rim, around the vortex finder strong downward flow can be observed due to short circuit effect as discussed earlier.

The most noticeable feature of the vertical velocity component is the locus or envelope of zero vertical velocity, which is conical in shape (Fig 3.6). The LZVV, which was believed to be conical in shape (Kelsall,1952) has been found to be slightly different. From the images observed due to dye injection Bradley and Pulling (1959) have concluded that the LZVV is cylindrical in the cylindrical section of the cyclone (known as 'Mantle') and extends in this form into the conical section until a level at which the wall radius is $0.7R_c$. The shape then becomes conical and extends to the apex of the cone (Fig 3.7), though the exact position of the conical locus is less determinate due to the flow split and underflow discharging conditions.

3-7
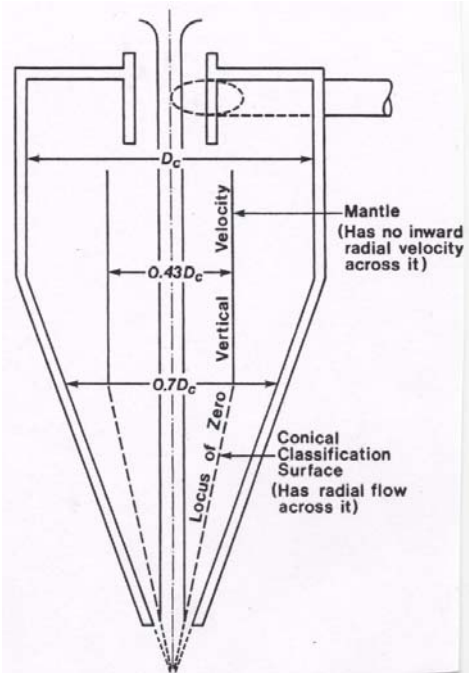
Fig. 3.7 LZVV observed by Bradley & Pulling (Kelly & Spottiswood 1985)

3.2.3   Radial Velocity (V_r)

It is the velocity component against which the particles must settle because of the centrifugal force. Usually, it is much smaller than the other two components and as such very difficult to measure accurately. Inward radial flow is maximum near the cone wall and diminishes with decrease in radius (Fig 3.8). The locus of its zero velocity, however is not known (Svarovsky 1990). As discussed earlier, at levels above the rim of the vortex finder there may be outward re-circulatory flows, and near the roof of the cyclone there is a strong inward flow due to short circuiting.

This short account of velocity profiles in a hydrocyclone is only qualitative. The flow patterns are highly complex even for fluid with low specific gravity and viscosity and may be incorrect to assume that precisely similar profiles occur in a cyclone with a considerably different geometry (Svarovsky, 1990).
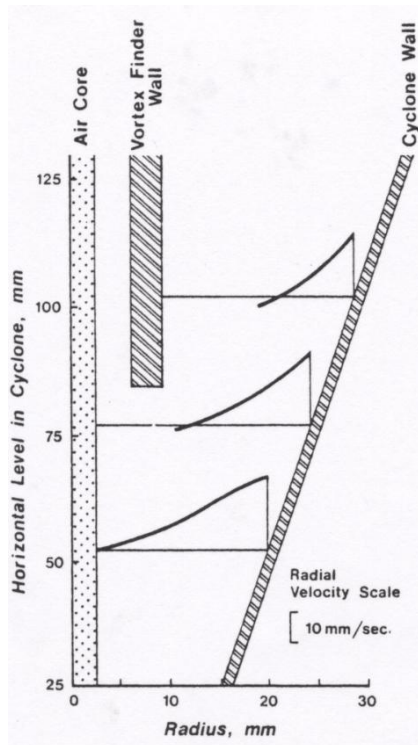
Fig. 3.8 Radial velocity distribution of fluid measured by Kelsall (Kelly & Spottiswood 1985)

The velocity distribution discussed above was observed in a hydrocyclone with air core at the center and that for other conditions are slightly different. Using a Laser Doppler Anemometer (LDA) Luo et al.(1989) have found higher tangential velocity for a water-sealed hydrocyclone with increased wall thickness of the vortex finder. The radial velocity distribution was found to be similar to the tangential velocity in contrast to Kelsall's findings. Due to the increased thickness of vortex finder, they were able to find wider zone of zero vertical velocity instead of locus of zero vertical velocity. Similarly, the velocity distributions in a cyclone without forced vortex have been found to be different than that of the conventional cyclones. Carrying out a study in an 82 mm diameter cyclone and eliminating the air core in a cyclone with thicker vortex finder Xu et al. (1990) were able to find higher tangential velocity but lower radial velocity and slightly lower axial velocity near solid core liquid interface (Fig.3.9).

3-9
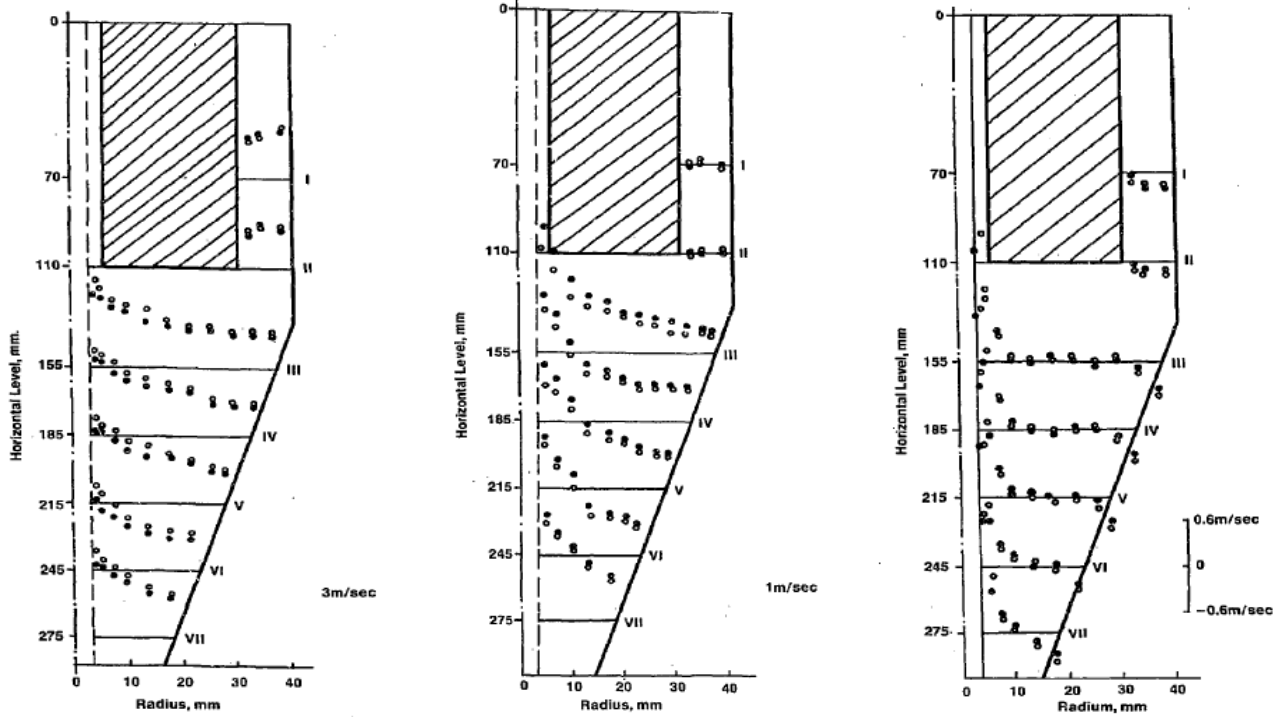
Fig. 3.9 Tangential (left), radial (middle) and axial (right) velocity distributions in a cyclone without forced vortex (Xu et al., 1990)

3.3 Parameters of Particle Separation

3.3.1 Separation Efficiency

Rietema (1961) has defined four principle factors affecting the separation, which are: the centrifugal field; the radial velocity pattern; the residence time of the particles; and, the turbulence which develops. Separation efficiency of a hydrocyclone is one of the main performance indicators. Measure of separation efficiency of solid liquid separation equipment is assessed in terms of total and grade efficiency curves.

3.3.2 Total Efficiency

The most obvious definition of separation efficiency is simply the rate of mass recovery in the underflow, M_u as a fraction of the feed mass, M and mathematically,

$$E_T = \frac{M_U}{M}$$

Eq- 3.4

If there is no accumulation of solid particles in the cyclone, an overall mass balance leads to

$$E_T = 1 - \frac{M_O}{M} \qquad\qquad \text{Eq- 3.5}$$

There are two problems associated with total efficiency. First, if a hydrocyclone delivers both liquid and solid to the underflow and nothing to the overflow, an ideal total efficiency of one (100 per cent) will result. Second, without any separation, a hydrocyclone, by simply splitting the flow to underflow and overflow will attain any guaranteed total efficiency. In order to overcome these weakness, several alternative definitions of efficiency are used.

3.3.3 Grade Efficiency

Grade efficiency, $G(x)$ is defined in a similar way as the total efficiency, except that its value corresponds to only one particle size. Usually the feed mixture is heterogeneous, therefore, the underflow also receives particles of different sizes. If the performance of the separator for each particle size is evaluated and represented in a graphical form, it is called the grade efficiency curve or selectivity curve (Kraipech et al. 2002). As the value of the grade efficiency has a character of probability, it is sometimes referred as partition probability curve.
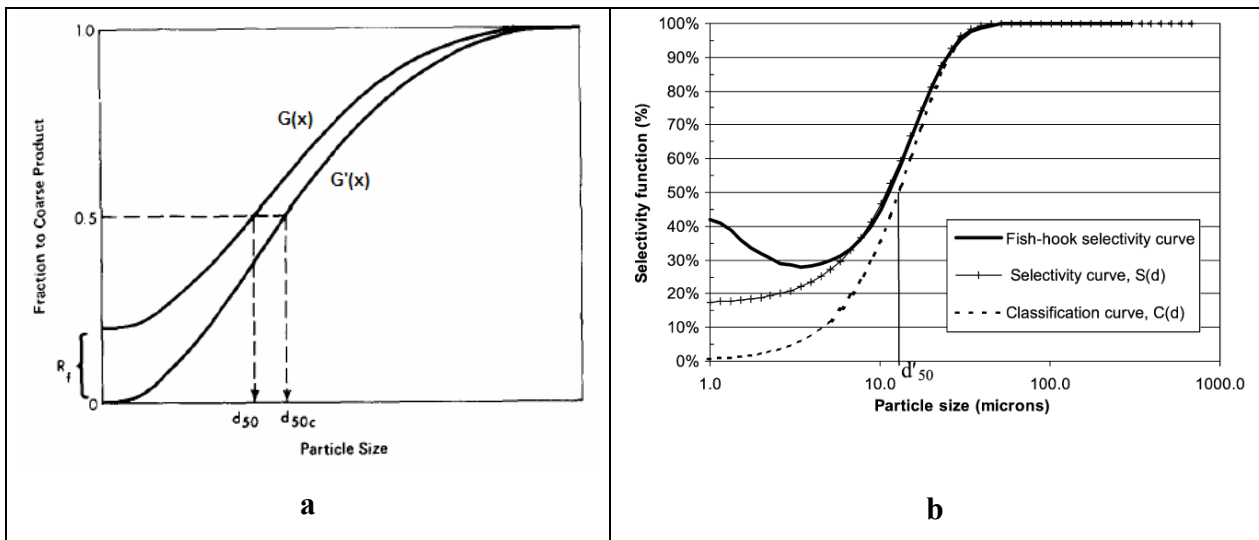
Fig. 3.10 Separation curves with corresponding cut sizes a) (Plitt & Kawatra, 1979) b) Kraipech et al. (2002)

For a hydrocyclone, the form of separation curve is usually S-shaped. The classical approaches postulate that the finest particles can not be classified by the hydrocyclone. Their presence in underflow stream is argued simply due to the result of flow split and hence their separation efficiency at the beginning is equal to the flow ratio, Rf (Fig. 10.a). However, recent research has shown that the efficiency of separation of finest particles is higher than the flow

ratio (Fig. 3.10.b) resulting in a shape called fish-hook (Kraipech et al., 2002; Neesse et al., 2004). It is argued that the finest particles are dragged together with the coarse particles due to the entrainment effect (Neesse et al.,2004).

3.3.4   Reduced Grade Efficiency

In certain applications in solid-liquid separation, when relatively dilute underflow occurs, such as with hydrocyclones, the overflow as well as underflow receive some unclassified flux "dead flux" due to the effect of flow splitting. This is because any separator functions as a flow divider and it also divides the solids in at least the same ratio as is the underflow to total flow ratio, $R_f = Q_u/Q$ (Plitt & Kawatra, 1979). The total efficiency defined earlier includes such dead flux as well and do not reflect the separation capacity of the equipment. Therefore, a concept of reduced efficiency', E_T , is introduced (Tenbergen & Rietema,1961; Kelsall,1966), which is described as

$$E_T' = -\frac{E_T - R_f}{1 - R_f}$$
<div align="right">Eq- 3.6</div>

The splitting effect shows unrealistic separation efficiency of the equipment. As a result the curve does not start from the origin of the coordinates (Fig. 3.10.a), but has an intercept, the value of which usually equals to R_f. This is simply because the very fine particles simply follow the flow and are split in the same ratio as the fluid.

3.3.5   Cut Size

The cut size is a particle size which in some way characterizes the position of the grade efficiency curve along the x-axis, for a strongly size dependent separation process. Although some manufactures use other definitions as well, most generally accepted and logical definition is that particle size which has a 50 per cent chance of being separated or going through the overflow when presented in the separator. The majority of the particles finer than the equiprobable size x_{50} in the feed will go through overflow, while the majority of those coarser than x_{50} will be separated. If the 50 percent particle size is deduced from the reduced grade efficiency curve, $G'(x)$, it is known as corrected (reduced) cut size d'_{50}(Fig 3.10, Svarovsky,1984).

3.3.6 Sharpness of Separation

As the same cut size may imply different separation possibility, a sharpness of separation is defined through the steepness of the grade efficiency curve. In mathematical term it is the slope of the tangent at $x=x_{50}$ to a plot on linear graph paper of the normalized grade efficiency.Or more often as the ratio of two sizes corresponding to two different efficiencies on either side of x_{50} on grade efficiency curve. The ratio of x_{10}/x_{90}, x_{25}/x_{75} and x_{35}/x_{65} are also considered. Sometimes, a reverse ratio is also used.

3.4 *Classification in a Hydrocyclone*

Classification is the separation of particles into two or more products according to their settling velocity in a fluid. The classical model postulated that the classification takes place throughout the whole body of the cyclone. However, later, studies carried out by Renner & Cohen (1978) indicated that the major classification in the hydrocyclone takes place only in some regions. Using high-speed probe, they were able to extract the samples from several selected positions within a 150-mm diameter cyclone. The PSD analysis showed that in terms of classification, the interior part of a hydrocyclone can be divided into four regions (Fig 3.11).

Essentially unclassified feed exists in a narrow region *A*, adjacent to the cylinder wall and roof of the hydrocyclone. Region *B* occupies most of the space of conical part and contains fully classified coarse material, i.e. the size distribution is practically uniform and resembles that of the coarse underflow product. A fully classified fine material is contained in region *C*,
a narrow region surrounding the vortex finder and extending below it. The authors found classification to occur only in the fourth toroid shaped region *D*, surrounded by regions *A, B* and *C*. Across this region, size fractions are radially distributed, the smaller sizes being closer to the region of decreasing radial distances from the axis and vice versa. This indicates that this region is the locus of active classification. Poor classification can occur when region *D* fails to form well, because of poor design or poor operation. This was also confirmed by
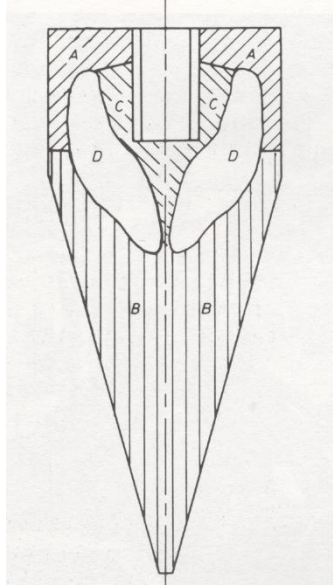
Fig. 3.11 Regions of similar size distributions by Renner & Cohen 1978 (after Wills 1992)

Xu et al. (1991) in 82 mm dia cyclone reducing the pre-separation zone by 16 mm and increasing the width of zone *D* by the same magnitude, which resulted in an increase of coarser particles separation by 8.0 per cent.

3.5   *Motion of Solid Particles in a Hydrocyclone*

Although the fluid flow pattern was understood in early fifties by Kelsall (1952), the motion of particles inside a hydrocyclone was not understood until early nineties. By using a particle dynamics analyzer, Chu & Chen (1993) were able to measure the velocity patterns as well as the concentration of the particles in an 80 mm diameter hydrocyclone.

3.5.1   Radial Velocity

Chu & Chen (1993) have measured the radial velocity of particles starting from the wall of the conical section towards the center of the hydrocyclone. The radial velocity increases from the wall of the conical section towards the center of the hydrocyclone, until a maximum value is reached near the air water interface (Fig 3.12). The velocity again decreases towards the center with a relationship very similar to tangential velocity of the fluid described by Eq- 3.1.
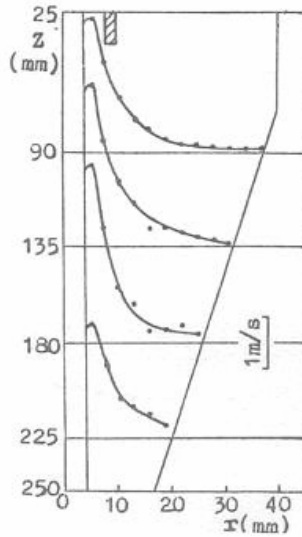
Fig. 3.12 Radial velocity of solid particles (Chu & Chen 1993)
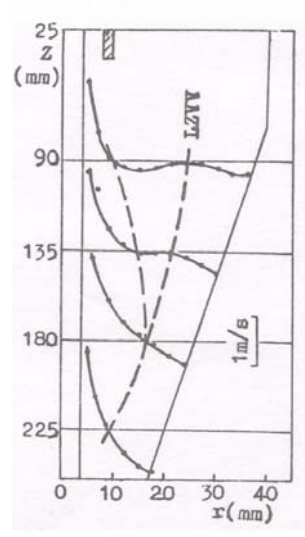
Fig. 3.13 Axial velocity of solid particles (Chu & Chen 1993)

3.5.2 Axial Velocity

There was a belief that the axial velocity of the particles in a hydrocyclone are the same as that of liquid. However, recently it has been found that it is significantly different than axial velocity of the fluid (Chu & Chen,1993, Fig 3.13). Further, a region of stationary layer between two loci of zero vertical velocity in the upper part of the cone was noticed as observed earlier by Bradley & Pulling (1959). Looking at the low radial velocity and region of stationary layer, they concluded that this part doesn't contribute to the particle separation and hence contradicts the postulation put forwarded by Renner & Cohen (1978).

3.5.3 Particle Size Distribution and Their Concentration

Due to the centrifugal effect, the larger particles are transported to the wall and smaller ones to the center of the hydrocyclone (Chu & Chen, 1993, Fig. 3.14). However, it is interesting to see that the concentration of solid particles is maximum not near the wall but near the region of LZVV of solid particles (Fig. 3.15). Since both the velocity components in this region are minimum, the particles have a tendency to accumulate there. Earlier, Renner & Cohen (1978) have also found higher residence time of the particles in this region.
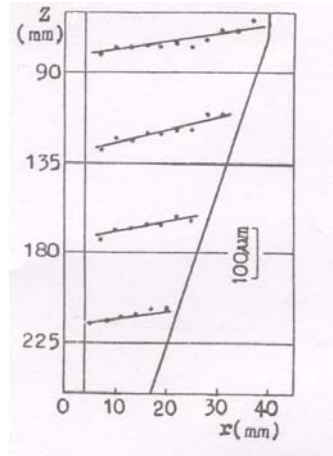
Fig. 3.14 Particles size distribution (Chu & Chen 1993, p. 1884**)**
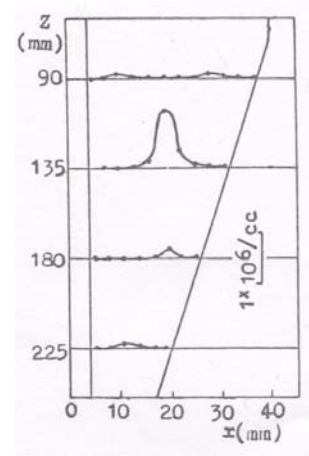
Fig. 3.15 Concentration distribution of solid particles (Chu & Chen 1993, p. 1885)

3.6   Theories of Hydrocyclone

As the flow process is fairly complex, and influenced by many variables, separation process in a hydrocyclone has been described by different approaches. Two schools of thoughts, namely the equilibrium orbit and the residence time theories are known as fundamental theories of separation in a hydrocyclone. These theories take no or little account of the effect of split ratio, feed concentration and PSD.

3.6.1   The Equilibrium Orbit Theory

The equilibrium orbit theory is based on the concept of the equilibrium radius. According to this concept, particles of a given size attain an equilibrium radial orbit position in the cyclone, where terminal settling velocity is just equal to the radial velocity of the liquid (Criner 1950; Driessen,1951; Kelsall,1952; Dahlstrom,1954, Yoshika & Hotta,1955 and Lilge, 1962). It is then argued that if this radius lies within the LZVV the particle will go to the overflow while those with an equilibrium radius outside of the LZVV region will go to the uderflow. The particle whose radius is coincident with the position of LZVV is assumed on this basis to be equal to d_{50}.

Stokes' law is usually assumed to hold and the particle diameter is calculated balancing two opposing forces acting on particle: an outward centrifugal force, F_c and an inward drag force, F_D which reads as

$$d_{50} = \left[\frac{18\mu}{(\rho_s - \rho)} \frac{V_r \, r}{V_t^2} \right]^{0.5}$$

Eq- 3.7

where d_{50} is the cut size of the particle which has equal probability to go to underflow as well as overflow, V_r and V_t are the radial and tangential velocity components.

This approach demands detailed knowledge of inward radial velocity, which is quite complex and has been estimated by different assumptions. As a result the relations derived by different researchers differ from each other. A detailed review of different approaches is given by Bradley (1965) and Svarovsky (1984).

The equilibrium orbit theory and the relations proposed by various authors can be criticized on the ground that it takes no account of the residence time of the particles in the cyclone and assumes that this residence time is so large that all particles can actually attain their equilibrium orbit (Rietema 1961). The theory also disregards the effect of turbulence, which also affects particle separation. Despite these drawbacks, reasonable predictions of cyclone performance at low concentrations have been found, particularly, when used under similar conditions as applied by respective authors (Svarovsky 1990, 1996).

3.6.2   The Residence Time Theory

Figuring out the drawback of the equilibrium theory, Rietema (1961) was the first to propose this theory, who assumed a homogenous distribution of all particles across the inlet. The cut size, d_{50} will then be the size of the particle, which, if entering precisely in the center of the inlet pipe will just reach the wall in residence time T. Then, as the radial velocity is not constant, the settling depth for d_{50} is $D_i/2$, which can be estimated by integrating the radial velocity over the time period, T:

$$\frac{D_i}{2} = \int_0^T V_r \, dt$$

Eq- 3.8

Rietama's theory, however does not take into account the radial fluid flow It also neglects any effect of inertia, turbulence, as well as hindered settling at higher concentrations. A more recent version of residence time theory due to Holland-Batt (1982) takes into account the radial flow. The simply used the hold-up time of the liquid cyclone (flow rate per cyclone volume) as the residence time, average radial fluid velocity (flow rate per wall are of the cyclone) and a general continuity equation for two dimensional flow to derive an expression for the cut size.The original equation for the cut size does not include the important effects of the inlet and outlet diameters. Neither the split ratio was included in the model. Though, Holland-Batt suggests that their omission is compensated by to some extent by pressure drop and volumetric capacity of hydrocyclone as input variables. Nevertheless, omission of these parameters have been found to be very sensitive with regard to cut size (Svarovsky,1984). One important consideration made by Holland-Batt(1982) was the inclusion of hindered settling.

Another theoretical approach to cut size prediction based on residence time theory is due to Trawinski(1969), who used the direct analogy of gravity settling , Stokes' law, an effective clarification area and an average acceleration to derive an expression for the cut size. The same author also proposed a rather simple correlation for pressure drop-flow rate relationship.

3.6.3   Hydrocyclone Correlations

The relations describing the hydrocyclone behavior and separation efficiencies have been based primarily on simple fundamental theories. As these theories lack full description of the flow inside the hydrocyclone, they are often combined with regression and dimensional analyses as well to deduce hydrocyclone correlations. With the invent of powerful computers and more understanding of physics of flow inside hydrocyclones, there is an increased trend of using CFD. Differential equations describing turbulent two-phase flow, flow pattern, particle trajectories, including the boundary layer flow, the short circuit flow and the internal eddies are solved using CFD.

Most of the early researchers used cut size as the representative of the separation efficiency. The equations for the cut sizes developed are based mostly on fundamental theories combined

with regression analysis. Bradley (1965) and later Svarovsky (1984) have reviewed such relations.

3.6.4 Cut Size (d_{50})

One of the more rigorous correlations based on equilibrium orbit theory is due to Bradley & Pulling (1959), which includes both design as well as operating variables. They were able to discover a more precise boundary of LZVV and the region inscribed by it, so called 'mantle' where there is no inward radial velocity. After defining the new classification surface area, the authors have derived more precise relations than that earlier developed by Yoshika & Hotta (1955) and Bradley(1958), which reads as

$$d_{50} = \frac{3.2(0.43)^n}{\alpha} D_i^2 \left[\frac{\tan\theta/2\mu(1-R_f)}{D_c Q(\rho_s - \rho)} \right]^{0.5}$$
Eq- 3.9

And after comparison with experimental values carried out in a 37.5 mm diameter cyclone, and in dimensionless form

$$\frac{d_{50}D_c}{D_i^2} = \frac{3(0.38)^n}{\alpha} \left[\frac{\mu D_c(1-R_f)\tan\frac{\theta}{2}}{Q(\rho_s - \rho)} \right]^{0.5}$$
Eq- 3.10

The another well known relation based on residence time theory propounded by Rietema(1961) is as follows

$$\frac{d_{50}^2 \Delta\rho}{\mu} L \frac{\Delta p}{\rho Q} = \frac{36}{\pi} \frac{w}{V} \frac{R}{D_i}$$
Eq- 3.11

Rietema found the right hand side parameters to be constant and defined as a characteristic cyclone number, Cy_{50}. Based on the above relation, Rietema optimized different parameters by changing length of the cyclone, inlet and outlet diameters in a 75 mm diameter cyclone. By using the data of Kelsall (1952) and Dahlstrom (1954). Rietema derived optimum geometry defined by: L/D as 5; D_i/D_c as 0.28; D_o/D_c as 0.34; and, Cy_{50} as 3.5.

However, the experimental investigations carried out at Bradford University with three sizes of Rietema's optimum design (22, 44 and 88 mm diameter) at one per cent volume feed concentration have produced Rietema's results but only with very dilute underflows

(Medronho & Svarovsky, 1984). They further add that the values of Cy_{50} about twice as large have been found under more practical operating conditions.

Using the test data, empirical relations have been developed which are based on regression analysis. These correlations are due to Dahlstrom (1984), Lynch et al.(1968, 1974, 1975), and Plitt (1976), Kawatra et al.(1996). More recently the cyclone manufacturers such as Krebs Engineers (Olson & Turner 2004) have also developed relations specific to their products. Of the many empirical correlations for d_{50}, the one developed by Dahlstrom (1954) is still widely accepted, which reads as:

$$d_{50} = \frac{0.001(D_u D_i)^{0.68}}{Q^{0.53}(\rho_s - \rho)}$$

Eq- 3.12

Empirical relation based on extensive data including the large diameter cyclones and accounting effect of concentration, Plitt (1976) obtained the following relation:

$$d_{50} = \frac{0.00269 \ D_c^{0.46} D_i^{0.6} D_o^{1.21} \exp(3.9C_v/d_m)^{0.052}}{D_u^{0.71}(L-l)^{0.38} Q^{0.45}(\rho_s - \rho_v)^{0.5}}$$

Eq- 3.13

Later using an online viscometer, Kawatra et al. (1996) were able to notice the influence of viscosity of the mixture and included in the equation as follows

$$d_{50}(c) = \frac{K D_c^{0.46} D_i^{0.6} D_o^{1.21} (100C_v)^{0.41} \mu^{0.35}}{D_u^{0.71}(L-l)^{0.38} Q^{0.45}(\rho_s - \rho)^{0.5}}$$

Eq- 3.14

3.6.5 Flow Split, (S) and Flow Ratio (R_f)

The distributions of flow among the outlets have been described either by Split (S) or flow ratios (R_f) and defined by the relations:

$$S = \frac{Q_U}{Q_O}$$

Eq- 3.15

$$R_f = \frac{Q_U}{Q} = \frac{S}{S+1}$$

Eq- 3.16

As the performance curve of the hydrocyclone is affected by the fraction of liquid leaving the underflow, Plitt (1976) has established a correlation between the split ratio (Q_u/Q_o) and design variables for a free discharging spray or vortex type flow which reads as

$$S = \frac{Q_u}{Q_o} = \left[\frac{34.3 \left(\dfrac{D_u}{D_o} \right)^{3.31} h^{0.54} (D_u{}^2 + D_o{}^2)^{0.36} \exp(C_v)}{\Delta p^{0.24} D_c{}^{1.11}} \right]$$
<div align="right">Eq- 3.17</div>

3.6.6 Pressure Drop (ΔP)

The pressure drop across the cyclone is fundamental for estimating the driving power requirement. In dimensionless form, it reads as (Bradley,1965)

$$\frac{\Delta p / \rho}{V^2 / 2g} = \frac{\alpha^2}{n} \left[\left(\frac{D_C}{D_O} \right)^{2n} - 1 \right]$$
<div align="right">Eq- 3.18</div>

As with his previous correlation for cut size, α and n need to be known, which limit the usefulness. Despite the simplicity the relation developed by Dahlstorm (1954) has been found to be much reliable and reads as (Kelly & Spottiswood,1982):

$$\frac{Q}{(\Delta p)^{0.5}} = 7.4 * 10^{-6} \left(\frac{D_O}{D_I} \right)^{0.9}$$
<div align="right">Eq- 3.19</div>

Including all the parameters affecting the pressure drop, Plitt (1976) derived a more cumbersome empirical correlation as follows (Kelly & Spottiswood,1982):

$$\Delta P = \frac{1.3 * 10^5 Q^{1.78} \exp(0.55 C_v)}{D_C{}^{0.37} D_I{}^{0.94} h^{0.28} (D_U{}^2 + D_O{}^2)^{0.87}}$$
<div align="right">Eq- 3.20</div>

Besides, most of the cyclone manufactures (Tarr, 1976; Olson & Turner, 2002; Arterburn, 2004) have developed empirical relations based on the results obtained from their particular products correlating design and operation variables and presented them in graphical forms. These graphical relations help user select the desired product based on their requirement. A detailed review of hydrocyclone correlations using different approaches is given in Bradley (1965,) and Svarovsky (1984).

3.6.7 Hydrocyclone Scale-up

The scale-up of hydrocyclones is based on the concept of cut size. On the basis of the 3 models (22,44 and 88 mm dia) developed and tested using Rietema's geometry and low feed concentration (~ 1% v/v) at University of Bradford, the following dimensionless equations

were developed for scaling-up hydrocyclones (Svarovsky,1984, Medronho & Svarovsky, 1984):

$$Stk'_{50}\, Eu = 0.074\big(\ln(1/R_f)^{0.742}\big)\exp(8.96C_v) \qquad\qquad \textbf{Eq- 3.21}$$

$$Eu = 371.5\,\mathrm{Re}^{0.116}\exp(-2.12C_v) \qquad\qquad \textbf{Eq- 3.22}$$

$$R_f = 1218(D_U/D_C)^{4.75}\,Eu^{-0.30} \qquad\qquad \textbf{Eq- 3.23}$$

where Stk_{50} is the Stokes' number (for x_{50}) and estimated by the following relations:

$$Stk_{50} = \frac{x_{50}^{2}(\rho_s - \rho)V}{18\mu D_C} \qquad\qquad \textbf{Eq- 3.24}$$

and the Reynolds number, $Re = VD_C\rho/\mu,$. Euler number is a pressure loss factor and

$$Eu = \frac{\Delta P}{\rho V^2/2} \qquad\qquad \textbf{Eq- 3.25}$$

All the above equations use the superficial velocity in the cyclone body as the characteristics velocity, i.e.

$$V = \frac{4Q}{\pi D^2} \qquad\qquad \textbf{Eq- 3.26}$$

3.7   *Effect of Design Variables on Efficiency of a Hydrocyclone*

The variables that affect hydrocyclone design can be divided into two groups: those which are dependent on hydrocyclone size and proportions, known as design variables and those which are independent of size and proportions, known as operating variables. The design variables include inlet, overflow and underflow openings and shape as well as the size of the main body. Operating variables depend on feed mixture characteristics, which include pressure drop; particles characteristics and fluid properties. Because of the interrelation between these variables, it is not possible to consider them individually. Therefore, hydrocyclone performance is evaluated in terms of the following parameters.

3.7.1   Effect of Cyclone Size

The key parameter, collecting efficiency of a cyclone is governed chiefly by the cross sectional areas and lengths of individual flow channels (Storch et al., 1979).The diameter of the cyclone, coupled with the diameter of the vortex finder (and to a lesser extent, the diameter ratio of

vortex finder to apex) create the centrifugal force, which is one of the two forces, which determine the separation (Kelly and Spottiswood,1982). Therefore it serves as a main parameter to which all the other dimensions are related .

At the same pressure drop and geometrically similar cyclones, the cut size decreases with decreasing cyclone diameters leading to higher mass recoveries. Analyzing the relations given by various authors, for low concentrations ($C_v<1$) the following relation is valid (Bradley,1965).

$$x_{50} \propto D_C{}^n \qquad\qquad \textbf{Eq- 3.27}$$

where n varies from 1.36 to 1.52 for constant flow rate and varies from 0.41 to 0.5 for a constant pressure drop. At higher concentrations, Plitt (1976) found the value of n as 1.18.

Over the wide range of design variables and operating conditions studied in 10.2-, 25.4- and 38.1-cm diameter hydrocyclones, Lynch et al. (1975) and Rao et. al (1976) found that the critical design variables are the inlet and outlet diameters and the cyclone diameter is merely the size of housing required to carry these diameters for a normal cyclone classifier operation.

Nevertheless, despite the dependency of cut size on the diameter of the cyclone in general, it is possible to have the same reduced efficiency curve from geometrically similar cyclones of varying diameter, design and operating variables (Lynch et al. 1974).

3.7.2   Effect of Inlet Geometry

3.7.2.1   Geometry of Approach

Despite the ongoing debate on the influence of geometry of approach on the efficiency of hydrocyclone, different geometries of approach have been reported in the literature (Fig. 3.16). The original cyclones offered prior to 1950 featured outer wall tangential feed entry or standard entry. One of the demerits of the tangential entry is the significant energy loss due to the impingement of entering and rotating fluids, especially at the entrance (Boadway,1984; Pandit et al., 2007) although early researchers such as Rietema (1962) didn't find any significance of involute entry in a 75 mm diameter cyclone.

Recognizing the limitations of standard tangential feed entries as early as 1953, the Krebs Engineers were able to invent involute feed entry and claimed an additional 25 % capacity. It is reasonable to assume that the full involuted feed provides a smooth transition from pressure energy to rotational momentum. As the rotational flow does not collide with the feed inlet flow, it eliminates the turbulence that influences the rate of sedimentation. Bradley (1965) has reported that for a gas cyclone, the ratio between peripheral velocity to average inlet velocity, $\alpha < 1$ for standard type, and $\alpha = 1$ for involute type. Bradley further argues that the change in α should have a pronounced effect on pressure drop in Rietema's investigations. Bradley's argument is supported by the fact that in recent years, cyclone manufacturers such as Vortex Ventures have introduced modified involute inlet designs such as Spintop^{TM}, which have been found to perform better (www.vortexventures.com). Separation efficiency being same, an increase of throughput by 16.4 % have been observed in gMax series (Krebs Engineers, 2000).
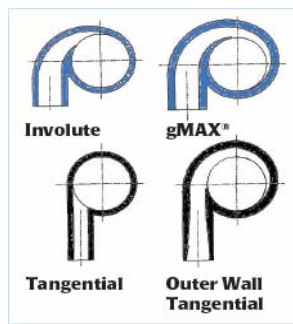
Fig. 3.16 Principal entry geometries of hydrocyclone (www.krebs.com

More recently, Chu et al. (2000) have comprehensively studied the performance of a 75 mm dia hydrocyclone through the structural modification of different parts using Rietema's optimum geometry. It included the modification of: inlet geometry; vortex finders; cone parts; central insertion; underflow; and, the length of the cylindrical portion. The performance indices observed were: reduced separation efficiency, $d_{50,c}$; separation sharpness; feed handling capacity; flow split; and, energy loss coefficient. These indices were investigated through 25 number of experiments adopting an orthogonal design method.

Six basic inlet configurations: involute, tangent, arc, slanting pipe and spiral with equivalent cross sections were adopted by Chu et al.(2000). Unlike other researchers they have operated

the hydrocyclone in combination with other structural modifications. Except for length of the cylindrical portion, all the design variables were kept constant.

Their results showed that the structural modification didn't result in any improvement in separation efficiency compared to the traditional tangent type entry. In contrary to what Bradley (1965) reported earlier and conventional wisdom, the reduced efficiency and corrected cut size due to other entry types resulted in some 30 per cent lower than that due to conventional tangent type. In terms of feed handling capacity, again the tangent type entry was found superior to all types and about 26 per cent higher than that due to involute one (even for lower split ratio).

The results on energy loss coefficient also seem to be somewhat unexpected and contradictory to the findings of Boadway (1984) and Pandit et al.(2007). Chu et al. (2000) also found the energy loss coefficient with tangent type entry the lowest among all types and 40 % lower than that due to involute type. Their argument for the lower efficiency with the involute and arc types is due to the fact that these types influence the flow structure not only at the entrance but also in the cylindrical or even the conical parts. As a result liquid moves in a state of circular motion for some time before it changes to helical motion to fit in the fluid flow pattern inside the hydrocyclone.

3.7.2.2 Shape of Inlet Cross Section

Early researchers such as Kelsall(1953) and manufacturers such as Krebs Engineers have found narrow and deep cross section to be slightly superior than the circular ones. However, there have been cases when the efficiency due to circular inlet have been observed to be better (Chu et al. ,2000; Soccol & Botrel,2004)

As the settling of particles is dependent on settling depth, which is obviously smaller for a narrow and deep cross sections compared to the circular ones, for the given sectional area, the former shape is always superior to the latter one. The findings of Chu et al.(2000) and Soccol & Botrel (2004) can be questioned on a ground that they didn't consider different shapes for the same geometry. Further, the residence time would have been sufficient for the shapes they considered.

3.7.2.3 Effect of Inlet Size

As the inlet diameter determines the inlet velocity and thereby controls the tangential velocity in the cyclone, the size of inlet opening plays an important role in particles separation and capacity of the cyclone. Smaller inlets, while reducing cyclone capacity, lead to higher efficiency and therefore lower cut size. Based on Bradley's review (Bradley, 1965) empirical relations take the form:

$$x_{50} \propto D_I{}^n$$

where n varies from 0.6 to 0.68.   However, using the approach of dimensional analysis Medronoho & Svarovsky (1984) have proved experimentally that the x_{50} is independent of the inlet diameter for a family of geometrically similar cyclones (with variable inlet sizes).

Rietema (1961, I) found an optimum size of inlet as $D_I = 0.28D_C$ for the chosen geometry, while Bradley chose a range of (0.14-0.17) D_C as a suitable compromise. The practical size of inlet based on the survey of manufacturers' product is 0.13-0.29 D_C (Svarovsky, 1984). One important requirement to be satisfied is that the entrance jet should not impinge on the vortex finder, because this would lead to turbulence as well as to excessive wear due to erosion.

3.7.3   Effect of Vortex Finders

3.7.3.1 Geometry of Vortex Finder

Renner & Cohen (1978) have found that the narrow region surrounding the vortex finder is occupied with unclassified feed. Therefore, there is a belief that the reduction of the width of the pre-separation zone won't have unfavorable effects on the performance of the hydrocyclone. On the other hand, Luo et al. (1989), have found improved performance of separation while using thicker vortex finder. Therefore Xu et al. (1991) hypothesized that this would significantly reduce the short circuit flow and reduces the energy loss near the entrance. The experiment carried out by them in an 82 mm diameter hydrocyclone changing the overflow diameters and pre-separation width from 26 mm to 10 mm revealed a reduction of short circuit flow by 8 per cent (10 against 18) compared to that in a conventional one.

Chu et al.(2000) studied the performance of 5 basic geometrical configurations of vortex finders including those suggested by Arato (1984); Boadway (1984); Xu et al.(1991) and Chu

& Luo (1994): straight pipe with 2.5 mm thick wall; straight pipe with thick wall (7.5 mm); 30^0 diffuser with cone; and, 20^0 diffuser with annular teeth.

Except for the increase of reduced separation efficiency by 9% due to straight pipe with siphon compared to conventional design, there was no performance improvement due to other geometries. Earlier, Bradley (1960) also reported insignificant effect of the shapes other than cylindrical one. A 'skirt' at the end is found sometimes beneficial in reducing pressure loss (Spintop Hydrocyclones, 2004; Duijn & Rietema, 1982).

3.7.3.2 Cross Section

Throughput of a hydrocyclone, is approximately proportional to the overflow diameter. The exponent on D_o is slightly less than one (.68-0.73) for higher concentrations (Svarovsky, 1984). Both the split ratio, S, as well as flow ratio, R_f are strongly affected by the diameter of the vortex finder. While Plitt (1976) found the exponent on D_u/D_o as 3.31, the review of empirical relations revealed it to vary from 1.75 to 4.4 (Bradley,1965).

Because of its strong influence on cut size, manufacturers prefer to use replaceable vortex finders in order to cover a wide range of performance characteristics with a limited number of standard cyclone diameters (Svarovsky,1984). Decrease in vortex finder diameters within certain limits lead to decrease of cut size due to increased pool effect and residence time. However, decrease of diameter beyond the radius of maximum tangential velocity lead to increase in cut size again because the short circuit flow do not encounter strong centrifugal force as it passes the bottom edge of the vortex finder. Bradley (1965) has suggested a minimum overflow diameter as $D_c/8$. Some manufactures often reduce the overflow diameter, while keeping thick walls to promote re-entrainment of particles from the short circuit flow.

The convincing argument for maximum limit of diameter of vortex finder is due to Bradley & Pulling (1965), which is based on the concept of LZVV. Their study revealed that increasing the diameter beyond LZVV ($0.43D_c$) can cause collapse of the normal pattern of inward radial flow. While the standard geometries given by Rietema and Bradley suggest the diameter of vortex finder as $0.34\ D_c$ and $0.2\ D_c$, the diameters in practice range from 0.16 to 0.5 D_c.

3.7.3.3 Length

Since the vortex finder was introduced to minimize short circuit effect, its length has direct implication on separation. Extension of the vortex finder, however, shortens the natural vortex in the cyclone body and reduces the separation of finer particles from the vortex Svarovsky (1984). Therefore, while the longer vortex finders minimize the entry of coarser particles, they generally increase cut size (Fig. 3.17). The optimum length of the vortex finder is therefore a compromise between the above two conflicting effects.

Although the length of the vortex finder is critical in small diameter cyclones, it is insensitive in large diameter cyclones (> 600 mm) operated at low pressure and coarser feeds (Bradley,1965).
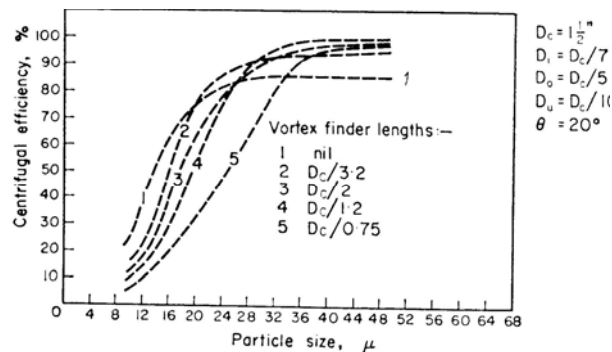
Fig. 3.17 Effect of vortex finder length on grade efficiency and cut size in a 38 mm dia hydrocyclone, after Bradley (1965)

While the length of $0.33D_c$ and $0.4D_c$ is recommended in their optimum geometries by Bradley(1965) and Rietema(1965), it varies from $0.3 D_c$ to D_c in practice (Svarovsky,1984). Bradley (1965) recommended that the vortex finder should not end at the same level as the bottom of the inlet opening or near the joint between the cylindrical and conical sections, in order to avoid turbulence. Unlike most researchers, Plitt (1976) has included its effect in his correlations.

3.7.4 Effect of Conical part

3.7.4.1 Geometry

Chu et al. (2000) considered five basic geometric configurations in their study: parabola, hyperbola, and cone with spiral, cone with rings and smooth cone. Their study showed the parabola type to be better than the conventional one in terms of separation efficiency, separation sharpness and split ratio. Though the separation efficiency of spiral type was comparable to that of parabolic configuration, split ratio was found to be 155 % compared to that in a conventional cyclone. More recent study carried out by Chu et al. (2004) with central insertions have also confirmed superiority of the performance indices due to parabolic configuration. Better performance was also observed in a modified geometry with a parabolic chamber in Spintop^{TM} series (www.vortexventures.com).

3.7.4.2 Length of the Cylinder and Cone

Reviewing the works of many researchers, Bradley (1965) concluded that increase in overall length gives an increase in both capacity and efficiency. While the cylindrical section may be omitted, the conical section is necessary:

- To compensate the loss of momentum due to the fluid lost inwards, while vortex moves downward and thereby maintain similarity of tangential velocity profiles at all levels within the cone

- To reduce secondary circulation flows unlike in wide-angle cyclone, hence to attract more fines towards underflow

After investigating with a family of narrow angle long cyclones, Bradley (1965) found the role of the length of the cyclone cylinder mere for housing purpose, which in practice varies from $0.67D_c$ to $2D_c$. Rietema (1961) suggested a length of $0.2D_c$ for the cylindrical part and an overall length of $5D_c$ for his optimum geometry.

A review of hydrocyclone in practice shows the total length to vary from 2.7 to $7.7D_c$ Svarovsky (1984). A recent study carried out in 82 mm dia hydrocyclone using Rietema's optimum geometry Chu et al.(2000) found the optimum length of the cylindrical section as $1.6D_c$.

3.7.4.3   Cone Angle

The capacity increases, while the pressure drop goes down due to increase of the length of the hydrocyclone by reducing the cone angle   (Dahlstrom 1949 ;Bradley,1965).Changing cone angle from 20^0 to 15^0 , Dahlstrom (1949) found the capacity to increase by 16%. Bradley observed capacity increase by 33 per cent by reducing cone angle from 20^0 to 9^0 (Fig. 3.18).

Loyola et al.(1996) found the sizes of fully trapped particle by underflow as 20 and 4.5 μm respectively in *2D2D* and *1D3D* cyclones. Better separation efficiency was observed in a double-cone cyclone (Krebs Engineers, 2000).

The conventional, narrow angle hydrocyclones usually vary from 6^0 to 25^0 for solid liquid separation and as small as 1.5^0 for liquid-liquid separation. Othmer (1980) reported that smaller cone angles are more usual on high efficiency units. Svarovsky (1984) found better sharpness with larger cone angles and suggest the largest angle as 25^0.
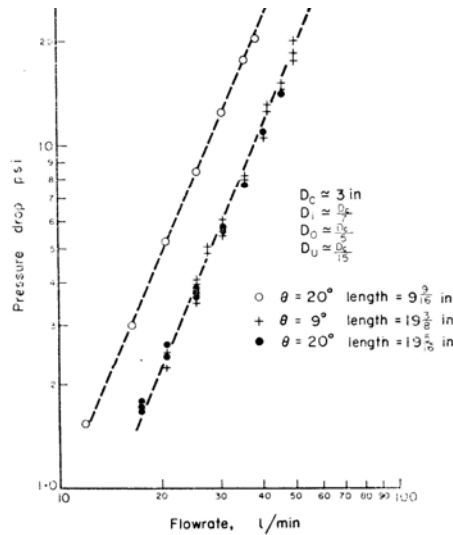
Fig. 3.18   Pressure drop versus capacity for cyclones of different length and cone angle (Bradley, 1965)

3.7.5   Effect of Underflow Configuration

3.7.5.1   Geometry
The flow and solid discharge pattern are dependent on the geometry of the underflow outlet, which will decide the mode of collection of underflow discharge.   It also influences the performance of hydrocyclone. Discharge through a narrow and converging geometry leads to a

rope like discharge at underflow, whereas a diverging type or open exit configuration gives a spray type of discharge.

Improved performance of the hydrocyclone is found due to the diffusive type of underflow geometry (Arato,1984). Greater tangential velocity and thereby better performance is found by eliminating air core in a water sealed hydrocyclone (Luo et al et al.,1989). This also leads to lesser susceptibility of blockage of the apex due to the higher ratio of apex to vortex.

Chu et al. (2000) have studied five different geometries of underflow: conventional; 20^0 and 30^0 diffusers recommended by Arato(1984); straight pipe with cone; and, straight pipe with water sealed tank recommended by Luo et al. (1989). Reduction of cut size by 8 μm compared to that in a conventional hydrocyclone was found in a straight pipe with cone and water sealed underflow setups.

3.7.5.2   Diameter
As the flow ratio is one of the main parameter for classification of feed, underflow plays a vital role in a hydrocyclone. The minimum size of the underflow aperture is fixed based on the amount and size of the solids to be separated and the amount of water entrained in the pores. In practice, it is preferable to oversize the underflow and to do the final adjustment during operation to provide desired solid concentration. A normal underflow diameter size is in the range of $D_c/10$ to $D_c/5$ with a control valve to give a further possible reduction in cut size and increase solid concentration by at least a factor of two (Bradley 1965). Storch (1979) recommends a range between 0.18 and 0.40 the higher ratios being common on the larger cyclones. Bradley recommended an underflow aperture as $D_o/3$ (with $D_o=D_c/5$) for his optimum geometry for his 75 mm dia hydrocyclone.

3.7.6   Effect of Central Insertion

Although the early researchers such as Bradley (1965) and Rietema (1961) argued that the formation of the air core is necessary to have stability of vortex flow, its negative effect on capacity of cyclone and energy consumption have been pointed out by recent studies. Inserting a 6.75 mm diameter thin solid insert in the center of an 82 mm diameter hydrocyclone with thicker vortex finder wall of 12 mm internal diameter, Xu et al.(1990a, 1990b) were able to

eliminate the forced vortex (air core) and studied its behavior. Both the tangential velocity and its gradient were increased, whereas the radial velocity was reduced compared to that in the conventional setup with forced vortex. The other significant improvement they noticed was the reduction of relative turbulence level both in radial and tangential direction. These results implied a better separation and hence a smaller cut size.

Xu et al.'s postulation was further investigated by Lee & Willliams (1993) carrying out investigations in a 44 mm dia Mozley's cyclone with varying size of the inserts, vortex finders as well as operating variables and noticed a maximum increase of volumetric throughput by 44 per cent compared to that in conventional setup. Further study by Chu & Luo (1994) in a 75mm diameter hydrocyclone installing a vortex finder attachment with special form and a cone below it found an improvement of sharpness index (d_{35}/d_{65}) from 0.176 to 0.702 but an increase in cut size from 19 μm to 44 μm. Later, Chu et al.(1996) have found that the energy consumption in a hydrocyclone can be significantly reduced by reducing turbulence level.

In a new Spintop^{TM} series, Vortex Ventures (www.vortexventures.com) have introduced a solid core below the vortex finder and found the core to promote a more constant rotational velocity (stable flow) between the primary and secondary vortices and eliminated the unstable fluctuating air core in a conventional design.

More recently Chu et al. (2000) studied the efficiency of hydrocyclone with the insertion of different geometries together with the structural modification of other components. Five different insertion geometries considered were: conventional; solid core (Xu et al. 1990) ; central cone (Chu et al. 1994); inner diffuser; and, a winged core.

Although the performance due to all types of insertions resulted in enhancement of the key performance indicators, the winged core was found to be the best one. The energy loss was found to be mere 51 per cent compared to that in a conventional cyclone resulting an increase in feed and overflow capacities by 35 per cent and 15 per cent respectively. Although the d_{50} was found to be slightly coarser (33.66 μm against 31.73 μm), higher separation sharpness indicated better elimination of coarser particles than that in conventional hydrocyclone, which

is more desirable in reducing the wear and tear of hydro mechanical equipment and accessories.

The performance improvement of the hydrocyclone with the insertion of central winged core argued by Chu et al. (2002) is that the forced vortex in the inner helical flow is broken up by the insert leading to better control of turbulence and energy loss.

3.7.7 *Effect of Cyclone Inclination*

The effect of inclination of hydrocyclone on its performance was studied by Asomah & Napier-Munn (1996) in 102 and 508 mm diameter hydrocyclones by changing the angle of inclination of cyclone axis from 0^0 to 135^0 (with respect to vertical axis). Solid concentration varied from 22 to71 percent (w/w) in the larger cyclone while that varied from 30 to 50 percent in the smaller one.

Their results in both the cyclones showed d_{50} to be in very weak dependence with the cyclone inclination below 45^0 for all feed concentration. However beyond this limit d_{50} increased quite rapidly, the stronger relation being on the larger cyclone with higher concentration . Other finding they observed was the increase in d_{50} with the increase in feed concentration for all cyclone inclinations. The other interesting result they observed is the increase of recovery of solids to underflow with the inclination of cyclone.

Further study carried out by Rong & Napier-Munn (2003) also confirmed above findings. The results obtained from a 200 mm diameter, modified geometry under different inclinations showed increased sharpness and recovery but reduced flow ratio. The reduced flow ratio nearly compensates the decreased feed flow, the cut size doesn't change significantly (54 μm instead of 53 μm) while cyclone is positioned in 75^0- 80^0 .

The question arises as to what is the contributing factor for better solid recovery when the fluid mixture has to travel against the gravity, which causes decrease in tangential velocity thereby reducing the centrifugal force. As the cyclones have been operated under high pressure, it indicates generation of much higher centrifugal force as compared to gravity. Therefore, the

effect of gravity on tangential velocity has been insignificant. But on the other hand, since the downward axial velocity has been diminished with the inclination of the cyclone, the particles are subjected to longer residence time, which causes higher degree of separation. As the apex is subjected to lower pressure with the inclination, larger spigots can be designed to achieve the split ratio, which is helpful in reducing the risk of apex blockage.

3.7.8   *Optimum Geometry of Narrow Angle Hydrocyclones*

This group of design is the most widely used cyclones in the industry. They are characterized by relatively long cyclone body length and included angles of the cone of less than 25^0. Such cyclones are capable of operating at low cut size and suitable, where high mass recoveries are desirable (Svarovsky, 1984). The parameters and scale-up constants of the optimum geometries suggested by well known researchers and manufacturers are presented in Table 3.1 (Svarovsky,1984; Krebs Engineers,2000).

Table 3-1   Characteristic parameters of geometries and respective performance constants of wellknown hydrocyclones

Authors	Parameters						Scale-up constants			Running cost criteria
	$D_{c\ (mm)}$	D_i/D_c	D_o/D_c	l/D_c	L/D_c	Cone angle, deg	$Stk_{50}.Eu$	K	n_p	$Stk_{50}^{4/3}.Eu$
Rietema	75	0.28	0.34	0.40	5.00	20	0.0611	316	0.134	2.12
Bradley	38	0.13	0.20	0.33	6.85	9	0.1111	446.5	0.323	2.17
Mozley	44	0.16	0.25	0.57	7.71	6	0.1508	4451	0	4.88
D15LB-T Krebs Engineers	381	0.23	0.31	0.12	6.84	10.5	na	na	na	na
gMax-Krebs Engineers	381	0.23	0.31	0.12	6.4	18 and 6	na	na	na	na

3.8   Effect of Operating Variables on Efficiency of a Hydrocyclone

3.8.1   *Effect of Feed Flow Rate*

Bradley & Pulling (1959) and Plitt (1976) has found to increase the separation efficiency with the increase in feed flow rate in accordance with the relationship:

$$d_{50} \propto \frac{1}{Q^n}$$

where, n varies from 0.45 to 0.64. However for an extremely low pressure cyclone ($h<1.5m$), where G force < 1, Shakya (2004) have shown the separation efficiency to be decreasing with the increase in feed discharge.

Similarly, the total flow increases with the increases in pressure difference in accordance with the relationship:

$$\Delta p \propto Q^n$$

where, n from different relations, varies from 2.0 to 2.6 for dilute suspensions and as low as 1.78 with higher concentration (Bradley,1965).

3.8.2   Effect of Pressure Drop

Increase in pressure drop usually leads to : higher throughput, smaller d_{50} ,increase in total efficiency and decrease in R_f. The capacity of the cyclone is increased with the increase in pressure drop with an exponent varying from 0.38 to 0.56. Increase in pressure drop generates greater tangential velocities, and thus leads to higher separation efficiency. This means that the grade efficiency curve moves to the left, to finer sizes, and the cut size reduces. The pressure drop has significant effect and has most stable relation in the following form:

$$d_{50} \propto \frac{1}{\Delta p^{0.25}}$$

The range of pressure drop in common use is 3.5 m to 35 m with the lower limit dictated by vortex stability and the upper limit largely by economy The upper limit 'economy' are decided by pump availability and cost, and in many applications by wear (Bradley, 1965).

3.8.3   Effect of Concentration

The concentration has three major effects on cyclone performance. Firstly, that of causing hindered settling and departure from Stokes' Law; secondly, that of causing even higher concentrations near the apex area of the cone resulting in the alteration of character of the underflow stream; and thirdly, that of causing a change in pressure drop or capacity.

The effects of hindrance on performance are negligible below a feed concentration of 11 per cent (v/v) or 25 per cent (w/w) for a solid of density as 2700 kg/m^3 with spherical or nearly spherical material in suspension (Fontein & Dijksman, 1952). Other limits, as high as 17 per cent (v/v) by Zhevnovatyi (1962) and as low as 2 per cent (v/v) by Rietema (1961) have been reported.

The change in concentration may lead to the change in discharge pattern through the underflow, which may cause severe reduction in removal efficiency. Dahlstrom (1949), who for otherwise identical experimental conditions obtained gross efficiencies of 61.7 per cent and 7.3 per cent for vortex and overloaded discharge respectively.

Fortunately, in water projects, the effect of concentration on performance efficiency may not be severe as the sediment load in the river hardly exceeds 1-2 per cent (v/v). And removal of solid by 50 percent with R_f as 0.10 results in about 5-10 percent (v/v), which will not alter the flow pattern. Further, as the weak relations between the concentration and flow rate as well as concentration and hindered settling are observed for low concentrations, any profound effect on these parameters is not envisaged.

3.8.4 *Effect of Feed Density*
The density of the fluid mixture play an important role as the separation depends on density difference. The relationship that arises from Stokes' Law and experimentally confirmed for cyclones > 75 mm is (Dahlstrom,1949):

$$d_{50} \propto \frac{1}{(\rho_s - \rho)^{0.5}}$$

3.8.5 *Effect of Split and Flow Ratio*
It can be concluded that the flow ratio, R_f or the volume split, S depend very little on the pressure drop and in practice this effect is often neglected. As pointed out earlier, control of underflow plays a vital role in the overall control of a hydrocyclone. Each can be achieved either by changing the size of the underflow orifice or by changing the back pressure on either or both of the outlet streams. Most authors find the volume split proportional to the ratio

$$S \propto \left(\frac{D_U}{D_O} \right)^n$$

where n varies from 3 to 4.4 and has strong effect on cut size and separation efficiency. Comparing the relations given by various authors, Svarovsky(1984) has found the following correlation between reduced cut size and flow ratio:

$$d_{50,c} \propto (1 - R_f)^{0.5}$$

4 EXPERIMENTAL INVESTIGATIONS

The present research was carried out by installing laboratory test rigs consisting of hydrocyclones of two different diameters and geometries. The smaller hydrocyclone having a diameter of 0.22 m was investigated during Jan-Jul 2005 in the Hydraulic Laboratory of Institute of Engineering (IOE), Nepal. Whereas the experimental work in a larger hydrocyclone of 0.38 m diameter with a double cone configuration was carried out during Mar- Dec 2006 in the Hydraulic Laboratory of Norwegian University of Science and Technology (NTNU), Norway.

The hydrocyclones having a cylindrical chamber connected to a conical bottom were investigated. The sizing and proportioning of the hydrocyclone were carried out based on the information due to Bradley (1965), Rietema (1961) and commercial cyclone manufacturers such as Krebs Engineers. The hydrocyclones were kept vertical throughout the experiment. Fiberglass was primarily used for fabricating the hydrocyclones. Nevertheless, the cylindrical chamber including the inlet and outlet part of the larger hydrocyclone were made up of transparent acrylic sheet in order to have better visualization of hydraulic phenomena in the hydrocyclone. The experiments were conducted in pressurized rigs for a turbulent flow under steady flow conditions.

4.1 Investigation in a 0.22 m dia Hydrocyclone

Although the application of hydrocyclone is common in industries, it is very little known in the field of Civil Engineering. Neither the relevant literature was available in Nepal nor the specific shortcomings of the hydrocyclone were known to the researcher. Therefore, the objective of the installation of the first test rig was to study the flow phenomena, its performance and the specific shortcomings of the hydrocyclone particularly relevant to the water projects.

4.1.1 Design of a 0.22 m dia Hydrocyclone

The size of the hydrocyclone was decided considering two criteria. First, achieving the sediment simulation close to real-world problems, thereby minimizing scale effect of

sediment particles. Second, considering the available static head, discharge and space availability in the laboratory. Accordingly, the diameter of the hydrocyclone tested at IOE was chosen as 0.22 m, size capable of excluding most of the sand fraction as well as coarser silt (Arterburn, 2002, Olsen & Turner, 2004, Kelly & Spottiswood, 1980).

The geometry of the hydrocyclone was chosen as a cylinder in the upper part followed by a conical section in the bottom. A circular cylindrical chamber made up of fiberglass having an internal diameter as 0.22 m was adopted. The bottom of the chamber was given a cone angle of 22° to facilitate the sediment movement toward the underflow outlet and create stronger vortex motion in the chamber. Both the cylindrical and conical chambers were 0.44 m high. The underflow outlet pipe had an internal diameter of 0.05 m for flushing out the sediment moving along the wall of the hydrocyclone. The overflow outlet conduit (vortex finder) provided with internal diameter of 0.11 m was inserted 0.14m inside the chamber to the opposite side of the underflow outlet. Other characteristic parameters pertaining to the geometry and setup are presented in Fig. 4.1 and 4.2 as well as Table 4.1.

4.1.2 Experimental Setup of a 0.22 m dia Hydrocyclone

The flow into the hydrocyclone chamber was admitted tangentially through an inlet conduit of 0.063 m without any acceleration (Fig. 4.2). In order to have less interference with the liquid inside the chamber, the latter was connected through a narrow but deep rectangular inlet section. The inlet pipe was kept horizontal to the axis of the hydrocyclone. The discharge passing through the overflow outlet was discharged to the collection tank without any deceleration of the flow. An adjustable stand was used for supporting the equipment

The discharge to the hydrocyclone was supplied by a pump. The pump received required amount of flow from nearby tank having fairly constant water level. Three gate valves were used to control the discharge in the system. The first gate valve was installed at the discharge exit of the pump. Whereas the second and third gate valves were installed at the exit points of overflow and underflow conduits. The discharge passing through the system as well as the respective outlets could be varied by manipulating these valves.
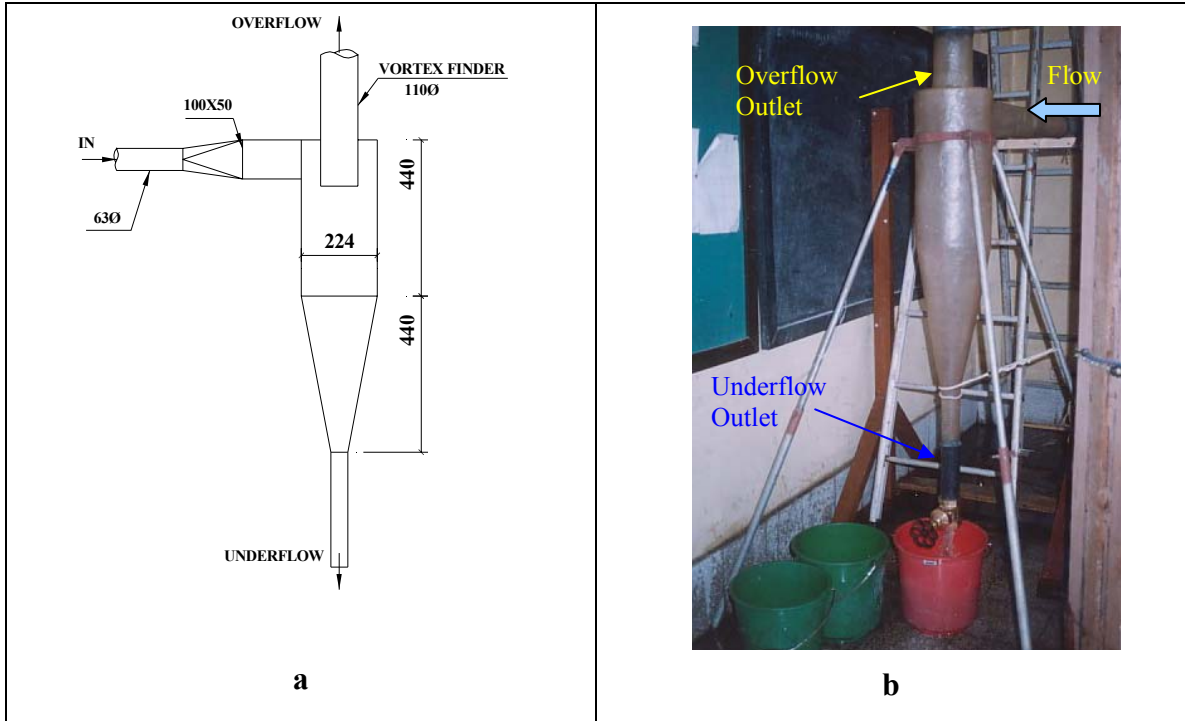
Fig. 4.1 The geometry of the 0.22 m dia hydrocyclone a) schematic view b) prototype view
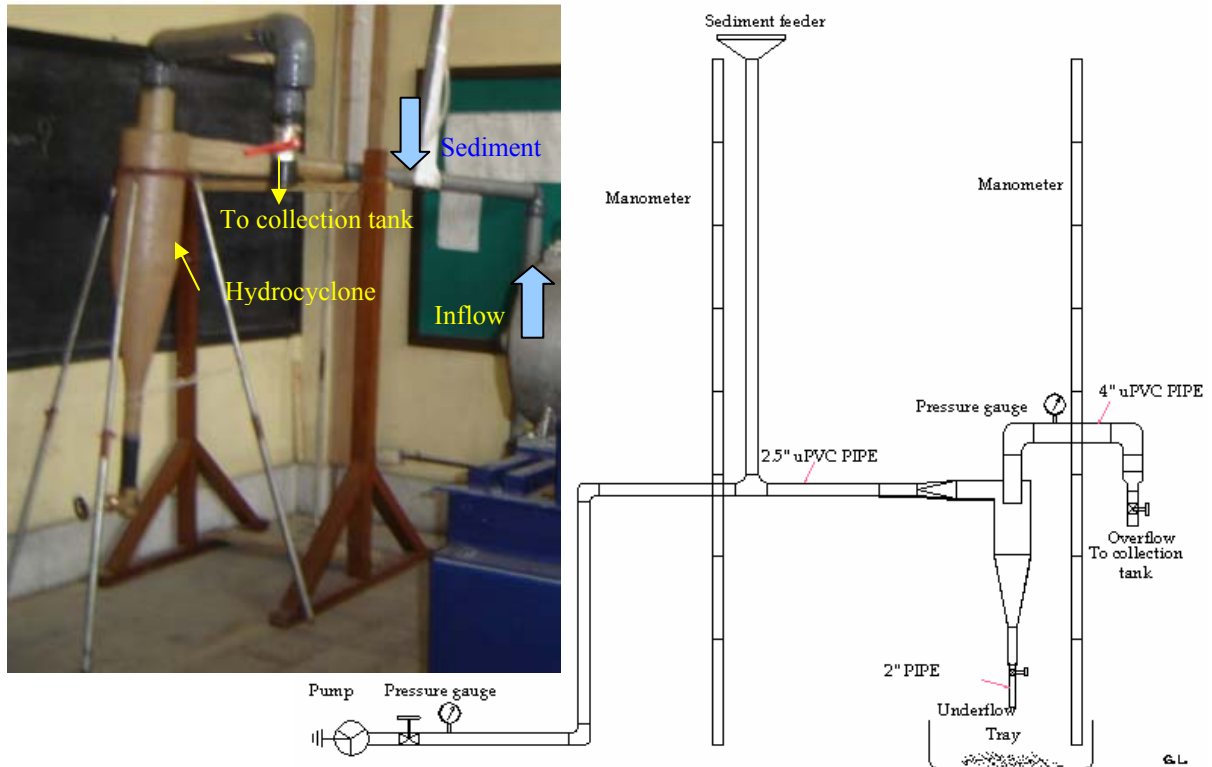
Fig. 4.2 Laboratory setup for 0.22 m dia hydrocyclone. Left: Prototype view, Right: Schematic sketch

Piezometers were installed near the inlet, outlet and along the conveyance conduits to measure the pressure head during each test run (Fig. 4.2). A sediment-feeding device consisting of a hollow circular PVC pipe of 0.063 m diameter connected to a funnel was used for feeding sediment into the test rig. Sediment feeding system being open and located only few meters above the inlet conduit, it was inconvenient to conduct the tests with higher inlet pressure. Further, all the sediment fed into the system could not reach the inlet of the hydrocyclone, the velocity in the feeding conduit and thereby the shear stress being not sufficient to transport coarser particles. Therefore, the test rig was later modified to incorporate a pressurized sediment feeding box.

4.1.3 Testing Procedure

The sediment removal efficiency of the hydrocyclone was studied for different flow conditions and sediment characteristics by systematically varying inlet, overflow and underflow discharge (Table 4.1). The discharge, head and sediment characteristics were considered as the main operating variables, whereas the parameters related to the geometry of the hydrocyclones and its components were assumed to be the design variables.

65 tests were conducted in a pressurized state for a turbulent flow under steady flow conditions. The velocity in the inlet varied from 0.10 m/s to 1.03 m/s, whereas the same in the outlet varied from 0.033 m/s to 0.40 m/s. Discharge from the underflow and overflow conduits were noted at the beginning of each test run. Properly dried cohesion less sediment was used in the experiment. The sediment in the system was fed once the steady flow in the system was maintained. Sediment having different particle size distributions was used in the experiment (Fig. 4.3). Attempts were made to maintain a fixed concentration by feeding sediment with constant rate. The observation continued for 5-10 min until the overflow tank was filled up.

The discharge together with the sediment passing through the underflow and overflow conduits were collected in separate tanks and allowed to settle for some duration. Clear water was drained out and the sediment settled in the respective tanks was collected. The sediment thus collected was properly dried and weighed. Sieve analysis of the samples

from each test was carried out to find out the grain size analysis and to ascertain the removal efficiency.

Table 4-1   Characteristic parameters of geometry and test runs of 0.22 m dia hydrocyclone investigated

Parameter	Unit	Symbol	Dimension
Diameter of hydrocyclone	m	D_c	0.22
Height of cylindrical part	m	h_{Dc}	0.44
Cone angle	deg	α_1	22^0
Height of first conical part	m	h_{c1}	0.44
Inlet discharge	l/s	Q_i	0.30-7.81
Underflow discharge	l/s	Q_u	0.03-.48
Flow ratio (Qu/Q)	%	R_f	0.48-18.63
Velocity in the inlet	m/s	Vi	0.10-1.03
Velocity in the outlet	m/s	Vo	0.033-0.40
Headloss	m	h_L	0.05-3.0
Sediment concentration, feed	ppm	C_i	1287-5092
Sediment concentration, overflow	ppm	C_o	8-942
Sediment concentration, underflow	ppm	C_u	734-186116
Particles size range	μm	d	65-1000
Median Particle size range	μm	d_{50}	76-397

Specific gravity of sediment
    Bulk
    Finer
		γ_s/γ	1.99-2.68
			2.5-2.7

Number of tests carried out	No		65

Although the sediment used in the test was quite fine, coarser particles in some tests, particularly with smaller flows were not reported to the discharging outlets. Therefore, the sediment recorded in the collection tanks was considered as the total sediment input to the hydrocyclone and subsequent estimation of the sediment concentration for each test. Whereas the sediment removal efficiency, E of the hydrocyclone was calculated using the following relationship

Fig. 4.3   PSD of sediment used in the tests

$$E = \frac{q_{su}}{q_{su} + q_{so}}$$

Eq- 4.1

where, q_{su} = amount of sediment received from underflow per unit time

q_{so} = amount of sediment received from overflow outlet per unit time

4.2　Investigation of a 0.38 m dia Hydrocyclone

4.2.1　Basis of Installation of a Larger Test Rig

The investigation in a 0.22 m dia hydrocyclone led to a better understanding of flow phenomena as well as particles separation characteristics of the hydrocyclone. It was found that the method of particles separation due to centrifugal action is superior than that due to gravity (Chapter 5). Nevertheless, the following shortcomings were observed in the smaller rig, which led to the installation of a larger rig:

- Poor hydraulics was observed near the inlet area, resulting in a significant headloss between the inlet point and the beginning of the cylindrical part of the hydrocyclone.

- The headloss in a high velocity zone such as in a hydrocyclone is highly influenced by the hydraulics of the approach conduits. Since the conduits of constant sectional area were used near the inlet and outlet regions, the effect of gradual acceleration and retardation of flow on the hydrocyclone could not be understood.

- The performance of only the hydrocyclone could be understood from the test rig. The test rig simulating part of the headrace of a water project along with the hydrocyclone/s would give a picture very close to the reality.

- As the flow used in the smaller rig was much smaller than that to be used in the water projects, the behavior of the finer particles didn't give a picture closer to real-world situation.

These underperformances of smaller hydrocyclone called for the installation of a test rig consisting of a larger hydrocyclone and further investigation. A test rig simulating part of the hydropower system of a headrace conveyance of a typical hydropower system (Fig. 4.4) was thus designed to improve the performance of the hydrocyclone.
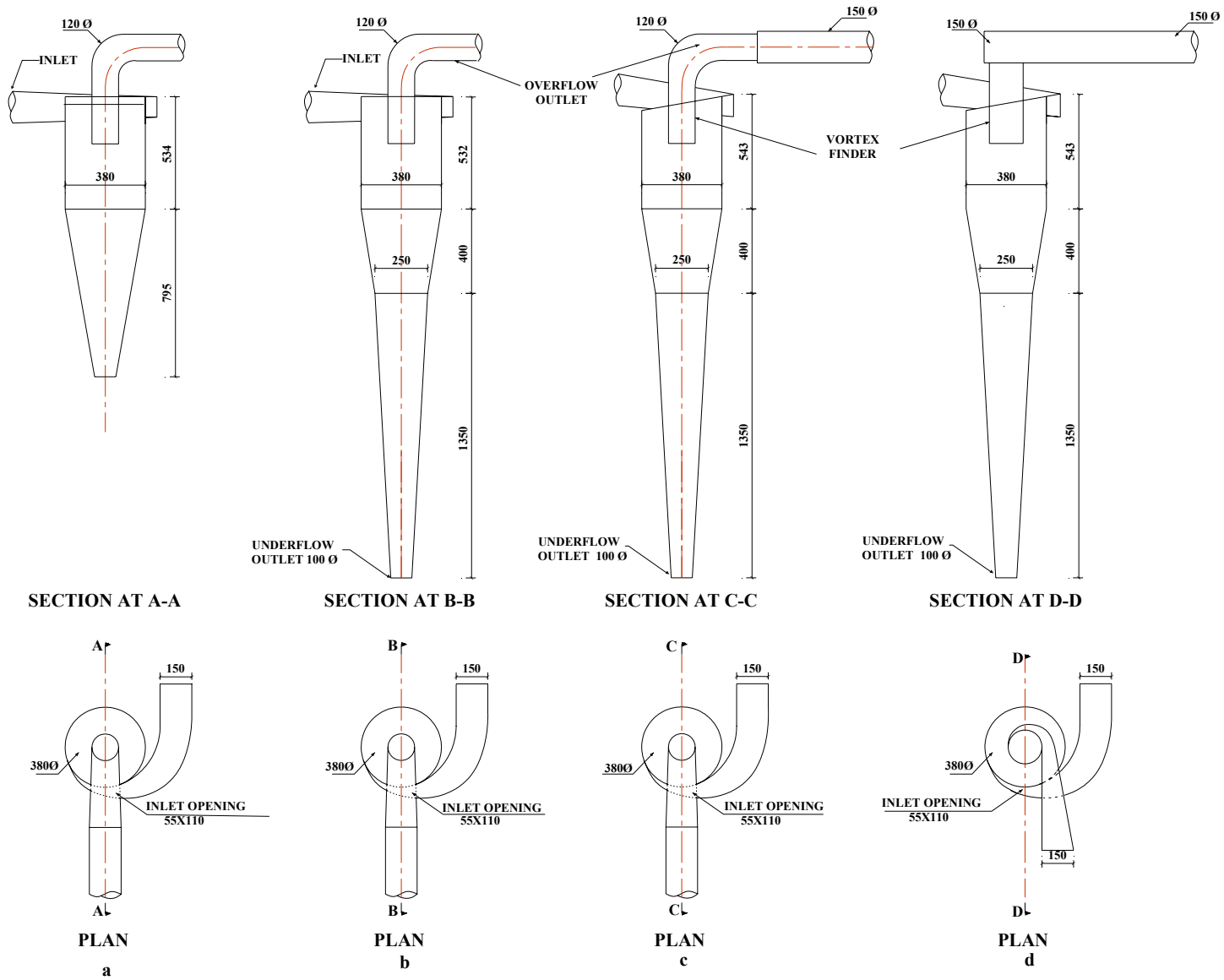
Fig. 4.4 Geometries of existing (a,b) and modified(c,d) hydrocyclones a) Standard hydrocyclone (b) Double cone hydrocyclone, gMax series of Krebs Engineers (c) Modified hydrocyclone with inclined inlet and axial outlet (d) Modified hydrocyclone with inclined inlet and tangential outlet.

4-7

4.2.2 Design of Hydrocyclone with Axial Setup

As the gMax series of Krebs Engineers have been found to be the better geometry in terms of particle separation efficiency, it was considered as principal reference geometry. The hydraulics of the conventional hydrocyclone (gMax series) was enhanced by introducing modification to inlet, outlet and roof of the device. The approach flow to the inlet was gradually accelerated by contracting 0.26 m wide square conduit at the headrace conveyance to 0.055 m wide and 0.11 m high rectangular section at the inlet opening of the hydrocyclone (Fig. 4.4.c & 4.5). Similarly, the high velocity flow leaving the cyclone was retarded to normal velocity. This was achieved by gradually enlarging 0.12 m diameter vortex finder at the axial overflow outlet to 0.26 m wide square conduit at the receiving conduit. The vortex finder was inserted 0.19 m inside the chamber to the opposite side of the underflow outlet. Inclined, involute type of inlet geometry was identified to streamline the flow inside the hydrocyclone.

Additionally, the roof of the hydrocyclone was also designed with inclined profile to further streamline the flow and minimize the short circuiting effect. The geometry of the remaining part of the device was similar to that of gMax profile (Krebs Engineers, 2000). The diameter of the 0.5 m high cylindrical part of the hydrocyclone was adopted as 0.38m, which was followed by conical section of two different cone angles. The upper conical part, 0.4 m high with a cone angle of 18^0 was followed by a 1.35 m long second conical section having a cone angle of 6^0 and terminating into an underflow outlet of 0.10 m internal diameter. The size and geometry thus chosen are capable of excluding most of the sand and coarser silt particles (Arterburn 2002; Turner and Olsen, 2004). The design also complies with available static head, discharge and space in the laboratory. Sectional and plan views of modified hydrocyclone along with Standard and gMax series hydrocyclone are presented in Fig. 4.4.

4.2.3 Experimental Setup

The discharge from the hydraulic system of the laboratory was admitted through a PVC pipe 0.20 m in diameter to a 3.0 m long square conduit of 0.26 m in size. From the center of the box the discharge was diverted to the hydrocyclone through a pipe 0.15 m in

diameter. A control gate was installed at the end of the feeding conduit to regulate the split proportion of flow. The discharge passing from the overflow was received in a conduit, identical to the feeding conduit. A gate valve was provided at the end of the receiving conduit to control the flow and maintain the desired pressure in the system. The discharge passing from both the outlets was collected in separate reservoirs.

Table 4-2   Characteristic parameters of geometry and test runs of 0.38 m dia hydrocyclone

Parameter	Unit	Symbol	0.38 m dia axial outlet	0.38 m dia tangential outlet
Diameter of hydrocyclone	m	D_c	0.38	0.380
Height of cylindrical part	m	h_{Dc}	0.50	0.50
First Cone angle	deg	α_1	18	18
Second Cone angle	deg	α_2	6	6
Height of first conical part	m	h_{c1}	0.40	0.40
Height of second conical part	m	h_{c2}	1.35	1.35
Variation of underflow aperture	mm	D_u	15 - 60	15 - 60
Inlet discharge	l/s	Q_i	10.4 - 19.9	15.0 - 23.70
Underflow discharge	l/s	Q_u	0.7 - 3.5	0.45 - 2.8
Underflow/inlet discharge	%	R_f	3.5 - 25.5	1.12 - 25.50
Velocity in the inlet	m/s	Vi	1.72 - 3.32	2.49 - 3.78
Velocity in the outlet	m/s	Vo	0.82 - 1.90	1.33 - 2.18
Headloss	m	h_L	1.16 - 3.94	1.6 - 3.8
Sediment concentration, feed	ppm	C_i	97 - 4,295	65 - 7,618
Sediment concentration, overflow	ppm	C_o	28 - 93	53 - 238
Sediment concentration, underflow	ppm	C_u	160 - 57,702	9,623 - 166,837
Particles size range	μm	d	0.4 -1000	I: 0.40 -1000 II : 0.40 - 340
Median Particle size range	μm	d_{50}	200.4	I: 200.4 II : 99.7
Specific gravity of sediment *Bulk* *Finer*		γ_s/γ	1.99-2.68 2.5-2.7	1.99-2.68 2.5-2.7
Number of tests carried out *Hydraulic* *With Sediment*	No	NA	75 26	58 17

NA: not applicable

The sediment into the system was injected through a sediment feeding box by creating a differential pressure between the feeding box and the test rig. Two electronic flow measurement valves (EMV) were installed to monitor the discharge entering the system and leaving through overflow conduit (Fig. 4.5). The discharge passing through the underflow was read from a rating curve established for the collection tank. Piezometers, P_1 to P_7 (Fig. 4.5, plan) were installed in seven different locations along the conveyance to monitor the pressure and headloss during each test.
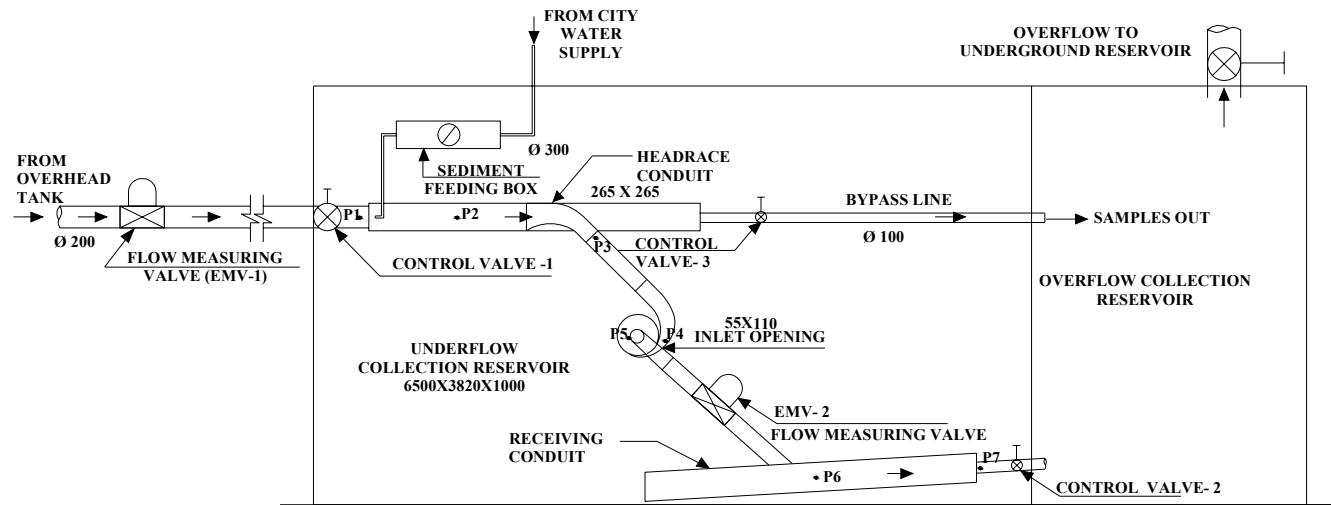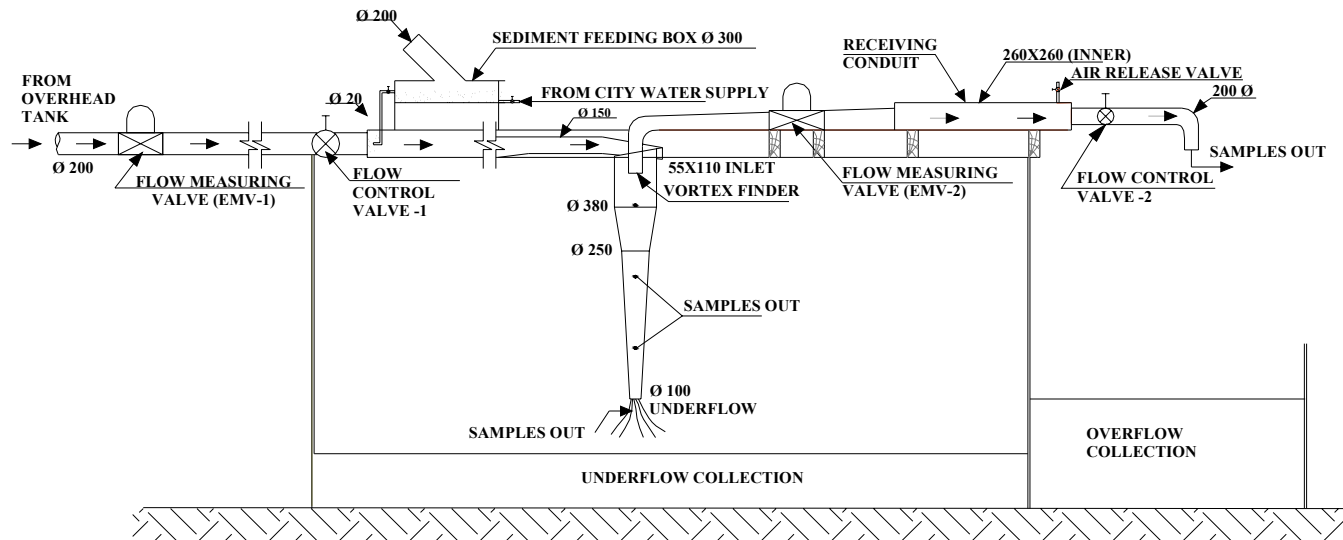
Fig. 4.5. Plan and Elevation of experimental setup: Plan view of general arrangement (top) & Sectional elevation along the conveyance (bottom)
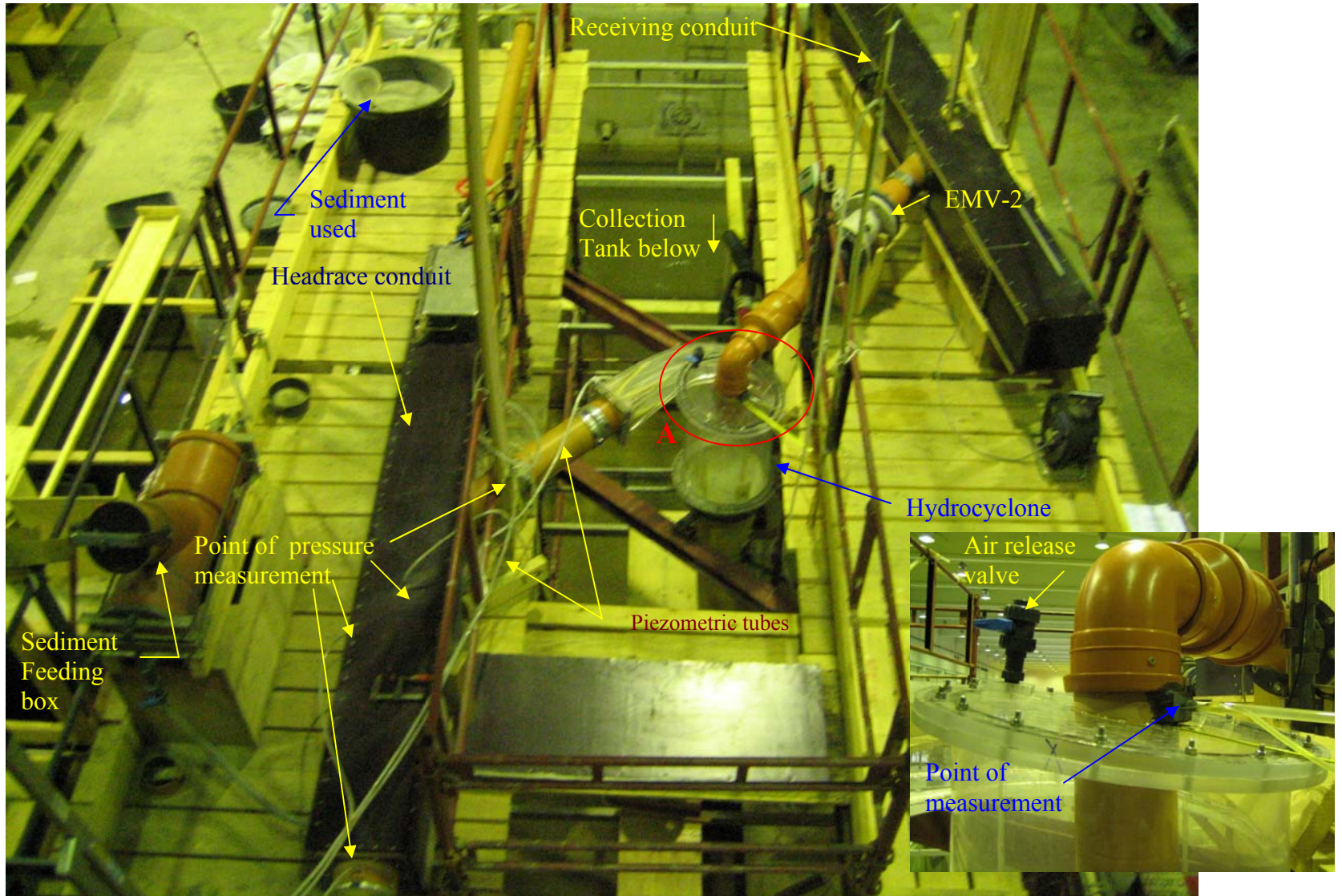
Fig. 4.6. General arrangement of experimental setup in laboratory

4.2.4 Testing Procedure

The testing procedure applied in the larger rig was similar to that adopted in the smaller rig. The sediment removal efficiency of the hydrocyclone was studied for different operating conditions and design variables (Table 4.2). The velocity in the inlet varied from 1.72 m/s to 3.32 m/s, whereas the same in the outlet varied from 0.82 m/s to 0.1.90 m/s. 75 tests were conducted without feeding sediment to assess the hydraulic performance of the hydrocyclone and the test rig, which was followed by 26 tests using two batches of sediment with different particle size distributions (Fig. 4.7).

Properly dried cohesion less sediment was used in the experiment. Attempts were made to maintain a fixed concentration in the rig by applying a constant pressure in the sediment feeding box. The sediment was injected into the system due to differential pressure between the system and the sediment feeding box. Each test continued until the sediment feeding box was emptied.

The duration of the experiment varied from 2.25 min to 11.50 min depending upon the amount of sediment and discharge chosen for particular test. The samples were collected from each discharging units before the discharge was admitted to the respective containers. The discharge together with the sediment passing through the underflow, overflow and bypass conduits were collected in separate tanks and allowed to settle for some duration. Clear water was drained out

Fig. 4.7 Particle size distributions of sediment fed into the system

and the sediment settled in the respective tanks was collected. All the sediment received in the overflow, underflow and bypass containers was collected in first three test runs and compared with that obtained from the samplers .to check the reliability of the data obtained from the samplers. The samples thus collected were properly dried and weighed. The particle size distribution (PSD) analysis of fine particles, especially in the silt and clay range obtained was carried out using coulter LS 230, a device working on laser diffraction principles.

Like in the smaller rig, coarser particles in some of the tests, particularly those conducted under smaller flows were not reported to the discharging outlets. Therefore, the sediment recorded in the collection tanks was considered as the total sediment input.   Sediment removal efficiency was computed using the relation given by Eq. 4.1.

4.2.5   Design of Hydrocyclone With Tangential Setup

Basis of Modification of Test Rig

Due to the improved design of geometry of the hydrocyclone and the test rig, the hydraulic and sediment removal efficiency of the larger test rig was found much better than that due to the Standard cyclone as well as conventional gMax series. However, there was a considerable amount of energy (head) lost at the exit area of the hydrocyclone, (Chapter 5.3.2). If recovered, this energy could be utilized for processing additional amount of flow through the same cyclone. Therefore the improvement to the hydrocyclone was made to minimize this loss by modifying the geometry of the hydrocyclone, particularly at the overflow outlet.

The Hypothesis for Modification of Outlet

Most of the energy in the flow in the headrace conduit before diversion to the hydrocyclone is retained in the form of potential energy. With gradual acceleration of the flow, part of this energy is converted to the kinetic energy. While this energy before entering the hydrocyclone remains in the form of axial velocity, it is retained in the form of tangential, axial and radial velocity components, once the flow enters into the hydrocyclone. Once it approaches the central region and the region of vortex finder, the radial component gradually vanishes, while the axial and tangential components get stronger. The velocity components are 2-3 times larger compared to that at the inlet of the hydrocyclone. Moreover, the tangential (spinning) component is usually larger by 2.0 -3.3 times than the axial components (Kelsall,1952). While the most of the energy is lost due to turbulence and friction while passing the flow through the hydrocyclone, significant amount of energy was still retained in the form of kinetic energy (velocity component) near the upper outlet of the hydrocyclone. And like in the headrace conduit, the energy in the receiving conduit is retained mostly in the form of

potential head. Therefore, most of the energy retained in the form of velocity component near the upper exit is converted to the potential energy before joining the receiving conduit.

Since an axial overflow outlet was adopted, the energy retained in both the velocity forms should be converted ultimately to the axial form. Further, the distance between the overflow outlet zone and the collecting conduit is only about 2.0 m and no devices involving major headloss are installed in this area. As the energy retained in the form of axial component shouldn't be lost considerably in a gradually expanded axial outlet, the above facts suggest that there must be a significant headloss during the conversion of energy retained in the tangential form to the axial form. Therefore, the following hypothesis was postulated. *" If the geometry of the overflow outlet of the hydrocyclone is similar to that of the inlet, most of the energy lost in the axial outlet can be regained"*. The geometry was designed accordingly and such an arrangement was named as a 'tangential setup'.
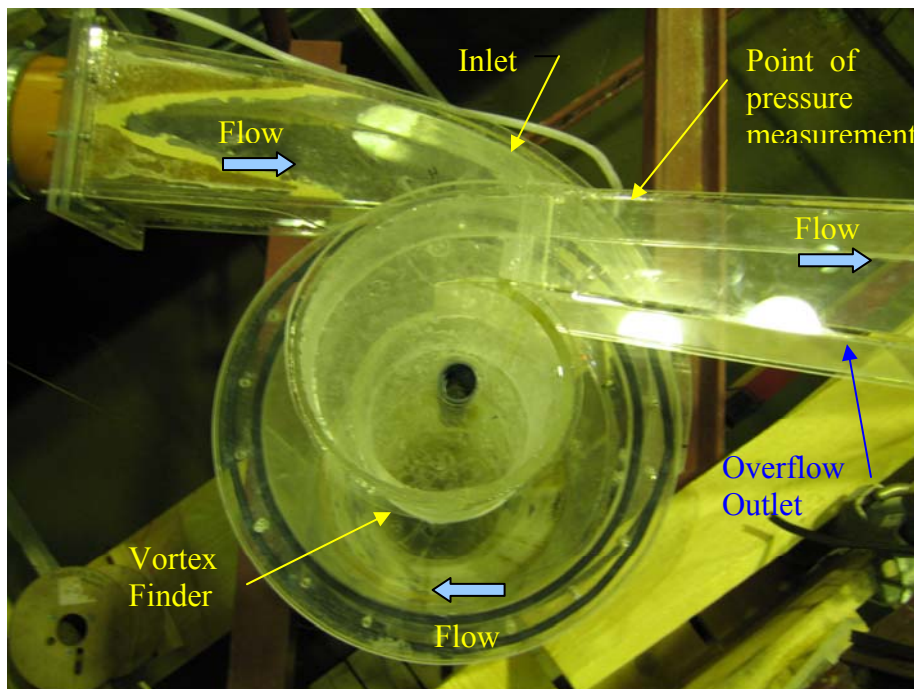
Fig. 4.8 Laboratory view : Modification of axial overflow outlet to tangential setup

4.2.6   *Design of Hydrocyclone With Tangential Setup*
The principal geometry of the hydrocyclone for tangential setup remained same as that of the axial setup except for the geometry at the overflow outlet. Instead of receiving the flow

axially at the overflow exit, the geometry was modified to receive the flow tangentially (Fig. 4.4.d and Fig. 4.8). The outflow passing through the vortex finder was gradually retarded to normal velocity by providing 0.06 m wide and 0.10 m high outlet at the exit of the vortex finder to a gradually expanding conduit ending to 0.15 m wide square section. A slightly larger diameter (0.16 m) of vortex finder was chosen to ease the fabrication of tangential outlet. The experimental setup remained exactly similar to that for axial overflow outlet.

4.2.7 Testing Procedure

The experimental procedure was similar to that adopted for axial overflow setup. Like in the axial setup the sediment removal efficiency of the hydrocyclone was studied for different operating conditions and design variables (Table 4.2). The velocity in the inlet varied from 2.49 m/s to 3.78 m/s, whereas the same in the outlet varied from 1.33 m/s to 2.18 m/s. 48 tests were conducted without feeding sediment to assess the hydraulic performance of the hydrocyclone and the test rig, which was followed by 17 tests using two batches of sediment of different particle size distributions (Fig. 4.7).

4.3 The Concept of a Bottom Outlet Hydrocyclone

4.3.1 Basis of Modification of the Bottom Outlet

It has been found that the new geometry investigated of the hydrocyclone is highly efficient in particle separation. Nevertheless, due to the driving head required for operation and long vertical dimension, hydrocyclones of such configuration may often require considerable rock excavation often inviting complexities in installation and may require considerable cost for installation. Therefore a concept, which utilizes relatively lower pressure head compared to that by the conventional design and draws all the flow from the bottom is introduced and investigated. And such a concept is named as " Bottom Outlet Hydrocyclone (BOH)" The concept aims to process the flow utilizing the potential head between the inlet and the underflow outlet
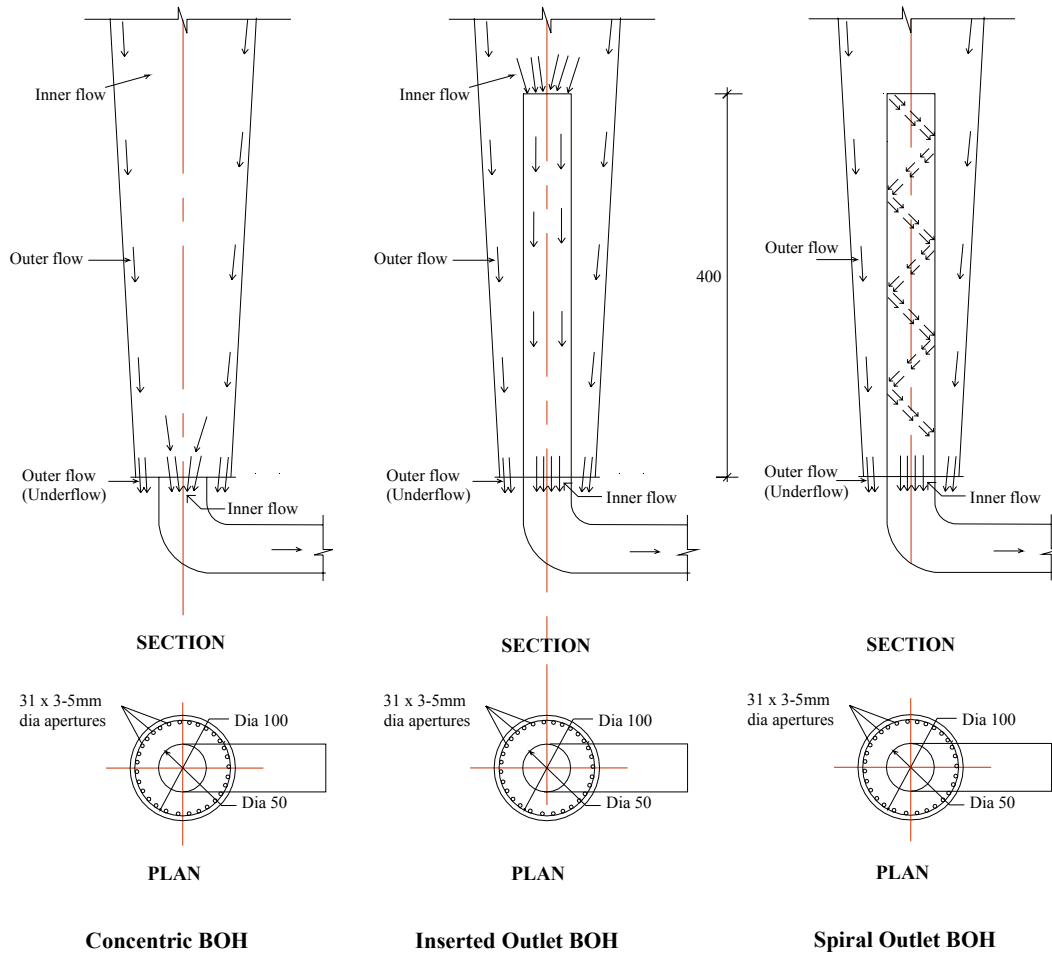
Fig. 4.9 Different geometries of Bottom Outlet Hydrocyclone investigated

4.3.2   Design of BOH

To achieve the objective, the   overflow as well as underflow discharge in the conventional setup is gradually received through the bottom part of the hydrocyclone. This was realized by allowing the inner flow pass through an aperture having 50 mm diameter at bottom center, whereas the outer flow through a number of apertures having 5.0 mm diameter along the periphery of the cyclone wall (Fig. 4.9). The openings of the apertures as well as configuration of the outlets at the end remained unchanged. But the tests were carried out with different geometrical configurations of the inner outlet. Three principal geometrical setups as presented in Fig. 4.9 were identified for the investigation of the BOH. In order to minimize the short-circuiting effect, the point of flow split was kept away by inserting the outlet 0.4 m from the bottom of the hydrocyclone. Further, for better streamlining of flow

and avoid congestion of the streamlines, apertures were made on the surface of the inserted outlet in spiral configuration.

To avoid further confusion, the terms used as overflow and underflow discharge in conventional hydrocyclone are often referred to *inner flow* and *outer flow* in BOH. Similarly, the head over the inlet is assumed as the headloss in both the hydrocyclones for comparison of results. Similarly, the concentric outlet means the one flushed with the bottom of the cone, and the inserted concentric outlet denotes the outlet pipe inserted inside the cone by 0.4 m. Whereas the spiral outlet indicates that the inner flow (central flow) is received from the periphery of the inserted pipe inside the cone, which has series of apertures having spiral configuration.

4.3.3 Testing Procedure

A number of hydraulic tests were carried out by varying the headloss in the system to assess the performance of the BOH. The testing procedure adopted was exactly similar to what was followed in the previous experiments. 6 number of tests were carried out to assess the SRE of BOH using the first batch of sand called Fugesand and varying operating and design parameters. The outer flow was freely discharged to the atmosphere in all the tests. Whereas the inner flow was discharged with and without pressurization of the outlet conduit.

5 RESULTS AND DISCUSSION

The results obtained from two test rigs described in previous chapter are presented and discussed in this section. The hydraulic and sediment removal efficiency (SRE) of hydrocyclone having 0.22 m diameter are presented in the beginning. The strength and weakness of the chosen hydrocyclone are discussed, which formed the major basis of further investigation of a test rig comprising a larger hydrocyclone having a diameter of 0.38 m. In the next part the results obtained from the investigation in the larger hydrocyclone with axial and tangential overflow outlet have been presented, discussed and compared with the data obtained by other investigators. Effect of operating and design (system) parameters are further discussed. In the end, the concept of a bottom outlet hydrocyclone is introduced and the performance of such hydrocyclone with different underflow configurations has been presented, analyzed and compared with that due to conventional hydrocyclone.

5.1 Results from 0.22 m Dia Hydrocyclone

65 test runs were conducted using cohesionless sediment of different concentration and particle size distribution. The particle size of the sediment used in the study varied from 65 μm to 1000 μm, whereas the median particle size varied from 76 μm to 397 μm. The concentration in the hydrocyclone varied from 1287 ppm to 5092 ppm, whereas the same for overflow and underflow varied from 8 ppm to 942 ppm and from 734 ppm to 186,116 ppm respectively. The hydrocyclone was tested for a wide range of operating parameters. Therefore, the average removal efficiency of the hydrocyclone under different operating conditions varied from 58% to 99%.

5.1.1 Hydraulics of the Cyclone

The flow into the hydrocyclone was fed through a pump. A high velocity was created near the inlet of the hydrocyclone to create a strong centrifugal acceleration (Fig 5.1). However both the acceleration and retardation of flow near the inlet as well as exit conduits were abrupt. A maximum velocity of 6.8 m/s for a corresponding discharge of 7.7 l/s was recorded near the entrance zone and hence inside the hydrocyclone.

The ability of hydrocyclone to process the flow for a given headloss is presented in Fig 5.2. The hydrocyclone was tested for a wide range of flows. The lowest discharge recorded was 0.30 l/s corresponding to a headloss across the cyclone as 0.05 m. Whereas the highest discharge observed was 7.81 l/s corresponding to a headloss between the entrance and exit outlet as 2.73 m. These tests were carried out by changing the

Fig. 5.1 Velocity profile along the conveyance (H_L= 2.73 m, Q = 7.7 l/s) in a 0.22 m dia hydrocyclone

flow ratio, R_f ($R_f = Q_u/Q$), which varied from 0.48 % to 18.6%. The discharge curve resembles a standard rating curve of a hydraulic device and best described by a power function as

$$Q_{Hc} = 4.51 H_L^{0.543}$$ Eq. 5-1

The hydraulic performance of the hydrocyclone has been found to be quite close to that of a standard hydrocyclone reported by Arterburn (2002).
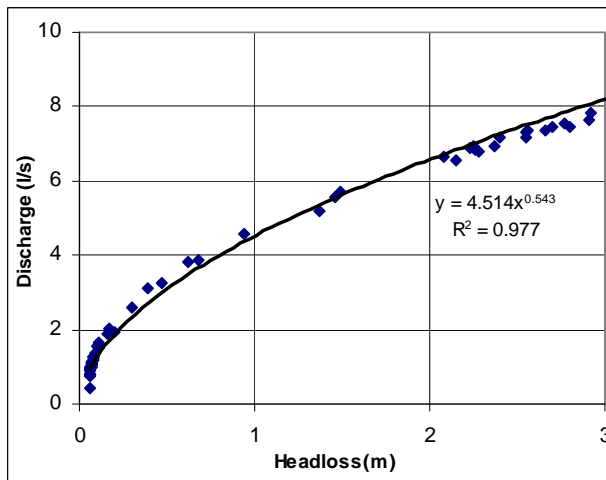
Fig. 5.2 Rating curve obtained from a 0.22 m dia hydrocyclone
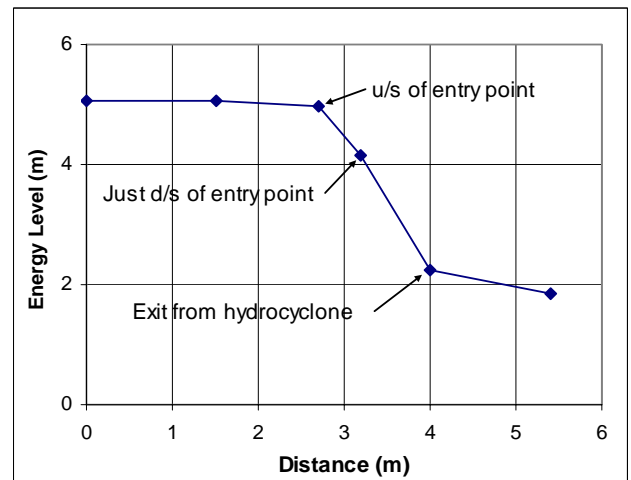
Fig. 5.3 Energy profile along the conveyance (H= 2.73 m, Q = 7.7 l/s) in a 0.22 m dia hydrocyclone

The energy level along the conveyance for a typical flow condition (H= 2.73 m and Q = 7.7 l/s) is depicted in Fig. 5.2. The energy profile before the entry to the hydrocyclone is quite

flat, which implies insignificant headloss occurring in this region. The central part of the profile is much steeper than that in upstream and downstream ends. This drop of 2.73 m indicates the total energy utilized by the hydrocyclone to pass a flow of 7.8 l/s through it. The profile after the exit point is flatter than the middle part but steeper than that before the entry to the hydrocyclone. It indicates that part of the energy available near the exit is not recovered properly.

Moreover, a sharp drop immediately after the entrance to the hydrocyclone has been observed corresponding to an energy dissipation of about 30%. The abrupt drop in energy level near the entrance as well as the exit point is believed due to the improper geometry near the inlet and outlet zones of the hydrocyclone. Improvement of hydraulics was therefore one of the objectives of the investigation in a larger hydrocyclone having a diameter of 0.38 m.

5.1.2   Sediment Removal Efficiency

PSD of samples received from overflow, feed and underflow for different   operating variables (headloss, total discharge, underflow discharge, feed PSD and concentration) were investigated. Fig. 5.4.a-d represent the PSD curves of the sample results, whereas Fig. 5.5.a-d depict the results on SRE by particles size. The results obtained from the tests conducted in a very weak centrifugal field are presented in Fig. 5.4.a & b, whereas that obtained in a relatively stronger acceleration field are presented in Fig 5.4.c & d. The common feature of the results is that the particles coarser than 200 μm are attracted towards the underflow stream despite the variation in centrifugal acceleration. On the other hand the degree of removal of particles finer than 200   μm was dependent on the operating parameters of the respective tests. The results presented in Fig. 5.4 and Fig. 5.5 also show the influence of operating parameters on SRE. Among them, the headloss (H_L), flow ratio (R_f) and sediment characteristics   were found to play a decisive role on SRE of the hydrocyclone.

In case of weak centrifugal field the removal efficiency, especially of finer particles (d< 200 μm) was found to be sensitive to underflow discharge and sediment concentration (Fig.5 5.a & b) and not on headloss across the hydrocyclone. The role of these operating variables

diminished gradually with the increase of centrifugal acceleration. In case of strongest centrifugal field, the SRE is literally insensitive to the operating parameters. (Fig. 5.5.c & d).
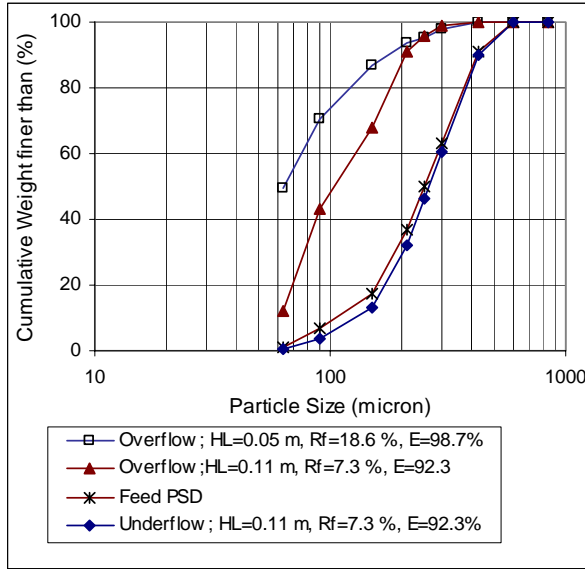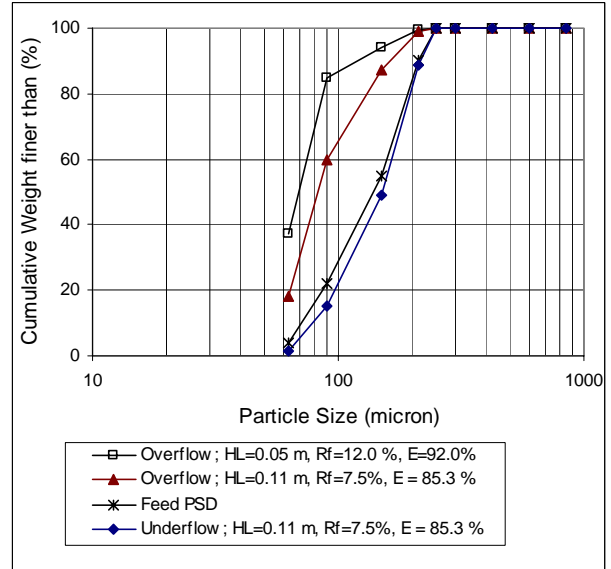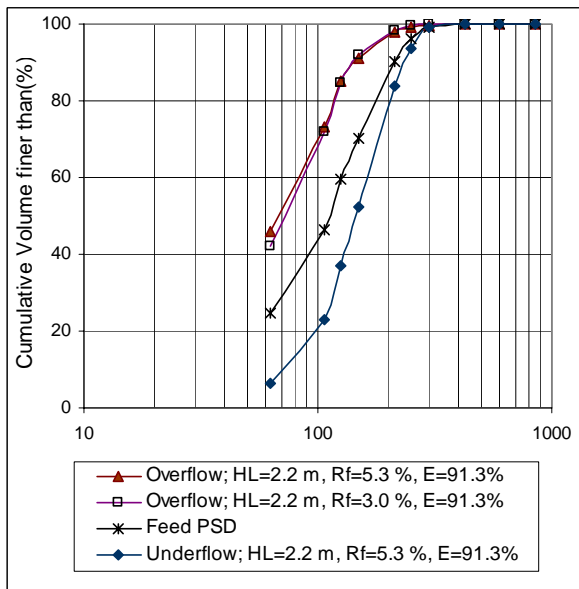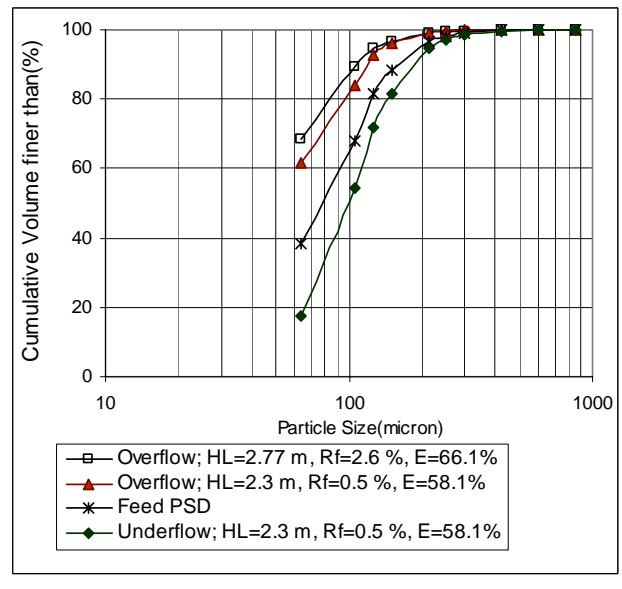
Fig. 5.4. PSD received from feed, overflow and underflow of an axial hydrocyclone for different operating conditions. H_L= Headloss, R_f = Q_u/Q, E = Sediment Removal Efficiency
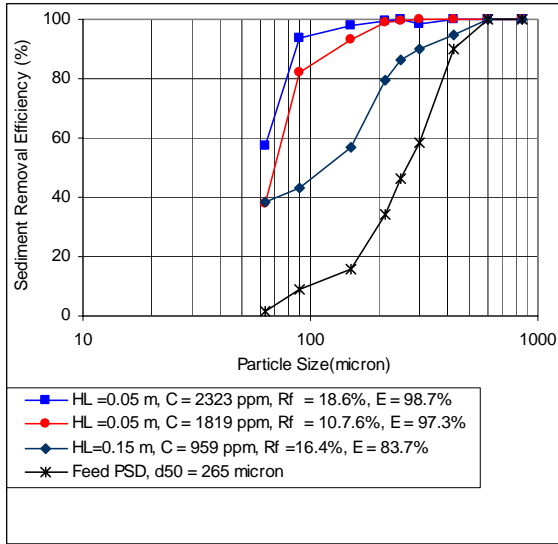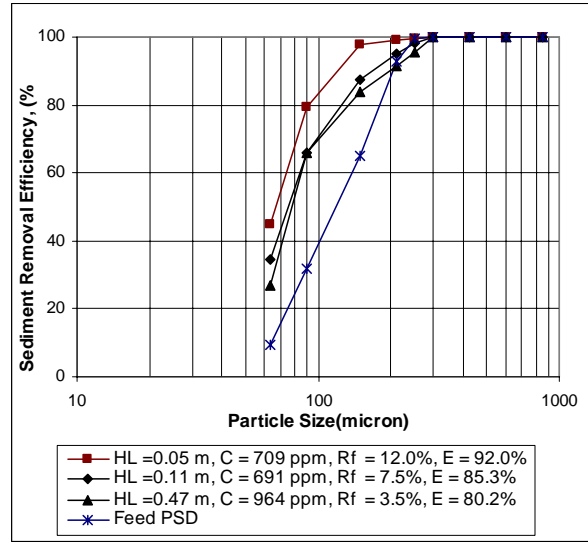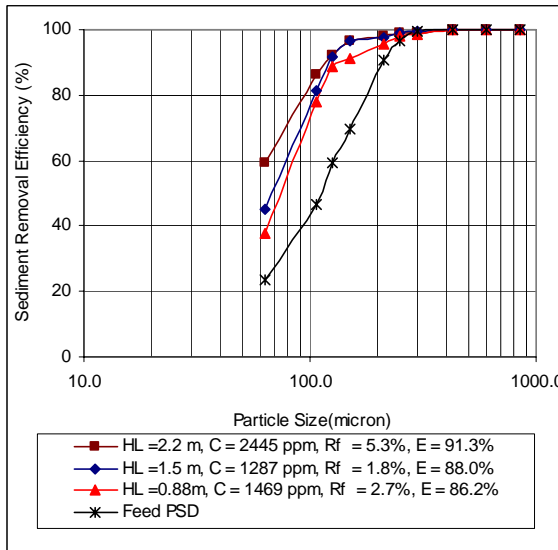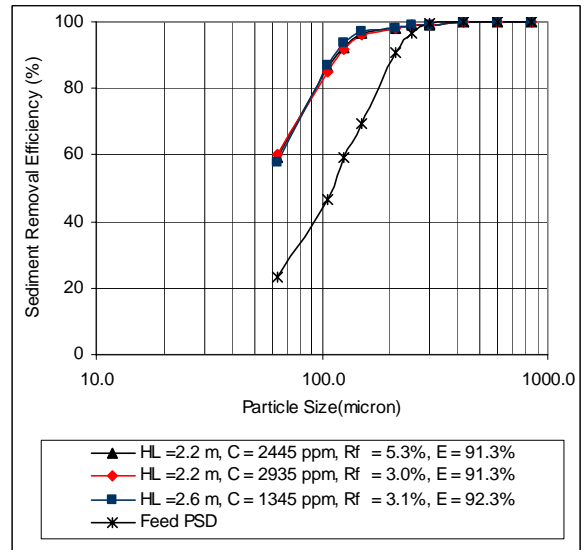
Fig. 5.5 Removal efficiency curves obtained by hydrocyclone with 0.22 m diameter using sand particles, G = 2.68 (a) Coarser feed, d_{50}= 265 µm (b) Finer feed, d_{50}= 123 µm (c) & (d) Finer feed, d_{50}= 111 µm. H_L= Headloss, R_f= Q_u/Q, E = Sediment Removal Efficiency

5.1.3   *Conclusions*

The results presented above followed by subsequent discussion conclude the followings:

- Significant headloss was observed immediately after the entrance of the hydrocyclone accounting about 30 % of the total loss occurred across the hydrocyclone.

- The SRE of the hydrocyclone even for smaller flows was found quite high. The lowest SRE of fine sand was observed as 35% for smaller flows. Whereas the

efficiency of removal of the same particle was recorded as 60 % in case of higher flows.

- In case of weak centrifugal field the SRE, especially of finer particles (d< 200 μm) was found to be sensitive to underflow discharge and sediment concentration and not on headloss across the hydrocyclone. The role of these operating variables diminished gradually with the increase of centrifugal acceleration. In case of strongest centrifugal field, the SRE is literally insensitive to the operating parameters.

- The performance of only the hydrocyclone could be understood from the test rig. The test rig simulating part of the headrace of a water project along with the hydrocyclone/s would give a picture very close to the reality.

- As the flow used was much smaller than that to be used in the water projects, the behavior of the finer particles didn't give a picture closer to real-world situation.

5.2   Results from 0.38 m -Dia Hydrocyclone with Axial Overflow setup

As mentioned earlier, the investigation in the larger hydrocyclone was carried out to improve the flow hydraulics near the inlet zone thereby minimize the headloss observed immediately after the entrance of the smaller hydrocyclone. The geometry of the cyclone body was chosen as that of gMax series of Krebs Engineers. Inclined involute inlet as well as inclined roof was proposed to minimize the loss in the inlet region. 26 test runs were conducted using two types of cohesionless sediment of different concentration (Table 5.1). The feed sediment concentration in the hydrocyclone varied from 97 ppm to 4295 ppm, whereas the same for overflow and underflow varied from 28 ppm to 93 ppm and from 160 ppm to 57,703 ppm respectively. Total discharge handled by the hydrocyclone varied from 10.4 l/s to 19.90 l/s,   whereas the flow ratio varied from 3.5% to 25.5%. The test results characterizing the operating parameters along with the SRE are presented in Table 5.1. The data of Arterburn (2004), Olson et al. (2001), Kraipech et al. (2002) and Neesse et al.(2004) have been used to compare the hydraulic and SRE of the hydrocyclone under study.

5.2.1   Flow Phenomena Inside the Hydrocyclone
The flow pattern inside the hydrocyclone was a spiral inside a spiral. The outer spiral can be seen in Fig 5.6 a, which was observed for a relatively smaller flow. The fluid on the entry commenced downward flow in the outer regions of the cyclone body. Because of the ability

of the underflow outlet to accommodate only a small proportion of the flow, most part of the flow was reversed to the upward direction to leave through the overflow outlet at the top. The existence of these two regions created a locus of zero vertical velocity, inside which a stagnant zone (mantle) was observed (Fig. 5.e & f). The rotation of the fluid created a low pressure axial core (Fig. 5.6. b,c,d), which mostly resulted in a free liquid surface. The diameter of the air core was dependent on the opening of the underflow aperture; smaller being for the smaller aperture size.

Table 5-1. Characteristic operating parameters and test results obtained from axial setup

Test No	Q_t (l/s)	Q_o (l/s)	D_u (m)	Q_u (l/s)	Q_{HC} (l/s)	Q_u (%)	C_{feed} (ppm)	H_L (m)	E (%)
S2-1	17.20	14.68	0.035	2.52	17.20	14.65	893	2.88	95.5
S2-2	14.30	12.31	0.035	1.99	14.30	13.92	4295	2.10	97.4
S2-3	19.40	17.30	0.035	2.10	19.40	10.82	1134	3.61	98.2
S2-4	13.60	10.13	0.035	3.47	13.60	25.51	1157	1.94	96.2
S2-5	17.85	15.45	0.035	2.40	17.85	13.45	2157	3.16	97.6
S2-6	15.09	12.44	0.035	2.65	15.09	17.56	1635	2.31	96.5
S2-7	18.14	15.54	0.035	2.60	18.14	14.33	1170	3.17	98.2
S2-8	16.60	14.33	0.035	2.27	16.60	13.67	1690	2.73	96.7
S2-9	14.72	11.99	0.035	2.74	14.72	18.58	752	2.22	96.1
S2-10	15.05	12.45	0.035	2.60	15.05	17.28	2020	2.38	98.3
S2-11	16.80	15.43	0.025	1.38	16.80	8.18	996	2.76	95.0
S2-12	19.05	17.77	0.025	1.28	19.05	6.69	2546	3.54	98.7
S2-13	15.27	13.98	0.025	1.29	15.27	8.45	848	2.31	93.6
S2-14	15.29	14.00	0.025	1.29	15.29	8.44	474	2.35	92.7
S2-15	12.67	11.54	0.025	1.13	12.67	8.92	176	1.64	66.2
S2-16	10.42	8.20	0.025	2.22	10.42	21.31	276	1.16	73.3
S2-17	19.85	19.15	0.025	0.70	19.85	3.53	1059	3.94	97.5
S2-18	14.60	13.88	0.025	0.72	14.60	4.93	125	2.14	66.5
S2-19	18.87	17.33	0.03	1.54	18.87	8.16	1862	3.46	97.9
S2-20	15.78	14.18	0.03	1.60	15.78	10.14	992	2.44	95.5
S3-BP-22	26.45	15.88	0.03	1.78	17.66	10.08	794	3.02	94.6
S3-BP-23	30.38	16.18	0.03	1.70	17.88	9.51	871	3.08	94.3
S3-BP-24	37.49	15.70	0.03	1.77	17.47	10.13	91	2.95	97.7
S3-BP-25	34.00	13.07	0.03	2.25	15.32	14.71	501	2.11	89.7
S2-26	19.67	18.97	0.02	0.70	19.67	3.56	2136	3.81	96.1
S2-27	15.21	14.30	0.025	0.91	15.21	5.98	1435	2.35	95.63

Q_t = Total discharge to the rig; Q_o = discharge through overflow outlet; Q_u = discharge through underflow outlet; Q_{Hc} = discharge through hydrocyclone; D_u = diameter of underflow aperture; C_{feed}= sediment concentration at the inlet of hydrocyclone; H_L =headloss across the hydrocyclone; E= sediment removal efficiency
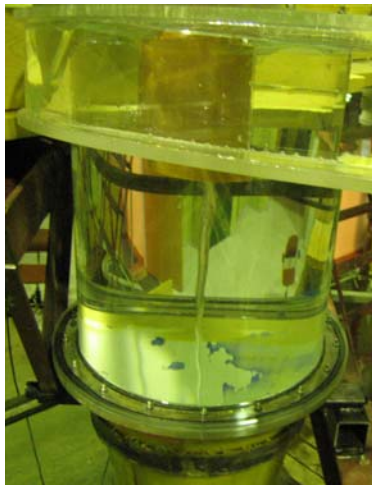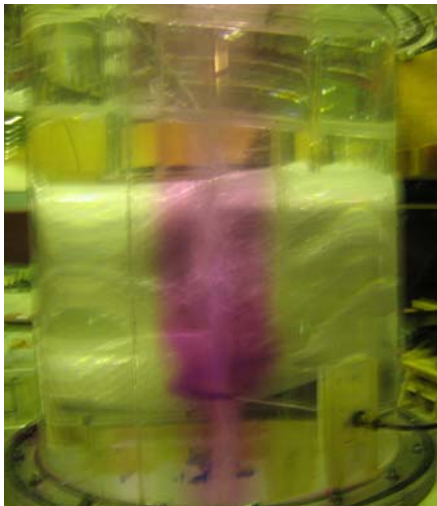
Fig. 5.6 Flow pattern inside a hydrocyclone; a) Outer spiral observed for low flows b) Established air core for normal flows c) Established air core for smaller underflow aperture d) Full air core observed from the top e) Mantle obtained by direct dye injection f) Mantle obtained by inner reversal

5.2.2 Velocity Profile

The flow was gradually accelerated to the entrance of the hydrocyclone. On the other hand, the exit flow at overflow was gradually retarded to normal velocity (Fig. 5.7). For a reference flow of 19.7 l/s, a velocity of 0.802 m/s was recorded at the bifurcation point which was further accelerated to 3.3 m/s at the entrance to the hydrocyclone. Whereas the exit flow of 3.1 m/s was gradually retarded to 0.75 m/s at the exit region to the receiving conduit.
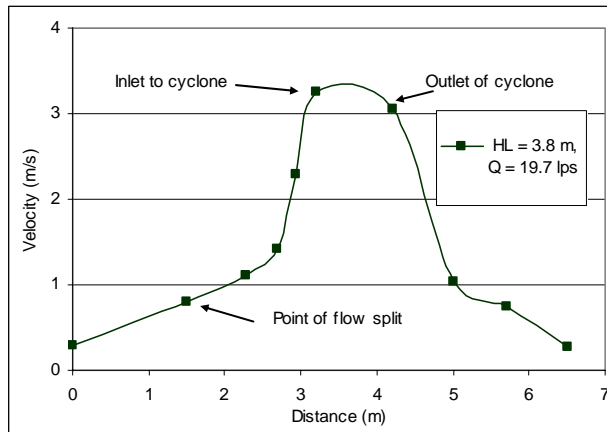
Fig. 5.7 Velocity profile along the conveyance
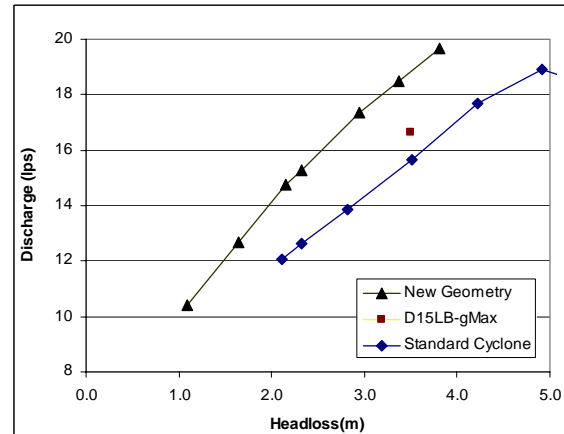
Fig. 5.8 Comparison of hydraulic performance of modified hydrocyclone with existing cyclones

5.2.3 The Hydraulic Performance

The hydraulic performance of the new geometry has been compared with that of standard cyclone (Arterburn, 2004) and D15LB-gMax (Olson et al., 2001). The results of the experiments show that the hydraulic performance of the hydrocyclone with the new geometry is better for entire headloss range under study (Fig 5.8). For a reference headloss of 3.5 m such an improvement in flow hydraulics increased the capacity of hydrocyclone by 21% and 13% more than that of Standard and D15LB- gMax cyclones respectively. And in terms of headloss, the efficiency of modified hydrocyclone over Standard and gMax cyclones is higher by 30% and 21.5 % respectively. The performance is even better for larger value of flow, a desirable feature for prototype situation.

The improvement of the performance of the cyclone can be explained by next reasoning. First, the gradual acceleration and deceleration of flow in inlet and outlet zones caused better streamlining of flow resulting in reduction of turbulence losses in high velocity zone. Second, the gradually inclined inlet geometry of cyclone under study, which is an

improvement over an involute, horizontal inlet of gMax series has also helped in better streamlining the inlet flow into main course of flow inside cylindrical and conical parts of the cyclone. These streamlines otherwise would have taken some additional path before matching with the streamlines inside the hydrocyclone. As the inlet and outlet zones are known as principal locations to have significant energy dissipation (Boadway 1984), the improvement of the geometry in these zones has minimized the turbulence losses. Since the performance improvement due to the involute type of entry and modified conical part against the geometry of the standard cyclone has been already described in gMax series (Krebs Engineers 2000), the modification in the inlet and outlet geometries thus should be the only factor to minimize losses and exhibit improved hydraulic performance over the gMax series.

5.2.4 Energy Profile

The energy profile observed along the conveyance of the test rig for a reference flow of 19.7 l/s is presented in Fig. 5.9. Like in the smaller hydrocyclone presented earlier, the energy profile before the entrance to the hydrocyclone is quite flat. The next part has the steepest gradient, the difference of which represents the total headloss across the cyclone. Further, a milder than the middle part but yet much steeper than the profile before the inlet as well as exit to receiving conduit was observed. This headloss alone constituted 21.5% of the total loss observed in the system.
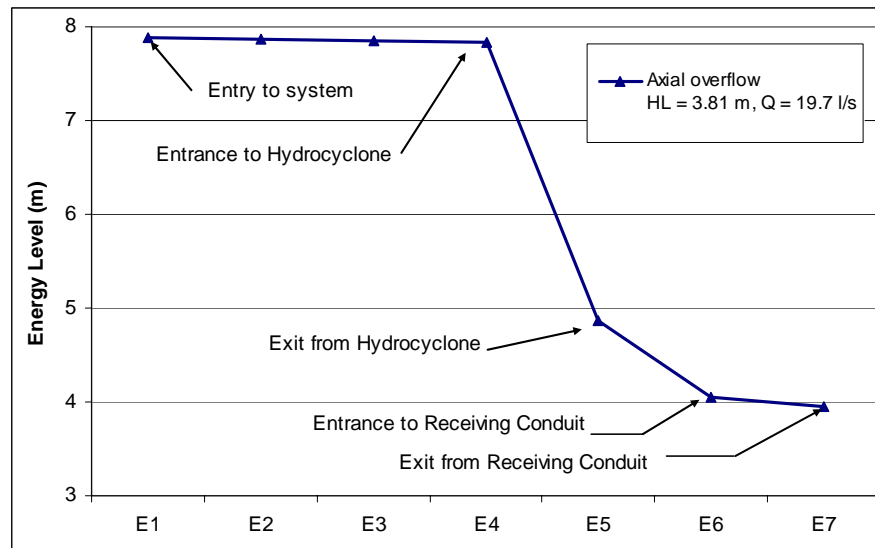
Fig. 5.9. Energy profile along the conveyance (H= 3.81 m, Q = 19.7 l/s) in a 0.38 m dia hydrocyclone

While the headloss involved between the entrance and exit points of the hydrocyclone is attributed to the processing of flow by a hydrocyclone, the headloss involved immediately after the exit region of the hydrocyclone is a wastage of energy. The associated headloss was believed due to the improper geometry of the hydrocyclone in overflow region. Further modification was therefore carried out intending to minimize this loss.

5.2.5   *Sediment Removal Efficiency*

The particle removal efficiency of a hydrocyclone is usually described by comparing the particles recovered in the underflow to the total particles fed into the system which are often presented in graphical form. These curves representing the removal efficiency by particle size have been given different names; performance curve (Kelly and Spottiswood,1982), grade efficiency curve (Svarovsky 1984, 1990), selectivity function (Kraipech et al. 2002), and separation function (Neesse et al. 2004). Typical results illustrating PSDs of the samples collected from overflow, underflow and feed for different operating variables are presented in Fig. 5.10.

From the test results presented in Table 5.1 and PSD of representative tests illustrated in Fig. 5.10, it can be observed that the sediment removal performance of the hydrocyclone is influenced by operating parameters, such as headloss, flow ratio and the concentration of feed. In general the SRE has been found to increase with the increase of all the operating parameters. The SRE is quite low, when the headloss is lower than 2.3m (Fig 5.10.a). The SRE in this range is more sensitive to flow ratio. The higher SRE (73.3%) of test S2-16 conducted under a headloss as 1.16m and flow ratio as 21.3% compared to SRE as 66.5 in test no S2-18 under a headloss as 2.14m and a flow ratio as 4.93% is credited mainly to the higher flow ratio in the former test. However, the SRE is less sensitive to the operating parameters, in the region of higher headloss.
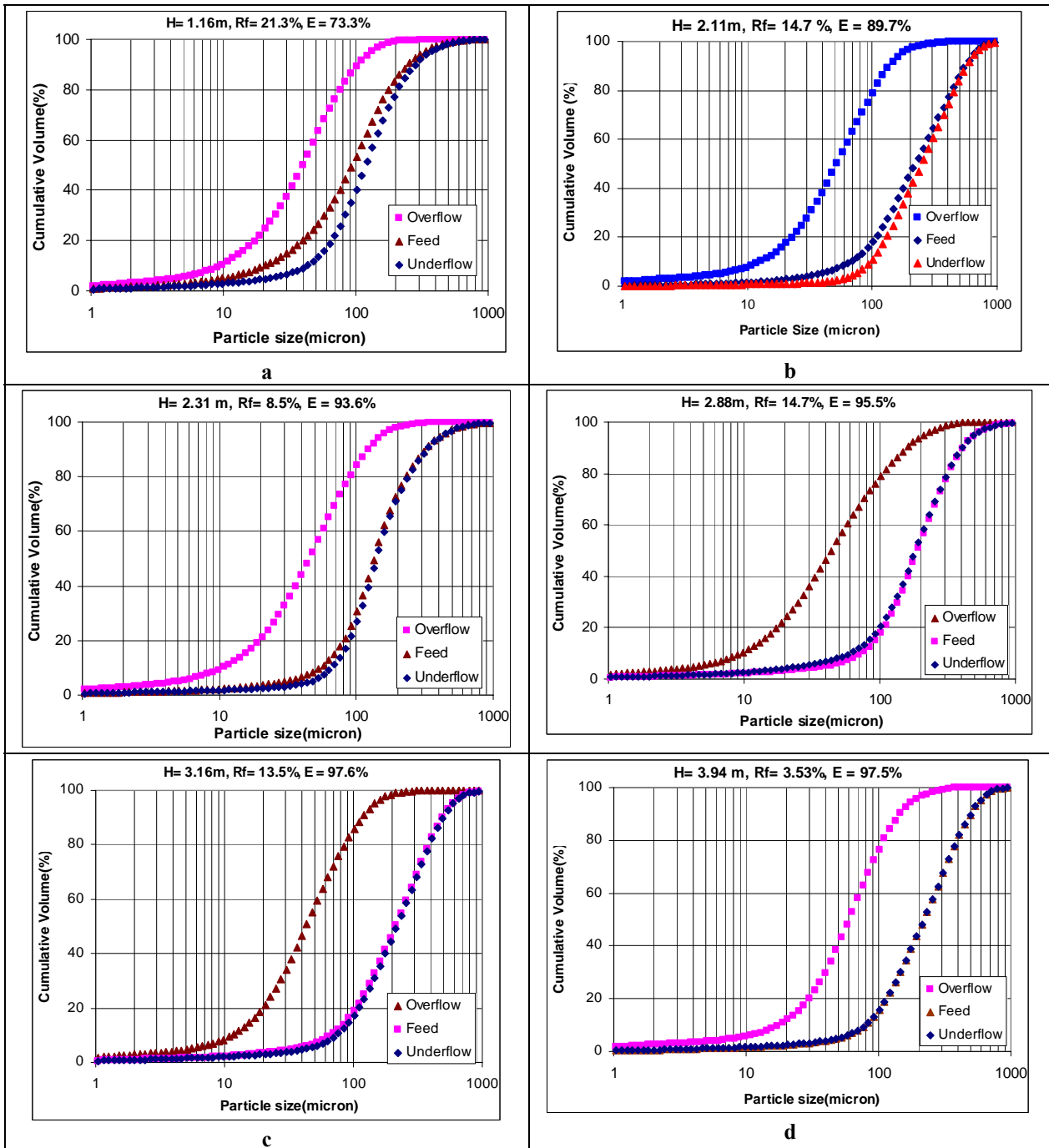
Fig. 5.10 PSD obtained from feed, overflow and underflow conduits for different operating conditions in a hydrocyclone with axial overflow geometry. H_L = Headloss, R_f = Q_u/Q_c, E = Sediment Removal Efficiency

The shape of the PSD curves is alike in all the tests. However, PSD curve of underflow moves closer to that of feed with the increase in headloss. The shift is rapid in lower headloss range (HL< 2.3 m), and literally insensitive in higher headloss range. The underflow PSD

curves in these cases have been overlapped with that of feed, which indicates that most of the sediment fed into the system is captured by the underflow.

The SRE being quite low for the first case can be explained due to next reasoning. First, although the sediment fed into the box is of the same characteristics, actual feed into the hydrocyclone remained different in each case. Shear velocity being quite low, most of the coarser particles have been settled elsewhere along the conveyance. Whereas the additional coarse particles deposited along the conveyance have been picked up by the flow when the transport capacity was sufficiently high. Accordingly, the d_{50} of the feed in case 'a' is 94.3 μm compared to 217.7 μm in case 'd'. The finer being the feed PSD, it is reasonable to have lower efficiency. Second, the flow magnitude being smaller, the magnitude of resulting tangential velocity and centripetal force, a major actor for separation is also weaker, which led to lower removal efficiency. Third, because of the finer feed, the population of the coarser particles is smaller than that in other tests. This lead to less entrainment of finer particles when the coarser particles are dragged towardss the wall of the cyclone. This resulted in the shift of the fish-hook curve, which is witnessed in Fig. 5.11d, where the trapping efficiency curve has dropped down to a level of 20% as against 60% in most of the tests.

5.2.6 *Comparison of Sediment Removal Efficiency of Hydrocyclone*

SRE of the modified geometry has been compared in terms of sediment trapped (recovery curves) by underflow. Actual recovery curves obtained in the present study have been compared with those obtained from hydrocyclones ranging from 40 mm to 250 mm dia hydrocyclones manufactured by Richard Mozley and Krebs Engineers. SRE curves for particles with different specific gravity obtained by Kraipech et al. (2002), Neesse et al. (2004) and Krebs Engineers (2000) have been considered for the comparison. The characteristic parameters used by these authors together with that used in the present study have been presented in Table 5.2. SRE of the hydrocyclone by particle size observed in the representative tests have been presented in Fig. 5.11 for comparison.
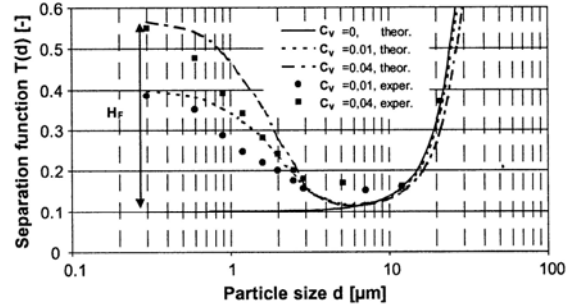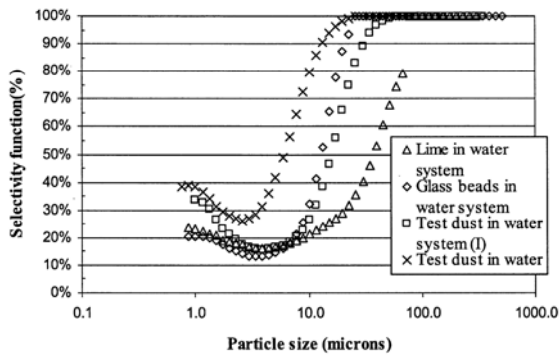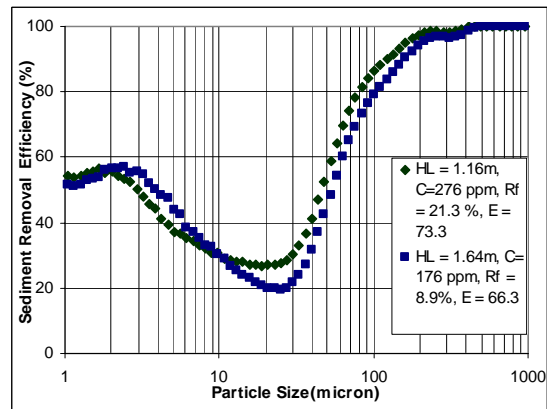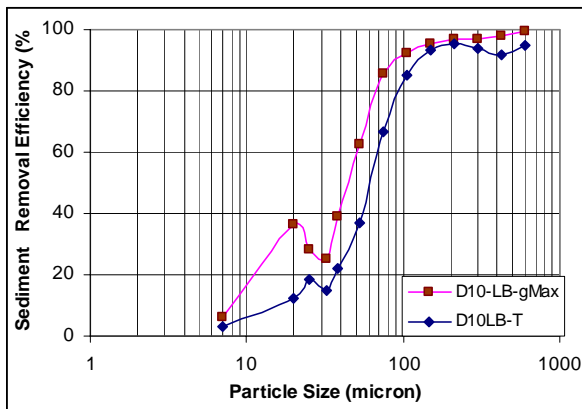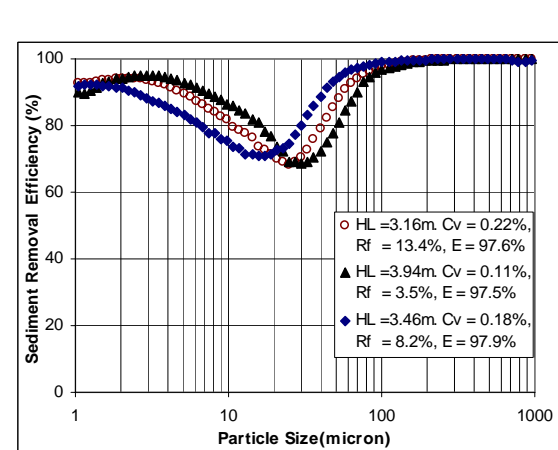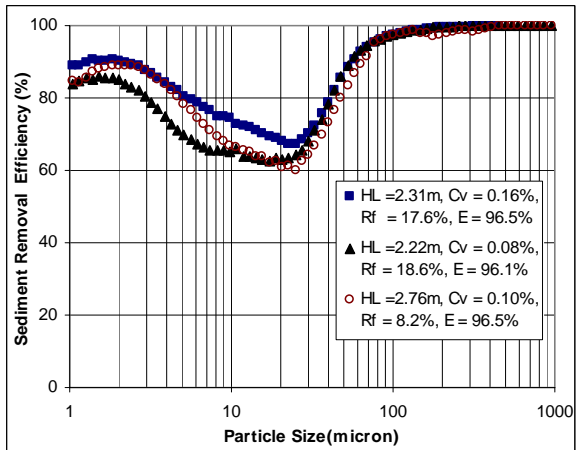
Fig. 5.11 Particles Removal Efficiency obtained in different cyclones observed by (a) Kraipech et al.(2002) (b) Neesse et al.(2004) (c) Krebs Engineers (d),(e),(f) Present study in an axial overflow setup. H_L= Headloss, R_f= Q_u/Q_c, E = Sediment Removal Efficiency

Table 5-2. Characteristic parameters of tests used by different investigators

Parameters	Neesse et al.	Kraipech et al.	Krebs Engineers	Present Study
Cyclone diameter (mm)	40	100 & 50	250	380
Cyclone geometry due to	Krebs Engineers	Krebs Engineers & Richard Mozley	gMax	Modification to gMax
Operating headloss (m)	15	20 & 30	14	1.16-3.94
Concentration by vol. Cv (%)	1.0-4.0	NA	NA	0.03-0.08
Particle size(micron)	<50	<100	2-600	1-1000
Particle type	quartz	Test dust & glass beads	coal	quartz > 80%
Specific gravity of sediment	2.65	NA	1.32	2.63
Fluid medium	water	water	water	water

NA: Not available

All the removal efficiency curves observed in the present study exhibited inherent fish-hook property. In addition, the removal efficiency of any particle in the fish-hook zone observed in the present study was higher to those observed by all the authors considered for comparison. Nevertheless, the shape of the fish hook curve is slightly different in each test and also different from that obtained by other investigators. This is believed mainly due to the feed particle size in this range being in a small quantity. The variation of operating variables in each test may also have considerable influence.

The particle removal efficiency is much higher for all headloss range above 2.22 m and, almost comparable to that obtained by Kraipech et al., Neesse et al. and Krebs Engineers in the range of smaller headloss. Further, all these authors have carried out investigation in smaller hydrocyclones. This implies that the removal efficiency in such cases should have been better than what was observed in the present study according to prevailing theory (Bradley 1965, Svarovsky 1984). It can be inferred from the above discussion that the improved removal efficiency of the hydrocyclone is due to the improved inlet, outlet and roof arrangement.

Nevertheless, as the efficiency of the hydrocyclone is influenced by many parameters, the comparison of the results thus presented give general impression only. Therefore, the influence of each operating parameters is discussed in subsequent sub-chapters later. Further, as the test data of other investigators, except for Neesse et al. (2004) were obtained using particles other than quartz, comparison of total removal efficiency of the hydrocyclone under

study with that obtained by these authors may not be fully comparable. However, the comparison of the shape and depth of the fish-hook curves obtained in the present study also provides a meaningful conclusion while evaluating the SRE of the new geometry.

5.2.7 *Conclusions*

The results presented above followed by subsequent discussions concluded the followings:

The investigation of the modified hydrocyclone lead to the following conclusions:

- A new geometry of the axial overflow hydrocyclone with modification of inlet, outlet and the roof was identified, which has been found more efficient than conventional hydrocyclone. The same amount of flow in the modified hydrocyclone can be processed with a reduction of headloss by 30 % and 21.5% compared to Standard and gMax cyclones respectively.

- The inherent fish-hook property of the hydrocyclone was also conserved in the modified hydrocyclone. However, the removal efficiency of any particle in the fish-hook zone was higher than those observed by Kraipech et al. (2002), Neesse et al. (2004) and Krebs Engineers (2000).

- Despite the improved performance of the modified hydrocyclone, about 21.5 % of the total headloss occurred in the system was observed near the exit region of the hydrocyclone. As the spinning component of the velocity in a hydrocyclone is much higher than the axial component, most of the energy retained in the form of tangential velocity component was lost in an axial outlet while being converted into potential energy.

5.3 Results from Tangential Overflow Hydrocyclone with 0.38 m Dia

Despite better hydraulic and SRE of the hydrocyclone with axial outlet setup compared to that of existing devices, about 21.5 % of the total headloss involved was noticed near the overflow conduit of the hydrocyclone (Fig. 5.12). As discussed in Chapter 4, it was believed this loss was attributed to the geometry of the overflow outlet, adopted for the setup. The energy retained in the form of tangential velocity component near the exit outlet of the hydrocyclone couldn't be converted to the form of potential energy properly in an axial outlet. As the spinning component of the velocity is much stronger (2-3 times) than the axial one, significant headloss was involved near the outlet area. Therefore, the main purpose of

the modification of the axial outlet was to minimize the headloss that took place at the upper outlet by changing the axial setup adopted previously to the tangential one.

Table 5-3 Comparison of removal efficiency of cyclones with axial and tangential setups

A. Similarity in Headloss

Test No	Qc (l/s)	Qo (l/s)	Qu (l/s)	Qu/Q (%)	C_{feed} (ppm)	d_{50} (feed),μm	H_L (m)	E (%)	Setup Type
S2-15	12.67	11.54	1.13	8.92	176	96.48	1.64	66.25	Axial
S6-M-BP-35	15.06	13.47	1.59	10.58	1348	98.64	1.58	84.21	Tangential
S2-11	16.80	15.43	1.38	8.18	996	105.01	2.76	95.03	Axial
S6-M-39	19.90	19.20	0.70	3.52	3592	105.87	2.79	95.14	Tangential
S2-1	17.20	14.68	2.52	14.65	893	200.40	2.88	95.48	Axial
S4-M-30	19.90	19.16	0.74	3.72	1768	127.38	2.88	97.13	Tangential
S2-8	16.60	14.33	2.27	13.67	1690	105.01	2.73	96.68	Axial
S6-M-36	20.70	18.38	2.32	11.21	4481	107.50	2.73	96.97	Tangential
S2-5	17.85	15.45	2.40	13.45	2157	214.25	3.16	97.63	Axial
S2-M-29	20.33	18.18	2.15	10.58	3119	180.40	2.98	97.53	Tangential
S2-26	19.67	18.97	0.7	3.56	2136	182.90	3.81	96.10	Axial
S6-M-BP-34	31.83	21.92	0.926	4.05	2790	107.93	3.81	97.13	Tangential

B. Similarity in flow ratio (Qu/Qc)

Test No	Qc (l/s)	Qo (l/s)	Qu (l/s)	Qu/Q (%)	C_{feed} (ppm)	d_{50} (feed),μm	H_L (m)	E (%)	Setup Type
S2-17	19.85	19.15	0.70	3.53	1059	235.1	3.94	97.47	Axial
S6-M-39	19.90	19.20	0.70	3.52	3592	105.9	2.79	95.14	Tangential
S4-M-30	19.90	19.16	0.74	3.72	1768	127.4	2.88	97.13	Tangential
S2-8	16.60	14.33	2.27	13.67	1690	105.0	2.73	96.68	Axial
S6-M-44	20.37	17.655	2.715	13.33	5522	109.3	2.69	97.35	Tangential
S2-3	19.4	17.3	2.1	10.83	1134	235.1	3.61	98.25	Axial
S2-M-29	20.33	18.18	2.15	10.58	3119	180.4	2.98	97.53	Tangential
S6-M-36	20.70	18.38	2.32	11.21	4481	107.5	2.73	96.97	Tangential

C. Similarity in d_{50}

Test No	Qc (l/s)	Qo (l/s)	Qu (l/s)	Qu/Q (%)	C_{feed} (ppm)	d_{50} (feed),μm	H_L (m)	E (%)	Setup Type
S2-15	12.67	11.54	1.13	8.92	176	96.48	1.64	66.25	Axial
S6-M-BP-35	15.06	13.47	1.59	10.58	1348	98.64	1.58	84.21	Tangential
S2-8	16.60	14.33	2.27	13.67	1690	105.01	2.73	96.68	Axial
S6-M-39	19.90	19.20	0.70	3.52	3592	105.87	2.79	95.14	Tangential
S2-11	16.80	15.43	1.38	8.18	996	105.01	2.76	95.03	Axial
S6-M-39	19.90	19.20	0.70	3.52	3592	105.87	2.79	95.14	Tangential
S2-1	17.20	14.68	2.52	14.65	893	198.90	2.88	95.48	Axial
S2-M-29	20.33	18.18	2.15	10.58	3119	180.40	2.98	97.53	Tangential

D. Similarity in Feed Concentration

Test No	Qc (l/s)	Qo (l/s)	Qu (l/s)	Qu/Q (%)	C$_{feed}$ (ppm)	d$_{50}$ (feed),μm	H$_L$ (m)	E (%)	Setup Type
S2-12	19.05	17.77	1.275	6.69	2546	NA	3.54	98.70	Axial
S6-M-BP-34	31.83	21.92	0.926	4.05	2790	107.93	3.81	97.13	Tangential
S2-2	14.30	12.31	1.99	13.92	4295	NA	2.10	97.44	Axial
S6-M-36	20.70	18.38	2.32	11.21	4481	107.50	2.73	96.97	Tangential
S2-19	18.87	17.33	1.54	8.16	1862	NA	3.46	97.88	Axial
S4-M-30	19.90	19.16	0.74	3.72	1768	NA	2.88	97.13	Tangential

17 tests using two batches of sediment (Fig. 4.7) were conducted varying mostly the operating parameters and a few design parameters. In order to facilitate the better comparison of results with those obtained from the axial setup, sample test results have been presented dividing them into four principal categories; similarity in headloss, flow ratio, feed concentration and median particle size, d$_{50}$ of feed material (Table 5.3). The PSD of the samples obtained through underflow and overflow outlets as well as feed received from some of the tests (Fig. 5.14) are also presented in subsequent sub-chapters, which are followed by SRE curves (Fig. 5.15).

5.3.1 *The Hydraulics of the Cyclone*

The flow pattern inside the hydrocyclone remained exactly similar to what was observed in the cyclone with axial overflow. The streamlines leaving the hydrocyclone were directed tangentially due to the modification of the overflow. The observation through the dye injection revealed that there was no significant discrepancy in the velocity profiles across lateral and longitudinal directions near the outlet of the overflow region.

5.3.2 *Energy Profile*

The shape of the energy profile for both the axial as well as tangential setups is alike. However the energy profile for the axial setup is higher than that for the tangential setup. As noticed from Fig. 5.12, the energy level at the inlet of the hydrocyclone for the axial setup is higher by 0.90 m compared to that for tangential setup to process almost the same amount of flow. A difference of about 0.50 m in energy levels was also observed at the overflow outlet resulting in a total headloss in the system as 3.81m in axial setup as against 2.98 m in a tangential setup. This means most of the energy lost in the axial overflow conduit is recovered once the geometry of the overflow conduit is configured tangentially. The more

important aspect is there was a significant impact on the hydraulics of the whole system due to the enhancement of the hydraulics at the overflow outlet
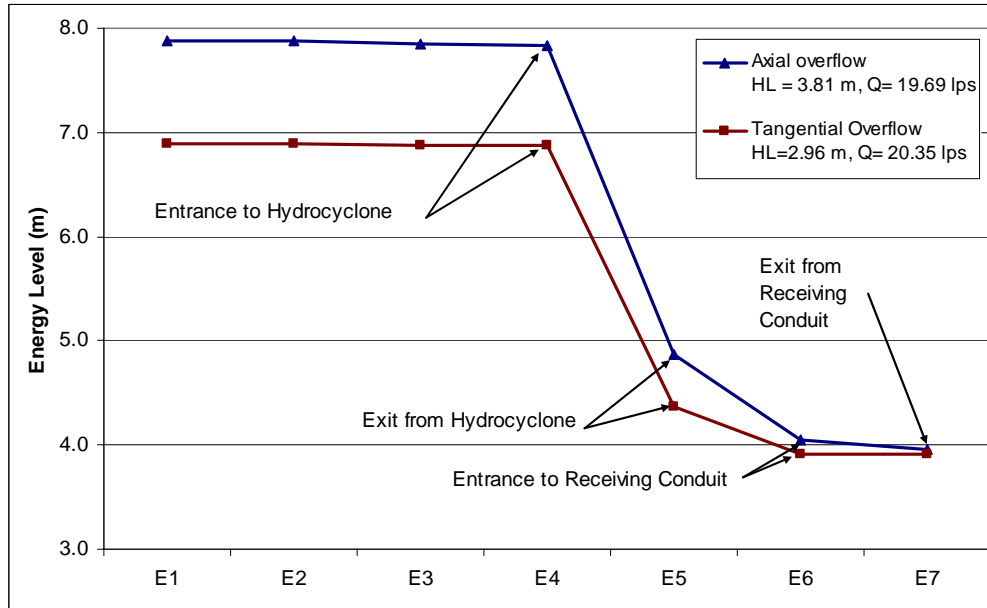
Fig. 5.12 Comparison of energy profiles in cyclone with tangential and axial overflow geometries

5.3.3 *The Hydraulic Performance*

The rating curves (Fig. 5.13.a) prepared for both the setups with underflow aperture as 25 mm as well as the curves prepared from overall observations (Fig 5.13.b) further illustrate the performance enhancement due to the modification of axial overflow outlet to tangential one. These illustrations demonstrate a higher performance for all range of headloss and underflow aperture. For instance, the discharge in two tests running under headloss as 3.7 m and 1.2 m increased by 16% and 22% respectively compared to that in a setup with axial overflow outlet. In other words the same amount of flow with a tangential outlet can be handled minimizing the headloss by 25.5% and 32.7% respectively.

The improvement of the hydraulic performance due to the tangential overflow outlet over the axial setup can be explained by the following reasoning. First, the energy retained in the form of tangential velocity near the overflow outlet of the hydrocyclone has been recovered substantially, most of which would have been lost in the setup with axial overflow. As the tangential component of the velocity is much stronger than the axial component, the

modification has resulted in a much higher efficiency. Second, the increase in overflow diameter by 25% in the tangential setup has also minimized frictional losses along the vortex finder.

| a | b |
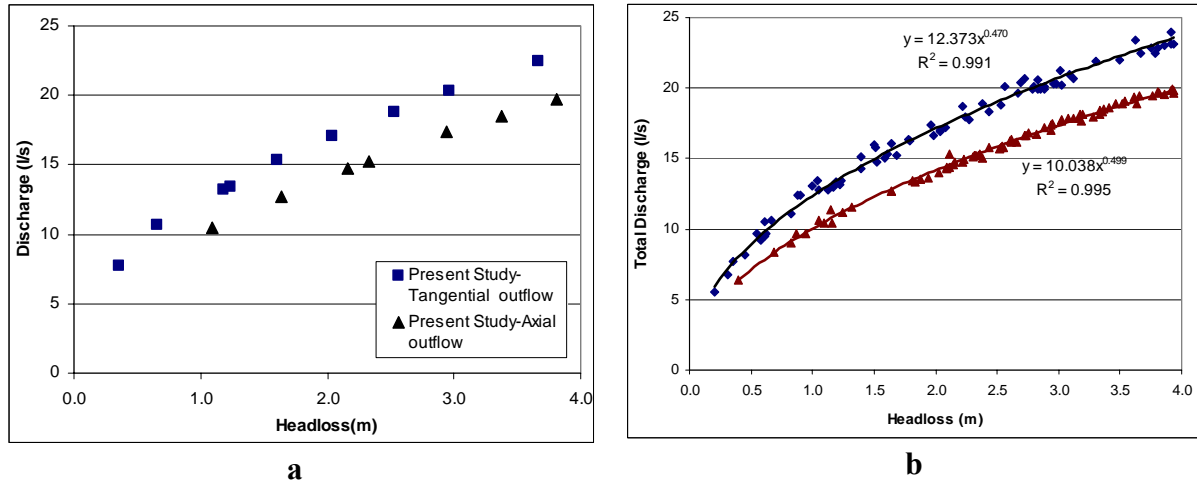
Fig. 5.13 Comparison of hydraulic performance of axial overflow and tangential overflow setups using rating curves for : a) underflow aperture as 25 mm b) overall data

5.3.4   Sediment Removal Efficiency(SRE)

SRE using two batches of sediment having d_{50} as 200.4 μm and 99.7 μm was investigated analyzing the PSD curves obtained from overflow, feed and underflow streams (Fig. 5.14). In addition, the SRE curves by particle size were derived from PSD curves and compared with those obtained from hydrocyclone with axial overflow geometry (Fig. 5.15).

In Table 5.3, 34 numbers of selected test results obtained from axial and tangential setups have been presented. Each pair of results was formed matching the similar operating conditions of the tests from each setup. Better performance due to tangential overflow, particularly for smaller flows can be noticed. For instance, the lowest removal efficiency of the cyclone with tangential overflow was observed as 84.2 % for a reference headloss of 1.58 m as against 66.3 % in the cyclone with axial setup for a corresponding headloss of 1.64 m. Similar conclusion is valid for higher flows as well.
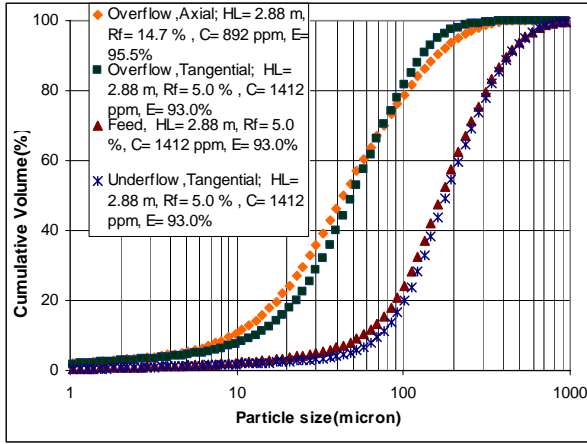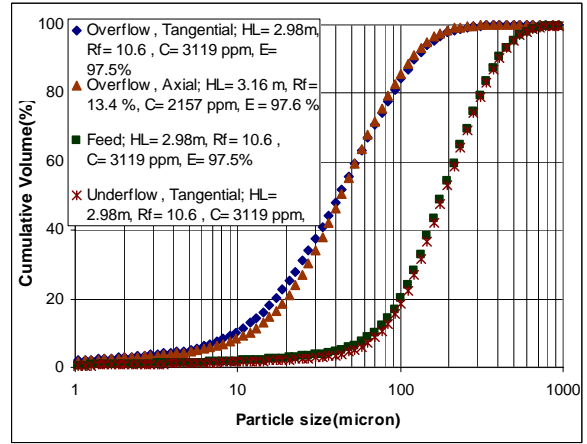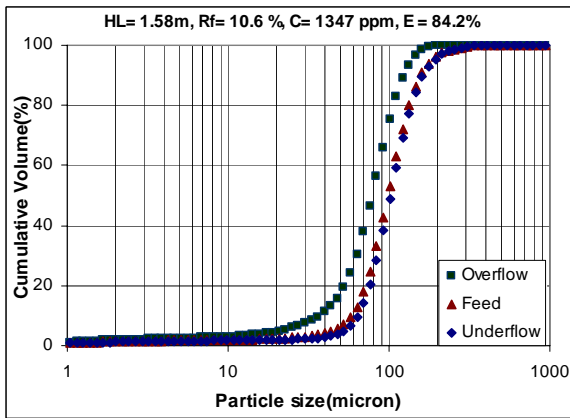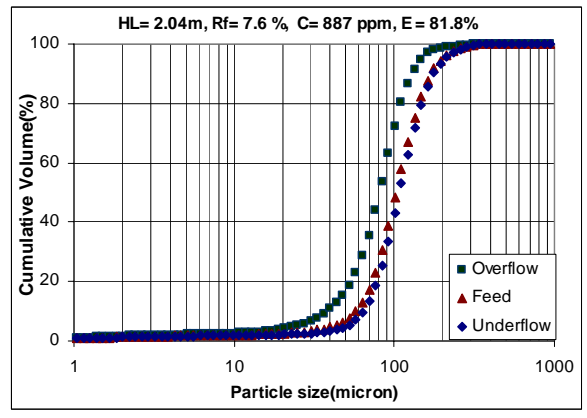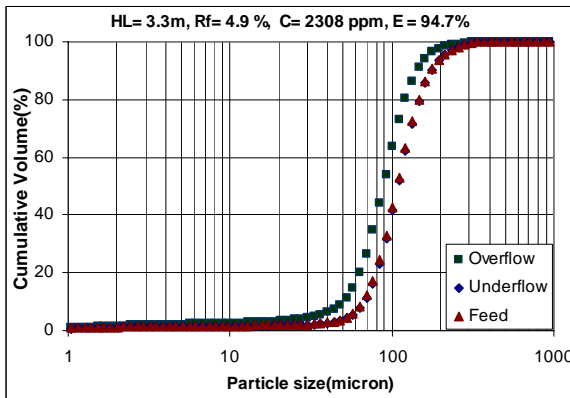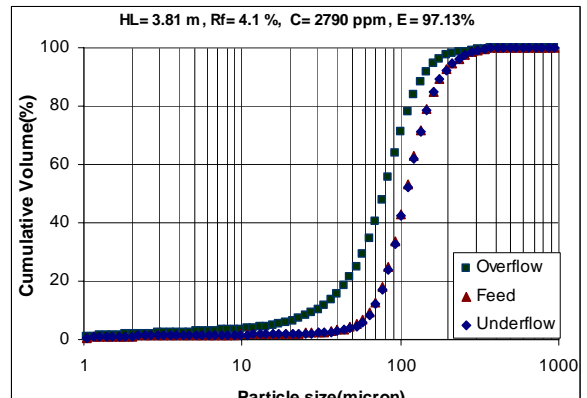
Fig. 5.14 PSD received from feed, overflow and underflow under different operating conditions in cyclone with tangential overflow. Test results a,b are obtained using Fugesand whereas 'c,d,e,f' are obtained using Baskarpsand. H_L = Headloss, $R_f = Q_u/Q_c$, E = Sediment Removal Efficiency

The results on PSD obtained from two different tests conducted under similar operating conditions but with two different overflow geometries have been presented in Fig 14.a & b for comparison. Although the overall SRE of cyclone having axial overflow is marginally

higher than that with tangential overflow geometry, when operating both the cyclones under a head of 2.88 m, the coarser particles (d > 60 μm) were better separated by the cyclone with tangential overflow (Fig 5.14.a). On the other hand, exactly the same efficiency was

a

b

c

d

e

f
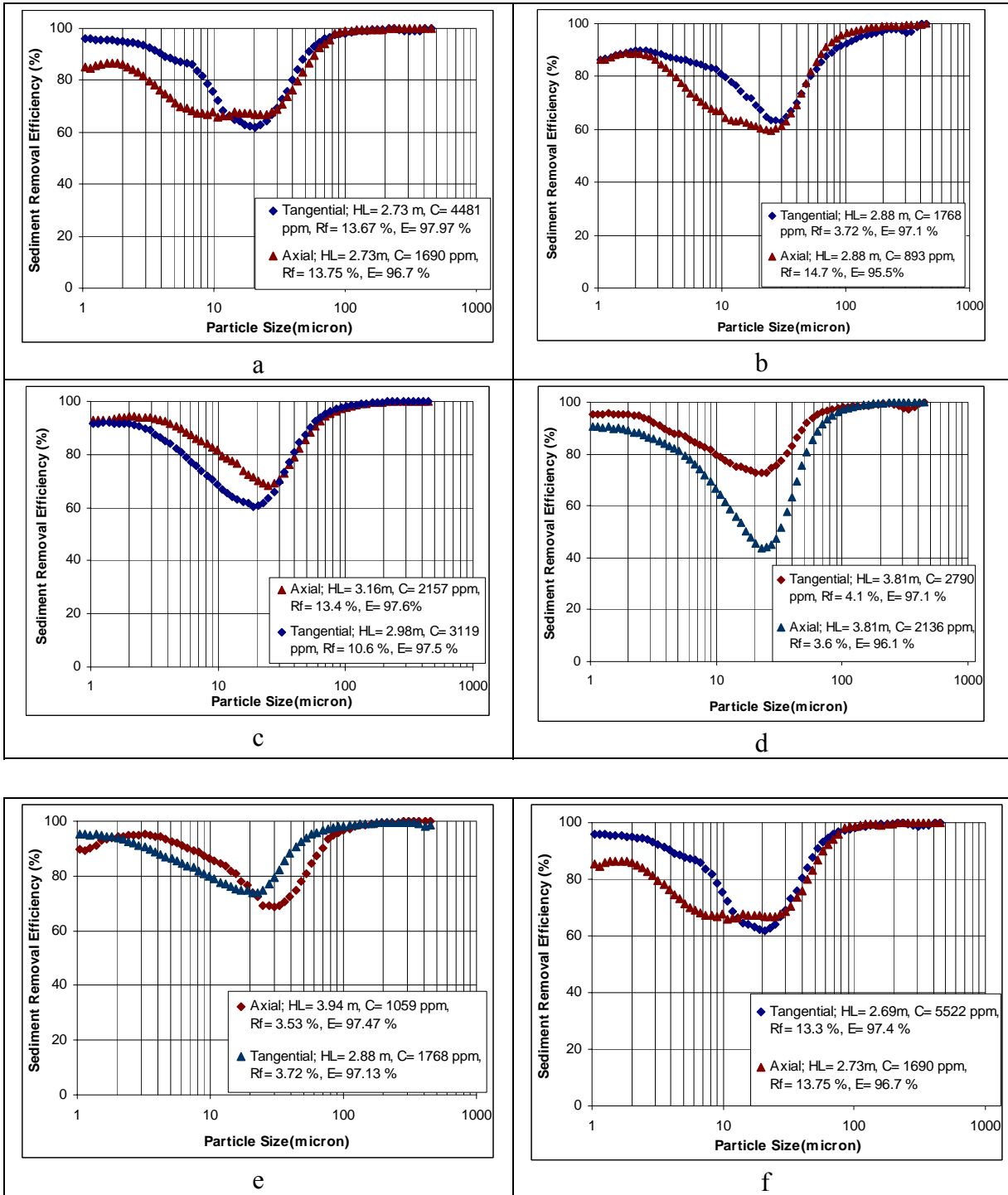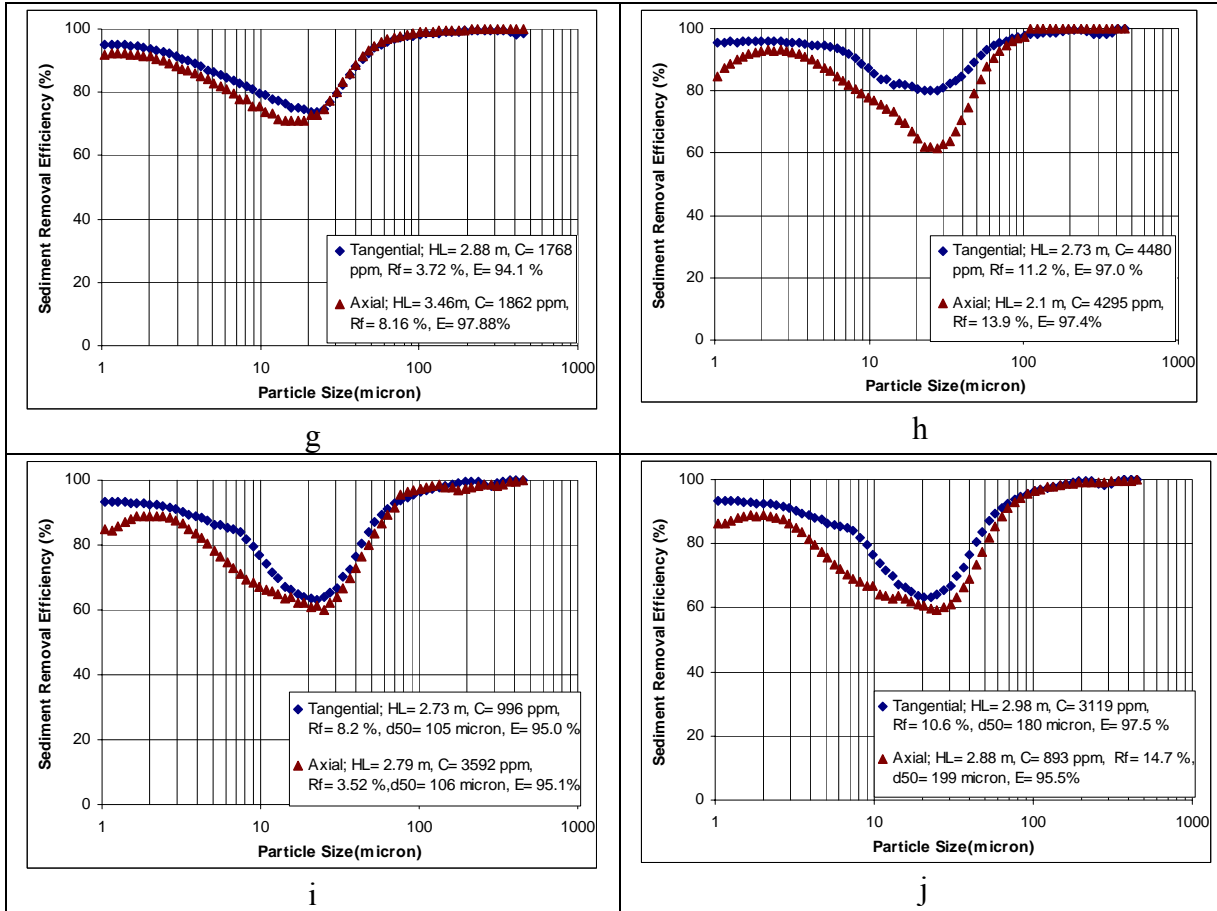
Fig. 5.15 Comparison of SRE (Actual recovery) curves obtained by cyclone with axial and tangential overflow setup: a,b,c,d: Similarity in headloss; e,f: Similarity in flow ratio, *Rf* ; g,h: Similarity in sediment concentration; i,j: Similarity in d50; H_L= Headloss, $R_f = Q_u/Q_c$, E = Sediment Removal Efficiency

observed in both the devices even when the cyclone with tangential overflow was operated under a head lower by 5.7%. In Fig. 5.14.c-f the PSD obtained from the tests conducted in a tangential setup using very fine and more homogeneous sediment have been presented. The results obtained under headloss starting from as small as 1.58 m to as high as 3.81 m have been depicted. Despite the sediment used being much finer, most of the sediment fed into the system was captured by the underflow resulting in higher efficiency even for smaller flows. However, like in an axial setup the SRE was more influenced by operating parameters, such as flow ratio in lower headloss range compared to that in higher range.

Sample results describing the SRE by particle size for axial as well as tangential setups have been presented in Fig. 5.15. As witnessed from these figures, the recovery curves are similar,

fish-hook effect is prominent in tangential setup as well. From overall data as well as the sample results presented in Fig 5.14 and Fig 5.15, it can be inferred that there is no compromise on SRE of cyclone with tangential outlet over the one with axial overflow provided the operating conditions are similar. For instance, the removal efficiency of tangential setup was 97.1% compared to 95.5% for axial setup while tested under a same headloss as 2.88 m (Fig. 15.b). The same efficiency of both the cyclones have been observed when cyclones were operated under higher head range(Fig. 5.15.c & d). Similar results were also observed, when tests were run under similar flow ratio, sediment concentration and median particle size (Fig. 5.15, e-j). The marginal difference in each comparison is believed not due to the geometry of the hydrocyclone, but due to the difference between the respective operating conditions in the tests. The role of these operating parameters on SRE has been discussed in next sub chapter 5.5

5.3.5 *Conclusions*
- The inherent fish-hook property of the hydrocyclone was conserved in the setup with tangential overflow as well.
- The hydraulic performance of cyclone with tangential overflow has been found much higher than that of hydrocyclones studied. For a reference headloss of 3.5 m the discharge increases by 16.8% compared to that with axial setup resulting in reduction of headloss by 28%. When compared with standard and gMax series hydrocyclones, the discharge increased by 41% and 33.7% respectively resulting in energy saving of 52% and 46% respectively.
- For similar operating conditions, SRE due to tangential outlet is better than that due to axial outlet.

5.4 Comparison of SRE of Hydrocyclones of Dia 0.22 m and 0.38 m

It was not possible to conduct tests in both the cyclones under exactly the same operating conditions. Nevertheless, the results obtained from 8 number of tests conducted under the similar operating parameters in both the hydrocyclones have been presented in Table 5.3 for comparison. It was found earlier that the SRE of a hydrocyclone is quite sensitive to operating parameters (refer sub-chapter 5.5 for detailed analysis) in smaller flow conditions.

Nevertheless, the observed results show that the SRE of both the cyclones are comparable in this region.

However, for moderate and higher flow conditions ($H_L > 2.0$ m), the efficiency of the larger hydrocyclone was better in separating coarser as well as finer particles. For example, while operating both the cyclones under similar operating conditions (S_{II}-12 vs. S_2-27), the efficiency of removal of 150 μm particle in larger hydrocyclone is 99.1 % as against 96.3 % in smaller cyclone. When compared the efficiency of removal of the same particle size with that in S_{II}-9 test with exactly the same headloss, the same difference is witnessed. Similarly, considering the same test results as considered above, the efficiency of smaller cyclone to remove particles with d_{50} as 125 μm and 106 μm, the smaller cyclone was found lower by 6.5 % and 12.5 % respectively.

Table 5-4 Comparison of Efficiency of cyclones with 0.22 m and 0.38 m diameter

Test Run	Diameter (mm)	Feed d50	C_feed (ppm)	Head (m)	Rf (%)	G Force	E_particles			E_avg (%)
							106 μm	125 μm	150 μm	
S_{II}-9	224	105.14	1287	1.49	1.84	10.8	81.16	91.9	96.64	87.96
S_{II}-12	224	111.18	2446	2.23	5.3	14.4	85	91.8	96.31	91.3
S_{II}-11	224	111.06	2935	2.56	3.13	18	86.96	93.83	97.21	92.3
S2-15	380-Axial	91.84	176	1.64	8.92	2.4	80.1	85.2	89.20	66.3
S6-41	380-Tangential	102.88	887	2.01	7.64	4.2	86.11	90.2	93.20	81.8
S2-9	380-Axial	160.35	752	2.22	18.58	3.2	97.5	98.3	99.02	96.11
S2-27	380-Axial	153.57	1435	2.35	5.98	3.4	97.51	98.53	99.10	95.63
S6-44	380-Tangential	109.36	5522	2.66	13.33	6.1	98.42	98.7	99.22	97.35

In a field of centrifugal acceleration, the general belief is that the greater the G-force (ratio between centrifugal and gravitational forces), the higher the particle removal efficiency. Nevertheless, this principle did not hold in the present study. Despite G- force being 4.2 times higher in the example considered above, the removal efficiency of the same particle size and characteristics has been found even better in the larger hydrocyclone. From this discussion and other data presented in Table 5.4, it can be concluded that overall geometry and the hydraulics of the system, which enable sufficient residence time is equally important as to the headloss and resulting G-force across the hydrocyclone to have desired level of particle separation efficiency.

5.5 Comparison of Cut size (d50)

The performance of hydrocyclone, especially SRE is commonly assessed in terms of cut size or d_{50} of the particles, which have equal probability to report to overflow as well as underflow outlets. Fig. 5.16 compares the d_{50} values observed in the present experiment with those predicted by other investigators. The relation due to Bradley and Pulling (1959) was developed based on equilibrium orbit theory, whereas that due to Rietema (1961) was based on residence time theory and optimum geometry defined by the researcher. On the other hand, the empirical relation developed by Plitt (1976) was based on extensive data covering the wide range of design and operating variables. Whereas the prediction of Dahlstrom (1954) was based on extensive study in a hydrocyclone having 23 cm diameter.
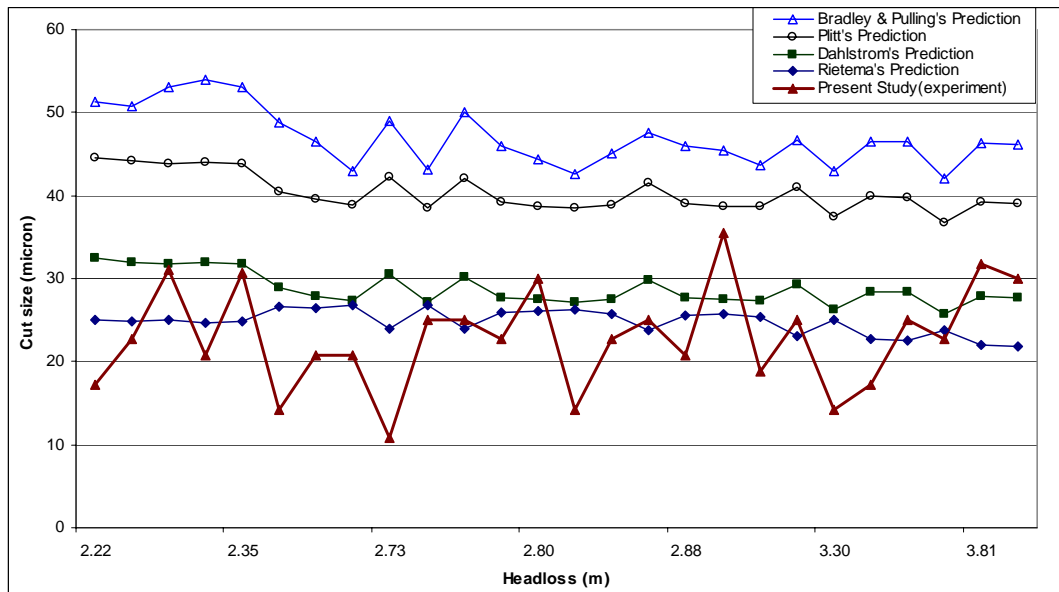
Fig. 5.16 Comparison of cut size under study with the cut size predicted by other investigators

The comparison of the results presented in Fig. 5.16 clearly show that the d_{50} values observed in all the tests of the present study are much smaller than that predicted by Bradley and Pulling (1959) and Plitt (1976). Further, except for a couple of test results, which were obtained under extremely low flow ratio (~ 3%), the d_{50} values observed in the present study are finer than that predicted by Dahlstrom (1954) and Rietema (1961).

While Plitt (1976) used the data of smaller as well as larger cyclones, the predictions of Dahlstrom and Rietema's were based on much smaller diameter. The characteristics cyclone

number, Cy_{50}, as 3.5 defined by Rietema was based on the experimental results obtained in a cyclone having 7.5 cm diameter. These facts suggest that the d_{50} values predicted by these investigators should have been smaller than what were observed in the present study. Therefore, the comparison of results obtained in the present study with those predictions based on theory as well as extensive experimental results shows a remarkable performance improvement of the modified hydrocyclone. This enhancement in the performance of the hydrocyclone is attributed to the better geometry and thereby the better hydraulic conditions near the inlet and outlet. However, unlike those predicted by previous investigators, there is a considerable variance in the cut size. This is believed due the feed material near the cut size in the present study being in a very small quantity.

5.6 Effect of Parameters on SRE of Hydrocyclone

The influence of operating parameters on the performance of the hydrocyclone is discussed in this section. Each chart in Fig. 5.17 presents two test results obtained from hydrocyclone having 0.38 m diameter having axial and tangential overflow setups. Each of these pair of tests conducted under similar operating conditions resulted in exactly the same results. Therefore, the effect of only these operating parameters (H_L, C, Rf and d_{50}) is believed to play important role on the performance of the hydrocyclone, which is discussed in the ensuing sub-chapters. Since the experiments were carried out using only two batches of sediment, effect of variation of sediment particle size is not considered.
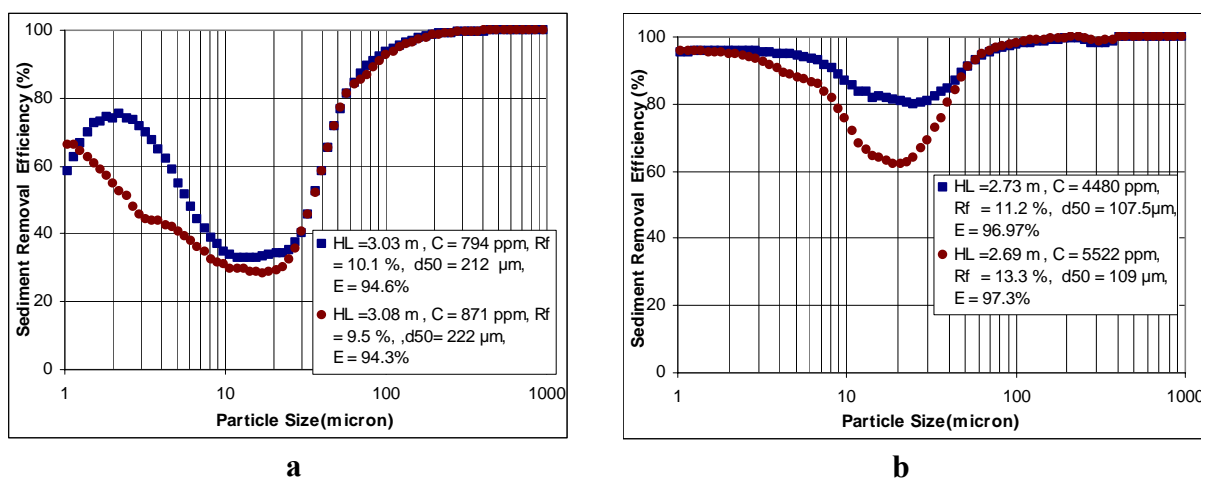
Fig. 5.17 SRE by particle size of a-380-mm dia hydrocyclone considering similar operating conditions: (a) with axial setup (b) with tangential setup. H_L= Headloss, R_f= Q_u/Q_c, E = Sediment Removal Efficiency

5.6.1 Effect of Headloss Across the Hydrocyclone

The test results representing the dependency of SRE of hydrocyclone on headloss are presented in Fig. 5.18 to Fig.5.20. The efficiency curves derived for overall tests with varying operating conditions have been best described by a parabolic relation (Fig. 5.18.a). As the results presented in Fig. 5.18.a show behavioral distinction of hydrocyclone in the zone of smaller and larger flows

The test results representing the dependency of SRE of hydrocyclone on headloss are presented in Fig. 5.18 to Fig.5.20. The efficiency curves derived for overall tests with varying operating conditions have been best described by a parabolic relation (Fig. 5.18.a). As the results presented in Fig. 5.18.a show behavioral distinction of hydrocyclone in the zone of smaller and larger flows further analysis was carried out dividing the results into two parts.
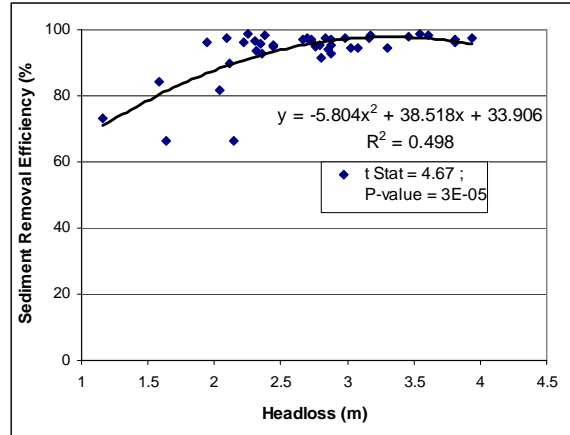
a) Overall data, R_f= 2.4- 25.5 %; C = 91- 7618 ppm
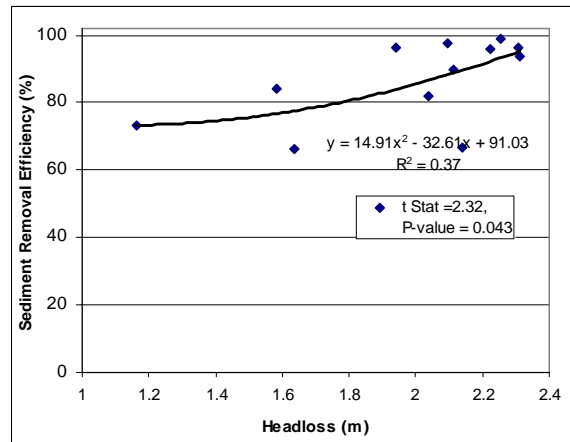
(b) R_f =4.9- 25.5 % ;C= 125-7618 ppm
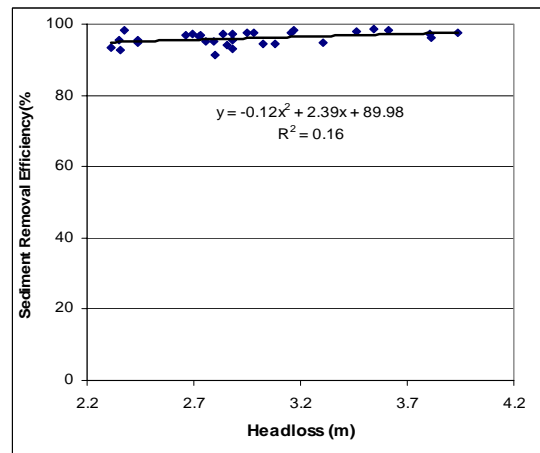
c) R_f = 2.4- 17.3 %; C = 91-5522 ppm

Fig. 5.18 Relation between E and H_L for: (a) overall data (b) smaller flows (c) higher flows.

a) R_f=2.43 %- 5.0 %
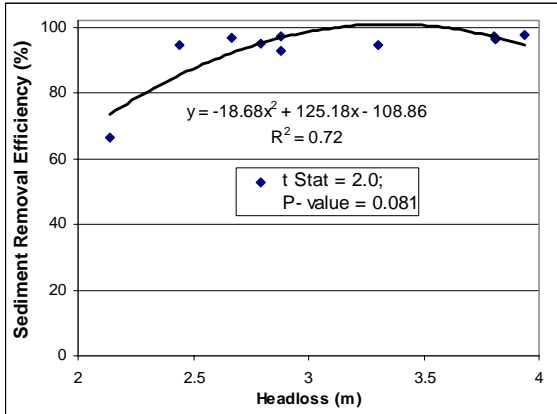
b) R_f=6.0 %- 10.6 %
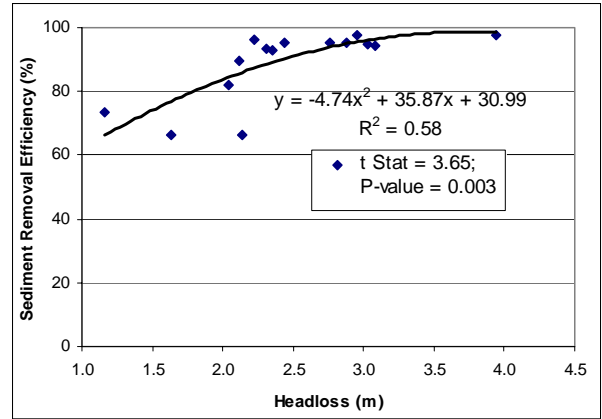
c) R_f=10.6 %- 25.5 %

d) C_{feed} =91 ppm – 1060 ppm
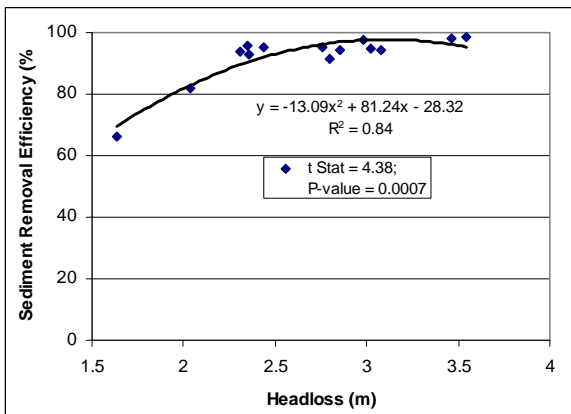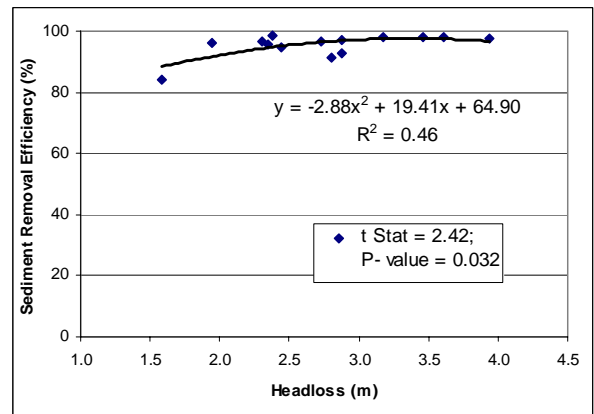
e) C_{feed} = 1060 ppm - 2020 ppm
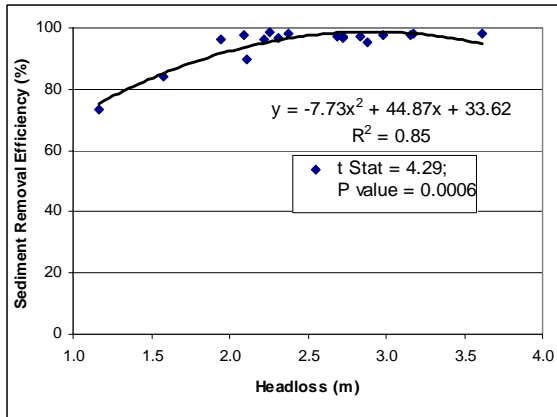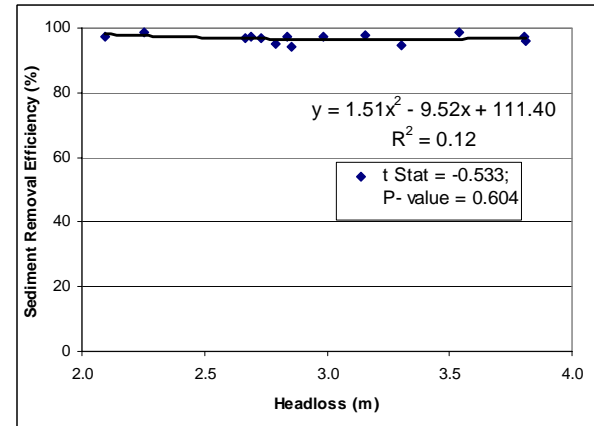
f) C_{feed} = 2136 ppm - 7618 ppm

Fig. 5.19 Relation between E and H_L for: (a,b,c) influence of flow ratio (d,e,f) influence of feed concentration

Accordingly, the results obtained from tests with headloss 2.31 m or less were considered as smaller flows, and those obtained with greater than 2.31 m as larger flows (Fig. 5.18.b and Fig. 5.18.c. As can be observed from these illustrations, the curve is steeper in the range of steeper headloss and opposite is true in the region of higher headloss (larger flows). A steeper gradient at the beginning and an *R square* value as 0.37 indicates a relatively stronger dependency of the SRE on headloss for smaller flows (Fig. 5.18.b). On the other hand, a flatter gradient with an *R square* value as 0.16 reveal a much weaker relation between these variables for larger flows.

Nevertheless, the efficiency of the cyclone might have been influenced by other variables as well. Therefore, in order to assess the influence of only the headloss, further investigation was carried out dividing the other operating variables into three levels; small, moderate, and large, while considering the variation of headloss (Fig. 5.19 and Fig. 5.20).

The illustrations presented in Fig 5.19. a,b,c and *R Square* values from regression analysis show that there is a strong correlation between SRE and headloss. Further, higher values of t Stat (0.84 and 0.85) but much lower P-values (0.0007 and 0.0006) suggest that such a relation is valid in the range of moderate and higher flow ratios as well.However, t Stat value being relatively low and P-value being much higher than 0.05, it can be concluded that such a relation is statistically insignificant in the region of smaller flow ratio (*Rf* < 5.0%).

On the other hand, *R Square* values from regression analysis as 0.58, 0.46 and 0.12 for smaller (91-1060 ppm), moderate (1060-2020 ppm) and higher feed concentration (2186 - 7618 ppm) indicates the effect of concentration on SRE seems to be weaker compared to flow ratio (Fig 5.19. d,e,f). Moreover, both the illustrations as well as statistical analysis signify a very weak relation between the headloss and SRE in the range of higher concentration of feed, implying that the SRE is literally insensitive in the range of higher feed concentration provided the H_L > 2.0 m.
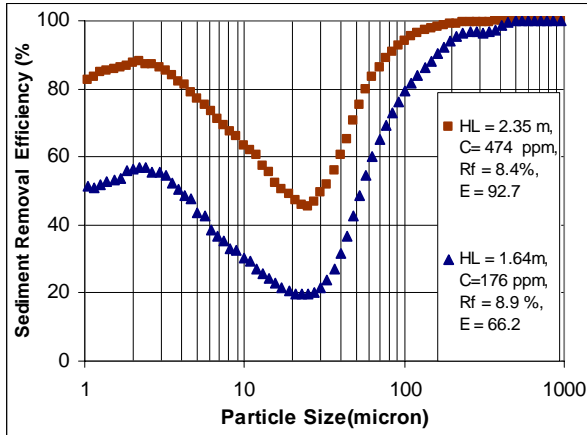
a) axial overflow setup
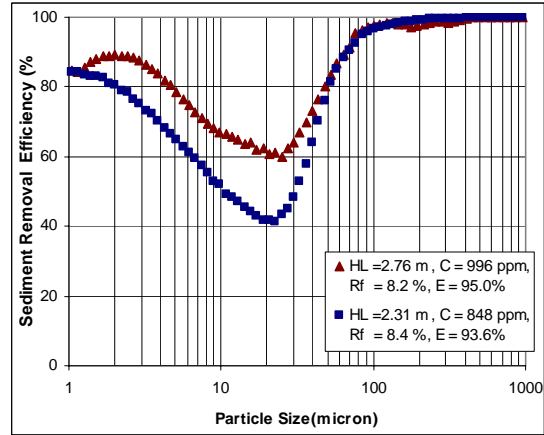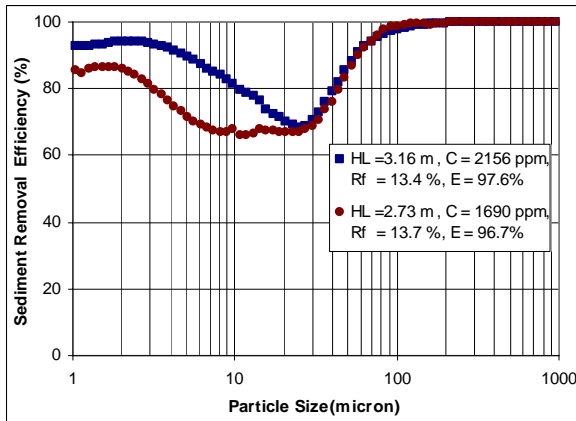
b) axial overflow setup

c) axial overflow setup
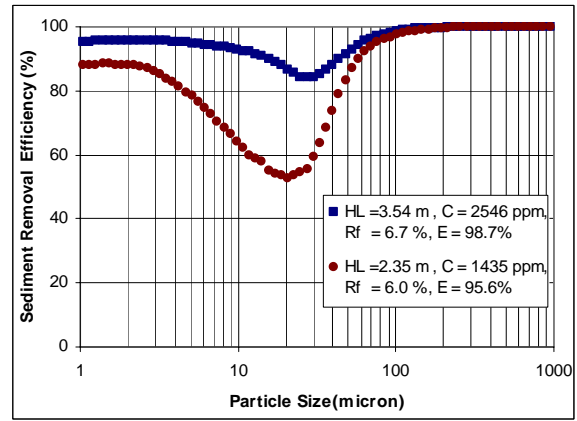
d) axial overflow setup
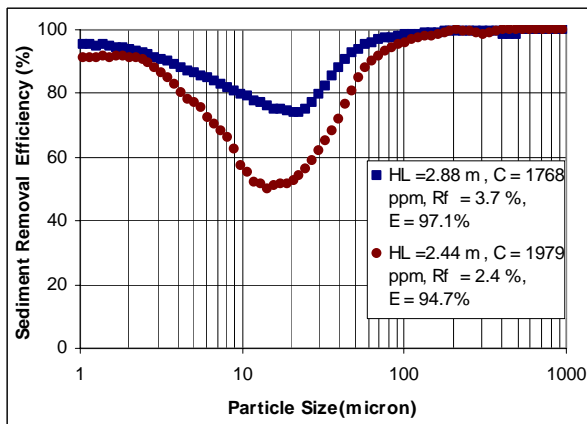
e) tangential overflow setup
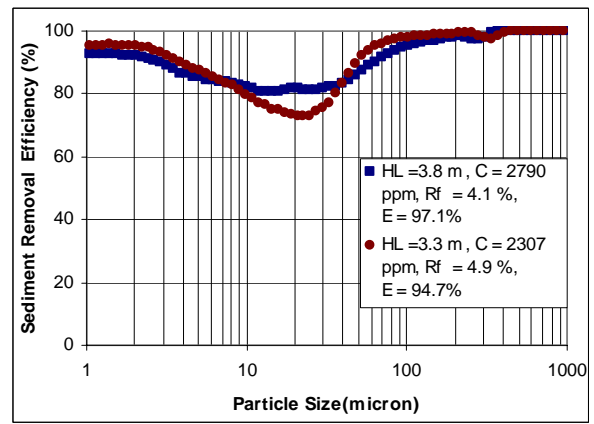
f) tangential overflow setup

Fig. 5.20 Comparison of SRE of a-380- mm dia. hydrocyclone by particle size under different operating conditions, with special reference to variation of headloss **.** H_L= Headloss, R_f= Q_u/Q_c, E = Sediment Removal Efficiency

The illustrations presented in Fig. 5.20 through SRE curves further prove the dependency of SRE on headloss especially in the region of smaller flows. For instance, a total difference in SRE by about 25% between two test runs conducted under a headloss of 1.61 m and 2.35 m having almost the same proportion of underflow discharge and sediment concentration (Fig 5.20.a) further demonstrates a stronger dependency of hydrocyclone performance on headloss for smaller flows. In this range of flows, not only the total efficiency but also the higher efficiency of each particle size were observed. Nevertheless, further observation of results obtained from axial as well as tangential overflow setups (Fig. 5.20.b, c,d,e,f) for larger flows revealed relatively weaker relation in this region.

The shape of all the SRE curves derived for the full range of flow conditions is similar. The fish-hook effect is prominent in all the tests. The common feature of all the curves is that the lowest point of the curve is located in the proximity of the same particle size having a mean diameter as 20 micron. However, the depth of the curve gets shallower and wider with the increase of headloss resulting in enhanced performance.

The steepness of the curve at the beginning followed by a flatter gradient (Fig. 5.18.a) can be argued with the following reasoning. While the centrifugal acceleration is sufficient to drag the coarser particles to the wall of the hydrocyclone, the same is not sufficient for fine particles in the range of smaller headloss. With the increase of headloss (flow), tangential velocity and hence the centrifugal acceleration increases leading to the separation of more fine particles and thereby steep SRE curve at the beginning. With further increase of headloss, the centrifugal force reaches a value which is sufficient to separate most of the sediment particles used in the tests leading to a flatter gradient in the range of larger headloss.

5.6.2   *Effect of Flow Ratio*

The role of the underflow discharge on sediment removal performance has been illustrated in Fig 5.21 and 5.22. The results obtained from all the tests conducted under different operating conditions are depicted in Fig 5.21.a. The flatness of the curve as well as very small *R square* value implies a weak dependence between the two variables.
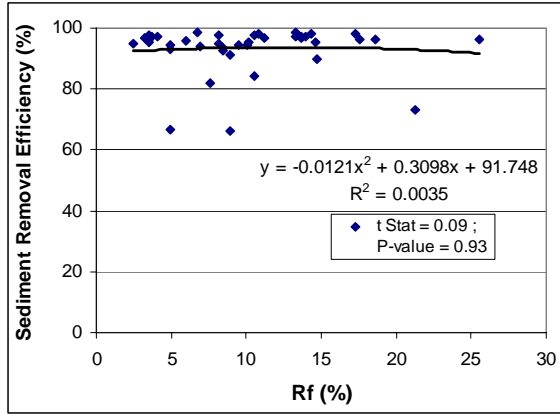
a) Overall data, R_f = 2.4- 25.5 %; C = 91- 7618 ppm
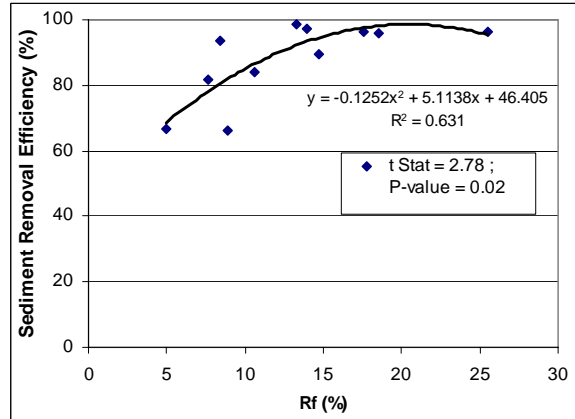
b) H = 1.58 -2.31 m ;C= 125-7618 ppm
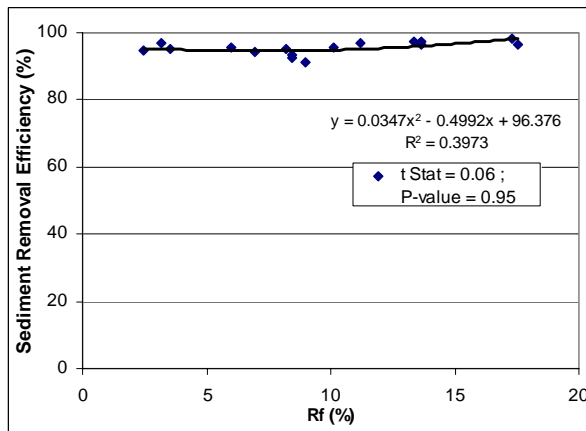
c) H = 2.3-2.8 m ; C = 474-5523 ppm
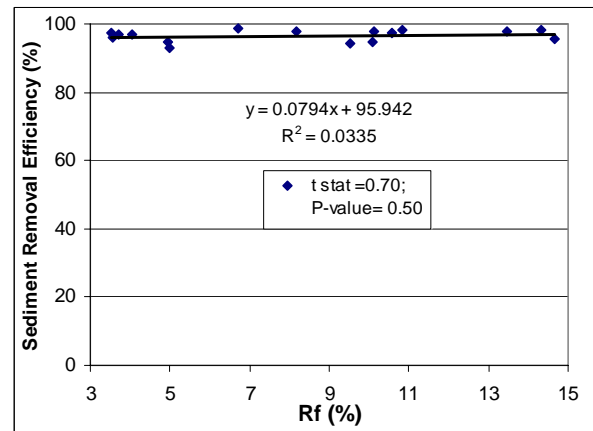
d) H =2.8-3.93 m ; C = 91-3119 ppm

Fig. 5.21 Relation between SRE and proportion of underflow discharge : (a)considering overall data (b), (c), (d) considering ranges of headloss . H_L= Headloss, R_f= Q_u/Q_c, E = Sediment Removal Efficiency

However, scatterness of the plot also suggested a possibility of dependency between these variables in some definite range of other variables, such as headloss. Therefore further investigation was carried out grouping the total data into three categories: tests with smaller, medium and higher flows (Fig. 5.21.b, c & d). Accordingly, it is evident from the test results obtained for smaller flows (Fig 5.21.b) that a strong relation between SRE and the flow ratio holds, the performance being enhanced with the increment of flow ratio. A *P-value* as 0.02 further indicates statistical significance of such a dependence. On the other hand, neither the visual observation nor the regression analysis witnessed a dependence of these parameters for medium and higher flows.
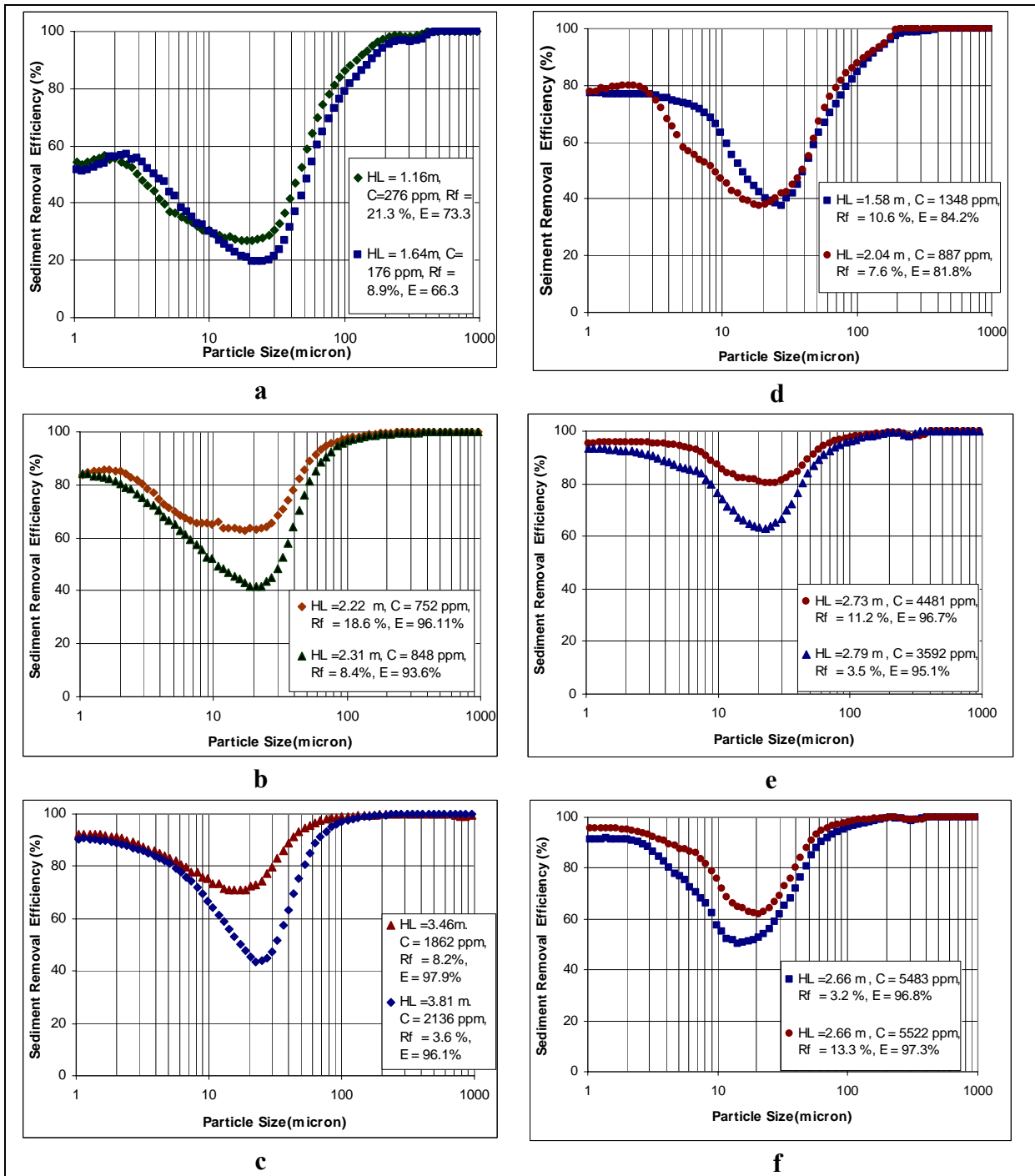
Fig. 5.22 Comparison of SRE of a 0.38 m dia hydrocyclone by particle size under different operating conditions, with special reference to variation of flow ratio. H_L = Headloss, $R_f = Q_u/Q_c$, E = Sediment Removal Efficiency

The influence of underflow discharge on SRE was further examined comparing the performance of two or more tests having variable flow ratio, but minimal variation of headloss and concentration (Fig. 5.22). This is illustrated through the PSD curves obtained

5-34

from the representative tests. A stronger influence of flow ratio on the performance of hydrocyclone once again can be witnessed for both the setups (Fig. 5.22.a & d). In axial setup, it was possible to obtain higher efficiency in a test with smaller headloss (1.16 m against 1.64 m) using a higher flow ratio (21.3 % against 8.9%). Similarly, increase in SRE by 2.4% could be obtained in tangential setup when a flow ratio was larger by 3% in a test conducted under a headloss lower by 0.46 m (Fig. 5.22.d). A slightly enhanced performance with the increase of underflow discharge in both the setups can be witnessed from the results obtained for medium and larger flows as well. However the degree of performance improvement in these cases is quite small compared to what was observed in case of smaller flows (Fig. 5.22.b,c,e,f).

The pattern of the performance efficiency curves for smaller as well as larger underflow discharge is same. The fish-hook effect is well established in both cases. However, the depth of the fish-hook curve gets shallower and flatter with the increase of underflow discharge. Further, the SRE curves for full range of particle size with larger flow ratio are always higher than that with smaller one.

For a constant head difference, the overflow discharge decreases with the increase of flow ratio. However, in a hydropower plant, a maximum flow through the overflow is always desired to minimize the cost incurred in hydraulic structure. Therefore, the above results suggest maintaining a minimum flow ratio considering the choking free criterion at the underflow outlet while operating hydrocyclone in the zone of higher flows. Since the sediment concentration in the river during operational hours hardly exceeds 1 % by volume (26,500 ppm), the amount of water passing through the underflow outlet will be insignificant compared to that in conventional settling basins.

5.6.3 *Effect of Feed Concentration*
The results illustrating the effect of concentration on sediment removal performance have been presented in Fig. 5.23 and Fig. 5.24. The results obtained from 43 tests conducted under a wide range of operating variables have been depicted in Fig. 5.23.a. As the role of concentration might be influenced by the magnitude of the flow processed by the

hydrocyclone, the results have been presented further dividing it into three groups; lower, moderate and higher headloss range (Fig. 5.23.b,c & d).
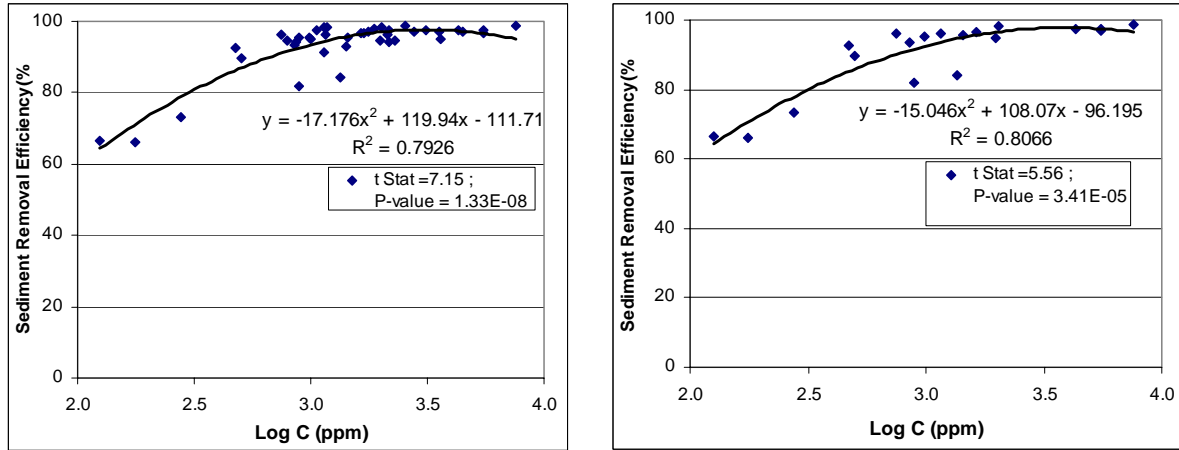
a) Overall data, H_L = 1.16 -3.94m; R_f = 2.4- 25.5 %; **b)** H_L = 1.16-2.69 m ; R_f = 2.4- 25.5 %;
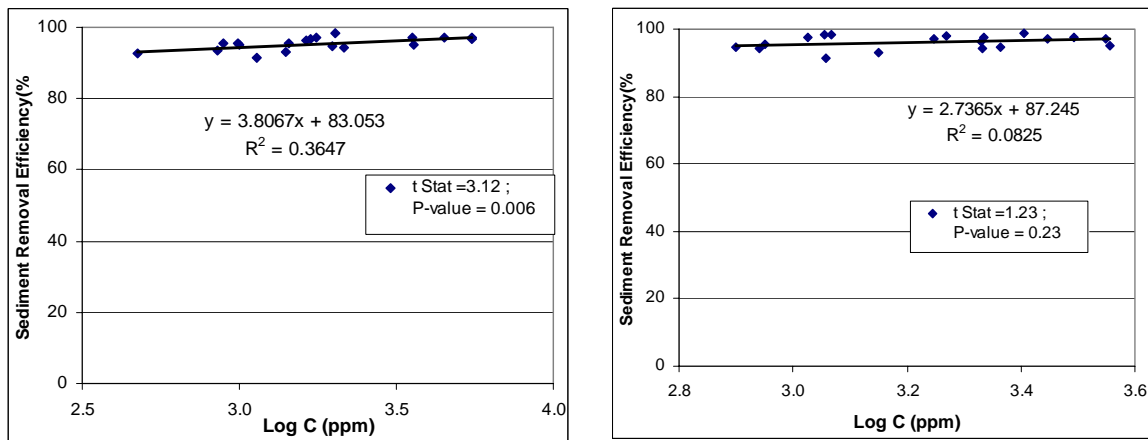
c) H_L = 2.31-2.88 m ; R_f = 2.4- 17.6 %;   **d)** H_L =2.98-3.94 m ; R_f = 3.5-14.3 %;

Fig. 5.23 Relation between SRE and concentration: (a)considering overall data (b), (c), (d) considering different range of headloss. H_L= Headloss, R_f= Q_u/Q_c, E = Sediment Removal Efficiency

It is interesting to note from Fig 5.23.a that sediment removal performance enhances with the increase in concentration. The visual observation on the results shows a strong dependency between these parameters. A very low *P-value* derived from regression analysis further substantiate the significance of such a relation. Further observation of the results presented in sub groups (Fig. 5.23.b,c & d) reveals that such a dependency diminishes gradually with the increase of flow. Although a weaker relation between these variables for medium flow can be
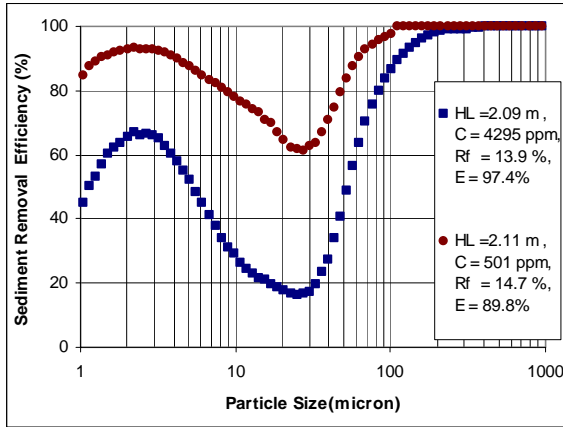
a) axial overflow setup
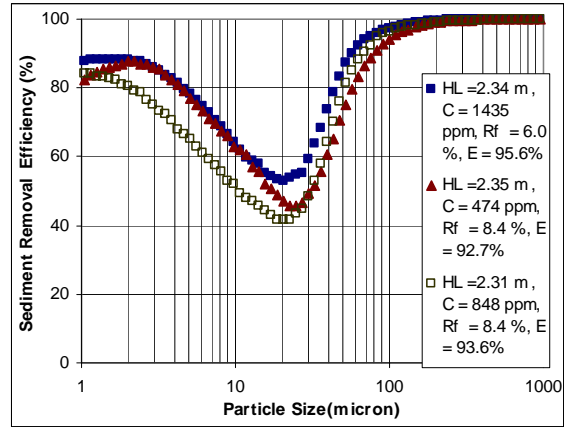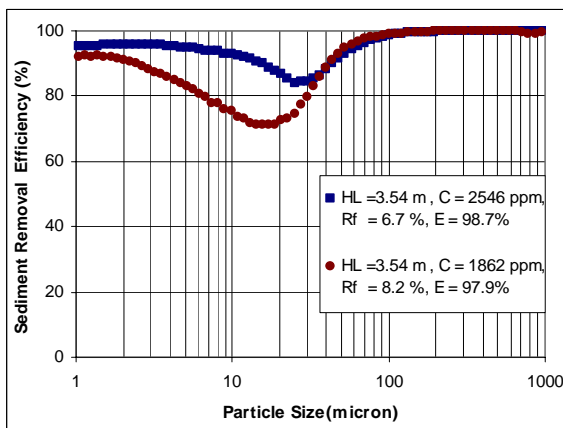
b) axial overflow setup

c) axial overflow setup
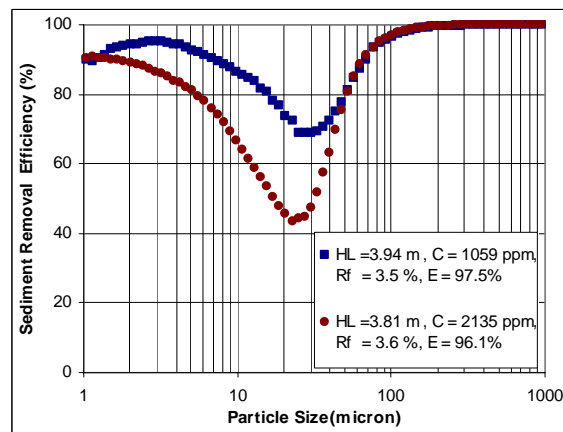
d) axial overflow setup
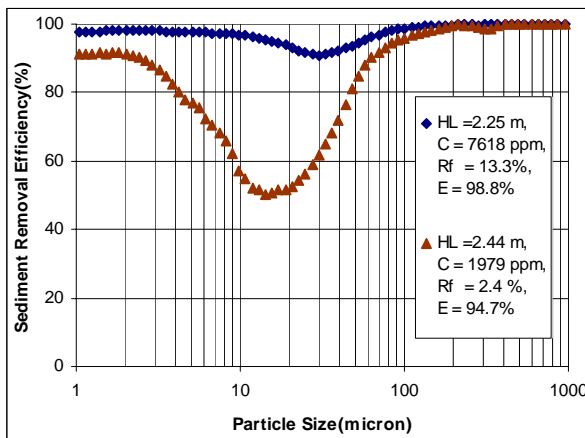
e) tangential overflow setup
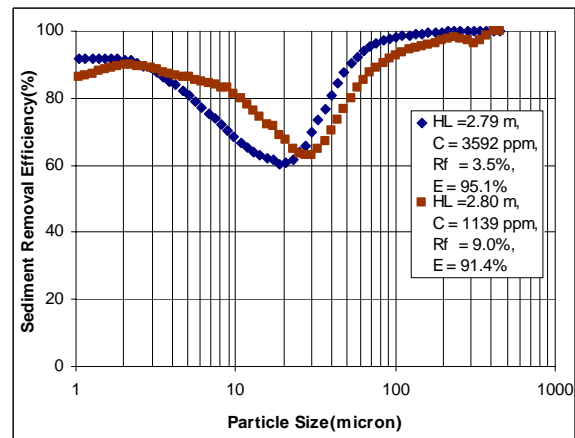
f) tangential overflow setup

Fig. 5.24 Comparison of SRE of 0.38 m - dia hydrocyclone by particle size under different operating conditions, with special reference to variation of feed concentration. H_L= Headloss, R_f= Q_u/Q_c, E = Sediment Removal Efficiency

witnessed by visual observation , the regression analysis of these data suggests such a relation to be statistically significant.On the other hand, visual impression as well as the regression parameters for larger flows signify no dependency between these two variables. The curves by particles size obtained for axial as well as tangential setups and presented in Fig. 5.24 further substantiate the above conclusion.

5.6.4   Effect of Underflow Opening on the Performance of the Hydrocyclone

The effect of opening of underflow outlet was studied by varying the size of the apertures of the underflow from 15 mm to 60 mm (corresponding to a sectional area of 177 mm^2 to 2827 mm^2). The discharge through the underflow outlet in both the setups decreased with the increase of flow (headloss) in the hydrocyclone (Fig 5.25.a) and tend to converge in the range of higher headloss. Further, under the same operating conditions, the axial setup produced a higher flow ratio for the full range of headloss compared to tangential setup.
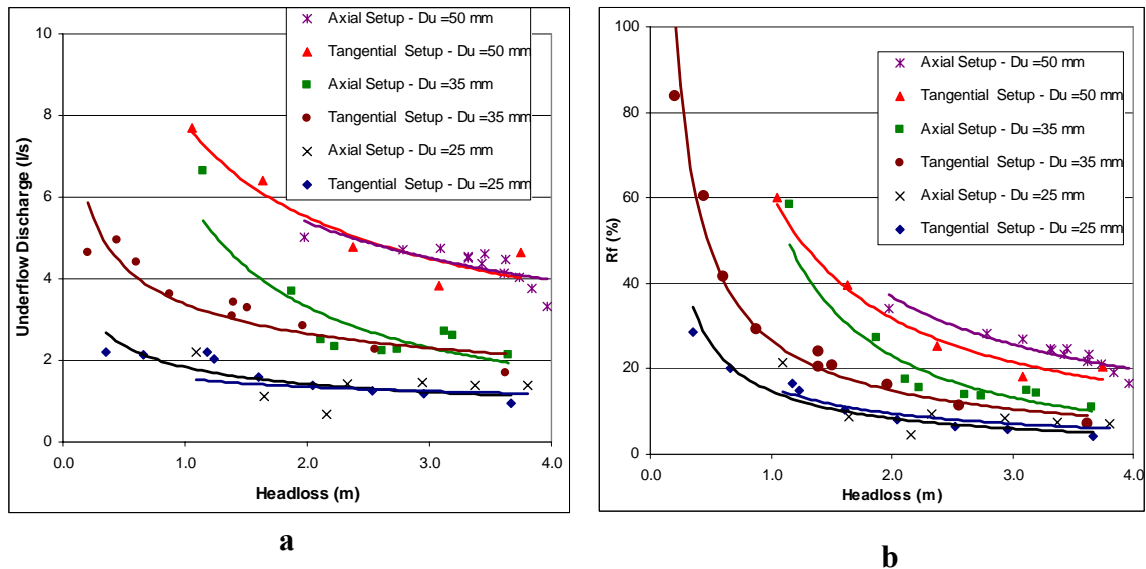
Fig. 5.25 Comparison of underflow hydraulics of hydrocyclone due to axial and tangential setups with different underflow apertures : (a) total discharge (b) flow ratio

The reason for having higher *Rf* at the beginning followed by a lower but a converging trend is attributed to the following arguments. When the flow was quite small, full swirl was not developed in the hydrocyclone. As a result the axial velocity of the flow was quite strong due to the gravity action. With the increase of headloss, the swirl inside the hydrocyclone was

fully developed resulting in a much stronger tangential velocity component than the axial one. Therefore, in a range of smaller headloss, the flow ratio of the respective outlets was quite high which gradually diminished with a tendency of convergence in the region of maximum flows.

Optimization of Underflow Outlet Opening

While the effect of the variation of underflow opening on discharge capacity of hydrocyclone was insignificant for axial setup, the same was found remarkable for hydrocyclone with tangential setup (Fig 5.26). Interestingly, the highest discharge in the hydrocyclone was observed not due to the lowest (50 mm) or the smallest (15 mm) underflow openings, but due to the one in between them (35 mm Ø, 962 mm^2(Table 5.5, Fig.5.26 and , Fig 5.27.a). The total discharge due to this aperture remained higher for the entire range of headloss with the deviation of discharge between the respective setups being higher in the range of higher headloss. For example, at a reference headloss of 4.0 m the total discharge with an aperture of 35 mm (962 mm^2) was higher by 8.5% compared to that due to 15 mm aperture. When compared the same due to 50 mm aperture, it was higher by 6%.

Nevertheless, the interest of a hydraulic engineer is to design a device which is efficient in terms of hydraulics as well as SRE. A device producing higher overflow without compromising the SRE is an ideal one. For this purpose, the overflow discharge obtained by the hydrocyclone with different underflow apertures were compared among themselves (Fig.5.27.b). In the region of higher flows, once again the setup due to 35 mm underflow aperture produced largest overflow discharge. In the region of smaller flows, however, the setup with the smallest underflow aperture (15 mm) exhibited the best hydraulic performance.
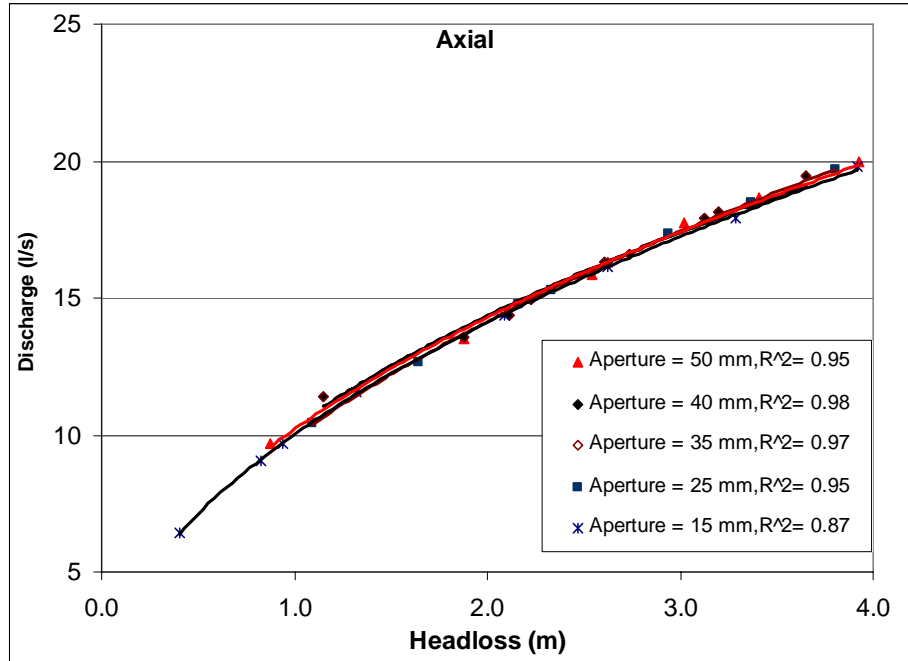
a
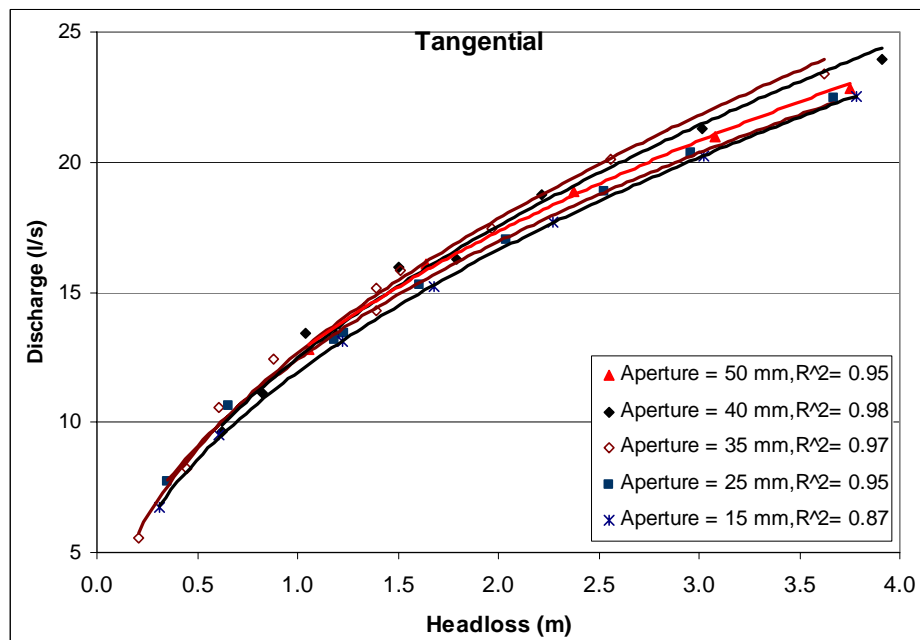
b

Fig. 5.26 Total discharging capacity of the hydrocyclone under different underflow apertures: (a) for axial setup (b) tangential setup

Table 5-5 *Comparison of discharge processed by hydrocyclone under different u/f aperture size*

Head (m)	Discharge (l/s) with u/f aperture dia (mm)					ΔQ (%) with underflow aperture dia (mm)				
	50	40	35	25	15	50	40	35	25	15
1	12.66	12.48	12.65	12.92	12.41	0.06	-1.36	0.00	2.10	-1.94
1.25	14.00	13.93	14.13	14.29	13.72	-0.90	-1.46	0.00	1.16	-2.98
1.5	15.21	15.23	15.46	15.52	14.89	-1.69	-1.55	0.00	0.38	-3.83
1.75	16.31	16.43	16.69	16.65	15.97	-2.36	-1.62	0.00	-0.28	-4.55
2	17.32	17.54	17.83	17.68	16.95	-2.95	-1.68	0.00	-0.85	-5.19
2.25	18.27	18.58	18.91	18.65	17.88	-3.47	-1.73	0.00	-1.36	-5.75
2.5	19.17	19.57	19.92	19.56	18.75	-3.93	-1.78	0.00	-1.82	-6.25
2.75	20.01	20.51	20.88	20.43	19.57	-4.36	-1.82	0.00	-2.23	-6.71
3	20.81	21.40	21.80	21.25	20.35	-4.75	-1.86	0.00	-2.62	-7.13
3.25	21.58	22.26	22.68	22.03	21.10	-5.11	-1.90	0.00	-2.97	-7.52
3.5	22.32	23.09	23.53	22.78	21.81	-5.44	-1.94	0.00	-3.30	-7.88
3.75	23.03	23.88	24.35	23.50	22.50	-5.75	-1.97	0.00	-3.60	-8.22
4	23.71	24.65	25.14	24.20	23.17	-6.05	-2.00	0.00	-3.89	-8.53
4.25	24.37	25.40	25.91	24.88	23.81	-6.32	-2.02	0.00	-4.16	-8.83
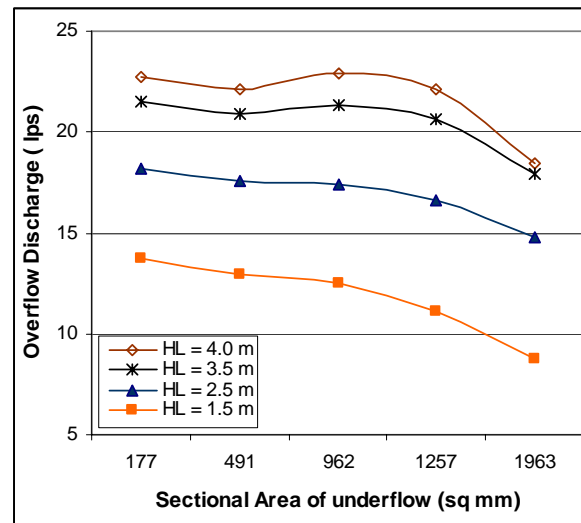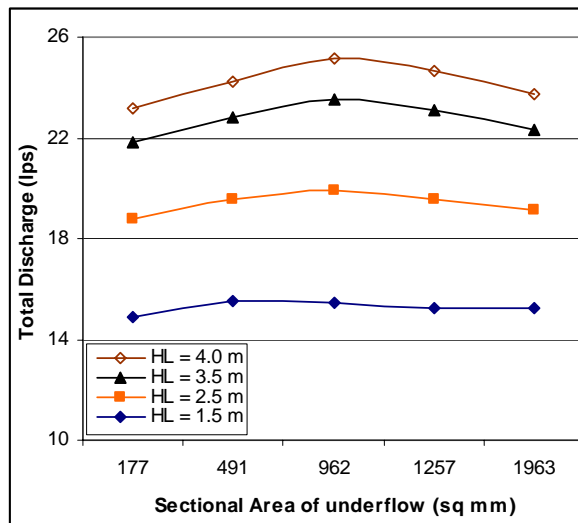
a	b

Fig. 5.27 Comparison of flow ratios in hydrocyclone with a) axial and b) tangential setups under different underflow apertures

5.6.5 Conclusions

The following conclusions can be made from the discussions held above:

- The SRE of a hydrocyclone increases with the increase in headloss. However, it is quite sensitive in the range of smaller headloss, but literally insensitive in the range of

higher headloss. The role of other operating variables such as flow ratio and sediment concentration is dominant in the range of smaller headloss.

- While the SRE increased with headloss for smaller as well as larger flow ratio, it remained sensitive to the headloss only in the range of smaller feed concentration (C < 1060 ppm).

- The increase in SRE with flow ratio is significant only in the range of lower headloss.

- Keeping the above facts in mind and uncertainties involved in the range o lower headloss, the hydrocyclone is recommended to operate under headloss > 2.0 m.

- While the shape of the SRE curve for both the setups is similar, the depth of the fish-hook curve gets shallower and flatter with the increase of flow ratio.

- The dependency of SRE on sediment concentration diminishes with the increase in headloss. While the relation is highly significant in the range of lower headloss, the same is insignificant in the range of higher headloss.

- The shape of all the SRE curves derived for the full range of flow conditions is similar. The fish-hook effect is prominent in all the tests. The common feature of all the curves is that the lowest point of the curve is located in the proximity of the same particle size having a mean diameter as 20 micron. However, the depth of the curve gets shallower and wider with the increase of headloss resulting in enhanced performance.

- The pattern of the performance efficiency curves for smaller as well as larger underflow discharge is same. The fish-hook effect is well established in both cases. However, the depth of the fish-hook curve gets shallower and flatter with the increase of underflow discharge. Further, the SRE curves for full range of particle size with larger flow ratio are always higher than that with smaller one.

- For a constant head difference, the overflow discharge decreases with the increase of flow ratio. As the maximum flow through the overflow is always desired to minimize the cost incurred in hydraulic structure, a minimum flow ratio is recommended complying choking free principle at the underflow outlet while operating hydrocyclone in the zone of higher flows.

- The total discharge of the hydrocyclone is dependent on the aperture size of the underflow. The highest discharge in the hydrocyclone was observed not due to the

largest (50 mm) or the smallest (15 mm) apertures, but due to the intermediate one (35 mm Ø, 962 mm^2). The total discharge due to this aperture remained higher for the entire range of headloss with the deviation of discharge between the respective setups being higher in the range of higher headloss. At a reference headloss of 4.0 m the total discharge with an aperture of 35 mm (962 mm^2) is higher by 8.5% compared to that due to 15 mm aperture. When compared the same due to 50 mm aperture, it is higher by 6%.

5.7 Combined Effect of Operating Parameters; Multiple Regression Analysis

As the performance of the hydrocyclone is mainly guided by the combined effect of each operating parameter, multiple regression analysis was carried out to assess the significance of these variables. Because of the significant difference between the geometries of the hydrocyclone of smaller and larger hydrocyclone, only the results obtained by the larger hydrocyclone are considered for analysis. As the results presented in the preceding section showed relatively stronger relationship of these variables with SRE for smaller flows but a weaker relation for both medium and larger flows, the results have been analyzed dividing them into two categories: smaller, and higher flows.

Proposed Relationship

For the purpose of developing a prediction equation for SRE, the following functional relationship is assumed:

$$E = f(Q_i, Q_u, H_L, Z_h, D_c, d_{50}, C_v, v, g)$$
<div align="right">Eq. 5-2</div>

Here Q_i = discharge entering to the hydrocyclone, Q_u = discharge passing through underflow outlet, H_L = Headloss across the hydrocyclone, Z_h = difference between overflow and underflow outlets, D_c = Diameter of the hydrocyclone, d_{50} = mean particle diameter of the sediment, C_v = concentration of sediment by volume, v = kinematic viscosity of fluid.

Although gravity is predominant at the beginning, its role in a hydrocyclone becomes insignificant once the full swirl is developed and vortex is stabilized. Similarly, the concentration of the fluid mixture in a river and thereby in a diverted flow rarely exceeds

26,500 ppm(1 % by volume, considering G =2.65). As the maximum concentration as 7618 ppm was observed in the tests under study, kinematic viscosity of fluid mixture did not influence the SRE of the hydrocyclone (Plitt, 1976). Therefore, these parameters were disregarded for further analysis. Following the dimensional analysis the following expression can be written:

$$E = f(\frac{Q_u}{Q_i}, \frac{H_L}{Z_h}, \frac{d_{50}}{D_c}, C_v)$$
Eq. 5-3

Since the tests were carried out using only two batches of sediment, and the diameter of the hydrocyclone remained constant, the parameter, d_{50}/D_c didn't vary much during the tests. Therefore, the parameter d_{50}/D_c was disregarded and hence abandoned in multiple regression analysis as well (Table 5.5).

Table 5-6 *Parameters from the regression analysis of the results data*

Category	H_L	R^2	Regression Equation	P-values (95 % Conf. lev.) for			
				Inter.	H_L/Z_h	C_v	R_f
Overall data (Eq.1)	1.16 - 3.94	0.73	$E = 97.32(\frac{H_L}{Z_h})^{0.195} C_v^{0.056} R_f^{0.052}$	2E-49	8E- 06	1E-06	0.0012
Smaller flows (Eq.2)	1.16 - 2.31	0.92	$E = 80.51(\frac{H_L}{Z_h})^{0.336} C_v^{0.061} R_f^{0.146}$	2.2-10	0.004	0.0037	0.0034
Larger flows (Eq.3)	2.31 - 3.94	0.39	$E = 95.38(\frac{H_L}{Z_h})^{0.054} C_v^{0.012} R_f^{0.014}$	1E-48	0.012	0.02	0.014

Higher *R square* value in the range of smaller flows suggest that the SRE of the hydrocyclone has a stronger relation with the operating variables in this range. This can be also witnessed by the power coefficients of each parameter, which are higher by a factor of 5 to 10 than that in the range of higher flows, the highest factor being attributed to the flow ratio. This implies that the flow ratio is literally insensitive in the range of higher flows. Further, the *P-values* of the regression analysis obtained at 95% confidence level are much smaller than a threshold value as 0.05. This means, that the relation between *E* and all the three parameters is statistically significant. The lowest *P-values* for H_L/Z_h (dynamic head

to potential head) in all cases of the regression analysis implies that the statistically most significant relation exists between SRE and the head ratio. Furthermore, smaller P-values for concentration, C_v compared to flow ratio, Rf in all cases of analysis suggests a better relation between E and C_v.

5.7.1 *Accuracy of Proposed Relationships*

For the purpose of checking the accuracy of the proposed relationships, the predicted values were compared with the observed ones (Fig. 5.28). The first three plots in Fig. 5.28compare the predicted efficiency computed by Eq. 1, Eq. 2 and Eq. 3 respectively. Whereas the Fig. 5.28d depicts the comparison of predicted efficiency according to Eq.2 as well as Eq. 3 considering the range of headloss under which they were developed. The accuracy of these equations were assessed evaluating the goodness of fit of the function. The sum of the residuals squared and *R square* values were used as the main criteria as to the goodness of fit.

Table 5-7 Parameters of goodness of fit

Regression Equation used	$\sum(E_{cal}\text{-}E_{obs})^2$	*R square*
Overall data (Eq.1)	746.64	0.71
Smaller flows (Eq.2)	1826.60	0.6
Larger flows (Eq.3)	1735.05	0.73
Eq.2 for H_L< 2.31, Eq.3 for $H_L \geq$ 2.31 m	145.98	0.94

The results depicted in Fig. 5.28.c and Fig. 5.28.d as well as parameters of goodness of fit (Table 5.7) illustrate that the efficiency predicted by Eq. 2 and Eq. 3 and applied to the full range of operating parameters involves a significant degree of error, especially outside the range of data, these equations were developed. On the other hand, the prediction due to Eq. 1 based on overall data avoids the peaks of the residuals, and thus improves the accuracy compared to the prediction made by Eq. 2 and Eq. 3 alone. Nevertheless, the scatter ness of the results in Fig. 5.28.a implies still imperfection. Therefore, prediction based on equations developed for particular range of headloss which resulted in a much improved *R square* value (0.94) and least sum of the residuals squared seems the most reliable functional relationships between SRE and operating parameters.
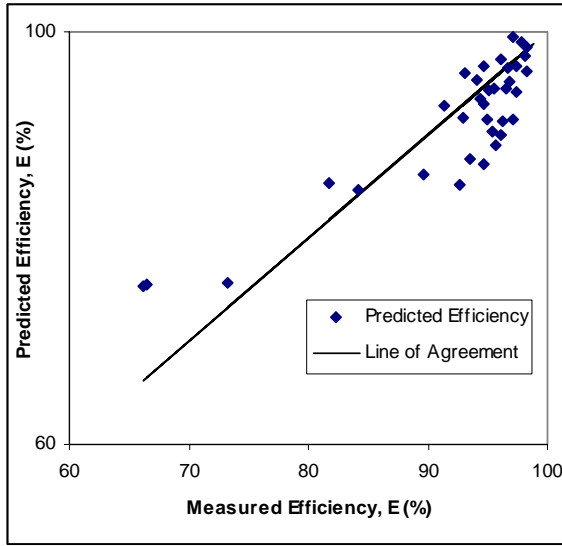
a. Prediction due to Eq. 1 (Overall data)   **b.** Prediction due to Eq. 2 (Smaller flows)
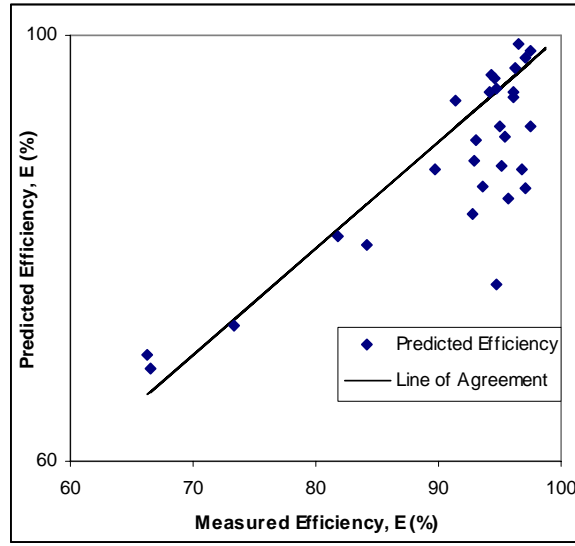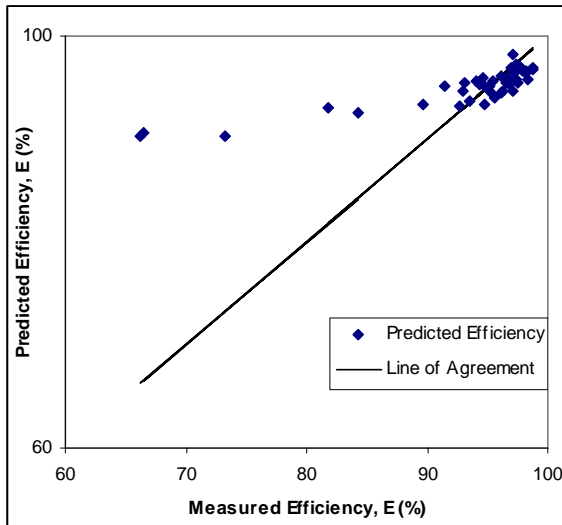
c. Prediction due to Eq. 3 (Larger flows)   **d.** Prediction due to Eq. 2 & Eq. 3
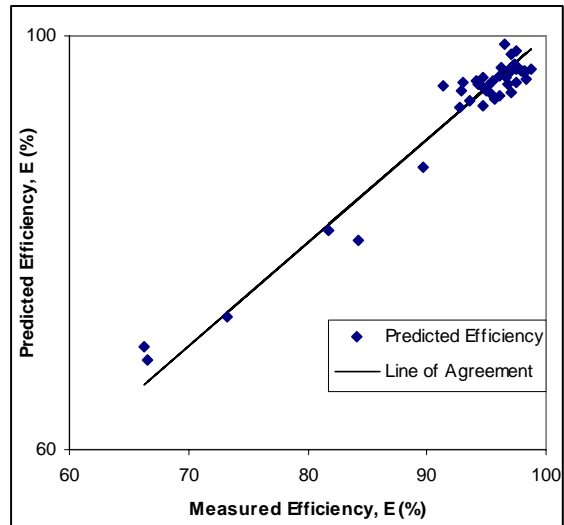
Fig. 5.28 Prediction of SRE due to different regression equations

5.7.2 *Sensitivity Analysis*

The sensitivity of the operating parameters was studied by increasing the magnitude of each of the parameters from 10% to 50 % while keeping the other two parameters unchanged. The efficiency of the hydrocyclone due to such effect was assessed applying the relations developed earlier. The sensitivity was judged with respect to R square value (coefficient of correlation) and the coefficient of variation (Fig. 5.29).
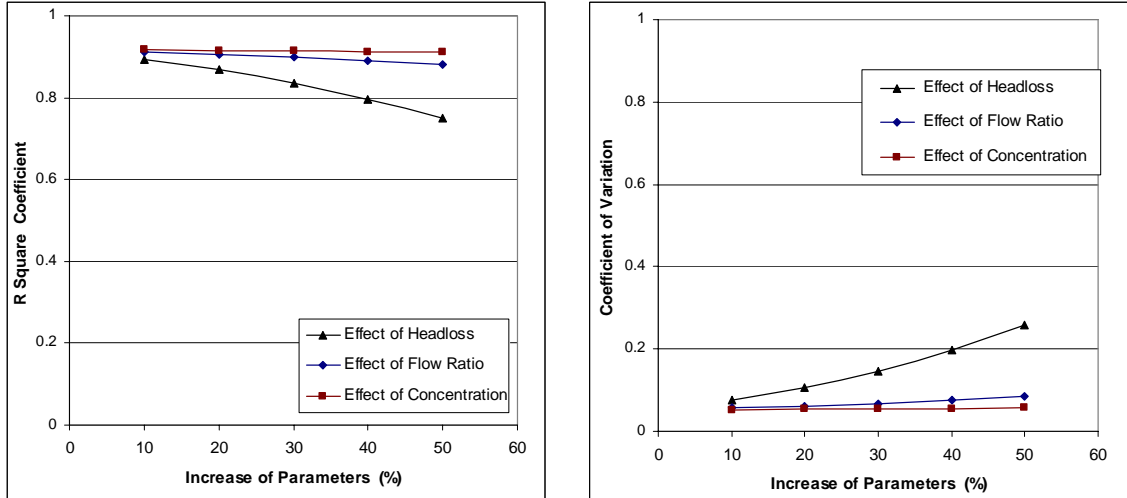
Fig. 5.29 Sensitivity of *E* to operating parameters; (a) change in *R square* value(b) change in coefficient of variation

The outcome of the analysis shows that the efficiency of a hydrocyclone is insensitive to the small changes (<10%) of the operating parameters. Furthermore, the results of the sensitivity analysis imply that the performance of the hydrocyclone is sensitive only to the head ratio. With the increase of head ratio by 50%, while keeping two other parameters unchanged, about 25% variation in efficiency can be expected. The illustrations in Fig. 5.29 also suggests that the SRE is literally insensitive to any deviation of C_v and R_f from the respective observed values.

5.7.3 Conclusions

The multiple regression analysis of the results obtained has shown that there is a relation between SRE and the parameters influencing it and such relation is statistically significant. The relation is best described if the data are divided into two groups; smaller flows ($H_L <$ 2.31 m) and larger flows ($H_L >$ 2.31 m) by the following equations, which resulted in an *R square* value as 0.94:

$$E = 80.51(\frac{H_L}{Z_h})^{0.336} C_v^{0.061} R_f^{0.146}$$
(for $H_L <$ 2.31 m)

$$E = 95.38(\frac{H_L}{Z_h})^{0.054} C_v^{0.012} R_f^{0.014}$$
(for $H_L >$ 2.31 m)

Further, the sensitivity analysis revealed that the SRE of the hydrocyclone is sensitive only to the head ratio (H_L / Z_h).

5.8   The Concept of a Bottom Outlet Hydrocyclone

As mentioned earlier in Chapter 4, the concept of a bottom outlet hydrocyclone (BOH) is introduced, aiming to process the flow utilizing the potential head between the inlet and the underflow outlet. To achieve the objective the   overflow as well as underflow discharge in the conventional setup is gradually received through the bottom part of the hydrocyclone. This was realized by allowing the inner flow pass through an aperture having 50 mm diameter at bottom center, whereas the outer flow through a number of apertures having 5.0 mm diameter along the periphery of the cyclone wall. The openings of the apertures as well as configuration of the outlets at the end remained unchanged. But the tests were carried out with different geometrical configurations of the inner outlet. Three principal geometrical setups were identified for the investigation of the BOH.

 In subsequent pages, the hydraulic and of BOH with these setups have been presented and compared with that of conventional hydrocyclone having axial overflow at the top. In the end, the of BOH with different setups have been compared among themselves. To avoid further confusion, the terms used as overflow and underflow discharge in conventional hydrocyclone are often referred to *inner flow* and *outer flow* in BOH. Similarly, the head over the inlet is assumed as the headloss in both the hydrocyclones for comparison of results. Similarly, the concentric outlet means the one flushed with the bottom of the cone, and the inserted concentric outlet denotes the outlet pipe inserted inside the cone by 0.4 m. Whereas the spiral outlet indicates that the inner flow (central) is received from the periphery of the inserted pipe inside the cone, which has series of apertures having spiral configuration.

5.8.1   The Hydraulics
Fig 5.30 compares the respective inflow, overflow and underflow discharge received from the hydrocyclone having conventional axial setup and BOH. Although the BOH envisages little or no discharge passing through the overflow, the hydraulic test was carried out for the full range of headloss keeping the overflow outlet open to compare its performance with conventional hydrocyclones. Due to the larger opening at the bottom center, the smaller

flows fully passed through the bottom outlets; most of it through the bottom center and part of it through the peripheral outlets. But, with the increase of headloss, the bottom outlet could not accommodate full discharge. Therefore, part of the inner flow passed through the overflow outlet as well.
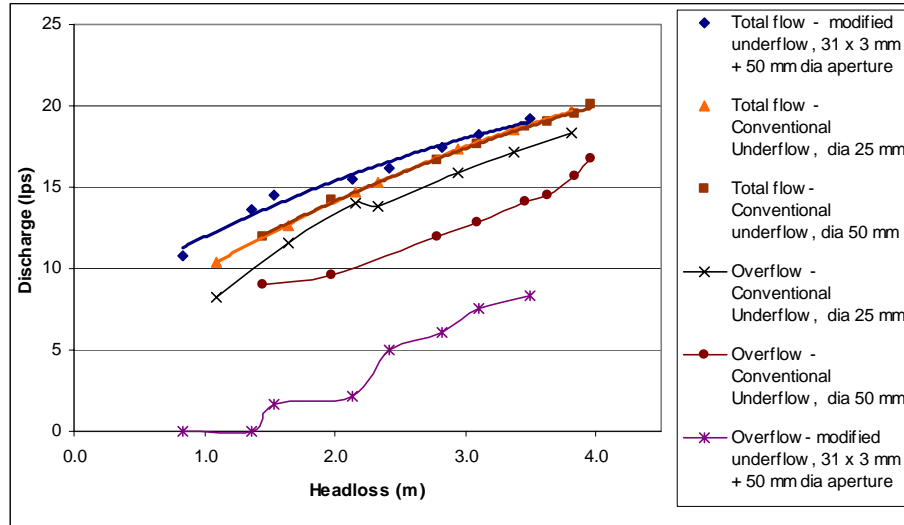
Fig. 5.30 Comparison of hydraulics of conventional axial setup with the hydraulics of BOH

The benefit of the BOH over the conventional setup, especially for lower flows can be noticed from the results. Utilizing the potential head over the bottom outlet, the BOH processes more flow than the hydrocyclone with conventional setup does. For a reference headloss of 1.0 m (over the inlet), the total flow is larger by 19.4 % and 16.6 % compared to that of conventional setup with the underflow apertures as 25 mm and 50 mm respectively. Nevertheless, with the increase of inflow, the discharge passing through the overflow gradually increases resulting in insignificant difference between the flows processed by three setups. These rating curves converge with each other in the zone of higher head.

5.8.2 Sediment Removal Efficiency

The SRE has been evaluated through PSD and particles removal efficiency analyses (Fig. 5.31- 5.33). The SRE of BOH of each setup has been compared to that with the conventional setup tested under similar operating conditions. Then for the purpose of comparison among themselves, these curves have been plotted together as a function of particle size.

5.8.2.1 Comparison of SRE of BOH with SRE of Conventional Setup

Comparison of SRE of axial and BOH is made using differential as well as cumulative PSD and SRE curves obtained by the similar tests in respective setups. The sediment removal performance obtained from a concentric and spiral bottom outflow, installed at the bottom end has been presented and compared in Fig. 5.31. It. illustrates typical PSD along with the frequency observed in overflow underflow and feed sediment for axial as well as BOH setups. As can be noticed from the results, the shapes of the PSD curves obtained from the outlets of BOH as well as conventional setups are identical. However, there is a shift in phase on theses curves derived for BOH towards the direction of increased particle size despite the median particle size of the sediment fed being similar.
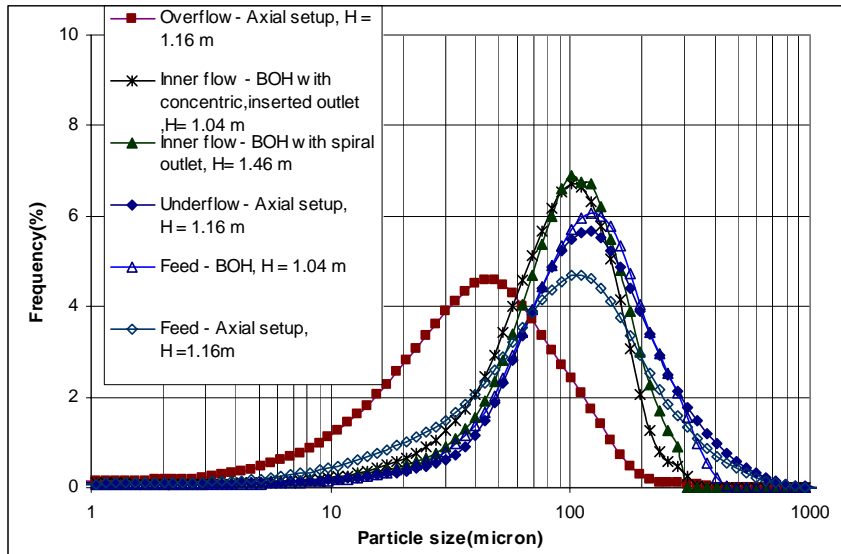
Fig. 5.31 Comparison of PSD (differential) received from conventional axial and BOH setups

The cumulative PSDs of both the concentric setups of BOH have been found to be identical, therefore, only the results of one test have been presented in Fig. 5.32. for the purpose of clarity of the graphical presentation. Although the actual sediment fed in the BOH is finer than that in the conventional setup, the PSD obtained from the inner outlet of BOH is skewed towards the direction of coarser particles size. This has resulted in lower SRE of BOH in comparison to the conventional axial setup when compared under similar operating conditions. However, a marked influence of pressurization of the outlet can be witnessed. The removal efficiency in such a case has gone up from 33.4 % to 39.6 % despite the head

across the hydrocyclone being less by 0.20 m (Fig 5.32.b). While the efficiency of removal for finer particles remained almost unaffected, the same for coarser particles has been influenced significantly with the pressurization of outlet conduit. The fish-hook effect can also be noticed, however it is much flatter compared to that due to conventional axial setup.
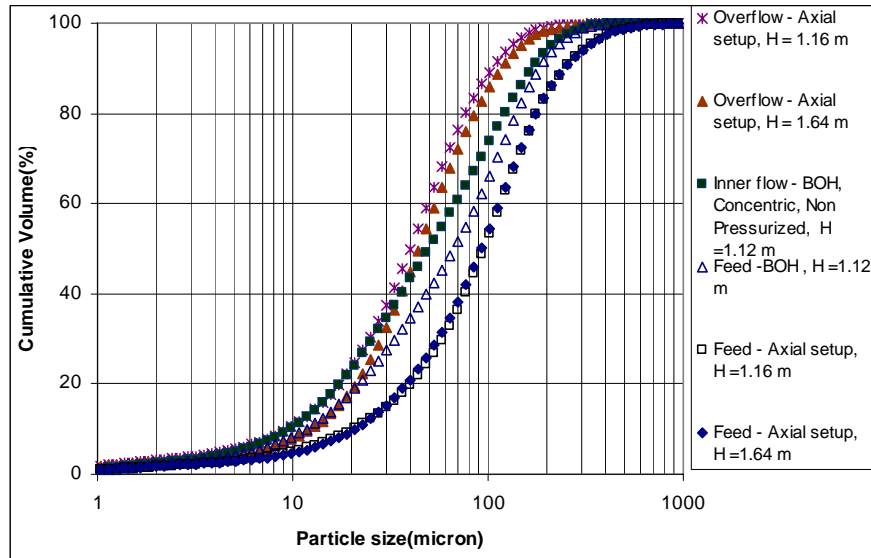
a
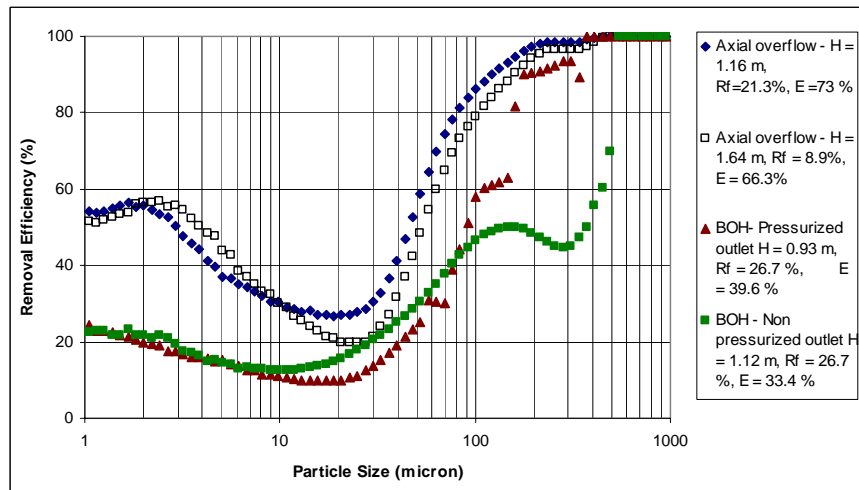
b

Fig. 5.32 Comparison of conventional axial and BOH with concentric bottom outflow setups: (a) PSD, cumulative (b) SRE by particles size

The improvement of the performance of a pressurized bottom outlet can be argued due to next reasons. First, part of the energy retained in the form of tangential velocity has been recovered by pressurizing the outlet conduit for some distance. Second, the low pressure

zone being farther from the zone of flow split at the bottom end of the hydrocyclone, short-circuiting effect has been minimized.

5.8.2.2 Effect of Modification of the BOH Outlets on SRE

The performance of the concentric bottom outlet has been further improved once the outlet was installed 0.4 m above the bottom end. For similar flow conditions, the SRE increased by 13.5% compared to BOH with concentric outlet. The fish-hook curve is very close to the one due to axial setup under similar flow conditions, indicating similar SRE for fine particles. However, SRE curve in the range of coarser particles is more skewed towards the coarser particles leading to the performance inferior compared to that due to axial setup.
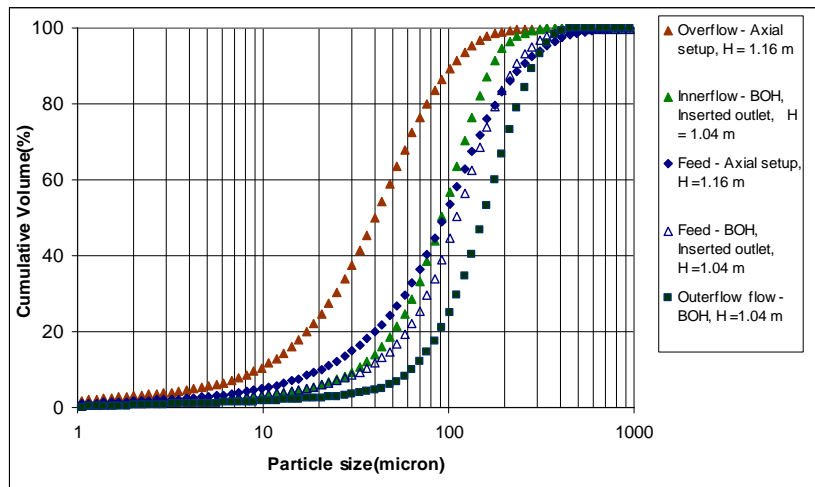
a
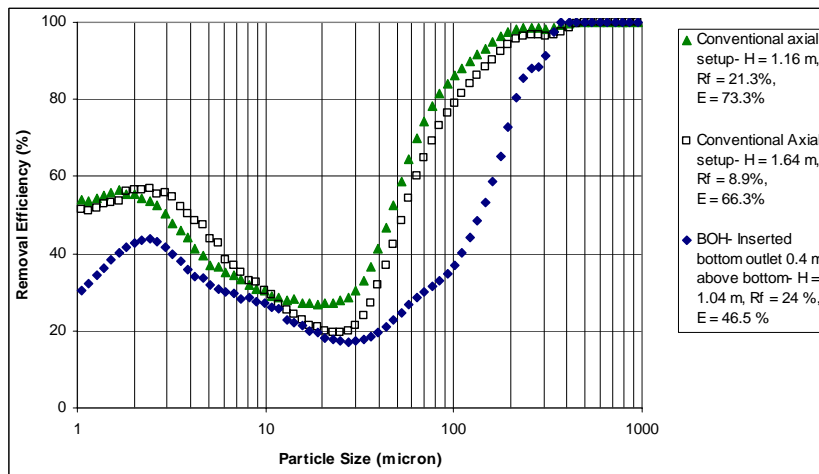
b

Fig. 5.33 Comparison of BOH with centrally inserted bottom outlet with the efficiency of conventional axial overflow setup : (a) PSD (b) Removal efficiency by particles size
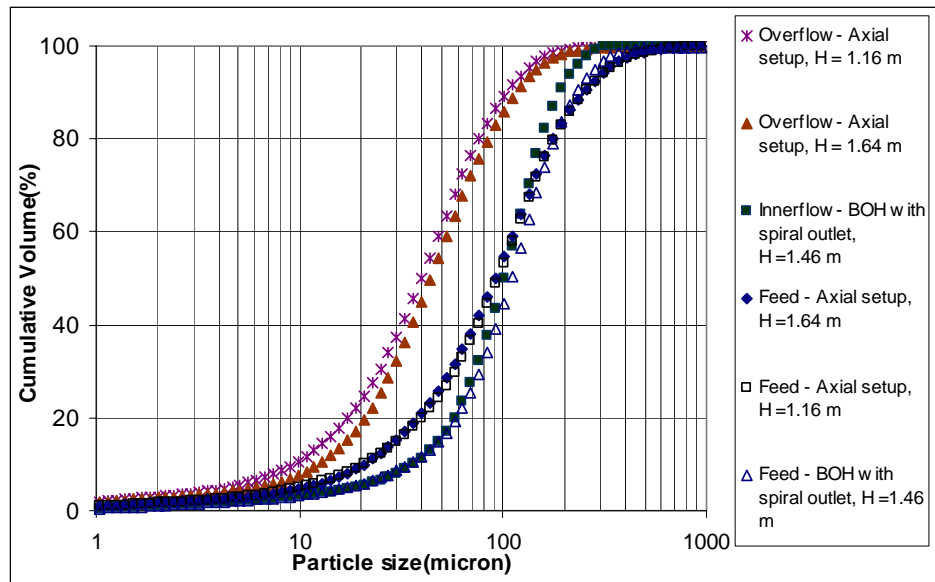
a
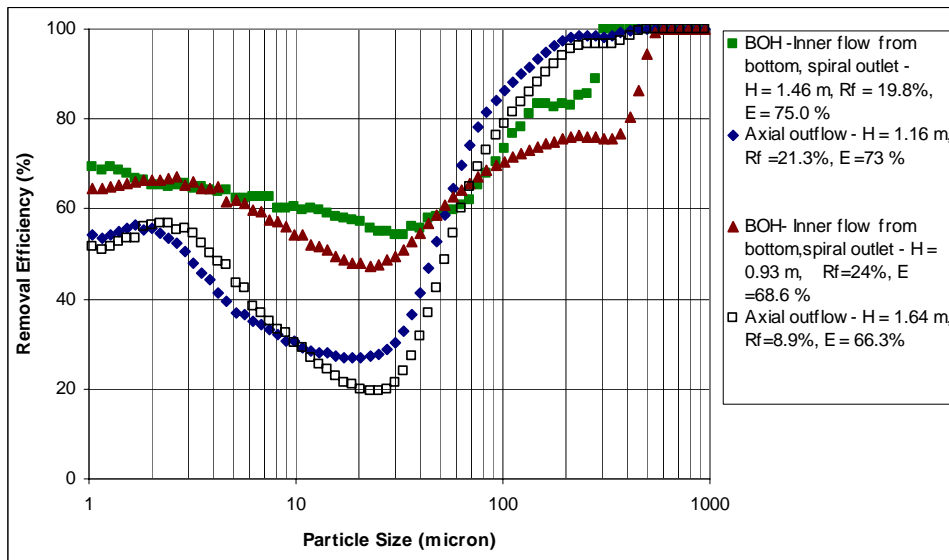
b

Fig. 5.34 Comparison of conventional axial overflow and BOH with spiral bottom outflow setups: (a) PSDs (b) Removal efficiency by particles size

The SRE of concentric outlet BOH has been further enhanced by providing the apertures in the inserted outlet in a spiral mode. The particles, especially the fine ones were better separated when the outlet was modified to spiral setup (Fig 5.34). Fish-hook effect could be easily noticed. More interestingly, the curve is much flatter than that due to conventional setup, a desirable feature for rivers dominated with finer particles containing hard minerals.

However, contrary to the enhanced performance of BOH for finer particles, inferior performance for coarser particles was witnessed compared to that due to conventional setup. The SRE is highly influenced by the headloss. For instance, with the increase of head acting on hydrocyclone by 0.42 m, the removal efficiency increased significantly, from 46.5 % to 75%. The performance of BOH here for finer particles is much better to that due to conventional setup with similar operating conditions.

5.8.3 SRE Comparison among BOH hydrocyclones

Comparison of the performance of BOH hydrocyclones is carried out by overlaying the curves of BOH with different outflow setups (Fig. 5.35). The comparison among the efficiency curves has revealed that inserted concentric bottom outlet is highly preferable to the one flushed with the bottom. The performance of such a geometry in separating the coarser particles can be further improved by pressurizing the outlet conduit. Further improvement in SRE can be achieved replacing the outlet with spiral geometry. Nonetheless, all of these setups exhibited inferior performance with respect to the separation of coarser particles compared to that due to conventional setup. As implied by the results obtained from pressurized concentric outlet such a deficiency can be overcome by pressurizing the outlet conduit for sufficient distance.
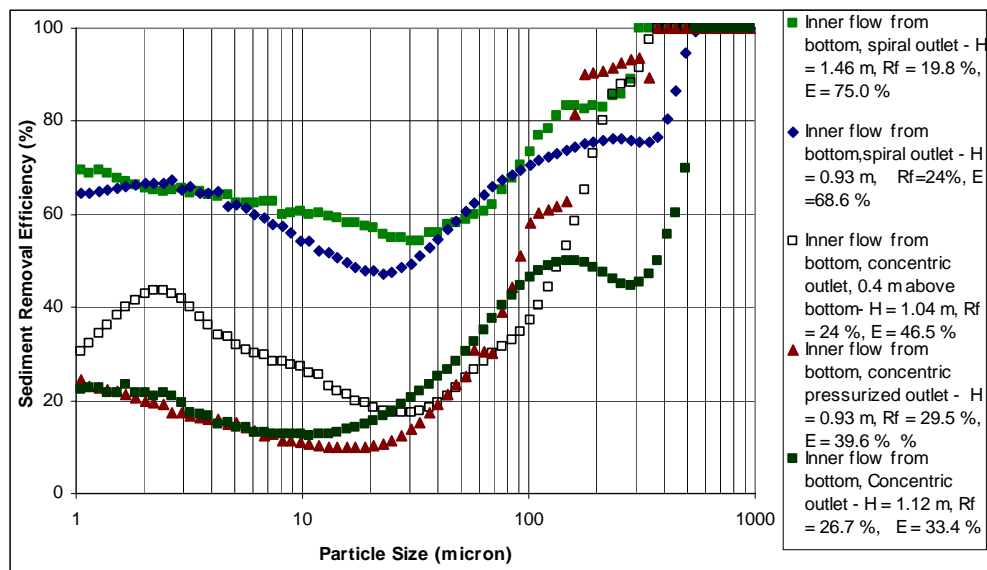
Fig. 5.35 Comparison of BOH with different design and operating variables

The results obtained from the BOH point out a scope for implementing such device in hydropower plants, where the conventional setup is not desirable due to topographical or economic reasons. However, as the tests were carried out in a very narrow range of operating and design parameters, detailed investigation with variation of design and operating variables may lead to meaningful conclusion.

5.8.4 Conclusions

- Like in the conventional setup, the SRE of BOH is enhanced with the increase of headloss. For instance, with the increase of head acting on hydrocyclone by 0.53m, the SRE due to spiral outlet increased considerably, from 68.6 % to 75%. The performance of BOH here for finer particles is much superior to that due to conventional setup with similar operating conditions.

- In general the SRE of BOH, especially of coarser particles has been found slightly lower than that due to conventional hydrocyclone, which is believed due to the residence time being shorter in BOH.

- The SRE of the concentric BOH can be enhanced by pressurizing the conduit receiving the inner flow. For similar operating conditions the SRE due to pressurized outlet was improved by 6% .

- The SRE of the concentric BOH can be enhanced by inserting the outlet into the bottom of the cyclone. For similar operating conditions, the performance of the inserted outlet BOH was increased by 13%

- The SRE of the inserted outlet BOH has been further enhanced by providing the spiral outlet. For similar operating conditions, the SRE due to spiral outlet enhanced by 22% compared to that due to inserted outlet BOH and 35% compared to that of concentric pressurized outlet.

- The shape of the SRE curves due to BOH are similar to that due to conventional hydrocyclone, however, it is wider and flatter compared to that due to axial overflow setup.

6 SEDIMENT HANDLING IN JHIMRUK HYDROPOWER PLANT: PRESENT PRACTICES AND PROPOSED MITIGATION MEASURES

Jhimruk Hydropower Project (JHP) is located in Pyuthan District in Mid-Western Region of Nepal (Fig.6.1). The plant is a Run-of-River (RoR) type, which utilizes a gross head of 210 m between the Jhimruk and Mari rivers. A headworks consisting of a 255 m long concrete dam (Fig. 6.2, 6.3) diverts a design discharge of 7.05 m^3/sec. The plant is equipped with three units of Francis Turbines, each with a rated flow of 2.35 m3/sand generating 4.0 MW of power. The project was commissioned on 17th August 1994.

Although, everything went fine before commissioning of the plant, it did not perform as expected from the very beginning of the operation. Therefore, the turbines were inspected shortly after the operation of five months, including one month of monsoon period. Although the turbine and accessories were subjected to less than half the sediment load of the month of July (Pandit, 2005) severe abrasive damage was observed in the runner, guide vanes, casing and other parts of the hydro-mechanical equipment (Basnyat, 1997). More severe damage have beeen observed in subsequent years of operation, when the hydro-mechanical equipment and accessories were subjected to the sediment load of full monsoon period. Therefore, the JHP is recognized as one of the severely affected projects in terms of sediment related damages.

Fig. 6.1 Location Map of Jhimruk Hydropower Project including Central to Far Western Part of Nepal (Source: **www.thamel.com**)

Fig. 6.2 Headworks of JHP, looking from upstream, non operational mode (Source: Hydro Lab, Nepal)

Fig. 6.3 General layout of Headworks of Jhimruk Hydropower Project

In this chapter, issues related to sediment induced wear and tear are briefly addressed. Especially, the measures adopted and efforts made to minimize wear and tear in hydro-mechanical equipment at JHP are critically assessed. This will be followed by two proposals of additional measures to solve the fundamental problem at JHP.

6.1 Hydrological Data

The Jhimruk River is a major tributary of the West Rapti River located in Mid-Western Region of Nepal. This is a non snow fed river. The catchment area of the river upstream of the headworks site is 645 km^2. The highest elevation of the catchment is 3000 m, whereas the lowest near the headworks is 740m above the mean sea level (NEA, 1986). The long-term average flow and mean monthly flow of driest period (May) of the river have been estimated at 27.0 m^3/s and 3.2 m^3/s respectively. The design flood of 1800 m^3/scorresponding to a period of return of 1000 years has been considered for headworks design (BPC,1997). The mean annual rainfall recorded in the Jhimruk catchment is about 1,610 mm, of which, 83 % appears during monsoon. Time series discharge monitored by BPC, during a period of 1994-1997, have been presented in Fig. 6.4. It can be seen that the variation of discharge during summer and winter periods is quite high. The highest flood recorded during the four year period is 893 m^3/s, which was observed in August 1995. Although the highest peaks of the years are different, general trend of hydrograph of each year is similar.

6.2 Sediment Data

6.2.1 Suspended Sediment Load

During the planning and design stage of JHP, sediment data were not available. Due to the lack of the data, the design was based on the general design criteria, the experience of the design of similar projects in Nepal and on general references to sediment transport in the Himalayan Rivers. The annual sediment load as (4700–5600) m^3/km^2 estimated by Norpower (1992) in the Kaligandaki River basin during the detailed feasibility study of Kaligandaki 'A' Hydroelectric Project has been taken as a reference. Out of which, 85% of the load as recommended by Snowy Mountain Engineering Corporation (SMEC) was considered as suspended load.
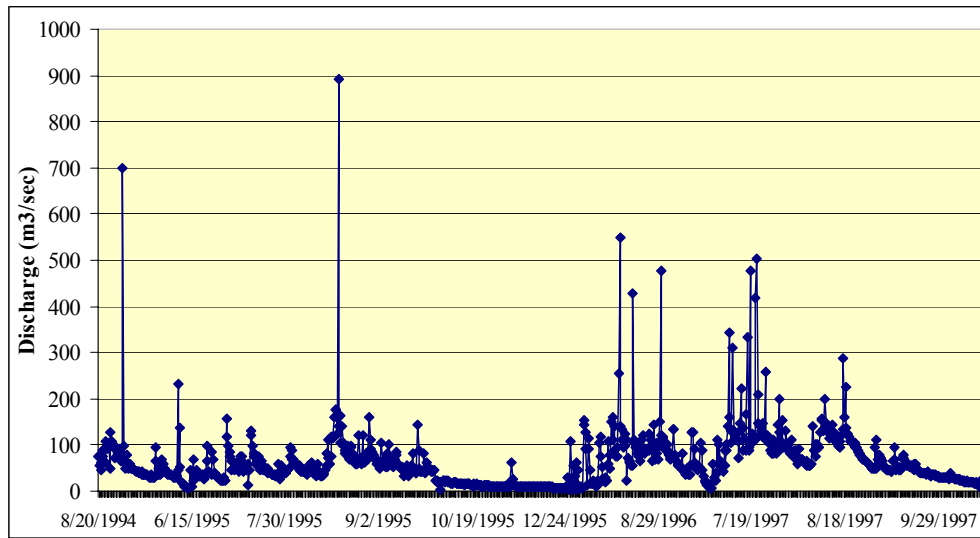
Fig. 6.4 Daily discharge recorded in Jhimruk River at JHP (Source: BPC, 2004)
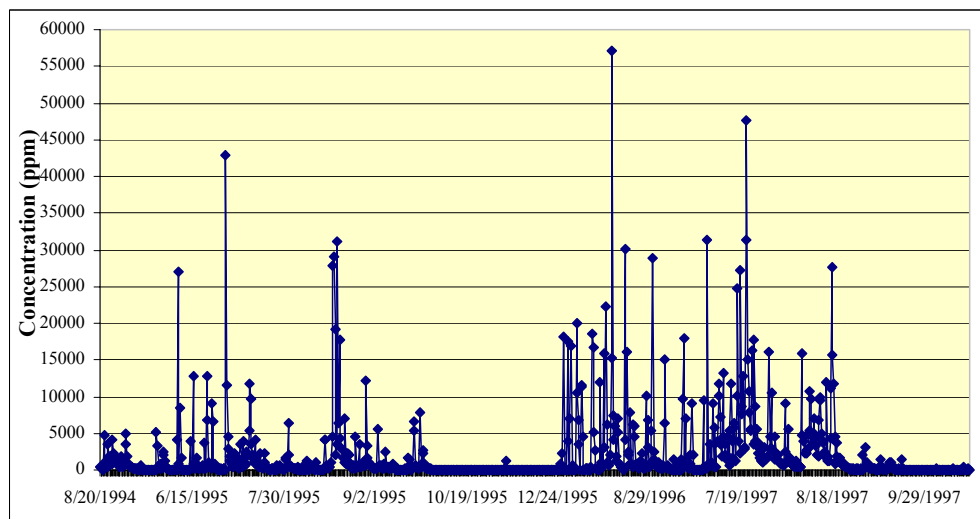
Fig. 6.5 Suspended sediment concentration recorded in Jhimruk River at JHP (Source: BPC, 2004)

Due to the lack of sediment data for the Jhimruk River, a regular sediment monitoring programme was carried out from the very beginning of the operation of the power plant. Time series data of suspended sediment monitored in JHP during the period of 1994-1997 have been presented in Fig 6.5. Witnessed by the highest concentration (57,094 ppm) recorded (Table 6.1, Fig 6.6) in July 1996 and several records of 25,000 ppm or more each year (Fig. 6.6), it can be inferred that it is one of the extreme rivers of Nepal in terms of sediment load. The particle size analysis of the sediment samples collected from intake area

(Table 6.2, Fig. 6.7.a) suggests that the suspended sediment load in the Jhimruk River is dominated by fine sand and silt particles.

Table 6-1 Measured Sediment Concentration in Jhimruk River (Computed from data recorded by BPC during 1994-1997)

Month	Jun	Jul	Aug	Sept	Oct
Max	27,037	57,094	311,30	28,950	26
Avg	3,396	4,626	2,368	854	14
Min	4	4	39	18	5
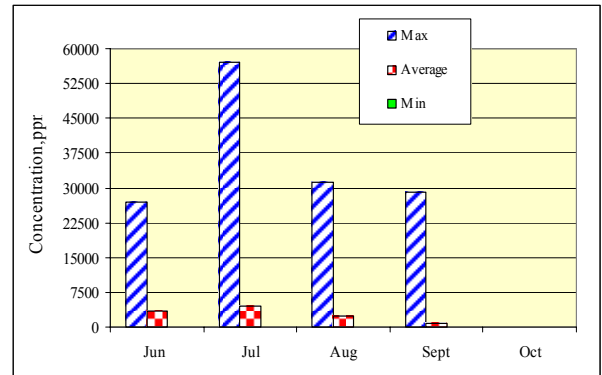
Fig. 6.6 Extreme and Average concentration in the Jhimruk River (Computed from data by BPC, 2004)
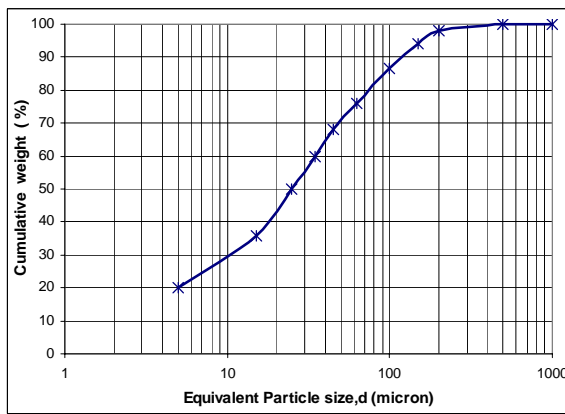
a
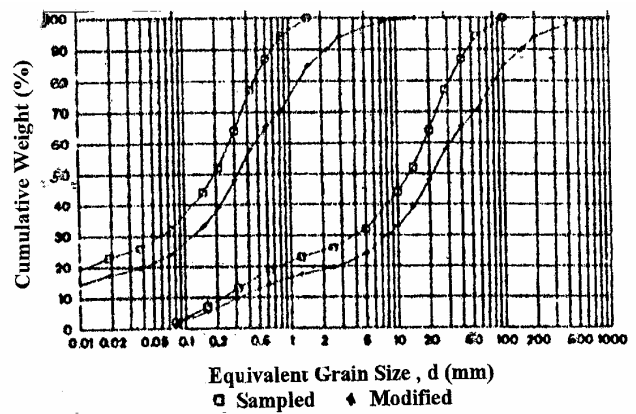
b

Fig. 6.7 Particle size distribution of the sediment in the Jhimruk river (a) Suspended sediment (Hydro Lab, 2004) (b) Bed material; Curves on LHS- model; Curves on RHS- prototype (Source: BPC, 2004)

6.2.2 Bed load

Data on bed load were also not available during the design stage. Neither, it was monitored after the operation of the JHP. However, rapid filling up of the river bed upstream of the dam planned within a few years implied that the magnitude of the bed load was much higher than what was anticipated during the planning and design stage of the project.

The samples taken from the river bed consisted of boulders, cobbles, gravels and coarse sand. The boulders as big as 0.5 m was found in the main channel as well as in flood plain. The median particle size of the bed material (d_{50}) was found as 20 mm, which indicated domination of gravel material in the bed (Fig. 6.7.b).

6.2.3 *Mineralogical Content of the sediment*

The mineral content analysis of suspended data collected in the Jhimruk River revealed that the river sediment is dominated by very hard minerals, and mainly quartz. Moreover, the content of the quartz particles was observed to be higher in finer particles (< 90 micron) by about 13% compared to that in coarser particles (d > 90 micron, Table 6.2, Fig. 6.8). Theses quartz particles in this range have been found quite abrasive in hydropower plants.

Table 6-2 *Mineral content of suspended sediment in the Jhimruk River (Dhakal, 2007)*

Particle size range (micron)	% mineral content (vol)		
	Quartz	Feldspar	Mica & others
>500	0	0	0
200-500	15	2	83
90-200	57	2	41
<90	85	1	14
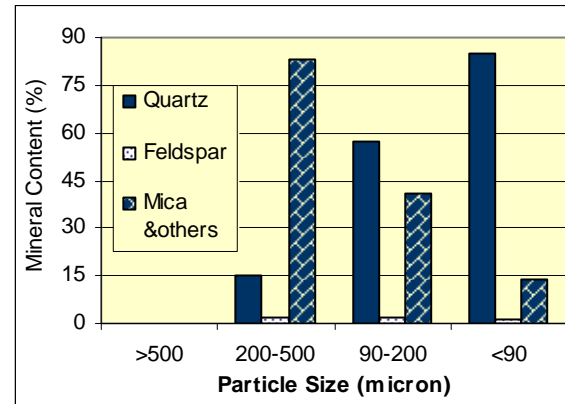
Fig. 6.8 Mineralogical content of suspended sediment in the Jhimruk River (Dhakal, 2007)

6.3   Sediment Exclusion Measures

The Jhimruk river near the headworks site is quite wide. The river plan form has a braided pattern at this stage, which is most unstable in nature. Therefore designing a headworks in a braided river is a very challenging task. Unless structural measures are taken, a stable and reliable channel, which controls the thalweg can't be expected in such a stretch. Realizing this fact, the concept of a trained channel was introduced during the model study and design of the JHP. Such a channel was intended to control the thalweg geometry and transport most of the bed load, which eventually would pass through three undersluice orifices (Fig. 6.3).

In addition to the measures for passage of bed load downstream, two settling basins have been designed to trap coarser particles. Due to the lack of data pertaining to sediment characteristics, the settling basin was designed based on the design experience of other projects in Nepal. As a result, the settling basins of JHP have been designed to trap 90% of particles equal or larger than 200 micron. Following a physical model study, two basins, each having an effective length as 36.0 m and width as 5.5 m, corresponding to a transit velocity of 0.19 m/s were designed (Fig. 6.3). Serpent Sediment Sluicing System (S4) was installed for flushing the deposited sediment in settling basins. The observed data from the plant operation reveals that the settling basin has performed as designed. S4 units have been functioning quite well, which has facilitated continuous operation of the power plant.

6.4   Sediment Related Damages

The four years (1994-1997) of headworks and power plant operation of JHP has revealed that sediment transport in Jhimruk River during the monsoon is higher than what was expected during the planning and design stage of the project. This has resulted in excessive wear and tear of the turbines and accessories leading to generation losses and high maintenance costs. The excessive wear and tear have been reported primarily due to three reasons:(i) high sediment load,(ii) the dominance of hard minerals such as quartz, and (iii) the entry of coarser particle sizes (63 μm < d >200μm).

Severe damage due to abrasive erosion was observed in turbine runners, guide and stay vanes, casing and other part of the hydro-mechanical equipment (Fig. 6.9).The types of erosion observed in turbines and accessories with the underlying reasons have been identified as follows (Hydro Lab, 2004):

1. Turbulence erosion of the stay vanes due to high velocity of fine grain sand
2. Turbulence erosion at the outlet region of the guide vanes and face plate due to high velocity of fine grain sand
3. Secondary flow erosion in the corner between guide vane and face plate creating horseshoe shape grooves
4. Leakage erosion at the clearance between guide vane and face plate due to local separation and turbulence

Fig. 6.9 Typical wear and tear observed at JHP in : (a) turbine runner (b) guide vane (c) stay vane, and (d) facing plate (Source: Hydro Lab, 2004)

5. Erosion of the guide vanes due to acceleration of large particles in the main flow
6. Erosion of the runner blades due to acceleration of large particles in the main flow
7. Erosion of the upper and lower seal rings.

6.5 Assessment of Adopted Measures

As mentioned above, the extent of wear and tear in hydro-mechanical equipment and accessories was unusual compared to that in other hydropower plants in Nepal and abroad. Therefore attempts were made to find the underlying causes and apply remedial measures from the very beginning of the operation of the pant. The efforts were primarily made to

improve hydraulics of the system, exclude more sediment from diverted flow and apply protective coatings to the equipment and accessories. These measures are described in the ensuing sub-chapters.

6.5.1 Installation of Tranquilizers in Settling Basins

Because of the curved entry of flow at the entrance of the settling basins and shorter transition zone to the right chamber, about one third of the length of this basin was subjected to increased turbulence (Basnyat, 1999). This has reduced the effective length of the settling basin considerably. Therefore, a study was carried out to install tranquilizers at the entrance to the basins, so that the turbulence could be minimized. The tranquilizers were designed and installed accordingly. Such an installation was helpful in reducing turbulence, however, there has been literally no impact in minimizing the wear and tear of hydro-mechanical equipment and accessories.

6.5.2 Application of Coatings to Turbine and Accessories

Application of high-strength coatings to the erosion prone surface of the equipment and accessories is one of the well known protective measures in engineering. Therefore, several attempts have been made to control wear and tear by applying coatings to the surface of turbine and accessories. Nevertheless, the application of Plasma nitriding and ceramic spray 25050 were not helpful in solving the acute problem. Although the performance of Neyrco coating applied by Gec Altsthom and the surface coating applied by GE Hydro have been found to be better than the coatings applied earlier, the BPC authority seems still unconvinced about their significance in JHP (Dhakal, 2007).

6.5.3 Forced Shutdown of the Plant Based on Concentration Limit

Following the severe wear and tear, there have been attempts to shutdown the power plant during exceptional sediment load. Sediment concentration as 3000 ppm in the river has been adopted as a limiting value. Since the monitoring mechanism for discharge and sediment concentration has been installed in the plant, the plants is put out of operation once the concentration exceeds moe than 3000 ppm. The actual shutdown period of the plant considering this operating rule, while complying other obligations such as PPA with NEA is presented in Fig. 6.10.

As the sediment induced wear and tear due to exceptional load lasting even for a short duration has been found to be more detrimental than that due to normal sediment load lasting for a prolonged duration, this operating rule has protected hydro-mechanical equipment and accessories considerably. However, the sediment duration curves derived for monsoon months suggest that plant should be put out of operation for about 28% of the time during June, July, August and about 5% of the time in the month of September (Pandit, 2005). In a monetary term according to prevailing energy price. (U$ 0.06 /kWh), this involves a revenue loss of about U$ 0.5 million annually

On the other hand, Nepal presently is reeling under acute load shedding. The system experiences considerable shortfall even during summer. This implies that there is a possibility of selling all the energy during this period resulting in violation of set rules quite often.
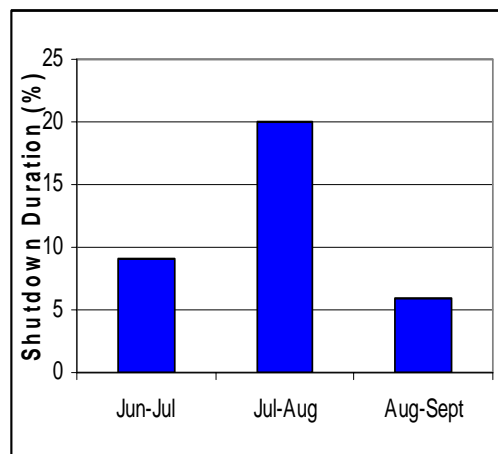
Fig. 6.10 Actual forced shutdown due to excess sediment concentration (Dhakal, 2007)

6.6   Future Plan of Actions Drawn by JHP

6.6.1   Addition of Settling Basins

The existing settling basins have shown satisfactory performance in excluding particles 200 micron or larger. However, the particles size distribution (PSD) of sediment collected in the tunnel as well as power house revealed that the basins exhibited very poor performance in excluding particles finer than 200 micron. As the fine particles are dominant in the Jhimruk River, the existing settling basins were able to trap mere 17% of the total load when all the units were operational. The rest of the load consisting of fine particles passing to powerhouse

were believed to cause severe abrasive effect on turbine and accessories. The plant has been normally operated at about one-third of its capacity during monsoon to avoid excessive wear and tear of hydro-mechanical equipment and accessories (Dhakal, 2007). Therefore, a viability for increasing the trapping efficiency during the monsoon was sought.

Additional settling basins were found one of the best alternatives for solving the said problem. The study was carried out by Hydro Lab with the objective of increasing sediment exclusion and reducing turbine wear. Two basins, each having effective length as 36 m and width as 12 m adjacent to the existing settling basins were found to be the suitable alternative. As a result, overall trapping efficiency of 32.5 has been expected (Fig. 6.11). In other words there will be an improvement of sediment removal by about 15.5 % with the new arrangement. Nevertheless, it also means about 85% of the sediment load subject to the turbine and accessories will still continue to pass in the new arrangement .
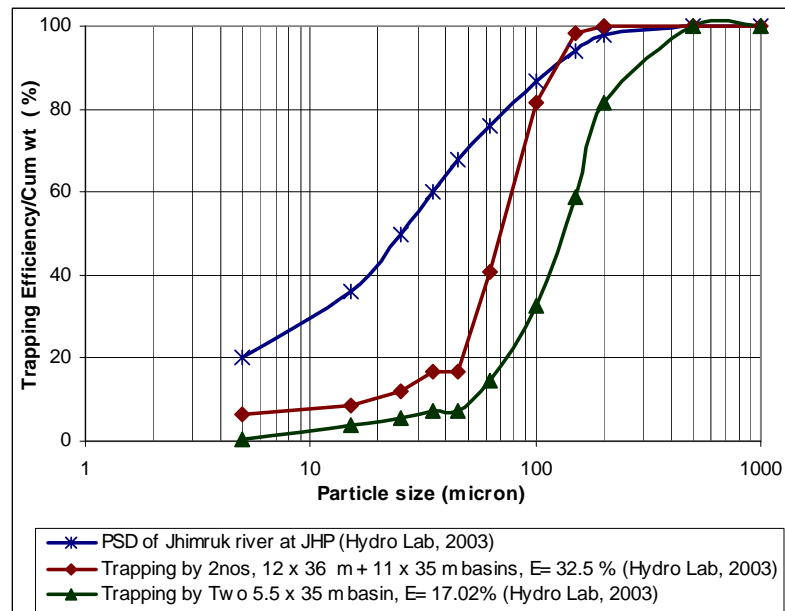
Fig. 6.11 Comparison of trapping efficiency due to existing and new arrangement with additional settling basins

Although the removal of coarser particles in the range of 100 micron or higher have been increased significantly, the same of finer particles didn't improve appreciably. As the sediment load due to the finer sand as well as coarser silt is also responsible for wear and tear of the hydro-mechanical equipment and accessories (Biswakarma, 2008; Bajracharya, 2007),

the new arrangement may not reduce the damage drastically. Due to the significant resources requirement for additional settling basins (U$ 3.0 mln, Basnyat, 1999) and uncertainty of degree of reduction of wear and tear, the plant owner seems reluctant to implement this proposition.

6.6.2 Running Plant With Spare Units

As the addition of settling basins will reduce the sediment load to power plant by 15.5 % and there was no significant impact of the tranquilizers in reducing wear and tear in the plant, BPC is considering to have a set of spare units. One set of units (existing) is proposed to run during monsoon period, whereas the other one during rest of the period, when literally no sediment is anticipated. It is expected that the units which will be run during off-monsoon period will not require considerable repair and maintenance. However, the units subject to monsoon sediment load should be repaired each year.

Although optimum efficiency of the units can be expected during the off monsoon period due to the better condition of the equipment, there is a question as to whether the units designated for monsoon period work properly. Since the units presently, are heavily damaged even when the units run for 33% of the monsoon time, there is a question as to whether these units will sustain if operated for full monsoon period. Even if they sustain, their reparability after heavy damage is questionable. Moreover, periodic repair and maintenance of those units run for off-monsoon period is also unavoidable, which eventually increases the repair maintenance cost compared to that at present level.

6.6.3 Installation of Real Time Sediment Monitoring System

Even if the additional settling basins are added to the existing setup, the new arrangement will not be capable of handling extreme sediment load. Since, from the operational point of view, the extreme sediment load lasting for a short duration is much more harmful than the normal sediment load lasting for a prolonged duration, a reliable sediment monitoring system is desirable. As the present method of sediment analysis using 'soil hydrometer' requires 1-2 hours (Basnyat,1999) to assess the sediment characteristics, the authority desires to get installed a real time sediment monitoring system, so that the power plant is operated according to turbines operating rules.

6.6.4 Installation of Split and Settle Concept

Unless suspended particles are extremely fine or very high turbulence is created, the concentration of suspended sediment across the cross-section of a conventional water passage is usually non uniform. The concentration profile is guided by well known Rouse relation. Because of the gravity, the sediment particles are attracted towards the bed of the conduit. As a result, the concentration in a conduit is much higher close to the bottom than that near the surface. Introduced by Prof. Dr. Haakon Stole, the split and settle concept utilizes this advantage of this difference in sediment concentration over the depth (Stole, 1997). There was a proposal to install such a system at the end of the headrace tunnel by constructing an additional tunnel parallel to the existing one. However, it was argued that a side cover of about 35 m might be insufficient in a geologically weak area . Therefore, BPC could not decide as to whether to go for such a concept (Basnyat, 1999).

6.6.5 Managing Turbine Operating Conditions

It has been reported that operating a plant under part or full overload conditions during monsoon is not desirable. It was noticed that sharing the plant output among several units operating at part load causes more overall damage than having a few units operating at full load (Basnyat, 1999). Therefore, the plant will run at full load condition as far as practicable.

Although, the above mentioned rules in this sub-section are desirable to minimize the level of wear and tear of the equipment and accessories at JHP, the grid operation may not comply with these operating rules. Witnessed by the power shortage even during the monsoon of 2007 and 2008, periodic maintenance of other plants commonly being in the same period and part load often being unavoidable due to the demand pattern in the grid the operating rules desired by the plant often have to be violated. Therefore, new measures should be considered in order to have optimum efficiency of the plant in JHP, which are addressed in next sub-chapter.

6.7 Suggested Measures

The proposed plan of actions set by JHP as well as the prevailing practices to minimize sediment related abrasion in JHP have been presented and assessed in the foregoing section. Although the plan of actions set by BPC seem to be quite logical, most often they may not be applicable from the operation point of view. Going through these plans of action it has been found that none of them envisaged by the plant owner is satisfactory in terms of solving fundamental problem that exist in JHP. Therefore, three measures are proposed to minimize the existing problem prevailing at JHP in the ensuing sub sections. The first measure proposes adopting Split and Spin method to increase trapping efficiency significantly. Whereas the two other measures present a quick and simple methodology to assess sediment concentration.

6.7.1 Installation of Split and Spin System

Excessive sediment induced wear and tear in JHP has been found due to the high concentration of silt as well as fine sand particles. Further, despite their wonderful performance under ideal operating conditions, the Francis turbines installed in JHP are very much delicate in terms of sediment induced wear and tear compared to Pelton turbines. Therefore, without removing coarse silt as well as well as fine sand particles, and thereby reducing the sediment load significantly, JHP will continue to suffer. Looking at the nature of sediment in the Jhimruk River, addition of settling basins seems not very promising in terms of removing the particles in the above mentioned range. Therefore, alternative method to conventional sediment exclusion practices (where gravity is exclusively used) should be introduced in JHP to drastically minimize the sediment load to turbines and accessories and thereby minimize the level of wear and tear significantly.

The sediment concentration at the end of the HRT in JHP shows that most of the sediment load is transported through the bottom part of the conduit. Further, the sediment particles transported through the upper layer are quite fine, which may be assumed relatively not objectionable. Therefore, if the flow is split into two parts and the bottom flow is diverted and processed through the efficient device such as hydrocyclone, relatively sediment free water will pass to the turbine and accessories.

The results obtained from the hydrocyclone in the present research have shown that such a device is highly efficient in removing very fine silt as well as sand particles (refer Chapter 5). The inherent fish-hook effect of the hydrocyclone helps remove the finest particles as well. The performance of hydrocyclone therefore has been compared with the trapping efficiency of existing basins as well as combination of existing and two additional basins (Fig. 6.13). The performance of hydrocyclone having 0.38 m and 1.0 m diameter has been considered for the comparison. The data of smaller hydrocyclone were directly monitored in the laboratory, whereas the data for hydrocyclone having 1.0 m diameter were generated according to scaling laws.
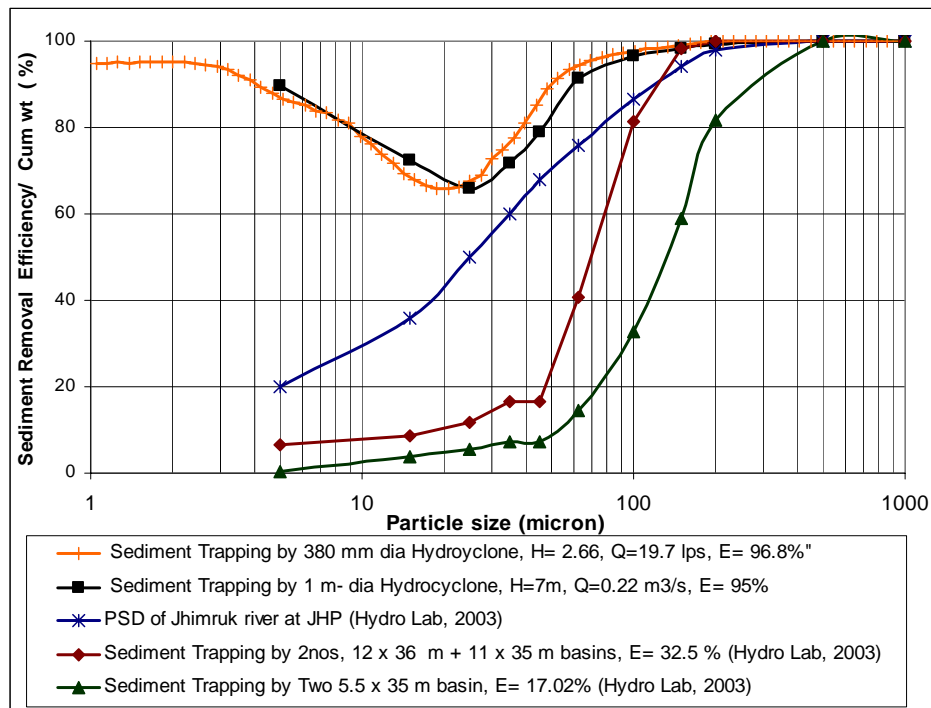
Fig. 6.12 Comparison of sediment removal efficiency due to hydrocyclone and settling basins

It is interesting to note that the removal efficiency of larger hydrocyclone is almost equal to that of smaller hydrocyclone (95% vs 96.8%). On the contrary, a very low efficiency of gravity settling basins can be noticed as compared to that of hydrocyclone. Due to the addition of two large settling basins (increasing trapping area by 3.3 times) overall efficiency of trapping has increased to just 32.5% from 17 %.

Although the efficiency of settling basins for coarser particles (100 micron or larger) has been improved drastically with the addition of two basins, the same for finer particles did not increase significantly. On the contrary, the hydrocyclone exhibited excellent removal efficiency for finer particles as well due to the fish-hook effect as discussed earlier. As the Jhimruk River transports extremely fine sediment, hydrocyclone seems to be a quite efficient alternative device for the exclusion of suspended sediment and minimizing the present level of wear and tear significantly.

Layout Possibilities

The existing access to the headrace conveyance and Surge Tank provided at the end of HRT can be utilized to incorporate the envisaged concept. Further, existing drainage channel provided at this location further ease the installation. Part of the bottom flow can be diverted making use of this channel to get processed through the hydrocyclones. The processed water, however, should be pumped back to HRT before the Surge Tank. The detailed layout possibilities and financial viability of this proposal is however, outside the scope of current research.

6.7.2   Installation of Real-time Sediment Monitoring System

The experience with the hydro-mechanical equipment and accessories has shown that the wear and tear due to excessive sediment load lasting for a day is much more harmful than that due to milder sediment load lasting for prolonged period (Reinhold, 2001). Therefore, real-time information on sediment load can give valuable input to the power plant operator as to what measures to apply.

The laboratory and subsequent field tests of SMOOTH online sediment monitoring system have shown satisfactory results in terms of recording sediment concentration automatically in a pipe flow in real-time (Biswakarma, 2008). Installation of such a system in JHP will provide real-time sediment information , which will give valuable input in terms of operation modality of the plant. This will help avoid severe incidents of wear and tear of hydro-mechanical equipment and accessories.

6.7.3 Sediment Monitoring Using Sediment Rating Curves

Because of the flash flood in mountainous river, the sediment load in the Jhimruk river may increase quite fast. However, the present method of sediment monitoring installed at JHP is capable of assessing the sediment load only after few hours. Hence, extreme load can also eventually pass all the way to power plant before proper assessment is made and proper action is taken. Therefore, the information obtained from sediment rating curves may be utilized to monitor sediment concentration, so that necessary precautions can be taken before hand. This method is proposed to implement in conjunction with the sediment monitoring method installed in JHP.

It has been discussed that the information on concentration of sediment in a power plant in Himalayan river is quite important from several aspects. However, monitoring/recording and assessing the reliable sediment data is often a cumbersome and quite an expensive task. On the other hand, discharge measurement at or near the headworks is unavoidable in any water project. Rather, it is a less expensive and much easier task compared to sediment measurement. Although, the sediment concentration is dependent on many parameters, in a particular river basin such as the Jhimruk, the analysis of the data collected during 1994-1997 at JHP showed that the sediment concentration is highly dependent with the discharge. And such a relation has been found to be statistically highly significant (Pandit, 2005). The regression equations thus obtained for different months with parameters of statistical analysis are presented in Table 6.3.

Table 6-3 *Parameters of Regression Analysis*

Months	Regression Equations	Multiple R	P -value (*x* var)	*Remarks*
June	$S = 0.577 * Q^{2.0454}$	0.887	1.040E-22	*S* in
July	$S = 0.8049 * Q^{1.7884}$	0.848	7.286E-66	ppm, *Q* in
August	$S = 0.0004 * Q^{3.3524}$	0.860	1.279E-45	m³/sec
September	$S = 0.0002 * Q^{3.449}$	0.808	2.75E-51	

6.7.3.1 Limitations of Sediment Rating Curves

The regression equations show that the sediment load is highly sensitive to river discharge. However, the sediment load in a river may drastically rise due to mass wasting in some of the tributaries or at particular locations even when the river flow is relatively small. The sediment load derived as a function of discharge given here may not be correct in such instance. Therefore, the applications of these equations is recommended only when more reliable method such as reliable real-time sediment monitoring method is not available.

6.8 Conclusion

The status of Jhimruk Power Plant, specifically related to sediment induced wear and tear were briefly addressed. The extent of damage in hydro-mechanical equipment and accessories were presented. The efforts made by JHP in minimizing sediment induced wear and tear were critically assessed. It was found that the fundamental problem in JHP was high concentration of finer particles entering into the power plant. From this point of view, most of the measures adopted and planned were not found effective in solving the main problem.

Therefore, three measures are proposed to minimize the existing problems prevailing at JHP. The first measure, application of Split and Spin system consisting of hydrocyclones, can trap most of the particles in the diverted flow and allow the operation of the plant throughout the monsoon period. When using the PSD of the Jhimruk River, a trapping efficiency of a hydrocyclone with 1.0 m diameter is estimated at 95%, compared to 32.5% due to addition of two large settling basins. Other two measures proposed for receiving real-time sediment monitoring provide valuable input to the power plant operator in excluding sediment optimally and operating the power plant in a suitable mode., thereby protecting hydro-mechanical equipment from severe damage.

7   CONCLUSIONS AND RECOMMENDATIONS

7.1   *Conclusions*

An alternative method for suspended sediment exclusion from the hydropower plants in Himalayan Rivers is sought to exclude more and finer sediment, so that the excessive wear and tear in hydro-mechanical equipment can be minimized. The study was carried out by installing laboratory test rigs consisting of hydrocyclones of two different diameters (0.22 m and 0.38m) and geometries. 108 number of test were carried out by varying operating and design parameters. The results obtained from these tests and presented in the foregoing chapters followed by subsequent discussions conclude the followings:

7.1.1   The Performance Assessment of 0.22 m Dia Hydrocyclone

- Significant headloss was observed immediately after the entrance of the hydrocyclone accounting about 30 % of the total loss occurred across the hydrocyclone.

- The sediment removal performance of the hydrocyclone even for smaller flows was found quite high. The lowest SRE of fine sand was observed as 35% for smaller flows. Whereas the efficiency of the same particle was recorded as 60 % in case of higher flows.

- In general the SRE improves with the increase in headloss across the hydrocyclone. However, in case of weak centrifugal field the SRE, especially of finer particles (d< 200 μm) was found to be sensitive to underflow discharge and sediment concentration and not on headloss across the hydrocyclone. The role of these operating variables diminished gradually with the increase of centrifugal acceleration. In case of strongest centrifugal field, the SRE is literally insensitive to the operating parameters.

7.1.2   The Performance Assessment of 0.38 m -Dia Hydrocyclone

- A new geometry of the axial overflow hydrocyclone with modification of inlet, outlet and the roof was identified, which has been found more efficient than conventional hydrocyclone. The same amount of flow in the modified hydrocyclone can be processed with a reduction of headloss by 30 % and 21.5% compared to Standard and gMax cyclones respectively.

- Despite the improved performance of the modified hydrocyclone, about 21.5 % of the total headloss occurred in the system was observed near the exit region of the hydrocyclone.

- The hydraulic performance of cyclone with tangential overflow outlet has been found much higher than that of the hydrocyclones studied. For a reference headloss of 3.5 m the discharge increases by 16.8% compared to that with axial setup resulting in reduction of headloss by 28%. When compared with standard and gMax series hydrocyclones, the discharge increased by 41% and 33.7% respectively resulting in energy saving of 52% and 46% respectively.

- The inherent fish-hook property of the hydrocyclone was also conserved in both the setups of the the modified hydrocyclone. However, the removal efficiency of any particle in the fish-hook zone was higher than those observed by Kraipech et al. (2002), Neesse et al. (2004) and Krebs Engineers (2000).

- For similar operating conditions, SRE due to tangential outlet is better than that due to axial outlet.

- The cut size of most of the tests observed in a 0.38m dia hydrocyclone is smaller than that predicted by previous investigators; Bradley and Pulling (1959), Plitt (1976 Dahlstrom (1954) and Rietema (1961).

- The SRE of smaller as well as larger hydrocyclones in the region of smaller headloss ($H_L > 2.0$ m) are comparable. However, in the range of higher headloss ($H_L > 2.0$ m), the efficiency of the larger hydrocyclone is better in separating coarser as well as finer particles. Such a discrepancy is believed due to the longer residence time of larger cyclone and better streamlining of flow compared to that in the smaller one.

7.1.3 Effect of Design and Operating Parameters on SRE of Hydrocyclone

- The SRE of a hydrocyclone increases with the increase in headloss. However, it is quite sensitive in the range of smaller headloss, but literally insensitive in the range of higher headloss. The role of other operating variables such as flow ratio and sediment concentration is dominant in the range of smaller headloss.

- While the SRE increased with headloss for smaller as well as larger flow ratio, it remained sensitive to the headloss only in the range of smaller feed concentration (C < 1060 ppm).

- The increase in SRE with flow ratio is significant only in the range of lower headloss.

- The shape of all the SRE curves derived for the full range of flow conditions in axial as well as tangential setup is similar. The fish-hook effect is prominent in all the tests. The common feature of all the curves is that the lowest point of the curve is located in the proximity of the same particle size having a mean diameter as 20 micron. The SRE curves for full range of particle size with larger flow ratio are always higher and flatter than that with smaller one.

- The dependency of SRE on sediment concentration diminishes with the increase in headloss. While the relation is highly significant in the range of lower headloss, the same is insignificant in the range of higher headloss.

- For a constant head difference, the overflow discharge decreases with the increase of flow ratio.

- The total discharge of the hydrocyclone is dependent on the aperture size of the underflow. Among the aperture sizes (15 mm to 50 mm) considered, the highest discharge was observed due to 35 mm aperture. At a reference headloss of 4.0 m the total discharge with an aperture of 35 mm is higher by 8.5% compared to that due to 15 mm aperture. When compared the same due to 50 mm aperture, it is higher by 6%.

7.1.4 Evaluation of a Bottom Outlet Hydrocyclone

- Utilizing the potential head over the bottom outlet, the BOH processes more flow than the hydrocyclone with conventional setup does. For a reference headloss of 1.0 m (over the inlet), the discharge due to BOH is larger by 16.6 % compared to that of conventional setup with the same size (50 mm) of underflow aperture.

- The SRE of the concentric BOH is enhanced by inserting the outlet into the bottom of the cyclone and pressurizing the outlet.

- Among the geometries of BOH studied, the SRE due to Spiral outlet has been found better. For similar operating conditions, the SRE of spiral outlet BOH is comparable to that due to conventional hydrocyclone, however, the finer particles are better separated in BOH, whereas the coarser particles in conventional hydrocyclone.

7.1.5 Evaluation of Sediment Handling Practices in JHP

It was found that the fundamental problem of excessive wear and tear in hydro-mechanical equipment in JHP was high concentration of fine quartz particles entering into the power plant. None of the measures adopted and planned to minimize wear and tear were found successful in solving the main problem. Therefore, the following measures by priority are proposed to minimize the existing problems.

- Application of split and spin system. While the top flow relatively clean will directly pass to the power plant, sediment laden bottom flow will be processed by hydrocyclone and returned to main flow. A trapping efficiency of a hydrocyclone with 1.0 m diameter is estimated at 95%, compared to 32.5% due to addition of two large settling basins.

- Proper sediment handling in accordance to the information on sediment load to be received from
  - real-time sediment monitoring system
  - sediment rating curves prepared for monsoon months in the absence of the above system

7.2   Recommendations

- Considering the sensitivity of SRE on various parameters and uncertainties involved in the range of lower headloss, the hydrocyclone is recommended to operate under a headloss larger than 2.0 m.

- As the overflow discharge decreases with the increase of flow ratio for a constant head difference, a minimum flow ratio complying choking free principle is recommended while operating hydrocyclone in the zone of higher flows.

- Although the headloss incurred at the exit region of the hydrocyclone has been minimized due to the modification of axial overflow outlet to the tangential setup, energy level at the overflow outlet in the tangential setup is still much higher than that in the receiving conduit. It indicates, that part of the energy is still lost in this area. Further study is recommended to minimize this loss.

- The performance of the BOH has been found promising, however, as the tests were carried out in a very narrow range of operating and design parameters, detailed investigation with variation of design and operating variables is recommended to better

assess the hydraulics and particles separation performance of the hydrocyclone and draw meaningful conclusions.

- As the discharge handling capacity of a single hydrocyclone is much smaller than that due to a settling basin, large number of hydrocyclones are required in water sector projects, such as Hydropower. Therefore, its application is highly recommended in high-head (low discharge) hydropower plants and water supply projects where the finer sediment particles may also be objectionable.

.

REFERENCES

1. Albertson, M. L. (1952). "Effect of shape on the fall velocity of gravel particles". *Proc. 5th Hydraul. Conf.,* Iowa.
2. Arato EG, 1984, Reducing head or pressure losses across a hydrocyclone, *Filtration & Separation*, vol. 21, pp. 733-736.
3. Arterburn, RA 2004, *The sizing and selection of hydrocyclones*, Retrieved September 30, 2005, from http://www.krebs.com
4. Asomah, IK & Napier-Munn, TJ (1996), The performance of inclined hydrocyclones in mineral processing, pp. 273-286, in Claxton, D, Svarovsky, L & Thew, M (eds), *International Conference 'Hydrocyclone'96',* Cambridge, UK.
5. Athar, M., Kothyari, U. C., and Garde R. C. (2002). " Sediment Removal Efficiency of Vortex Chamber Type Sediment Extractor." *J. Hydraul. Eng.* 128 (12), 1051-1059.
6. Atkinson, E (1990). The vortex tube sediment extractor, Flow analysis and its design implications, Technical Note OD/TN 51, *HR Wallingford,* UK
7. Avery P., 1982 'The Problems of Sedimentation Modelling With Particular Reference to River Intake Models', *International Conference on Hydraulic Modelling of Civil Engineering Structures, Coventry, England,* pp. 167- 180.
8. Avery, P. (1989). "Sediment control at headworks- A design guide." *BHRA, The fluid engineering center,* Bradford.
9. Bajracharya, S.M. (1996). "Sediment exclusion at RoR projects, the Split and Settle concept, Master of Science Dissertation, *Norwegian University of Science and Technology,* Trondheim, Norway.
10. Bajracharya, T. (2007). Correlation between sand led erosion of Pelton buckets and efficiency losses in high head hydropower scheme, Doctoral Dissertation, *Institute of Engineering, Tribhuvan University*, Nepal.
11. Biswakarma M. B. 1998, Sediment Exclusion Optimization Study in Jhimruk Hydropower Plant, Nepal, Norwegian University of Science and Technology, Trondheim, Norway.
12. Biswakarma, M. (2008). Online sediment monitoring in RoR hydropower projects, Doctoral Dissertation*, Norwegian University of Science and Technology*, Trondheim, Norway.
13. Boadway, JD 1984, A hydrocyclone with recovery of velocity energy in, *Proceedings of the Second International Conference on Hydrocyclones,* Bath, England, pp. 153-162.
14. Bradley, D & Pulling DJ 1959, Flow pattern in the hydraulic cyclone and their interpretation in terms of performance, *Transactions Institution of Chemical Engineers*, vol. 37, pp. 34-45.
15. Bradley, D 1965, *The Hydrocyclone,* Pergamon Press, London.
16. Bradley, D, 1960, Design and performance of cyclone thickeners. In *Proceedings of International Mineral Processing Congress,* Group 2, Institute of Mining and Metallurgy, pp. 129-144.
17. Brekke, H., Wu, W.L., and Cai, B.Y. (2002). "Design of hydraulic machinery working in sand laden water." *Abrasive erosion and corrosion of hydraulic machinery.* Imperial College, London, 156-171.
18. Butwal Power Company (BPC), 2004, Sediment load and discharge records for the period 1994-1997, Kathmandu, Nepal
19. Butwal Power Company (BPC)/Hydro Lab, 2004, Additional Settling Basins at Jhimruk Headworks, Hydraulic Design and Model Study, Kathmandu, Nepal
20. Butwal Power Company (BPC, Operations Department, 1997, Jhimruk Hydropower Project, Design Report, Kathmandu, Nepal
21. Camp, T. R. (1943). " The effect of turbulence on sedimentation", *Proc. 2nd Hydraulic Conference,* Iowa.
22. Camp, T. R. (1946). Sedimentation and design of settling tanks", *Trans, ASCE,* 1946
23. Carson, B. 1985, Erosion and Sedimentation Processes in the Nepalese Himalaya. *ICIMOD Occasional paper No.1,* ICIMOD, Kathmandu

24. Chandra, S. and Sinha, A.K. (1996). "Hydro-abrasion of water turbines in Himalayas", in Varma, C.V. J (Ed), *Proc.,, Workshop on silt damages to equipment in hydropower stations and remedial measures*, July 25-26, New Delhi.

25. Chopra, V. and Arya, S. (1996). "Silt- its effect on hydropower components and remedial measures", in Varma, C.V. J (Ed), *Proc., Workshop on Silt Damages to Equipment in Hydropower Stations and Remedial Measures*, July 25-26, New Delhi.

26. Chu, LY & Chen, WM & Lee XZ 2002, Effects of geometric and operating parameters and feed characters on the motion of solid particles, *Separation Science & Technology,* vol. 26, pp. 237-246.

27. Chu, LY & Chen, WM 1993, Research on the motion of solid particles in a hydrocyclone, *Separation Science & Technology,* vol. 28, no. 10, pp. 1875-1886.

28. Chu, LY & Luo QL 1994, Hydrocyclone with sharpness of separation, *Journal of Filtration & Separation,* vol. no. 7, pp. 733-736.

29. Chu, LY, Chen, WM & Lee XZ 2000, Effect of structural modification on hydrocyclone performance, *Separation & Purification Technology,* vol. 2, no. 1-2 , pp. 71-86.

30. Chu, LY, Yu W, Wang GJ, Zhou XT, Chen, WM & Dai GQ 2004, Enhancement of hydrocyclone performance by eliminating the air core, *Chemical Engineering & Processing,* vol. 43, pp. 1441-1448.

31. Chu, LY, Chen, WM & Lee XZ 2002, Enhancement of hydrocyclone performance by controlling the inside turbulence structure, *Chemical Engineering Science,* vol. 57, pp. 207-212.

32. Chu, LY, Qin, JJ, Chen, WM & Lee XZ 2000, Energy consumption and its reduction in the hydrocyclone separation process, *Separation Science &Technology,* vol. 35, no. ?? , pp. 2679-2705.

33. Coulson, J. M., Richardson, J.F., Backhurst, J. R. and Harker, J. H.(1991). *Chemical Engineeering(2),Particle Technology and Separation Process,* Pergamon, Oxford.

34. Criner, HE 1950, in Svarovsky, L 1992, *Solid Liquid Separation,* p. 215, Butterworth, UK.

35. Cullivan, JC, Williams, RA, Dyakowski, T & Cross CR 2004, New Understanding of a hydrocyclone flow field and separation mechanism from computational fluid dynamics, *Minerals Engineering*, vol. 17, no. 5 pp. 652-660.

36. Dahlstrom, DA 1954, Fundamentals and applications of liquid cyclone, *Chemical Engineering Progress, Symposium Series, Mineral Engineering Techniques,* vol. 50, no 41.

37. Dahlstrom, DA, 1949, in Bradley, D, 1965, *Hydrocyclones*, Pergamon, Oxford, p. 117,136

38. Deshar, I. M. (2007). "O and M Experience in Sediment Management" *Workshop on Operations, Repair and Maintenance of Hydropower Plants*, BPC and Statkraft Norfund Power Invest AS, Jan 16, Kathmandu.

39. Dhillon, G.S. (1996). "Silt control works: can they be relied upon to give erosion free operation of power plants" *Proc.,* workshop *on silt damages to equipment in hydropower stations and remedial measures*, New Delhi, India, 203-212.

40. DOI (1990). "Design manuals for irrigation projects in Nepal." *Headworks, river training works and sedimentation manual, No 7,* Department of Irrigation, Nepal, 23-125.

41. Driessen, MG(1951) in Svarovsky, L 1992, *Solid Liquid Separation,* p. 215, Butterworth, UK.

42. Duijn, GV & Rietema, K, 1982 in Svarovsky, 1984, Hydrocyclones, Holt Rinehart, London, p. 115.

43. Fontein FJ, Van Kooy JG & Leniger HA 1962 in Bradley, D 1965, *The Hydrocyclone,* p.11, Pergamon Press, London.

44. Fontein, FJ & Dijksman, C, 1952 in Bradley, D, 1965, *Hydrocyclones, Pergamon*, Oxford, p. 133-134.

45. Fontein, FJ 1958 in Rietema, K 1961, Performance and design of hydrocyclones – I, General considerations, *Journal of Chemical Engineering Science*, vol. 15, p. 300.

46. Galay, V.J., Schreier, H. and Bestbier, R. (2000). Himalayan sediments issue and guidelines, Water and Energy Commission Secretarait, Nepal.

47. Garde, R.J. and Ranga Raju, K.G.(2000). "Sediment Control in Canals", *Mechanics of Sediment Transportation and Alluvial Stream Problems,* 3rd Ed, New Age International, New Delhi, pp. 531-568.

48.   He, P, Salcudean, M & Gartshore, IS 1999, in Cullivan, JC, Williams, RA, Dyakowski, T & Cross CR 2004, New Understanding of a hydrocyclone flow field and separation mechanism from computational fluid dynamics, *Minerals Engineering*, vol. 17, no. 5 pp. 652.

49.   Holland- Batt, AB 1982, A bulk model for separation in hydrocyclones, *Transactions of Institution of Mining and Metallurgy, Section C : Mineral Processing*, vol. 91, pp. 21-25.

50.   Hydro Lab (2004). *Sediment and Efficiency Measurements at Jhimruk Hydropower Plant – Monsoon 2003,* Kathmandu, Nepal.

51.   Hydro Lab (P) Ltd, 2004, Sediment and Efficiency Measurements at Jhimruk Hydropower Plant – Monsoon 2003, Kathmandu, Nepal

52.   hydrocyclone behavior, *International Journal of Mineral Processing,* vol. 3, no ?? , pp.357-363.

53.   Julien, P. Y. (1986). "Concentration of very fine silts in a steady vortex." *Proc., IAHR*, 255-264.

54.   Kawatra SK, Bakshi AK & Rusesky MT 1996, The effect of slurry viscosity on hydrocyclone classification, *International Journal of Mineral Processing,* vol. 48, pp. 39-50.

55.   Kayasta, G.P. (1992). " Marsyangdi Hydropower station. Sediment monitoring activities, Annul Report, *Nepal Electricity Authority,* Kathmandu.

56.   Kayasta,G.P. and Regmi, K.R.(1991). " Marsyangdi reservoir sedimentation", *Nepal Electricity Authority,* Kathmandu.

57.   Kelly, E. G., and Spottiswood, D. J. (1982). Classification. *Introduction to mineral processing,* Wiley, New York. 199-232.

58.   Kelly, EG & Spottiswood, DJ 1982, *Introduction to Mineral Processing,* John Wiley & Sons, USA.

59.   Kelsall, DF 1952, A study of the motion of solid particles in a hydraulic cyclone, *Transactions of Institution of Chemical Engineers*, vol. 30, pp. 87-104.

60.   Kelsall, DF 1953, A further study of the hydraulic cyclone, *Journal of Chemical Engineering Science*, vol.2, pp. 254-272.

61.   *Krebs gMax Cyclone Development, History in the Coal Industry*, 2002. Retrieved Dec 16, 2005, from *http://www.krebs.com/documents/71_gmax_development-coal-09-30-02.pdf*

62.   *Krebs gMax^{TM} Cyclones for Finer Separations With Large Diameter Cyclones,* 2000. Retrieved Dec 16, 2005, from http://www.krebs.com/documents/70_gmax_cyclones_for_finer_seps_-_aug2000.pdf

63.   Lane, E.W. (1953). "Sediment problems in irrigation projects in the United States", *Engineering Vol*. 176, July 1953.

64.   Llyod, P.J. and Ward, A. S., 1975 in Svarovky, L. (2000), *Solid Liquid Separation,* Butterworth, London.

65.   Luo, Q, Deng, C, Xu, J, Yu, L & Xiong, G 1989, Comparison of the performance of water sealed and commercial hydrocyclones, *International Journal of Mineral Processing,* vol. 25, pp. 297-310.

66.   Lynch, AJ, Rao, TC & Bailey CW 1975, The influence of design and operating variables on the capacities of hydrocyclone classifiers, *International Journal of Mineral Processing,* vol. 2, no ??, pp. 29-37.

67.   Lynch, AJ, Rao, TC & Prisbery, KA 1974, The influence of hydrocyclone diameter on reduced efficiency curves, *International Journal of Mineral Processing,* vol. 1, no ??, pp. 173-181.

68.   Lysne, D.K., Olsen, N.R.B., Stole, H., and Jacobsen, J. (1995). "Sediment Control: recent developments for headworks", *Hydropower and Dams,* March 1995, pp. 46-49.

69.   Lysne, D.K.., quoted by Stole H., 1993, ' Diversion Works, Planning Approach', *Withdrawal of Water from Himalayan Rivers, sediment control al Intake*s, Norwegian University of Science and Technology, Trondheim, pp.3-2-3.3.

70.   Ma, L, Ingham, DB & Wen, X, 2000 in Cullivan, JC, Williams, RA, Dyakowski, T & Cross CR 2004, New Understanding of a hydrocyclone flow field and separation mechanism from computational fluid dynamics, *Minerals Engineering*, vol. 17, no. 5 pp. 652.

71.   Medronoho, RA & Svarovsky, L 1984, Tests to verify hydrocyclones scale up procedure, *2nd International Conference on Hydrocyclones (Bath 1984)*, pp. 1-14.

72. Ministry of Water Resources, Nepal (MWRN, 2003). Nepal Country Report by Minister of Water Resources, *The Third World Water Forum*, Kyoto.

73. Mironer, A.(1979). " Engineering Fluid Mechanics" *Mc Graw Hill*, New York.

74. Mosonyi E., 1991, Water Power Development Vol. 2/A, High Head Power Plants, Academia Kiado Budapest

75. Mosonyi, E. (1991). "Water power development, High-head power plants, 2(a), *Akademia Kiado, Budapest, 9*-77.

76. Nagpal, R.K. and Tyagi, S.K., (1996). Unprecedented problems of heavy silt erosion of under water parts of hydropower stations in Ganga valley". in Varma, C.V. J (Ed), *Proc., Workshop on Silt Damages to Equipment in Hydropower Stations and Remedial Measures*, July 25-26, New Delhi.

77. Naidu B.S.K., 1996, Silt Erosion Problems in Hydropower Stations and their Possible Solutions, International *Conference on Silt Damages to Equipment in Hydropower Stations and Remedial Measures,* Central Board of Irrigation and Power, New Delhi, India.

78. NEA, 1986. Jhimruk Power Development, Feasibility Study, *Nepal Electricity Authority,* Kathmanudu.

79. Olsen, N.R.B. (1991). " A numerical approach for simulation of sediment movement in water intakes, Doctoral Dissertation". *Norwegian Institute of Science and Technology,* Trondheim.

80. Olson, TJ & Turner, PA 2004, *Hydrocyclone selection for plant design*, Retrieved September 30, 2005, from http://www.krebs.com

81. Pandit, H.P. 2005, Sediment Handling in Run-of-River Projects in Himalayan Rivers using Sediment Rating Cirves, *Nepalese Journal of Engineering,*V1(1), pp. 39-45.

82. Perry and Chilton (1973). Chemical Engineers' Handbook, *Mc Graw Hill*, Ohio.

83. Picenco International Inc., in Weiss NL 1985, ed, *Classification, SME Mineral Processing Handbook,* p. 3D-12, Society of Mining Engineers, AIMMPE, New York.

84. Plitt, LR 1976, A Mathematical model of hydrocyclone classifier, *CIM Bulletin,* vol. 69, pp. 114-123.

85. Ranga Raju, K.G., Kothyari, U.C., Srivastav, S., and Saxena, M.(1999). "Sediment removal efficiency of settling basins", *J. Irri. and drain. Eng, ASCE,* 125(5)*,* pp. 308-314.

86. Rao, TC, Nageswararao, K & Lynch, AJ, 1976. Influence of feed inlet diameter on the

87. Reinhold M., 2001, Wasserkraft Volk AG, Germany, personal communication.

88. Renner VG & Cohen HE 1966 in Wills BA 1992, *Mineral Processing Technology,* pp. 384-386*,* Pergamon, Oxford, UK.

89. Rietema, K 1961, Performance and design of hydrocyclones, Part I to IV, *Chemical Engineering Science,* vol. 15, pp. 298-325.

90. Rietema, K 1961, The mechanism of the separation of finely dispersed solids in cyclones in Rietema, K & Vermer, CG (eds), *Cyclones in Industry,* pp. 46-63, Elsevier, The Netherlands.

91. Rietema, K., 1962, *Paper C44, 3rd Congress of European Federation of Chemical Engineering,* London.

92. Rong, R & Napier-Munn TJ 2003, Development of a more efficient classifying cyclone, *Journal of Coal Preparation,* vol. 23, no 4, pp. 149-165.

93. Rouse, H. (1937). " Modern conception of mechanics of fluid turbulence" *Trans, ASCE* (102)

94. Sakhuja, V. S. (1996). "Measures to encounter sediment problems of hydropower plants." *Proc.,* w*orkshop on silt damages to equipment in hydropower stations and remedial measures*, New Delhi, India, 67-75.

95. Scholitsch, A. (1937). " Canal Intake Works in Hydraulic Structures, Vol II." *ASME*, New Work.

96. Schrimpf, W. (1991). "Discussions of 'Design of settling basins' by R.J. Garde, K.G. Ranga Raju and W.R. Sujudi" *J. Hydr. Res.,* The Netherlands, 29(1),136-142.

97. Shakya, B 2004, Performance study of an 8" hydrocyclone, MSc Thesis, *Institute of Engineering, Tribhuvan University,* Nepal.

98. Simons, D.B. and Senturk, F. (1977). "Sediment transport technology", *Water Resources Publication*, Fort Collins, Colorado, 163-177.

99.   SMEC (1978). "Gandaki river basin power study" *UNDP report,* Kathmandu, Nepal.

100.   Soccol, OJ and Btrel, TA 2004,Hydrocyclone for pre-filtering of irrigation water, Scientia Agricola, Vol. 61 (2), Piracicabe, Brazil. Retrived Mar 12, 2004 from http://www.scielo.br/scielo.php?script=sci_arttext&pid=S0103-90162004000200002

101.   Soknes S. & Tvinnereim K., 1982, Sediment Removal at the Bondhus Glacier Intake, *in International Conference on Hydraulic Modeling of Civil Engineering Structures, Coventry, England,* pp. 159- 166.

102.   Spintop Hydrocyclones, a non-pluging hydrocyclone, Retrieved , Sept 20, 2004, from *http://www.vortexventures.com/Products/SpintopHydrocyclone/SpintopHydrocyclone.htm*

103.   Stokes, G. G. (1851). "On the effect of internal friction of fluids on the motion of pendulums", *Trans, Cambridge Phil. Soc.,* 9(2), 8-106.

104.   Stole H., 1993, Sediment processes in Himalayan River Basins *in withdrawal of Water from Himalayan Rivers, sediment control at Intake*s, Norwegian University of Science and Technology, Trondheim, pp.2.1-2.3.

105.   Stole, H. (1993). "Withdrawal of Water from Himalayan Rivers, sediment control at Intakes." *Norwegian University of Science and Technology*, Trondheim.

106.   Stole, H. (1997). Split and Settle- A new concept for underground desanders, in Broch ??, Lysne, D.K., Flatabo, ?? and Holland-Hansen (eds), *Hydropower'97*, Trondheim, Balkema, Rotterdam.

107.   Storch, 1979 in Mohamed, D., Davis, S, & Heathman L., *Cyclone Separators, Team 1*, Retrieved September 2, 2004, from www.wsu.edu/~gmhyde/433_web_pages/ cyclones/CycloneRptTeam1.html [2004, Sept2]

108.   Svarovsky (1984), *Hydrocyclones*, Holt, Rinehart & Winston, London.

109.   Svarovsky, L 1977, *Solid liquid separation*, Butterworth, London.

110.   Svarovsky, L 1990, *Solid liquid separation*, Butterworth, London.

111.   Svarovsky, L 1996, A critical review of hydrocyclone models, in Claxton, D, Svarovsky, L & Thew, M, *International Conference on Hydrocyclone'96,* pp. 17-30, Mechanical engineering publications, Bury St Edmunds, Suffolk, UK.

112.   Svarovsky, L. (1977), *Solid Liquid Separation,* Butterworth, London.

113.   Swamee, P.K. and Ojha, C.S. P. (1991). "Drag coefficient and fall velocity of nonspherical particles." *JHE, Proc. ASCE* Vol 117(5).

114.   Tarjan G 1962, in Bradley, D 1965, *The Hydrocyclone,* Pergamon Press, London.

115.   Tarr, DT 1976, in Kelly, EG & Spottiswood, DJ 1982, *Introduction to Mineral Processing,* John Wiley & Sons, USA, pp 219-220.

116.   Thapa, B. (2004). " Sand erosion in hydraulic machinery, Doctoral Dissertation, *Norwegian University of Science and Technology*, Trondheim.

117.   Torobin, L.B. and Gauvin, W.H.(1959). "Accelerated motion of the particle." In Fundamental aspects of solid-gas flow, Part III, *Can. J. of Chem. Eng.* 38(224).

118.   Trawinski, HF 1969 in Svarovsky, L 1992, *Solid Liquid Separation,* p. 217, Butterworth, London.

119.   Uppal, H. L. (1951). "Sediment excluders and extractors" *Proc.s, IAHR 4ᵗʰ Congress,* Bombay.

120.   US Interagency Committee on Water Resources (1957). " Some fundamentals of particle size analysis", Report No 12,

121.   Vanoni, V. A. (1975). " Sedimentation Engineering (ed.)." *Manuals and reports on engineering practice,* ASCE, New York, No 54, 553-587.

122.   WECS (1987). "Erosion and sedimentation in the Nepal Himalaya, an assessment of river processes" *Water and Energy Commission Secretariat and ICIMOD*, Kathmandu, Nepal.

123.   White, S.M. (1981). Design manual for vortex tube silt extractors. Report No OD 37, HRS, Wallingford, UK.

124.   Wills, B.A.(1985). *Mineral Processing Technology,* Pergamon, Oxford.

125.   Xu, JR, Luo, Q & Qiu, JC 1990, Studying the flow field in a hydrocyclone with no forced vortex, Pat I: Average velocity, *Journal of Filtration & Separation ,* vol. 27, pp., 276-278.

126.   Xu, JR, Luo, Q & Qiu, JC 1990, Studying the flow field in a hydrocyclone with no forced vortex, Pat II: turbulence, *Journal of Filtration & Separation ,* vol. 27, pp., 356-359.

127. Xu, JR, Luo, Q & Qiu, JC 1991. Research on the pre-separation space in hydrocyclones. *International Journal of Mineral Processing,* vol. 31, pp., 1-10.
128. Yang, C. T.(1996). *Sediment Transport Theory and Practice,* McGraw-Hill.

APPENDIX A

List of Publications Made During the Research Period

1. Hydraulic and Sediment Removal Performance of a Modified Hydrocyclone. *International Journal of Minerals Engineering,* Vol 22(4), *Elsevier,* Mar 2009, pp. 412-414.

2. Hydrocyclones: Alternative Devices for Sediment Handling in Run-of - River Projects. *Hydro Sri Lanka*, 22-24 Oct,2007, Kandy, Sri Lanka.

3. Sediment Exclusion in Himalayan Rivers using Hydrocyclones. *ISH Journal of Hydraulic Engineering, Vol 14,* Sept 2008.

4. Sediment Handling in Himalayan Rivers Using Cyclone Type Separator, *Workshop on NUFU supported Research Programs at IOE.* Oct, 2007, Kathmandu

5. Sediment Handling in Run-of-River Projects in Himalayan Rivers using Sediment Rating Curves, *Nepalese Journal of Engineering,* Volume 1(1), pp. 39-45, 2005

6. Alternative Methods of Sediment Handling in Himalayan Rivers, *Hydropower 05* , 23-25 May,2005, Stavanger, Norway.